EFFECTIVE UTILIZATION OF DATA FOR ENHANCING THE PERFORMANCE OF MANUFACTURING

A Thesis Submitted in Partial Fulfillment of the Requirements
for the Degree of

DOCTOR OF PHILOSOPHY

by

Kaustabh Chatterjee
(Roll no 186103018)

Department of Mechanical Engineering

Indian Institute of Technology Guwahati

Guwahati 781039

INDIA

August 2023

TH-3282_186103018

TH-3282_186103018

Department of Mechanical Engineering,

Indian Institute of Technology Guwahati,

Guwahati-781039, INDIA

CERTIFICATE

It is certified that the work contained in the thesis entitled "**Effective Utilization of Data for Enhancing the Performance of Manufacturing**" is submitted by Mr. Kaustabh Chatterjee to the Indian Institute of Technology Guwahati for the award of the degree of Doctor of Philosophy. The work has been carried out under my supervision in the Department of Mechanical Engineering, Indian Institute of Technology Guwahati. This work has not been submitted elsewhere for the award of any other degree or diploma.

Dr. Uday Shanker Dixit

Professor

Department of Mechanical Engineering,

Indian Institute of Technology Guwahati,

Guwahati-781039, INDIA

Dr. Jian Zhang

Professor

Department of Mechanical Engineering,

Shantou University,

Shantou-515063, CHINA

TH-3282_186103018

TH-3282_186103018

DECLARATION

I declare that,

a. The work contained in this thesis is original and has been done by me under the guidance of my supervisor.
b. The work has not been submitted to any other institute for any degree or diploma.
c. I have followed the guidelines provided by the institute in preparing the thesis.
d. I have confirmed the norms and guidelines given in the ethical code of conduct of the institute.
e. Whenever I used materials (data, theoretical analysis, figure and text) from other sources, I have given due credit to them by citing them in the text of the thesis and giving their detail in references.

Signature of student
(Kaustabh Chatterjee)

TH-3282_186103018

TH-3282_186103018

Dedicated to Almighty, my late grandmother Mrs. Pratima Chatterjee, my beloved parents Mr. Pradip Chatterjee & Mrs. Kamala Chatterjee, my family and my teachers

TH-3282_186103018

TH-3282_186103018

Acknowledgement

I would like to begin by thanking the Almighty God for helping me remain mentally and physically fit throughout my PhD work. I am also thankful to everyone who had helped me either directly or indirectly during my PhD journey at IIT Guwahati. This thesis has been the result of the support that I have received in IIT Guwahati. I would like to acknowledge and thankful to everyone associated with this thesis.

I would like to express my sincere gratitude and appreciation to my supervisor, Prof. Uday Shanker Dixit, Department of Mechanical Engineering, IIT Guwahati, for his valuable guidance, patience and encouragement. It was only possible due to his continuous support that I was able to carry out this research work. I feel highly privileged for getting the opportunity to work under him as my PhD supervisor. I am also thankful to my co-supervisor, Prof. Jian Zhang, Department of Mechanical Engineering, Shantou University, China, for his valuable suggestions from time to time. It was indeed helpful in improving my research work. I am highly indebted to both of them.

I am also thankful to my doctoral committee members, Prof. D. Chakraborty, Prof. S.N. Joshi and Prof. A. Anand, for their valuable suggestions during the assessment period of my research work. I am also grateful to the former and present heads of the Department of Mechanical Engineering Department, Prof. S.K. Dwivedy, Prof. S. Senthilvelan and Prof. K.S. Krishna Murthy for extending various supports during my PhD tenure.

I would also like express my sincere gratitude to my father Mr. Pradip Chatterjee and my mother Mrs. Kamala Chatterjee for their immense motivation during my PhD journey. It would be unfair, if I don't mention my other family members, who also played an important role in motivating me during my PhD. I will always be grateful to them for understanding me during my tenure at IIT Guwahati.

I am thankful to my friends and colleagues Mr. Chandra Prakash Singh, Mr. Santanu Das, Mr. Ankan Hazra, Mr. Niraj K. Prasad, Mr. Dheeraj Kumar, Mr. Subhash Pratap, Mr. Ritam Sarma, Mr. Debtanay Das, Dr. Rajkumar Shufen, Dr. Vikas Kumar, Dr. Amit Raj, Dr. Faladrum Sharma, Mr. Nilkamal Mahanta, Mr. Nitish Bhardwaj, Mr. Bappa Das, Mr. Bhanu Prakash Bonthala, Mr. Abhijit Pal, Mr. Mussa, Mr. Dipankar Saha, Mr. Abhijeet Dhulekar and last but not the least Mr. Shyaman Saloi.

TH-3282_186103018

TH-3282_186103018

Abstract

The effective utilization of data is becoming increasingly important for enhancing the performance of manufacturing processes. In the era of Industry 4.0, advancements in technology have enabled the collection of vast amounts of data from various manufacturing processes, making it possible to analyse the data and derive insights that can help enhance the performance. One of the main advantages of using data-driven manufacturing is the ability to identify quality issues early in the production process. It reduces the likelihood of defective products, thereby enhancing customer satisfaction, reducing wastage and improving the profitability.

Literature review indicates that modelling of manufacturing processes using physics-based techniques requires unrealistic assumptions and complete knowledge of the deformation phenomenon. With the advancement in the computational capabilities, numerical techniques provide some hope. However, for complex geometries, numerical simulations take up several hours to complete and the associated computational cost also increases. In the era of Industry 4.0, data-driven models can be an alternative way to model a manufacturing process. It provides a quick and accurate estimation. An efficient data-driven modelling of manufacturing process can be achieved by focusing on building a reliable data bank, filtering out the noisy data and avoiding data explosion.

To explore the feasibility of data-driven manufacturing, two typical manufacturing process are considered, viz., turning and forging. Turning is a representative conventional machining process and forging is a typical example of bulk metal forming process. The first objective of the thesis is focussed on capturing veracious data and identification of outliers in turning. The strategy is explained by giving an example of cutting force estimation in turning operation. It attempts to utilise the concept of data analytics for collecting and building a data warehouse, termed as Central Database Repository (CDR). CDR uses multiple linear regression on the captured data and preserved in the databank. Uncertainties associated during machining are taken care of in a separate cloud-based repository termed as mini-repository. Cutting force estimation is carried out with 95% confidence and a new concept of dynamic reliability is attached with each data. Moreover, there is a provision to update the database based on the feedback and filter out the unnecessary data by evaluating the Cook's distance.

The second objective of the thesis aims towards efficient storage and prediction, thereby avoiding data explosion in turning. The methodology is explained by giving an example of surface roughness estimation in turning operation using an industrial big data. The main aim is to preserve the essential model parameters rather than the complete data so that the

TH-3282_186103018

burden on data storage is reduced. The scheme suggests the lower, most-likely and upper estimates of the surface roughness using 35000 datasets simulated using a virtual lathe. The complete region of data is divided into 81 cells and model fitting is carried out in each cell. The proposed methodology provides a reasonable accuracy in the estimation of surface roughness.

The third objective focusses on efficient utilization of the shop floor data for forging load estimation. The main focus is on using an empirical model for estimating the forging load in open and closed die forging. The empirical approach requires correct estimation of a correction factor termed as complexity factor. The complexity factor depends on the geometry of the product and the friction condition. All the data for validations is obtained from finite element method (FEM) simulations using ABAQUS®, that represents a virtual factory. For open die forging, the value of the complexity factor can be accurately estimated using a semi-analytical approach irrespective of the aspect ratio. However, the challenge lies in accurately suggesting the complexity factor for closed die forged products. A methodology is suggested for estimating the forging load in axisymmetric closed-die forged products using a fuzzy set-based methodology. Estimations are carried out using the most similar products in the database.

The last objective attempts to filter the noise from the shop floor data for improving the estimation of the forging load. Kalman filter is used to filter the noise from the shop floor data. In this case, both closed-die forged axisymmetric as well as non-axisymmetric products are considered. All the information is preserved in MySQL relational database. A novel feature of this work is that instead of one deterministic estimate, three estimates, viz. lower, upper and most likely, are obtained. There is also a provision for updating the preserved information in the database. Typical case studies are presented to show the fine tuning of the suggested forging load. When forging load is estimated under stable condition, Kalman filter helps in reducing the error drastically. When forging load is estimated under unstable condition, Kalman filter tries to follow the most-likely estimate.

Overall, the effective utilization of data is presented for two typical manufacturing processes, viz., turning and forging. A well-structured methodology is presented for preserving the veracious data by identifying the outliers. Data duplication is avoided and performance estimation if carried out by preserving only the model parameters, thereby reducing the chances of data explosion. Closed-die forging load is estimated by retrieving the information of the most similar product. Uncertain parameters are represented as fuzzy parameters. Kalman filter is used for tuning the estimate of a semi-analytical model.

TH-3282_186103018

CONTENTS

TH-3282_186103018

TH-3282_186103018

TH-3282_186103018

TH-3282_186103018

List of Figures

TH-3282_186103018

TH-3282_186103018

TH-3282_186103018

TH-3282_186103018

List of Tables

TH-3282_186103018

TH-3282_186103018

Nomenclature

Roman letters

a	Radial acceleration in m/s^2
A_p	Plan area of the forging including flash
C	Average ring-down count obtained from the acoustic sensor
C_p	Complexity factor
d	Depth of cut in mm
$d_{Euclidean}$	Euclidean distance
D_i	Cook's distance for the i^{th} observation
E_{mea}	Error in the measurement
E_{oest}	Error in overestimation
E_{uest}	Error in underestimation
E^u_{est}	Updated error in the estimation
f	Feed in mm/rev
f_i	Numeric/non-numeric attribute of the new product
$\hat{F}$	Best fit value of the cutting force
F_l	Lower estimate of the forging load
F_m	Most-likely estimate of the forging load
F_{mea}	Simulated forging load
f_r	Numeric/non-numeric attribute of the compared product already preserved in the database
F_u	Upper estimate of the forging load
F^u_l	Updated lower estimate of the forging load
F^u_m	Updated forging load
F^u_u	Updated upper estimate of the forging load

TH-3282_186103018

H	Final height of the disk
h	Height of the billet
h_i	Leverage of the ith observation
K	Regression constant
K_G	Kalman gain
L	Semi-width of the billet
$L_{diagonal}$	Length of diagonal of the cell
m	Number of predictors
n	Number of observations used for model fitting
n_a	Total number of attributes (numeric as well as non-numeric)
p	Die pressure at any location
P	Total forging load
$\hat{R}_a$	Best fit value of the surface roughness
R	Projected radius of the disk perpendicular to the loading axis
r	Radial coordinate in cylindrical coordinate space
R_a	Surface roughness in μm
$R_{ainterval}$	Upper and lower estimate of surface roughness using nearest neighbour approach
R_{apred}	Upper and lower estimate of surface roughness with 95% prediction interval
R_d	Difference between the maximum and minimum value of the attribute being compared
$R_{ecurrent}$	Current reliability of the observation
R_{enew}	Reliability of the new observation
$R_{eupdated}$	Updated reliability of the observation
$R_{excurrent}$	Reliability of current regression parameter value
R_{exnew}	Reliability of the new regression parameter value

TH-3282_186103018

$R_{exupdated}$ Reliability of updated regression parameter value

s Standard error of the estimate

t (n–4, 5%) Test statistic obtained from a t-table of two tailed t-test for the degree of freedom of (n–4) respectively with 5% significance level

t (n–5, 5%) Test statistic obtained from a t-table of two tailed t-test for the degree of freedom of (n–5) respectively with 5% significance level

t Time elapsed

V Cutting velocity in m/min

V_y Die velocity

w Height of wear land

x Axial coordinate in cartesian coordinate space

$x_{current}$ Current parameter value

x_{new} New parameter value

$x_{updated}$ Updated parameter value

Greek letters

α Regression exponent for cutting velocity

β Regression exponent for feed

γ Regression exponent for depth of cut

δ Regression exponent for radial acceleration

ε Equivalent plastic strain

μ Coefficient of friction

σ_o Flow stress

List of abbreviations

AI Artificial intelligence

ALE Arbitrary Lagrangian-Eulerian

BUE Built-up-edge

CDR Central database repository

TH-3282_186103018

CLA	Centre line average
CNC	Computer numerical control
CPS	Cyber-physical system
DNN	Deep neural network
FEA	Finite element analysis
FEM	Finite element method
GPR	Gaussian process regression
GUI	Graphical user interface
HSS	High speed steel
IOT	Internet of things
IP	Internet protocol
KDD	Knowledge discovery in database
ODB	Output database
SVR	Support vector regression
IE	Internal energy
FE	Frictional energy

TH-3282_186103018

Chapter 1
Background and Scope

1.1 Introduction

The effective utilization of data is becoming increasingly important for enhancing the performance of manufacturing processes. In recent years, advancements in technology have enabled the collection of vast amounts of data from various manufacturing processes, making it possible to analyse the data and derive insights that can help enhance the performance (Tao et al., 2018). One of the key benefits of data-driven manufacturing is the ability to perform performance prediction. By analysing data collected from manufacturing processes, industries can predict when equipment is likely to fail and carry out preventative maintenance. This can significantly reduce downtime and increase equipment lifespan, resulting in cost savings and increased productivity. Another key benefit of data-driven manufacturing is the ability to improve quality control. Analysing data collected from manufacturing processes can help in identifying the quality issues early in the production process, reducing the likelihood of defective products. This can enhance customer satisfaction, reduce wastage, and improve profitability (Zhang et al., 2023).

Data-driven manufacturing also provides opportunities for process optimization. By analysing data on manufacturing processes, companies can identify ways to optimize production and reduce waste. This can lead to significant cost savings and improved efficiency. In addition, real-time monitoring enabled by data-driven manufacturing allows for quick identification and resolution of the issues, thus, further improving the performance.

Notwithstanding various advantages, there are challenges associated with it (O'Donovan et al, 2015). Data management can be a significant challenge due to the sheer volume of data generated by manufacturing processes. It is essential to have efficient systems in place for collecting, storing, and processing this data effectively. The accuracy and completeness of data are crucial. Data quality can be impacted by sensor malfunction, human error, and data entry mistakes. Data analysis also is a complex task, and many manufacturing industries lack the necessary data skills to interpret the data effectively and make informed decisions. Finally, data integration can be challenging, as manufacturing processes often involve multiple systems and technologies that may not integrate seamlessly. These challenges must be addressed for effective data-driven manufacturing.

TH-3282_186103018

To address challenges associated with data, industries must have some mechanism for effective utilization of data to enhance the manufacturing performance. There is a need to establish a robust data management system that can handle large volumes of data effectively. Industries should also invest in tools and technologies that can help ensure data quality, such as sensors that can detect and correct errors in real-time (Tao and Qi 2017). Additionally, industries should build data analysis capabilities by investing in training and hiring data analysis experts or outsourcing to companies that specialize in data analysis. Finally, industries must prioritize data integration by ensuring that their systems and technologies are compatible and can be integrated seamlessly.

In recent times, the effective utilization of data has played an integral part in enhancing the performance of manufacturing processes. The benefits of data-driven manufacturing are significant, including predictive maintenance, quality control, process optimization, and real-time monitoring (Tao et al., 2018). However, industries must address the challenges associated with data-driven manufacturing, including data management, data quality, data analysis, and data integration. Reconfigurable manufacturing system (RMS) is a popular type of flexible manufacturing system that is used by industries to quickly adapt to the change in market demands (Mittal and Jain 2014). Data-driven insights enables manufacturing industries to make an informed decision on how to reconfigure the existing systems based on the market demands without hampering the productivity.

By adopting best practices for utilizing data to enhance manufacturing performance, companies can unlock the full potential of data-driven manufacturing and achieve significant improvements in productivity, efficiency, and profitability (Rai et al., 2021). The main focus of this thesis is on presenting effective data utilization for two typical manufacturing processes, viz., machining and metal forming.

1.2 Two typical manufacturing processes: machining and metal forming

Manufacturing processes plays a crucial role in the production of goods. From automobiles to electronics, an understanding of manufacturing processes is essential to understand the journey of a raw material into finished product. There are various types of manufacturing processes available. Casting is a mass containing manufacturing process. It involves pouring a molten material into a mould, allowing it to solidify and take the desired shape. Forming is also a mass containing process that involve reshaping materials without removing any significant amount of material. Machining is a subtractive manufacturing process that that utilizes cutting tools to remove excess material from a workpiece, resulting

TH-3282_186103018

in the desired shape and size. Joining processes are employed to connect two or more components together to create an assembly or a finished product. Additive manufacturing, also known as 3D printing, is a revolutionary process that builds objects layer by layer using a digital model. Among the available manufacturing processes, two typical manufacturing process: machining and metal forming are chosen for illustrating effective utilization of manufacturing data.

1.2.1 Machining

Machining is a subtractive manufacturing process where the excess material is removed from the work-piece in the form of chips with the help of a sharp-edged tool (Shaw 2005). A basic classification for the machining process is shown in Fig 1.1. Machining processes are broadly classified into the conventional and non-conventional machining process. The conventional machining involves physical contact with the work piece for the removal of the material. It is achieved by using either a single-point cutting tool or a multi-point cutting tool or abrasives. Non-conventional machining processes may or may not involve contact of the work-piece with the cutting tool for the removal of the material. Non-conventional machining processes utilize various energy forms, chemical reactions, or unconventional tools to achieve the desired results.

Conventional machining has always attracted researchers for a very long time. In-spite of the limitations involved in conventional machining such as cutting tool wear, difficulty in machining hard materials, difficulty in producing complicated profile, the research on conventional machining continues. One of the major reasons being the cost associated with machining, which is around 15% (Merchant, 1998). Hence, a long-cherished goal of the researchers has always been to enhance the machining performance.

Turning is one of the most popular conventional machining operations. A cylindrical turning in a lathe machine is shown in Fig. 1.2. Two kinds of relative motions are involved in conventional machining, one is the primary motion or the cutting motion and the other is the secondary motion or the feed motion. Major portion of the energy provided to a machine tool is spent in cutting motion. Generatrix is the line generated by the cutting motion and directrix is the line generated by the feed motion. One of the main focus of this thesis is to effectively filter, preserve and utilise the turning data for performance enhancement by overcoming the issues discussed in the subsequent section.

TH-3282_186103018

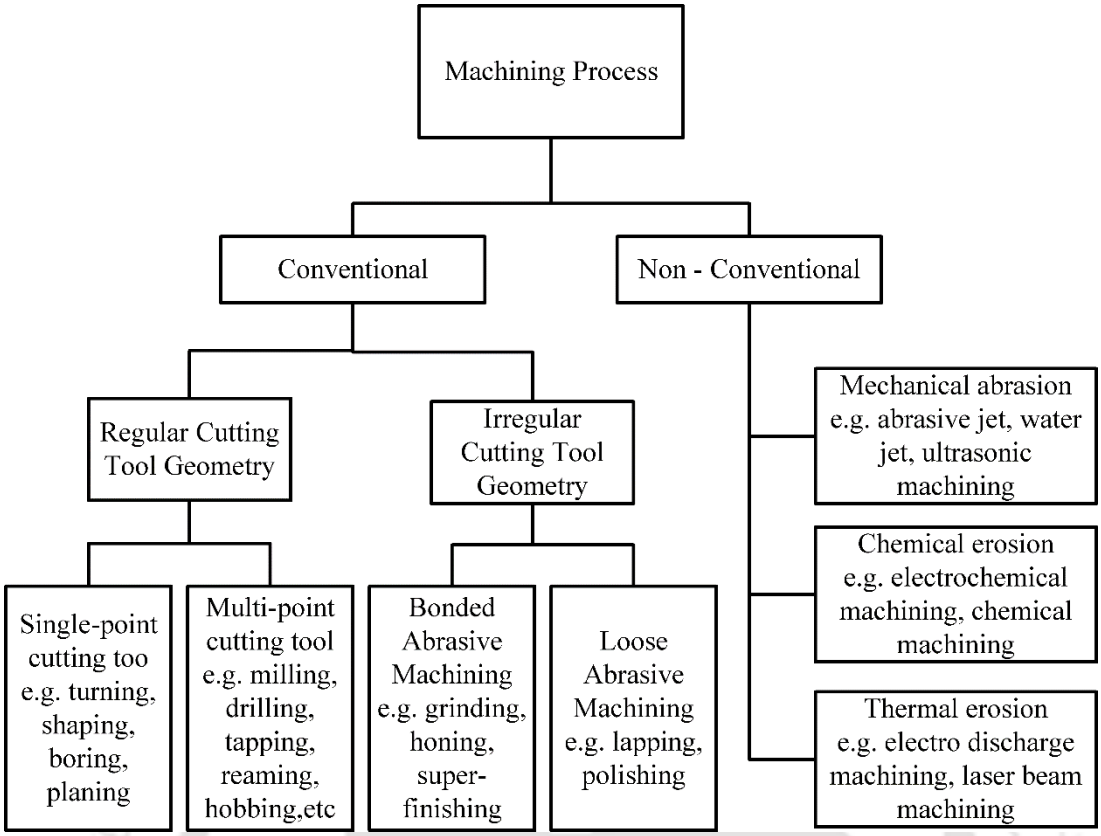

Figure 1.1 Classification of the machining processes

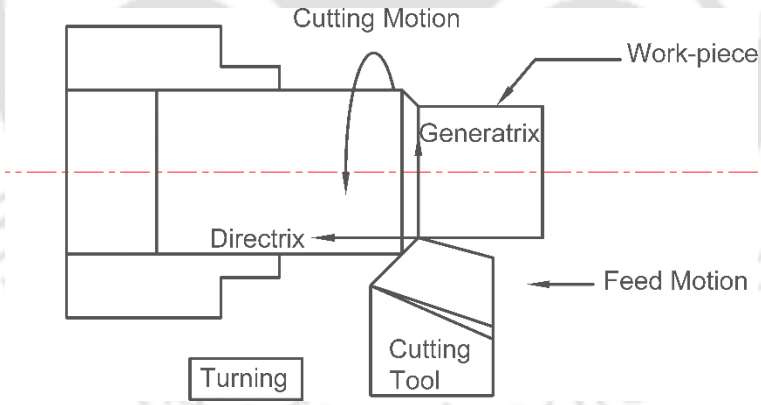

Figure 1.2 Turning Operation

1.2.2 Metal forming

Metal forming is one of the most widely investigated manufacturing processes (Dixit and Narayanan 2013). In forming operation, the material is plastically deformed to attain the desired product. It can be mainly categorized into two main categories— bulk metal forming and sheet metal forming. The conventional definition of bulk metal forming states that the product under consideration must have a high volume to surface area ratio. Rolling, forging, wire drawing and extrusion are examples of bulk metal forming processes.

TH-3282_186103018

On the other hand, in sheet metal forming, the product generally has a low volume to surface area ratio. The ideal situation for sheet metal forming is when there is little or no deformation along the thickness direction. For examples, deep drawing, stretch forming, spinning and bending operation. A basic classification of the metal forming process is shown in Fig. 1.3.

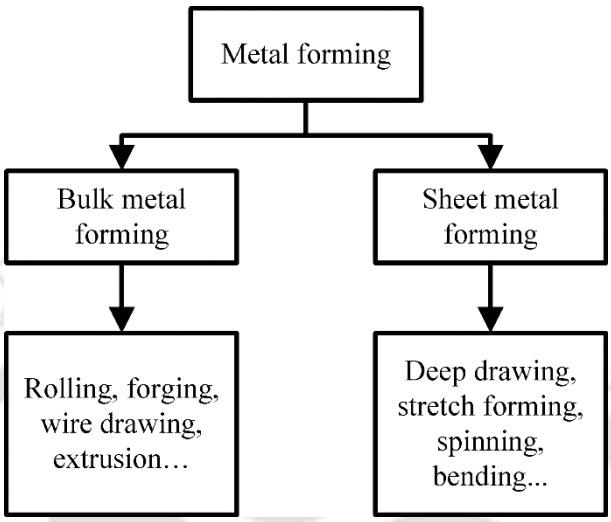

Figure 1.3 Classification of the metal forming processes

Forging is one of the most popular manufacturing processes that involves plastically deforming a material by hammering or pressing. Load requirement is less when forging is carried out under hot forming conditions (termed as hot forging). Occasionally, forging is also carried out under room temperature (termed as cold forging). Two kinds of forging processes exist: open die forging and closed die forging. In open die forging, there is no restriction in the material flow on the application of compression force from the die. An example of open die forging is the upsetting operation. In upsetting operation, the cylindrical billet is compressed between two flat dies as shown in Fig. 1.4. Due to the presence of friction between the workpiece and the platen, there is a restriction in the material flow at the top and bottom surface. However, the middle portion bulges out. Therefore, increasing the level of lubrication between the upper and lower surface can ease the level of restriction to a large extent. In closed die forging, the final product takes the shape of the impression of the die as shown in Fig. 1.5. The impression can be in either one half or in both half of the dies. The excess material is termed as flash that is removed from the final product. Besides turning, another major focus of this thesis is on effectively preserving and utilizing the forging data from the shop floor towards performance enhancement by taking care of the challenges discussed in the subsequent section.

TH-3282_186103018

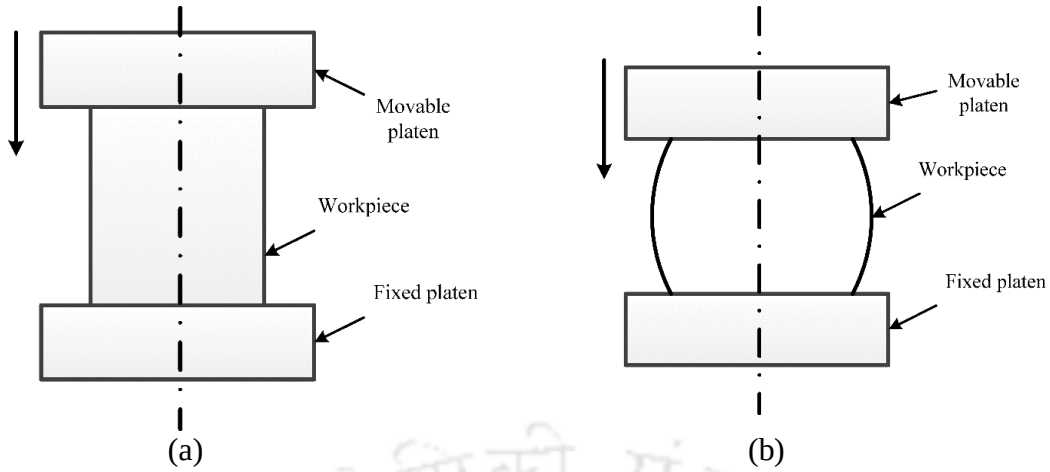

Figure 1.4 Open die forging. (a) Before upsetting. (b) After upsetting

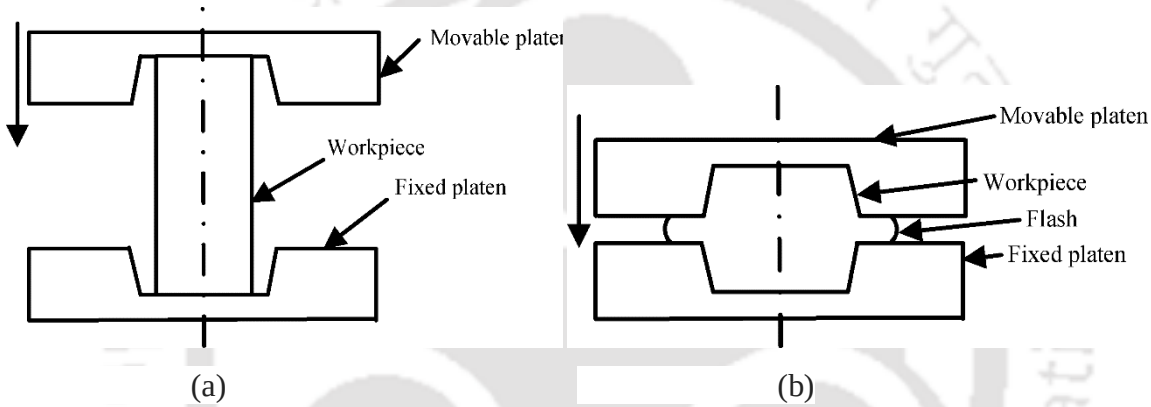

Figure 1.5 Closed die forging. (a) Before upsetting. (b) After upsetting

With the advent of the concept of Industry 4.0 (so called fourth industrial revolution), big data analytics has been the centre of attraction. With time, there has been an advancement in the field of artificial intelligence (AI). Manufacturing industries are trying to implement cloud computing, big data, mobile internet, cyber-physical system (CPS) and internet of things (IOT) in their systems (Tao and Qi 2017). This has triggered a lot of interest among the researchers across the globe towards data driven smart manufacturing (Tao et al., 2018). With manufacturing industries working in remoteness and devoid of a proper established mechanism for data storage, data scarcity is always considered as one of main hindrances towards the realisation of data driven manufacturing. Effective utilisation of manufacturing data for accurate performance prediction reduces the unnecessary downtime. Reduction of downtime improves the existing revenue of the organisation.

Recently, a large amount of manufacturing data is generated at an unprecedented pace due to the use of internet of things (Mourtzis et al. 2016). For machining industries,

TH-3282_186103018

such accumulated data are proposed to be used for machining optimization especially for the optimal selection of machine tool, cutting tool and machining condition (Ji et al. 2019). In contrast, there are scarce research works available that focuses on the timely and effective utilization of the accumulated forging data.

1.3 Issues in Manufacturing Process

Machining has always been a sought-after process in manufacturing. Even though researchers have always taken keen interest in machining, still it is one of the least understood process (Usui, 1988). Proper modelling of the process will greatly enhance the machining performance by optimizing the process without conducting a large number of hit-and-trail experiments. However, it is difficult to model such a complex process by analytical means. Finite Element Method (FEM), a numerical technique for solving differential equations, provided some hope. In spite of it, there is no reasonably accurate FEM model because phenomena involved in machining are not properly understood till date.

The common phenomenon taking place during chip formation in machining is considered to be yielding and shear (Shaw, 2005; Chattopadhyay, 2011). The shear strength of the work material is further used for the estimation of one of the major objectives of metal cutting, i.e., estimation of cutting force and associated cutting power. Later on, it was observed that there were much more mechanics involved in estimating the cutting force than that considered in the conventional Merchant's orthogonal cutting model (Astakhov and Outeiro, 2008). The equations used by Merchant and Ernst (1941) failed to explain the behaviour of AISI 1045 medium carbon steel and AISI 316L stainless steel. It was observed that despite having higher ultimate strength and yield strength, AISI 1045 medium carbon steel experiences lower cutting forces than AISI 316L stainless steel, which is having lower ultimate strength and yield strength. The primary reason being the energy spent in deforming the work material not only depends on the stresses, but also on the corresponding strains. Merchant's theories use only the stress associated with metal cutting for estimating the cutting force and cutting power. However, when it comes to practically determining the cutting force, the calibration of the dynamometer being used and the proper estimation of cutting force remains an issue for the researchers. Astakhov (1998) accurately estimated the cutting force during machining by breaking up the required cutting power into three major components. The components include power required for plastic deformation, power dissipated at the tool-chip and tool-work-piece interface, and power required for the

TH-3282_186103018

formation of the new surfaces. The inclusion of the three components improved the accuracy towards cutting force estimation.

Astakhov (2011) has analysed the reasons for poor performance of machining process models. He has pointed out the following worth considering issues in the modelling of machining operation:

1. It was believed since long that strain rates in machining are very high (Freudenthal, 1950) and can go up to 10^5 s^{-1} (Kronenberg, 1966; Stephenson and Agapiou, 1996). However, decrease of cutting force with cutting speed and absence of twinning deformation suggest that strain rate usually does not exceed 10 s^{-1}.
2. It is also believed that cutting temperatures being very high cause material softening. However, considering the fact that the most of generated heat goes away with the chips, it may not be prudent to consider machining as a cold working process. Most of the temperature rise in chip may be due to friction in the secondary zone without affecting the primary deformation zone. Therefore, the difficulty in understanding the physics behind metal cutting made finite element modelling a complex job.

Researchers in the field of machining also faced hurdles in modelling the contact conditions at the tool-chip and tool-workpiece interfaces. The general assumption of considering Coulomb's friction law for any pair of contacting surfaces did not produce any good results in case of modelling and simulation of a machining operation. There is a general perception to assume coefficient of friction to be independent of the area of the contact and the velocity of sliding. However, Hahn (1951) carried out experiments to suggest that coefficient of friction depends on the area of contact and the sliding velocity. Later on, apparent coefficient of friction was introduced by Kronenberg (1966). It considered the apparent area of contact between the mating surfaces and the sliding velocity, besides the normal load. The actual theory behind correct modelling of contact surfaces is still not clear.

In the late 20th century Luttervelt et al., (1998) addressed the following major hurdles in modelling a machining operation:

1. The large variety of machining operations available make it difficult for the researchers to have a generalized model for turning, milling or drilling. The process of material removal varies even within a particular category of machining. For example, there are various cutting tools available for turning serving different purposes.
2. It is observed that due to the complexity involved in the tool and workpiece interaction, the behaviour of the chips to be formed becomes difficult to understand.

TH-3282_186103018

3. Modelling a machining process involves a large number of fixed input variables as well as large number of free input variables. Fixed input variables are machine-tool, workpiece, cutting tool, fixture and tool holder. Similarly, free input variables are cutting speed, feed, depth of cut and width of cut available for introduction in the model. Hence, it is challenging to incorporate all the input variables in the machining model.

4. The effect of mechanical properties of the workpiece in machining is rarely utilised in modelling. The focus is generally on the phenomenon of chip formation and estimation of cutting force. Moreover, the difficulty in determining the properties of a work material while machining makes it difficult for the researchers to include the mechanical properties in modelling.

5. There is a need to develop an exhaustive database containing all the information regarding the machining operations, machining parameters, and other factors relevant to machining. This would enhance the researchers to model any machining operations with ease. The challenge lies in conducting expensive large-scale experiments to prepare such kind of database.

Apart from machining, another popular manufacturing process is forging. It is a bulk metal forming process that is subjected to three-dimensional compressive stresses. Estimation and control of metal forging process is of utmost importance, particularly in this era of global competition. Researchers have been carrying out estimation of forging load, mostly using analytical, numerical and empirical methods. Such efforts are still continuing (Mohskar and Ebrahimi, 1998; Hartley and Pillinger, 2006). The deformation mechanics of forging is extremely complex. Additionally, the material flow is non-steady and non-uniform. However, with time there has been sufficient progress in the field of analytical modelling that can accurately estimate the forging load. The main challenges in using analytical models are that they require the exact knowledge of the material behaviour during deformation and Coulomb's coefficient of friction. Assumptions such as homogenous deformation, temperature distribution due to different factors within and close to the deformation zone, and loading axes coinciding with the principal axes may be far away from reality. These drawbacks of analytical models were taken care by numerical models. With the advancement of processing power of computers, numerical models such as finite element method (FEM) provided quick estimation of forging load without the need to carry out expensive experiments (Ward et al., 1998). However, FEM simulations are computationally expensive and can take up several hours for simulating the forging of 3-dimensional products with complicated geometry. Empirical models require a lot of data

TH-3282_186103018

for accurate estimation of forging load. To overcome these problems, researchers have started to develop intelligent databases for estimating forging load. The advancement in automation and information technology provided a golden opportunity for the manufacturing industries to store and access large amount of data. Effective utilization of such large amount of data directly form the shop floor can be used for reliable prediction of forging load.

From the aforesaid discussion it is clear that there are several areas where the researchers are trying hard to clear the physics involved, resulting in greater confusion and attaining limited amount of success. The validity of any FEM simulation is also an issue due to following causes: unreasonable simplification of the process, lack of proper information about the process, poor assumption of boundary condition. The task in hand is to develop a reliable databank that can be used for modelling with a better accuracy considering all the challenges discussed.

1.4 Data-driven manufacturing in the era of Industry 4.0

Data-driven manufacturing has become an increasingly popular concept in the manufacturing industry with the advent of Industry 4.0. As a result of the rise in advanced technologies such as artificial intelligence, robotics, and sensors, manufacturers can now collect vast amounts of data about every aspect of their manufacturing process (Frank et al., 2019). This data can then be analysed using advanced analytics tools to identify patterns, trends, and insights, that can be used to make more informed decisions about how to improve manufacturing processes. The purpose of this thesis is to explore the concept of data-driven manufacturing, its benefits, challenges, and applications in turning and forging operations, and how it can transform the manufacturing industry.

Manufacturing is a critical sector in the global economy, responsible for producing everything from cars to household appliances. Traditional manufacturing processes have been manual and reliant on the expertise of workers. However, with the introduction of advanced technologies, the manufacturing process has become more automated and data-driven. By collecting data from various sources such as machines, sensors, and employees, manufacturers can gain insights into various aspects of the manufacturing process such as machine performance and quality control. These insights can then be used to make more informed decisions to improve efficiency and reduce costs.

Data-driven manufacturing offers many benefits to manufacturers. One of the key benefits is improved efficiency. By analysing data captured from sensors, industries can

TH-3282_186103018

identify bottleneck in the manufacturing process and take steps to address them. This can lead to significant cost savings and increased productivity.

Another benefit of data-driven manufacturing is improved quality control. By analysing data on product defects and other quality issues, manufacturers can identify the root causes of these problems and take steps to address them. This can lead to higher-quality products, increased customer satisfaction, and reduced costs associated with rework and recalls.

Data-driven manufacturing can also lead to better decision-making (Zheng et al., 2021). By analysing data on various aspects of the manufacturing process, manufacturers can make more informed decisions about how to allocate resources, optimize production schedules, and improve supply chain management. Despite the benefits of data-driven manufacturing, there is also a major challenge that is associated. The main challenge in data-driven intelligence is data security. Manufacturing facilities collect sensitive data such as trade secrets and customer information. Data must be protected from cyber threats and other forms of data breaches.

1.5 Digital Twin

The Fourth Industrial Revolution comes with digital tool that allows two-way interaction. Unlike the traditional forms of communication, where information flows in a single direction, digital tools enable the users to exchange feedback and opinion. This two way interaction creates a sense of connectivity through knowledge sharing. One of the most exciting innovations to emerge in recent years is digital twin technology. A digital twin is a virtual model of a physical object or system that is capable of simulating the behaviour of the real-world object or system. In the context of engineering, a digital twin can be used to simulate the performance of a product or system before it is built, thereby enabling engineers to optimize its design and performance. One popular tool for creating digital twins is the finite element analysis (FEA) software package ABAQUS.

A typical software package ABAQUS, is a powerful FEA software that is used to simulate the behaviour of complex mechanical systems. It allows researchers to simulate the behaviour of a system under different conditions and to optimize its design and performance. To create a virtual reality using ABAQUS, the following steps are required:

- Model Creation: The first step in creating a digital twin is to create a 3D model of the physical system. The model should be as accurate and detailed as possible to ensure accurate simulation results.

TH-3282_186103018

- Mesh Generation: Once the 3D model has been created, it needs to be converted into a mesh of small elements that can be used in the simulation.
- Material Properties: The next step is to define the material properties of the system being modelled. This includes defining the properties of individual components as well as their interactions with each other.
- Boundary Conditions: Boundary conditions are used to define the loads and constraints that the system will be subjected to during the simulation. These conditions should be as close to the real-world conditions as possible.
- Simulation: Once the model, mesh, material properties, and boundary conditions have been defined, the simulation can be run. ABAQUS provides a variety of analysis types and solvers that can be used to simulate the behaviour of the system under different conditions.
- Analysis: The results of the simulation are analysed to gather insights into the behaviour of the system. Researchers use the information to optimize the design and performance of the actual physical system.

ABAQUS is a powerful tool for creating digital twins that are used to simulate the behaviour of complex mechanical systems. By following the above-mentioned steps, researchers create accurate and detailed digital twins that are used for optimizing and controlling the design and performance of real-world systems.

1.6 Scope of the Thesis

In the previous sections, two typical manufacturing processes, i.e., machining and forging have been explained. On carefully analysing the issues in machining, it was observed that due to several simplified assumptions, the prediction capability of analytical models was limited. Most of the time constant material properties are taken; significant effect of temperature and strain rate is not accounted for. Additionally, friction is also incorporated in a highly simplified manner, mainly by applying Coulomb's model. It is well known fact that Coulomb's model is inappropriate in the processes involving plastic deformation. A numerical technique for solving differential equations are finite element method. FEM can be successfully applied only if the phenomenon involved in machining are completely known. Therefore, with the emergence of the fourth industrial revolution, an unprecedented rise of data has occurred due to the incorporation of sensor-based technologies that is commonly termed as Industrial Big Data. This has resulted in better monitoring and control.

TH-3282_186103018

On the other hand, in forging, the deformation mechanics is quite complex. Application of analytical models require exact knowledge of the material behaviour during deformation and Coulomb's coefficient of friction. Additionally, several assumptions such as loading axes coinciding with the principal axes, homogenous deformation and temperature distribution within and close to the deformation zone may not be real. The drawbacks were taken care of by numerical models. Finite element method (FEM) was successfully implemented for the quick estimation of the forging load. When simulations of three-dimensional products with complicated geometry are carried out, FEM takes several hours and is computationally expensive. Accurate estimation using empirical models require a lot of data. With the advancement in automation and information technology, there is a golden opportunity for the manufacturing industries to preserve and access such large amount of database.

The main focus of the present thesis is to suggest a framework for effective utilization of data for enhancing the performances of manufacturing processes. The emphasis will be on two typical manufacturing processes: turning and forging. Turning is a representative conventional machining process and forging is a typical example of bulk metal forming process. The overall objectives are classified into two main categories as explained in the following subsections.

1.6.1 A strategy to filter the captured veracious data with effective storage and utilization in turning operation

This objective is achieved by proposing a framework to filter the veracious data in turning operation. The strategy is explained by giving an example of cutting force estimation in turning operation. It attempts to utilise the concept of data analytics for collecting and building a data warehouse, termed as Central Database Repository (CDR). CDR uses multiple linear regression on the captured data and preserved in the databank. Uncertainties associated during machining are taken care of in a separate cloud-based repository termed as mini-repository. Cutting force estimation is carried out with 95% confidence and a new concept of dynamic reliability is attached with each data. Moreover, there is a provision to update the database based on the feedback and filter out the unnecessary data by evaluating the Cook's distance.

In the second part of this objective, efficient storage and utilization of the filtered data is carried out. The methodology is explained by giving an example of surface roughness estimation in turning operation using an industrial big data. The main aim is to

TH-3282_186103018

preserve the concise useful information so that the burden on data storage is reduced. The scheme suggests the lower, most-likely and upper estimates of the surface roughness using 35000 datasets simulated using a virtual lathe. The complete region of data is divided into 81 cells and model fitting is carried out in each cell. The proposed methodology provides a reasonable accuracy in the estimation of surface roughness.

1.6.2 Accurate estimation of the forging load in open and closed die forging with the help of the preserved data

This objective is achieved by estimating the forging load using the information of the shop floor data. The main focus is on using an empirical model for estimating the forging load in open and closed die forging. The empirical approach requires correct estimation of a correction factor termed as complexity factor. The complexity factor depends on the geometry of the product and the friction condition. All the data for validations are obtained from finite element method simulations using ABAQUS, that can be considered as a virtual factory. For open die forging, the value of the complexity factor can be accurately estimated using a semi-analytical approach irrespective of the aspect ratio. However, the challenge lies in accurately suggesting the complexity factor for closed die forged products. A methodology is suggested for estimating the forging load in axisymmetric closed-die forged products using a fuzzy set-based methodology. Estimations are carried out using the most similar products in the database.

In the second part of this objective, accuracy of the estimated forging load in closed-die forging is further enhanced by means of a Kalman filter. In this case, both closed die forged axisymmetric as well as non-axisymmetric products are considered. All the information are preserved in MySQL relational database. A novel feature of this work is that instead of one deterministic estimate, three estimates, viz. lower, upper and most likely, are obtained. There is also a provision for updation of the preserved information in the database.

1.7 Organization of the Thesis

The present thesis contains seven chapters. The present chapter introduces the importance of data-driven manufacturing by considering two typical manufacturing processes: turning and forging operations. The rest of the thesis is organized is as follows: Chapter 2 presents the literature survey and the detailed objectives of the thesis. Chapter 3 presents a filtration strategy of veracious data for cutting force estimation in turning operation. Chapter 4 presents an efficient storage and utilization framework of the captured

TH-3282_186103018

veracious data for surface roughness estimation in turning operation. Chapter 5 presents a methodology for the estimation of forging load in open and closed die forging from the already preserved data. Chapter 6 presents a strategy to improve the estimated closed-die forging load using Kalman filter. Chapter 7 highlights future challenges and scope of future work.

TH-3282_186103018

TH-3282_186103018

Chapter 2
Literature Review and Detailed Objectives

2.1 Introduction

In recent times, effective utilization of the manufacturing data has become quite critical for the manufacturing industries. A review on the modelling of machining and metal forming processes and the need for data-driven modelling in manufacturing, is discussed in this chapter in details. Section 2.2 presents a review of modelling of machining processes using analytical, numerical and semi-analytical techniques. Section 2.3 presents a detailed review on modelling of metal forming processes. The advancement in the field of physics-based models and numerical models over the years and the challenges associated are discussed. Section 2.4 presents a review on the use of data-driven modelling in manufacturing, indicating the recent trends in research. Section 2.5 presents the motives for carrying out the research on the effective utilization of manufacturing data in the era of Industry 4.0.

2.2 Modelling of Machining Processes

Machining has always been one of the most important process in manufacturing. In spite of the researchers taking keen interest in machining, it is one of the least understood process (Usui, 1988). Even till today attempts are being made to develop analytical models for machining (Utsumi et al., 2019). However, due to several simplifying assumptions, prediction capability of analytical models is limited. Most of the time, material properties are taken constant; significant effect of temperature and strain-rate is not accounted for. Friction is also incorporated in the model in the highly simplified manner, usually through Coulomb's model. However, it is well-established that Coulomb's model is inappropriate in the processes involving plastic deformation. Three-dimensional state of stress is also not considered in most of the analytical models, as it is next to impossible to solve all the three-dimensional governing differential equations analytically.

With time, there has been a rapid advancement in the computational capabilities. As a consequence, numerical techniques became popular. One such popular technique is Finite Element Method (FEM). FEM is a numerical technique for solving differential equations. It provided some hope to overcome the challenges associated with the analytical models. However, FEM model can be successful only if phenomena involved in machining

TH-3282_186103018

are properly understood. Astakhov (2011) analyzed the reasons for poor performance of machining process models. In particular, he refuted the claim of high strain rates (Kronenberg, 1966; Stephenson and Agapiou, 2016).

A semi-analytical method for the prediction of cutting forces is mechanistic modelling. Cutting force estimation using mechanistic modelling involves cutting edge discretization, evaluation of the force components at each discrete element based on cutting constants and edge coefficients, and summing up the obtained force components at each discrete element to evaluate the resultant cutting force. Hence, mechanistic models provide somewhat accurate results and are still in vogue. In the following sub-sections, a detailed review of the analytical, numerical and semi-analytical techniques is discussed.

2.2.1 Analytical Modelling

A well-established analytical method for the analysis of chip formation in machining is slip-line field analysis. Slip-line field analysis assumes the phenomenon of chip formation to be under rigid plastic and plane strain condition. Initially single shear plane model was suggested by Merchant (1944). The shear angle was estimated from the minimum energy principle. The main challenge was the velocity discontinuity associated with the single shear plane model. There have been a lot of work in the field of machining.

Modelling of self-excited vibration or chatter is also a challenging task. Doi and Kato (1956) took up this task and studied chatter analysis in turning. The authors assumed the system to be of single degree of freedom They claimed that the phase lag between the horizontal cutting force and movement of vibration induces chatter. During the same time, Salje (1956) assumed a two degree of freedom system to study chatter in turning operation.

Cutting process can be properly characterized by accurately estimating the dynamic cutting force coefficients. Tobias and Fishwick (1958) were one of the early researchers to analytically model the dynamic cutting force during machining. They assumed the chip thickness variation, penetration rate and cutting velocity. The results of the analysis were represented in the form of stability charts. They observed that chatter depends on the velocity of the workpiece, machined material, cutting tool geometry and the variation in the chip thickness.

In contrast to the algebraic methods developed so far, Gurney and Tobias (1961) graphically represented the dynamic characteristics of the machine tool structure. However, they suggested that graphical representation was possible only when the modes of vibration in a machine tool are distinguishable. Soon after, Tlusty and Polacek (1963) assumed an n-

TH-3282_186103018

degree of freedom system to analyze chatter. They carried out both experimental as well as theoretical analysis to observe that elliptical tool movement could overcome the damping losses due to chatter. Geometry of the cutting tool such as the shear angle, rake angle, friction angle and clearance angle affect the machining dynamics (Albrecht, 1965). Merritt (1965) studied chatter analysis for an n-degree of freedom machine tool system. He presented chatter using two feedback paths that he termed as primary and secondary. Most of the researchers represented dynamic cutting force to be proportional to instantaneous undeformed thickness.

Das and Tobias (1967) developed an analytical model that could estimate the cutting force coefficients accurately. They observed that the main cutting force and the shear force varies linearly with the shear plane area and universal machinability index. They assumed that the shear plane area was unaffected with respect to chip thickness. Oto and Kano (1974) observed that regenerative, wave cutting and wave removing effect causes chatter and instability. They suggested using a time lag concept for the thrust force and verified the concept in a boring operation. Nigm et al. (1977) suggested a model that estimated the dynamic cutting coefficients from steady state condition data. The authors assumed the theory of shear plane model. However, they considered angular oscillation of the shear plane with changes in the process parameters.

In the early 2000, Fang et al. (2001) suggested a robust universal slip line model that can be effectively used for modelling a machining process. The work of Fang et al. (2001) was further extended by Fang and Jawahir (2002) for the machining of strain hardened materials. They incorporated the effect of temperature and strain-rates in their model that could accurately estimate the cutting forces, chip thickness, chip curl radius, chip back flow angle and equivalent shear flow angle. The robust slip line field model was also used to estimate the stresses acting on the tool rake face during metal cutting (Wang and Jawahir, 2003).

Karpat and Ozel (2008) used the Johnson-Cook criteria to develop the slip-line field model in their analysis. They assumed a plastic contact between the tool and workpiece interface. Ren and Altintas (2000) estimated the shear angle using the minimization of total energy for machining using a chamfered cutting tool. Jin and Altintas (2011) even presented a slip-line field model for a micro-cutting. Therefore, it can be seen from the literature that there have been constant modifications for analytical modelling and till now researchers take a lot of interest in modelling using analytical techniques.

TH-3282_186103018

2.2.2 Numerical Modelling

Analytical modelling requires many simplified assumptions that may be far away from reality. Exact knowledge of the material deformation behavior is also required. Numerical models can be a suitable alternative. Several numerical techniques have been used in the literature. One of them is the finite element method (FEM). Two commonly used mathematical formulations applied in FEM are Eulerian and Lagrangian formulation.

In the Lagrangian approach, the mesh undergoes deformation over time with the material. This formulation is beneficial when there is an unconstrained flow of the material. On the other hand, the Eulerian approach involves a fixed mesh in space, known as a control volume. The mesh builds up the elements that are considered to be fixed in space and covers the assumed control volume. Both of these approaches allow implicit or explicit time integration procedures. One significant drawback of the Eulerian formulation is its assumption of a steady-state mesh configuration. This has resulted many researchers to adopt the computationally expensive Lagrangian formulation.

One such noteworthy research on Lagrangian formulation was carried out by Schermann et al. (2006) to analyze the interaction behavior between a machine tool and a cutting tool. The Lagrangian formulation also faces challenges when the metal cutting involves severe plastic deformation. Severe plastic deformation requires mesh regeneration. Additionally, it becomes difficult to distinguish the nodes during simulation with a negative rake angle or chamfered cutting tool. To overcome such hindrances associated with Lagrangian and Eulerian formulations, a hybrid approach termed as Arbitrary Lagrangian-Eulerian (ALE) is used.

ALE combines the features of Eulerian and Lagrangian approaches. ALE converges fast as compared to Eulerian or Lagrangian approach (Movahhedy et al., 2000; Ozel et al., 2011). There are few reasons for the fast convergence. Firstly, ALE uses an adaptive mesh technique that adapts and follows the motion of the solid boundaries. ALE provides better accuracy while simulating large deformation problems. Lagrangian formulation can become distorted and Eulerian formulation might not be able to capture the deformation well. ALE on the other hand, tracks the motion of the material points using a fixed Eulerian frame of reference, resulting in faster convergence of the solution. Arrazola and Ozel (2010) carried out FEM simulations of orthogonal machining process. They compared the FEM model using ALE approach with that of the FEM model using only Eulerian condition. They observed that the Eulerian formulation requires a predefined chip geometry. On the other hand, ALE formulation does not require such assumptions. They

TH-3282_186103018

even observed that the chip formation is different in the two aforesaid approaches. The chip formation phenomenon suggested by ALE was closer to the actual experimental results as compared to the Euler condition.

Apart from FEM, there are other numerical techniques that have been reported in literature for the modelling of a machining process. The other numerical techniques are based on conserving the mass, momentum and energy including techniques that does not require meshing. All the approximated values of the material properties as well as the state variables are indicated at discrete points or particles in the model. It thereby eliminates the problems arising from mesh distortion, remeshing and unexpected sudden contact conditions.

A notable numerical modelling technique is smoothed particle hydrodynamics (SPH). Calamaz et al. (2009) used SPH for the numerical modelling of turning operation. They studied the tool wear of tungsten carbide cutting tool during dry machining of titanium alloy Ti6AlV. SPH model was mainly used to understand the chip formation phenomenon with a worn-out cutting tool and also to supplement the experimental observation. Uhlmann et al. (2009) suggested a finite point set numerical technique and compared the chip formation phenomenon obtained from FEM simulation in machining of Inconel 718. The researchers claimed that Johnson-Cook model could accurately simulate the continuous chip formation phenomenon. However, Johnson-Cook model failed to accurately model the segmented chip formation phenomenon. In order to accurately simulate the segmented chip formation phenomenon of Inconel 718, they included a damage term in the Johnson-Cook model to accurately incorporate the softening phenomenon during chip formation. The improvement was incorporated in their numerical model and was validated with experimental results. Al-Athel and Gadala (2010) suggested a numerical technique termed as volume of solid (VOS) for modelling a metal cutting process. The proposed method involves estimating and tracking the fraction of the material occupying the Eulerian cells. Depending on the volume occupied in each Eulerian cell, the proposed VOS accurately tracked and estimated the actual deformed boundary of the material. The suggested numerical technique was validated with experimental results involving machining of P20 steel for studying the effect of chamfered or blunt cutting tool.

Constrained natural element method (CNEM) is another numerical technique does not require meshing. CNEM requires Voronoi diagrams and shape functions to track the workpiece boundary during deformation. Illoul and Lorong (2011) applied CNEM to understand the orthogonal and oblique cutting process. Research is still continuing to

TH-3282_186103018

accurately model machining processes numerically. However, they can be computationally expensive and, in many cases, difficult to predict the actual cutting phenomenon during machining operation. One such challenge is to accurately estimate the coefficient of friction during machining. Coefficient of friction directly influences the cutting forces, cutting temperature and plastic strain. Maranhao and Paulo Davim (2010) suggested using the numerical technique only where there is a proper knowledge of the coefficient of friction during machining. Otherwise, there is a significant difference in the experimental and numerical results. As a result, many researchers attempted to model using a hybrid model, termed as Mechanistic model.

2.2.3 Mechanistic Modelling

A semi-analytical method for the modelling of machining process is Mechanistic Modelling. Mechanistic models have been applied by researchers to estimate the cutting force. The main steps involve cutting edge discretization, evaluation of the force components at each discrete element based on cutting constants and edge coefficients, and summing up the obtained force components at each discrete element to evaluate the resultant cutting force.

Koenigsberger and Sabberwal (1961) were one of the early researchers to develop mechanistic models for analysing the tangential forces in end milling operations. They developed the mechanistic model to evaluate the empirical coefficients by measuring the forces during machining. The empirical coefficients were function of the instantaneous forces measured and the corresponding chip area. After more than a decade, Tlusty and MacNeil (1975) predicted the tangential and radial forces on the cutting tool during milling operation. The chip load was observed to be directly correlated with the tangential force and the radial force was observed to be scalar product of the tangential force and empirical cutting force coefficients. Researchers continued to explore ways to accurately estimate the cutting forces during milling operation. Gygax (1979, 1980) used convolution modelling method to determine the cutting force for multi-tooth face milling operation. He evaluated the tangential and the radial forces during machining. It was observed that the cutting coefficients were directly related to the tangential force and inversely with the undeformed chip area.

After the initial work of Sabbarwal, Kline et al. (1980) as well as Kline and DeVor (1983) incorporated uncertainties for the estimation of cutting forces during milling operation. They considered the effect of tool deflection and tool runout on the accuracy of

TH-3282_186103018

the machined parts. Kline's research was extended by Sutherland (1987). He focussed on further improving the accuracy of the Kline's mechanistic model for the estimation of the cutting force in end milling operation. He considered the effect of the tool deflection on the chip load. Interestingly, he successfully estimated the chip load by balancing the cutting force and the corresponding tool deflection. There were many noteworthy works available in literature for the mechanistic modelling of end milling and drilling operation (Armarego and Deshpande, 1991; Kolartis and DeVries, 1991; Chandrasekharan et al., 1995).

Mechanistic models were also used to analyse face milling operations. Fu et al. (1984) accurately modelled the force system by considering the cutter run out and spindle axis tilt. They analysed using a two-dimension orthogonal cutting force model consisting of the main cutting force component and secondary cutting force component on the rake surface of the milling cutter. Altintas and Spence (1991) used a tool path generation technique for simulation a milling operation. They estimated the cutting force using simulation. Besides cutter run out and spindle axis tilt, there are other uncertainties in milling operation such as accurate representation of the cutter and workpiece geometries. Therefore, it becomes necessary to incorporate them during modelling. Jayaram (1996) tried to simplify the representation of workpiece in his analysis. He assumed a number of closed polygons representing the actual workpiece under consideration.

Researchers have also applied mechanistic model for analysing turning and boring operations. Endres et al. (1990) measured the displacement of the tool holder and the workpiece using the vibration analysis. The displacements were further incorporated for studying the effect on the tool geometry and dimensional accuracy of the machined component. In cylindrical boring, Subramani (1990) measured the structural displacements by assuming the workpiece to be flexible and the cutting tool to be rigid. Later on, Jayaram (1996) attempted to modify the earlier works by enhancing the dynamic machining model. He claimed that his model could handle complicated cutting phenomenon representing the actual machining process.

Mechanistic models were also widely used to determine the surface topography during machining operation. Some of the noteworthy works was carried out by Kline et al. (1982), Montgomery et al. (1991), You and Ehmann (1991) and, Zhang and Kapoor (1991 a-b). Hong and Ehmann (1995) proposed a generalised framework that could determine the surface roughness for any type of machining operation.

TH-3282_186103018

Mechanistic models were even applied to analyse micromachining. Vogler et al. (2003) measured the cutting forces in micro-end milling operation using mechanistic models. The estimated cutting force was then validated with experimental results. Effect of the uncut chip thickness and rubbing effect of the cutting tool was considered by Ko and Heisel (2007). They considered both the cutting and the rubbing force for determining the overall cutting force. The model suggested by Wu and Liu (2010) drew correlation between flow stress with cutting tool geometry and the machining parameters. Wu and Liu (2010) observed that with reduction in the feed rate, the flow stress during machining increases. Jun el at. (2012) considered the phenomenon of ploughing, elastic recovery, effective rake angle and rubbing of the flank face. They proposed two mechanistic models, one for shearing and the other for ploughing. They observed that feed rate had minimum influence on the cutting force until the feed rate was twice that of the minimum chip thickness. Instead, the authors observed chip thickness and ploughing to have a significant effect for determining the cutting force.

Past works suggest that mechanistic models can model accurately and are still in trend. For example, recently, it has been applied to predict cutting force in orthogonal machining of an aluminum alloy with cutting speed, feed and edge radii as the input parameters (Sela et al., 2019). Nevertheless, it may be a good idea to combine mechanistic and data-driven models. In the combined models, the prediction can be made with mechanistic models but the coefficients of the model can be updated with the feedback of data. In fact, since long researchers have been stressing on the need to develop an exhaustive database for machining and overcoming the associated challenges in procuring such veracious data (Van Luttervelt et al., 1998).

Ultrasonic assisted turning (UAT) is a popular technique that is used to machine difficult to cut materials. Recently, Sharma and Pandey (2019) proposed a mechanistic model to accurately estimate the cutting forces during UAT. The authors used the free body diagram to analyze the forces acting on the chips. Governing force equations were derived using the momentum and force equilibrium equations. The authors took utmost care to model the self-lubricating cutting insert so as to investigate the effect of intermittent cutting action. Experimental validations were carried out to suggest a reasonable accuracy in the proposed mechanistic model.

Researchers are trying hard to incorporate all the uncertainties during modelling a machining process using analytical, numerical and mechanistic techniques. Research is still

TH-3282_186103018

continuing. The next section discusses on the research work carried out in the field of modelling of forging process.

2.3 Modelling of Forging Processes

Forging is a widely popular manufacturing process that involves subjecting metals to three-dimensional compressive stresses. In today's era of global competition, accurate estimation and control of metal forging process is vital. Over the years, researchers have made significant efforts to estimate forging load using various methods such as analytical, numerical, and empirical approaches (Moshksar and Ebrahimi, 1998; Fereshteh-Saniee and Jaafari, 2002; Hartley and Pillinger, 2006). While the deformation mechanics of forging are highly intricate and the material flow is non-steady and non-uniform, advancements in analytical modeling have allowed for more precise forging load estimation. However, analytical models face challenges as they require precise knowledge of material behavior during deformation and Coulomb's coefficient of friction. Assumptions made in these models, such as homogeneous deformation, temperature distribution, and alignment of loading axes with principal axes, may deviate from reality. To address these limitations, numerical models, like the finite element method (FEM), have emerged. FEM enables quicker estimation of forging load without costly experiments, although it can be computationally expensive and time-consuming for complex 3-dimensional geometries (Ward et al., 1998). Empirical models, on the other hand, require substantial data for accurate load estimation. To overcome these challenges, researchers have begun developing intelligent databases for estimating forging load, capitalizing on advancements in automation and information technology. The availability of large amounts of data from the shop floor presents an opportunity for manufacturing industries to make reliable predictions of forging load through effective utilization of such data. However, before discussing the data-driven aspects in manufacturing, the following two sub-sections discusses the research work carried out in the field of modelling of a forging process using analytical and numerical techniques.

2.3.1 Analytical Modelling of Forging Process

A number of analytical models have been developed over the past few decades. Among the analytical models, slab method is a popular technique that can approximately suggest the forging load and pressure distribution (Altan and Fiorentino, 1971). Slab method uses a differential equation by assuming a force balance in a very small element. It is assumed that the stress distribution is uniform across the thickness of the workpiece

TH-3282_186103018

under consideration. It is to be noted that under high friction condition, stress distribution may vary across the thickness direction and non-homogenous deformation may take place. Assumptions such as homogenous and isotropic material, neglecting the inertial effects, consider only the external friction, constant Coulomb's coefficient of friction and material deformation following von Mises rule may be far away from the actual case.

Altan and Boulger (1973) were one of the early researchers to use slab method for forging analysis. The authors accurately estimated the load and energies required during upset forging, closed-die forging and cold extrusion. In fact, slab method was widely used to estimate the load required to forge any specific product. One such example is manufacturing of connecting rod. Subramanian and Altan (1980) proposed a programmable calculator for estimating the forging load of connecting rods. The programmable calculator uses slab method to accurately estimate the forging that was verified by the experimental results obtained from the shop floor.

Monaghan (1993) in his work used the slab method analysis to accurately predict the forging load and die pressure for a countersunk forging operation. O'Connell et al. (1996) modified the existing slab method analysis to estimate the forging load in case of closed-die upset forging operation. They verified the results of the forging load with the experimental results. Mamalis et al. (1999) analysed the open die forging of a sintered porous product using the slab method analysis. They proposed a yield criterion based on the porosity content that was incorporated in the analytical model for the estimation of the load and the deformed shape of the final product. Research is still continuing on effectively using the slab method analysis for modelling a forging process (Kamble and Nandedkar, 2011; Gisbert et al., 2015).

Slab method is generally not applicable for high friction cases. If the friction between the interacting surfaces are high, stresses will vary across the thickness with non-homogenous deformation. In such cases, another popular analytical technique known as upper bound method (Alon and Kalai, 1985) is used. Upper bound method is used to evaluate the forging load, fold-over and bulging. This technique works on the principle of minimization of the total energy. The upper bound method starts by considering a set of admissible velocity fields within the material. These velocity fields define possible deformation paths that the material can follow during the forming process. The admissible velocity fields satisfy the conditions of continuity and compatibility, ensuring that the material deforms smoothly without any discontinuities or excessive deformation. Upper bound method has been widely used to estimate the forging load, bulging and fold-over.

TH-3282_186103018

Kudo (1960) was one of the early researchers to use upper bound theorem in forging and extrusion operations. The author used Coulomb friction model for the analysis. He carried out his analysis for perfectly plastic material as well as for strain hardened material. He estimated the working pressure using the upper bound theorem and validated the results with experimental results. Kudo (1961) extended his earlier work and carried out more detailed analysis in the estimation of working pressures in forging and extrusion operation. He introduced conical surfaces that represented surface of velocity discontinuity in the cylindrical deformation region by applying velocity fields analogous to plane strain condition. The velocity field is also responsible for the bulging phenomenon of the inner and the outer surface during forging of a hollow disk. Avitzur and Sauerwine (1978) used upper bound theorem to explain the deformation phenomenon of a hollow disk under the action of compressive forces. The authors tried to accurately estimate the bulge of the inner and the outer surfaces, neutral radius and relative average pressure.

The next challenge was to incorporate both bulge and fold in the analysis. Avitzur and Kohser (1978) assumed von Mises rigid and perfectly plastic material with no change in the shear stress friction between the interacting surfaces. They applied the upper bound theorem for the upset forging of rectangular strip and solid cylindrical disk. They found that the forging pressure depends on geometry of the product, friction between the interacting surfaces and the bulge formation with time. Till that point of time, the focus was mainly on the analysis of open die forging. Sagar and Juneja (1980) attempted to predict the forging die pressure in closed-die forging of hexagonal nuts. They assumed the von Mises yield criterion with the material to be rigid, perfectly plastic and isotropic. They observed that certain dimensional ratios require minimum die pressure.

Accurate estimation of the forging load is another aspect that researchers have always tried to investigate in forging. Yang et al. (1991) used the upper bound theorem to estimate the forging load and the deformed shape of the workpiece during upset forging of a cylindrical billet. They considered different friction conditions for the interacting upper and lower dies. All the theoretical results were validated with the experimental results.

Friction plays a key role in metal forming operation. It directly affects the tool life in forging. Ebrahimi and Najafizadeh (2004) assumed a constant friction model to evaluate the constant friction factor using the upper bound theorem. Upper bound theorem has also been used to analyze radial forging operation. Wu et al. (2015) predicted the forging load required in radial forging operation. They observed that the radial reduction was having more influence on the axial flow inhomogeneity as compared to the axial feed. Wu and

TH-3282_186103018

Dong (2016) extended their earlier work in the estimation of forging load in radial forging operation. They improvised the estimation technique using the upper bound theorem by developing admissible velocity fields without considering the velocity discontinuities. They observed that the final plastic strain depends on the reduction in the radial direction. However, for a single stroke, the plastic strain depends on the axial feed.

More recently, Alexandrov et al. (2017) used the upper bound method for quick estimation of the forging load or power in ring forging operation. They tried to generalize the kinematically admissible velocity field by assuming the existence of a rigid zone. Therefore, it is quite evident from the brief literature review that research is still continuing to analytically model a forging operation.

2.3.2 Numerical Modelling of Forging Process

Traditional analytical methods such as slab method, slip-line field method and upper bound method requires several simplified assumptions. Such assumption may be far away from the actual scenario. With the advancement in the processing capability of computers, numerical modelling has emerged as a powerful tool in the field of modelling a manufacturing process. This has enabled researchers to optimize the processes and improving the product quality. A widely used metal forming process is forging. Numerical modelling plays a pivotal role in simulating the complex thermomechanical behavior during deformation.

Finite element method (FEM) model is one such powerful numerical method to solve differential equations. The deformation behavior during any metal forming process can be accurately represented by using differential equations. Most importantly, FEM can incorporate the material inhomogeneity, process dependent material properties and suitable friction models.

Generally, there are three different modelling techniques in FEM. They are rigid-plastic model, elasto-plastic and visco-plastic model. The most popular one is the rigid-plastic model due to its simplicity and reasonable numerical accuracy (Tjotta and Heimlund 1992). Lee and Kobayashi (1973) developed the rigid-plastic model. It was later on used for analyzing various forming operations that include upsetting of solid cylinder, ring compression, extrusion and sheet bending operations (Shah et al., 1974; Chen and Kobayashi, 1978; Chen and Kobayashi, 1980). The main drawback of using the rigid-plastic model was that it neglects the elastic strains. Hence, such models cannot detect the

TH-3282_186103018

stresses that are below the yield point. In other words, rigid-plastic model cannot detect phenomenon such as spring back and residual stresses.

The initial applications of elasto-plastic models in the arena of metal forming were given to researchers such as Lee et al. (1977) applied in uniaxial tension tests, Yamada et al. (1978) studied upsetting of a cylindrical block and Cheng and Kikuchi (1985) analyzed head forming process. Lastly, visco-plastic model was first used by Zienkiwicz et al. (1981). It was further modified by Onate and Zienkiwicz (1983). As visco-plastic model include time-dependent properties of materials, such model is generally used in modelling a hot metal-forming operation. On the other hand, elasto-plastic is more relevant to model a cold metal-forming operation.

Oh (1982) developed a user-oriented computer code that could discretize the boundary conditions of the die. He analyzed the plane strain conditions of randomly shaped axisymmetric dies. Sun et al. (1983) carried out analysis on a three-bite flat bar forging using simplified three-dimensional elements. They assumed that the transverse coordinates had little or no effect on the longitudinal velocity of any point on the material being forged. Similar assumptions were observed in literature, such as Mori and Osakada (1984) applied in plate and edge rolling, and Li and Kobayashi (1984) analyzed spread during rolling. Researchers continued to explore the three-dimensional deformation using FEM. Park and Kobayashi (1984) used a hybrid rigid-visco-plastic model for analyzing compression of a rectangular and a wedge-shaped product. Radial forging of pipes and upsetting of rectangular prisms were also analyzed using a three-dimensional analysis (Mori et al., 1984). Later on, with the advent of the software packages it was easier for the researchers to model using FEM.

A number of researchers have employed FEM to analyze or utilize the results in process planning. In an early attempt, Osaka et al. (1990) tried to utilize the results FEM results of a cold forging process to prepare an expert system. They employed the developed expert system for the estimation of die fracture and defective product. Within two-year, Altan and Knoerr (1992) used FEM to optimize the process variable and die design using Design Environment for Forming (DEFORM) package. The main of their study was to reduce or eliminate the forging defect, carried our stress analysis and evaluate the lubrication in cold forging.

DEFROM was also used to analyze the tube forging process. Till then, researchers were more inclined towards analytical models. However, with the advent of the software packages, it was easier for the researchers to model using FEM. Domblesky et al. (1995)

TH-3282_186103018

used DEFORM package to analyze the hot radial forging process. They carried out thermo-mechanical analysis of the forged product using the rigid thermoviscoplastic FEM. They observed that deformation and strain-rates were sensitive to the axial feed rate. Jang and Liou (1998) studied the residual stresses for hollow shaft using non-linear FEM.

Accurate estimation of the residual stress is necessary for enhancing the service life of any forged product. The authors used ANSYS package for FEM analysis and assumed the material to be elasto-plastic in nature and validated the simulation results with the experimental results available in literature. They observed the presence of tensile residual stresses on the outer surface, compressive residual stress on the inner surface and highest tensile residual stress on the axial direction of the forged component.

It can be observed from the above discussions even though there has been significant advancement in the field of analytical and numerical techniques, still there are challenges associated with them. With the advancement in field of information and database technologies, researchers are focusing of effectively using the captured data from the shop floor. The following section discusses the opportunities that data provides and the works carried out in the field of data-driven manufacturing.

2.4 Use of Data in Manufacturing

Data-driven manufacturing refers to the approach where data plays a central role in decision-making and process optimization within the manufacturing industry. In recent times, the amount of high dimensional manufacturing data generated from various experimentations are piling up on a regular basis. Thus, it becomes impractical to perform any kind of manual analysis in order to discover possible inferences. Therefore, the need for artificial intelligence in data driven decision making arises, in order to draw useful insight from large data sets. For artificial intelligence in data driven decision making, the utilisation of knowledge discovery in databases (KDD) and data mining tools become extremely important. Data Mining involves applying specific set of algorithms for extracting information from data. In order to apply data mining algorithm, data preparation, data cleaning and data selection becomes necessary for ensuring proper interpretation of the data mining results obtained after the analysis (Mitra et al., 2002). The process of KDD includes the following steps (Fayyad et al., 1996; Mitra et al., 2002):

1. Knowledge about manufacturing: This includes having the right knowledge about manufacturing and the associated goal.

TH-3282_186103018

2. Collection of raw data: This includes the process of collection of raw data from various sources, selection of the dataset and focussing on those variables which address the manufacturing issue.

3. Data cleaning, pre-processing and transformation: This includes the pre-processing of data such as outlier removal, replacement of the missing values and filtering of the data. Finally, the data are organised in such a way which can be directly utilised for mining purposes.

4. Data integration: This includes integration of the heterogeneous data obtained from various sources in manufacturing.

5. Selection of appropriate functions of data mining: This includes applying the appropriate knowledge for various data mining functions (like clustering, classification, prediction, association, regression and summarization).

6. Choosing the relevant algorithm to apply data mining: This includes applying the appropriate technique to get the desired function so as to get logical patterns in the data.

7. Data mining: This includes applying a set of tasks to any data so as to get some representational pattern which can be logically inferred.

8. Inference and visualization: This includes the interpretation and visualization of patterns to obtain logical inference for further decision making.

9. Deployment of the obtained inference: The obtained information is deployed into the manufacturing system so as to enhance the performance of the system. The feedback which is obtained is used for further modification based on the requirement.

10. Knowledge storage, reuse and integration into the manufacturing system: This includes the requirement of a possible data storage system for further discovering of the knowledge and probable inclusion of the database in to the manufacturing organisation.

It becomes quite important for industries to adapt to data driven decision making in industrial processes, considering the complexity and nonlinearity of a real production process, the conventional physics-based processes become difficult to model. The reliability and accuracy of the results obtained cannot always be guaranteed. In recent times more and more focus is now towards introduction of the prediction strategy for feedback control, production scheduling and optimization of industrial processes (Jian and Gao, 2012).

The classification for the techniques used for forecasting or prediction of various tasks in industries is shown in figure 2.1 (Zhao et al., 2018). Forecasting and decision

TH-3282_186103018

making based on time series model are mostly used in the industrial processes. Methods such as linear regression, Gaussian process regression, artificial neural network and support vector machine are generally used for prediction based on several factors.

The nonlinearity of the dependent variables is trained easily by kernel based Gaussian process regression for time series prediction (Brahin-Belhouari and Bermak, 2004). Support vector machine is also a kernel-based approach which constructs a hyperplane or a set of hyperplanes for classification and regression (Deka, 2014). In case of factor-based prediction model, feedforward neural network, fuzzy set theory and support vector machines are very popular. In case of prediction within some level of confidence interval, the delta the Bayesian, the mean-variance estimates and the bootstrap approaches are very popular (Khosravi et al., 2011).

On the other hand, fuzzy modelling techniques are mostly preferred in case of long-term prediction interval. Therefore, it can be understood that there are various parameters based on which a specific algorithm is chosen to be implemented. On this note, in the subsequent subsections, a review of data-driven machining and data-driven forging is discussed.

2.4.1 Data-driven Machining

A detailed review on the performance prediction in conventional machining using soft computing techniques has been carried out by Chandrasekaran et al. (2010). The two main objectives of using soft computing techniques in machining is either for performance prediction or parameter optimization. They discussed the application of neural network, fuzzy set and genetic algorithm in turning, milling, grinding and drilling for the prediction of surface finish, dimensional deviation, tool life, tool wear, cutting force and overall process optimization. It is noticed that most of the researchers carried out their research using neural network. One of the pioneering works in the field of performance prediction in machining using soft computing was carried out by Rangwala and Dornfeld (1989). They used the feed forward neural network approach in turning process, where cutting speed, feed and depth of cut were the input variables and cutting force, power consumption, temperature and surface finish were the output variables.

Azouzi and Guillot (1997) carried out research for predicting the surface finish and dimensional deviation in turning using neural network. The neural network was trained based on the best combination of the input parameters obtained using the proposed sensor selection and fusion model. Feed, depth of cut, radial force and feed force were the input

TH-3282_186103018

parameters for the prediction of surface finish and dimensional deviation. Risbood et al. (2003) used neural networks for predicting the surface roughness and dimensional deviation in a turning process. Kohli and Dixit (2005) suggested a systematic procedure for the training of a multi-layer perceptron neural network that could be effective even when a limited amount of data was available. They also suggested a methodology to obtain the lower and upper bound estimation of surface roughness apart from the most likely estimate. Due to relatively faster training, radial basis function (RBF) neural networks have also been used in machining (Basak et al., 2007; Panda et al., 2008; Pontes et al., 2012).

Apart from neural network, fuzzy set theory has also been used for the performance prediction in conventional machining. A detailed review on the use of fuzzy set theory in the area of machining has been carried out by Adnan et al. (2015). Jiao et al. (2004) were one of the early researchers to use both neural network and fuzzy set theory for surface roughness modelling in turning operation. The combined framework of neural network and fuzzy set theory for surface roughness modelling was termed as fuzzy adaptive network (FAN), whose accuracy kept on improving with more data and learning experience. The predicted results by FAN were compared with the statistical regression technique for further justification and validation. Abburi and Dixit (2006) used both neural network and fuzzy set theory for predicting the surface roughness in turning. The data generated by a trained neural network, was used for developing a rule based module for fuzzy set based prediction. Hanafi et al. (2012) used fuzzy set theory for the prediction of cutting force, cutting power and specific cutting pressure in turning. The obtained results were further validated by comparing with the outcome of response surface methodology and experimental results.

The economic aspect in machining mostly depends on the amount of tool wear taking place and tool life of the cutting tool. In tool wear estimation also neural network became popular, with one of the early works for tool life estimation was done by Ezugwu et al. (1995). They used the backpropagation neural network for training the experimental data used for machining of grey cast iron with mixed oxide ceramic cutting tool. The experimental data contains information about flank wear, crater wear, surface roughness and also data related to catastrophic failure. The authors had limitation of the number of data sets being used for training and prediction.

Neural network for predicting the tool life in hot machining of magnesium was done by Tosun and Ozler (2002). They carried out machining operations for estimating the tool wear at four different temperatures, i.e., at room temperature, at 200 °C, at 400 °C and at

TH-3282_186103018

600 °C. The results obtained from neural network was better as compared with the results obtained from regression analysis.

A cost-effective method and faster method for estimating the tool wear involving neural network was developed by Ojha and Dixit (2005). They evaluated the tool life by applying the multiple-regression analysis in the steady wear zone and obtaining the time required for reaching a particular value of flank wear based on past literature and experience of the authors. They further used backpropagation neural network to obtain the upper, lower and most likely estimates of tool life analogous to the approach done by Ishbuchi and Tanaka (1991). The results obtained were found to be better as compared to multiple-regression model.

Neural network models are combined with various optimization techniques such as particle swarm optimization, genetic algorithm, simulated annealing, etc., for optimizing the model parameters. The similar kind of approach was adopted by Natarajan et al. (2007). They used backpropagation neural network for tool life prediction whose training time was reduced by using particle swarm optimization technique.

Estimation of cutting force using soft computing methodology has also attracted the attention of the researchers to reduce the downtime due to sudden tool breakage, tool wear and work piece deflection. Lee et al. (1995) used feedforward neural network for estimating the thrust force and cutting force. They considered undeformed chip thickness, chip width, cutting speed and tool rake angle as the input parameters for the cutting force estimation. The results obtained were further validated with experimental results. The utilization of neural network model for cutting force estimation was also done by Szecsi (1999). He considered the material properties, cutting tool angles and process parameters as the input variables for training 3200 data sets as compared to 1500 testing data sets. The cutting force which is estimated can be utilised further to predict the tool during machining (Lin et al., 2003).

The correlation between the independent and dependent variables makes it vital for developing a model while machining. One such work was done by Ezugwu et al. (2005) in high speed turning of nickel-based alloy. They modelled in neural network to find the correlation between the input and the output variables. The input process parameters considered were speed, feed, depth of cut, cutting time and coolant pressure and the output process parameters considered were tangential force, feed force, motor power consumption, surface roughness, average flank wear, maximum flank wear and nose wear.

TH-3282_186103018

The application of soft computing in parameter optimization is generally multi-objective type. The problems formulate to be of non-linear type containing multiple solutions. The popular optimization techniques used in soft computing are genetic algorithm (GA), simulated annealing (SA), particle swarm optimization (PSO) and ant colony optimization (ACO). Particle swarm optimization based neural network for modelling of surface roughness during single pass turning was performed by Karpat and Özel (2007). They carried out their research in finish hard turning processes using cubic boron nitride tool. The tool wear and surface roughness were predicted using neural network and PSO was used to achieve the optimum process parameters. The two major categories of GA based on the representation of design variables are real-coded genetic algorithm and binary coded genetic algorithm (RGA).

An optimization methodology consisting of a combination of RGA and sequential quadratic programming (SQP) were used by Abburi and Dixit (2007). The main objective was to minimize the production cost from the various pareto optimal solutions generated by using GA and SQP. The authors were able to find the global minima for multi pass turning process. RGA was also used by Kim et al. (2008) for obtaining the optimal machining condition in single pass turning. SA is another popular method of optimization in machining. Chen and Tasi (1996) used SA for minimizing the unit cost of production in multi pass turning process. Researchers such as Onwubolu and Kumalo (2001) found GA to perform better than SA in minimizing the unit production cost whereas researchers such as Chen and Chen (2003) found that the performance of GA and SA are very similar in minimizing the unit production cost.

Till now, most of the researchers carried out offline performance prediction and optimization. One of the early attempts for real time performance prediction or optimization was done by Wang and Wysk (1986). They developed an expert system for optimizing the overall production cost in machining using a data retrieval approach from a flexible database. The database was developed based on several empirical equations extracted from machining data book and literature. Later on, Dornfeld and DeVries (1990) monitored real time tool wear in turning using a neural network.

Yellowley and Adey (1992), carried out on-line optimization in contour turning. The authors controlled the feed rate to ensure a constant tool life with changing cutting direction and varying depth of cut with a constant cutting speed. Online monitoring of surface roughness while turning was carried out by Khanchustambham and Zhang (1992). They used backpropagation neural network for predicting the cutting force and surface

TH-3282_186103018

roughness for machining of ceramic material using the obtained cutting force signal and evaluating the surface roughness for real time monitoring. Real-time monitoring of tool-life while drilling was carried out by Malakooti et al. (1995) using a regression analysis. They also used neural network for supervising the drilling operation by optimally selecting the machining parameters. Employing real time optimization strategy with continuous learning becomes necessary as the performance of machining process is time-dependent (Chandrasekaran et al., 2012).

There are two approaches to optimization— adaptive control optimization (ACO) and adaptive control constraints (ACC). ACO carries out overall optimization, whilst the ACC maximizes one or more cutting variables without violating the constraint. Chandrasekaran et al. (2012) suggested to carry out machining optimization with the inclusion of an artificial intelligence (AI) module. The AI module contained an MLP network with three input variables (cutting speed, feed, depth of cut) and two output variables (surface roughness and tool life). AI module is continuously updated with new information.

Real time tool wear monitoring has also attracted the attention of the researchers for a long time. In direct type tool wear monitoring optical instruments are used for directly measuring the tool wear. In indirect method for evaluating the tool wear, parameters such as vibration and cutting forces are used for evaluating the tool wear. A thorough review for real time and indirect method for the evaluation of tool wear in turning was done by Sick (2002). He observed that neural network models were employed in real time tool wear monitoring utilising the feedbacks obtained from acoustic emission, torque, power, velocity and temperature sensors.

Das et al. (1996) considered cutting speed, feed and the cutting force components as the input parameters, and average flank wear as the output parameter in turning. They used backpropagation neural network for training the algorithm off-line and used feed forward neural network for testing the algorithm in real time. Silva et al. (1998) developed sensor based online tool wear monitoring using neural network. They used adaptive resonance theory (ART) neural network and self-organizing map (SOM) neural network for analysing the obtained frequency domain signals. The ART has the advantage of giving insight about the tool wear utilising a smaller number of sampled data and SOM is used for mapping a high dimensional data to a one- or two-dimensional data. Nadgir and Ozel (2000) also used neural network for tool condition monitoring using online cutting force measured by a piezoelectric dynamometer. Fuzzy neural network for online prediction of

TH-3282_186103018

tool wear was done by Chungchoo and Saini (2002). They used cutting force, acoustic emission signals, skew and kurtosis of force bands, and total energy of forces as the input parameters.

Another aspect of manufacturing is the web-based one that includes cloud computing based optimization. Wang and Jawahir (2004) were one of the early researchers who used the concept of web-based manufacturing in the area of metal cutting. They developed an interactive system in optimizing the cutting conditions by genetic algorithm in milling operation. The developed common gateway interface collects the input from the user side, based on which an HTML document gets generated. Later on, Zheng et al. (2008) attempted to achieve agile manufacturing in turning by developing a web based interface for process parameter selection in order to reduce the overall life cycle cost. In web based environment, the cloud can prove to be a platform for providing the computing services and warehouse of data as suggested by Chandrasekaran et al. (2013). In addition to web based manufacturing, a need arises for controlling the data having high volume, high velocity and having high variety (Woo et al., 2018). The necessity for data driven manufacturing comes into the picture. The next subsection focuses on research work in the field of data-driven forging.

2.4.2 Data-driven Forging

In the era of smart manufacturing, the factories are trying to become self-adaptive based on the real-time feedback from the shop floor. One of the key features of smart manufacturing is the ability to extract meaningful information from the already existing information. Initially computer aided techniques were focused mainly on the applications of knowledge-based expert systems for suggesting the sequence of steps required to forge a product. Such systems focus on using a knowledge database containing a set of rules. The sequence of steps to be followed is chosen based on the product to be forged is recognized.

Over the years, researchers have been trying to effectively incorporate expert system in the forging process optimization. Kim and Im (1995) initially used expert system in multi-stage cold forging process. They developed an algorithm in Prolog language to reduce the number of forming steps required to forge axisymmetric products. Prolog is a programming language known for its powerful logical reasoning. It is particularly well-suited for applications involving artificial intelligence, expert systems, and natural language processing.

TH-3282_186103018

Expert system was also used to determine the forging sequence design of turbine blades (Glynn et al., 1995) and for the process design of a cold forging process (Katayama et al., 2004). Forging involves optimal selection of the operating parameters. However, the operating parameters are often not deterministic or crisp. As a consequence, a lot of human expertise is required when it comes to suggesting a suitable process parameter for estimating the forging load. Additionally, transforming the human experience into a knowledge database is itself a challenging task.

The incorporation of both fuzzy logic and neural network made it possible to cope with the vague knowledge about the forging process parameters. Fuzzy logic based expert system was initially used for predicting the results of finite element analysis in compressing a rubber cylinder (Rao and Pratihar, 2007) and for the prediction of dimensional errors in forging (Park et al., 2007). Forging load and axial stress were then predicted for axisymmetric part using a fuzzy logic based expert system (Gangopadhyay et al., 2011).

Neural network was used for the estimation of wear depth in axisymmetric closed die products in a hot forging process (Yazdi et al., 2012). Later on, wear mechanisms of forging tools were also determined during hot forging using an expert system (Gronostajski et al., 2016). More recently, support vector machine has been used for identifying the product quality by collecting the sensory pressure data during multi-stage forging operation (Guo et al., 2020). Another research work using data from various sensors was carried out for process monitoring and fault detection (Ye et al., 2021). Deep learning techniques were the latest to be used for the condition monitoring of forging machines (Glaeser et al., 2021). Research is still going on to effectively use the accumulated forging data by applying data-driven techniques.

Another aspect of data that is vital towards accurate estimation of the forging load is the veracity of the data. The captured data from the shop floor may contain noise. It is important or vital to be cautious of the noise that may get accumulated with the data. On this aspect, a review on the usage of filters in manufacturing is carried out. Butterworth filter is one of the popular filters to be used in manufacturing.

A Butterworth filter is a type of analog or digital filter used in signal processing to suppress certain frequencies while allowing the rest of the frequencies to pass through. Butterworth filters are widely used in various applications, such as audio processing, communication systems, and image processing, to achieve specific frequency response characteristics. Butterworth filter has been commonly used as a technique for eliminating the noise from the captured signals due to the presence of various external disturbances.

TH-3282_186103018

There are several examples of Butterworth filter in the literature. About two decades ago, Liang et al. (2002) carried out experiments in end milling processes for optimizing the machining time by controlling the spindle power. The spindle power was regulated by adjusting the feed rate and spindle speed. Butterworth filter was applied on the signals received from the power sensor to reduce the effect of noise caused by the presence of cutter run out, belt oscillation and spindle motor. Dölen et al. (2004) developed a cutting force estimation technique for computerised numerical control (CNC) machines using the machine tool feed drives. They captured the signals from the feed drives to estimate the cutting forces.

Noise reduction of all the captured signals were carried out by using Butterworth filter. Ghosh et al. (2007) highlighted the importance of tool wear monitoring in a CNC face milling operation. They estimated the average flank wear by using multiple sensors. The information received from the sensors was used to train a neural network for accurate estimation of the tool wear. The authors conducted experiments both in laboratory as well as in industrial environment and used Butterworth filter for filtering out the noise introduced due to the breaking of the built-up-edge (BUE), local hardness variation over the work-piece and fluctuation in the supply voltage.

Bhattacharyya and Sengupta (2009) also studied the tool wear in a face milling operation. They suggested the use of multiple sensors. The information obtained from the sensors were fed in a regression model to estimate the average flank wear. The current signals received for estimating the power consumed was filtered using a Butterworth filter. Binsaeid et al. (2009) estimated the tool wear in an end milling process. The authors applied three techniques— support vector machine, multilayer perceptron neural network and radial basis function neural network— for evaluating the level of tool wear by using the information of cutting force, vibration and power consumption. Butterworth filter was applied to reduce the effect of noise on the signals received from the acoustic emission sensors. For other sensors, different types of filters were used.

Duro et al. (2016) carried out experiments to monitor the surface quality of a CNC milling process using an acoustic emission sensor. The signals received from the acoustic emission sensor was filtered using a Butterworth filter. Tool condition monitoring in machining of titanium parts was studied by Mou et al. (2019). They used accelerometer to capture the vibration signals for monitoring the cutting tool. Unwanted noise from the signals obtained from the accelerometer was reduced using a Butterworth filter. Butterworth filter produces a very flat smooth frequency response.

TH-3282_186103018

Moving average filter was also used in manufacturing processes for reducing the unwanted noise. Chatter or self-excited vibrations is a persistent problem in machining operation. Chatter signals are not only complex, but also noisy. Pérez-Canales et al. (2011) captured the acceleration signals for monitoring the instabilities caused due to chatter in a milling operation. The authors used the moving average filter for filtering the captured acceleration signals. Hu et al. (2012) carried out experiments on a CNC lathe machine to estimate the energy consumption during machining. They used a power sensor for capturing the energy input to the spindle motor.

Moving average filter was used for eliminating the noise from the power signals. Sun et al. (2016) monitored the chatter in a milling machine by capturing both the force and vibration signals. Moving average filter was then applied on the captured force and vibration signals to reduce the effect of unwanted noise. The main advantage of moving average filter is its simplicity but it requires a lot of memory for saving the data.

Kalman filter is a mathematical algorithm used for estimating and predicting the state of the system on the basis of noisy data. It is commonly used in various fields, such as robotics, aerospace, and control systems. Kalman filter is another popular technique that has been used in manufacturing domain for quick estimation in the presence of uncertainties (Meinhold and Singpurwalla, 1983). The early application of Kalman filter was about two and half decades back. Lou and Lin (1997) monitored the tool wear in a milling process. Tool failure was detected by capturing signals obtained from dynamometer and acoustic emission sensors. Back-propagation neural network was used to estimate the tool wear. Kalman filter was used within the back-propagation neural network to take care of various uncertainties associated with the milling process.

Niaki et al. (2016) monitored the tool wear in a milling process. The authors quantified the uncertainties associated with milling operation using a Kalman filter to accurately estimate the tool flank wear. Mirkoohi et al. (2018) developed an inverse method to estimate the cutting velocity and depth of cut for a desired cutting force. The estimation was carried out using an iterative gradient search method that uses Kalman filter. Tiwari et al. (2018) monitored the tool wear in an end milling process by capturing the cutting force data along with tool wear image. The obtained information was used to develop a linear regression model that was corrected at each stage by using Kalman filter.

Kalman filter has also been applied in the arena of metal forming. Zhang et al. (2019) measured the concentricity between large forging and upsetting or piercing rod using the principle of laser ranging. This type of measurement is crucial for maintaining

TH-3282_186103018

the accuracy and precision of forgings. The distance captured by the laser rangefinders contained random noise that was further refined by using Kalman filter. More recently, Yang et al. (2022) implemented fault detection and isolation in an accelerometer system for a drilling process. Accelerometers systems are used in drilling machine for process control and optimization. The authors used Kalman filter to cope with the uncertainties associated that naturally arise in a drilling process.

2.5 Gaps in literature

Modelling of manufacturing processes using physics-based techniques requires unrealistic assumptions and complete knowledge of the deformation phenomenon. Numerical techniques provide some hope with the advancement in the computation capabilities. However, with complex geometries, numerical simulations take up several hours to complete and the associated computational cost also increases. In hindsight, with the advancement in the information technologies, data driven models can be an alternative way to model a manufacturing process. It provides a quick and accurate performance estimation. An efficient data-driven modelling of manufacturing process can be achieved by focusing on building a reliable data bank, filtering out the noisy data and avoiding data explosion. This approach was not attempted by any researcher so far.

- Although researchers have started using the approaches of data analytics in manufacturing, especially in the quality prediction of steel and condition monitoring based maintenance of smart systems, there are few papers on the area of big data analytics especially in turning. Moreover, sharing of data would be beneficial for both small and medium scale industries. However, data should be properly filtered on the basis of the outliers and data updation facility should be there. These concerns received less attention from the researchers.
- It is evident from the literature that performance estimation in machining using data-driven modeling techniques have gained the attention of the researchers in recent times. Such models mainly require the complete dataset for accurate estimation. This makes the process computationally expensive and time consuming. Appropriate measures are required to avoid data explosion. This concern has gathered less attention from the researchers.
- A past few attempts in the field of metal forming focuses on the timely and effective utilization of the shop floor data. The works were mainly centered around determining

TH-3282_186103018

the number of forming steps required to manufacture a part, identifying the die defects in forging, determining the forging load and axial stress. However, a rigorous analysis is required for taking care of the uncertainties in forging and using the information of the similar products for estimating the forging load.

- Shop floor data may contain noise. Researchers in the past have applied filters to remove the noise from the data. The focus was mainly in the field of machining. Recently, researchers have started applying filters in the arena of metal forming. However, there is little or no focus on applying filter for accurate estimation of the forging load.

2.6 Objectives of the present thesis

To explore the feasibility of data-driven manufacturing, two typical manufacturing processes are considered, viz., turning and forging. Turning is a representative conventional machining process and forging is a typical example of bulk metal forming process. Therefore, based on the review of literature and the gaps in research observed, the following key objectives are decided:

- **Filtration of veracious data for cutting force estimation in turning**

  The first objective of the thesis is to filter the veracious data captured in turning operation. The main aim of this work is to propose a framework that can filter the already captured data during turning operation. The complete strategy is explained in details through an example of cutting force estimation in turning. Uncertainties associated during machining are taken care of and also there is a provision to update the database based on the feedback received from the shop floor.

- **Efficient storage and prediction of the captured veracious data: An example of surface roughness estimation in turning**

  The second objective of the thesis deals in effective storage and utilization of the filtered data during turning operation. The scheme is explained by giving an example of surface roughness estimation using an industrial big data. Different strategies are explained in details for preserving only the useful information that will ultimately reduce the burden on data storage.

- **Estimation of forging load in open and closed-die forging with the help of preserved data**

  The third objective of the study explores effective utilization of data in forging operation. The main aim of this objective is to correctly guess the forging load in

TH-3282_186103018

both open and closed die forging based on the data obtained from FEM simulations using ABAQUS that can be assumed as a virtual factory. Estimations in closed-die forging are carried out using fuzzy set by using the information of the most similar product in the database.

- **Improving the prediction with the help of Kalman filter: A case study of closed-die forging**

  The fourth objective is to enhance the accuracy of the suggested forging load in closed-die forging by using Kalman filter. The case study is presented for both axisymmetric as well as non-axisymmetric product. A novel feature of this study is that instead of one deterministic estimate, three estimates, viz. lower, most-likely and upper are obtained. Most importantly, as suggested for turning operation, for the study carried out for forging operation, there is a provision for preserving the updated information in the database.

  All the objectives are executed in a sequence and the research plan is presented in Figure 2.1.

TH-3282_186103018

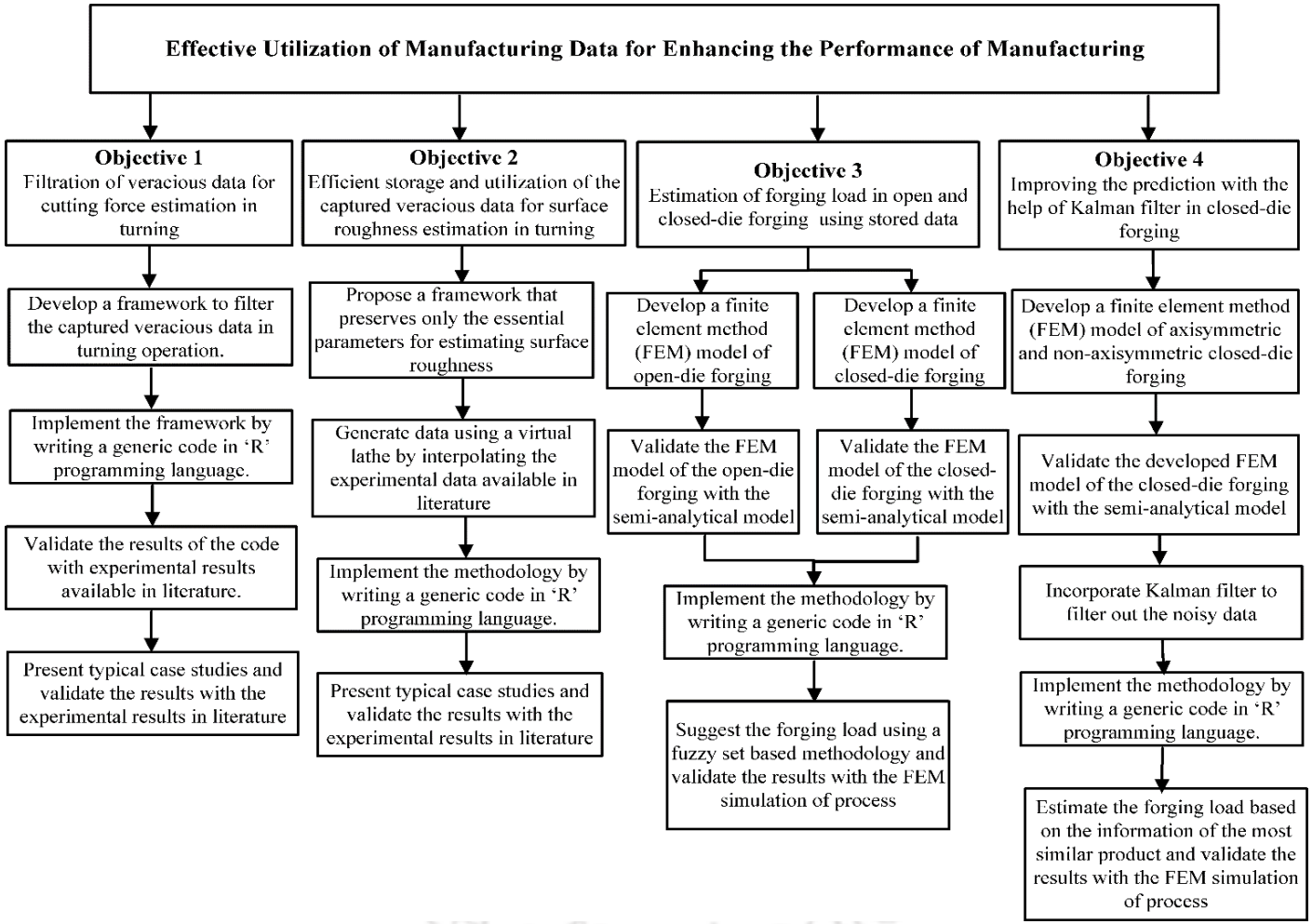

Figure 2.1 Flowchart of the research plan

TH-3282_186103018

Chapter 3
Filtration of Veracious Data for Cutting Force Estimation in Turning

3.1 Introduction

Filtration of veracious data plays a crucial role in cutting force estimation during turning operation. Turning is a widely used machining process in which a cutting tool removes material from a rotating workpiece to create a desired shape or size. Accurate estimation of cutting forces is essential for optimizing tool selection, minimizing tool wear, and ensuring the overall machining process's efficiency and productivity.

During turning, various factors affect cutting forces, such as cutting speed, feed rate, depth of cut, tool geometry, workpiece material properties, and machining conditions. Estimating these forces accurately is challenging due to the dynamic nature of the process and the presence of various sources of uncertainty and noise. To address this challenge, the filtration of veracious data is employed. Veracious data refers to the reliable and accurate information collected from sensors attached with the machine tool during the turning process.

In turning, prediction of cutting force, surface roughness and tool wear in machining keeps attracting the attention of researchers. Surface roughness has a long bearing on the quality of a product. Cutting forces influence dimensional accuracy, surface integrity, tool life and energy consumption. Tool wear modelling is very important for replacing the tool before it breaks or produces inferior quality product. A number of analytical and numerical methods have been developed to predict the surface roughness and cutting forces as a function of process parameters (Wang et al., 2019; Zhang et al., 2019). Attempts have also been made to predict tool wear during machining based on online signals from sensors (Kuntoğlu and Sağlam, 2019; Liu et al., 2019). However, these methods could attain only a limited success and prompted the researchers to develop soft computing-based methods (Laghari et al., 2019, Cherukuri et al., 2019). Soft computing-based methods such as neural network require a large amount of experimental data. With machining industries working in isolation and devoid of well-established mechanism for data storage, data scarcity has been a big hindrance to the effective utilization of soft computing-based methods. Fortunately, thanks to progress in information technology, industries are headed towards

TH-3282_186103018

implementing artificial intelligence (AI) in their activities. Industries are trying to get smart and intelligent by incorporating the technological concepts of cloud computing, Cyber-Physical System (CPS) and Internet of Things (IoT). These have been identified as the backbone of Industry 4.0 and Made in China 2025 (Ji et al., 2019). It appears that data scarcity will no longer be problem and proper analytics of big data can be a viable substitute for analytical and numerical methods.

The objective of this chapter is to sensitize the researchers in the application of big data and analytics in machining. Literature already contains a number of articles suggesting the prediction of performance parameters in machining using various techniques such as regression and neural network models. However, the biggest challenge is to acquire reliable data of different varieties in sufficient quantity. This chapter mainly focusses on how a reliable database repository can be prepared that will enable the modelling and optimization of machining processes. In order to present a proper framework for this task an example of main cutting force prediction in turning is taken, while fully acknowledging that in a real scenario the captured data will be supposed to carry out prediction of a number of parameters. Also, the data will be quite voluminous unlike that used in this chapter to illustrate the proposal.

The rest of the chapter is organised as follows. Section 3.2 presents the proposed methodology adopted for data collection and machining force prediction in turning. Section 3.3 discusses the data collection procedure when feed, depth of cut and cutting speed are available besides main cutting force. Section 3.4 presents the estimation of cutting force with 95% prediction interval. All the typical case studies are explained in Section 3.5. Section 3.6 concludes the chapter.

3.2 Proposed framework for data collection and machining force prediction in turning

Based on the review of literature on the modelling of machining process and past works on data driven manufacturing presented in the last chapter, the following issues have been identified in the context of a proper methodology for the capturing of veracious data in order to create a reliable data bank:

- Developing a proper methodology for data collection and building a reliable data bank for manufacturing industries is the need of the hour.

TH-3282_186103018

- Care has to be taken to avoid storing unnecessary machining data in the database in order to avoid data explosion.
- Data should be filtered to understand the effect of vibration, tool wear and sensory fault.

Realizing the issues in data driven approaches in machining, this chapter addresses them in the following ways:

- There is a long-awaited need of the machining industries to acquire a reliable methodology for data collection that will ultimately create a data bank. The developed data bank can be used by machining industries across the globe. Initially the approach would be to utilize the past machining data present in the literature to develop a data bank called Central Database Repository (CDR) here. In due course of time, with participation of machining industries, the data will increase in the CDR and eventually become *Big Data*.
- In the present study, a new concept of dynamic reliability is introduced, which is related to veracity of data. Dynamic reliability gets updated with each new information. It helps in building a highly reliable data bank as discussed in Section 3.3.2.
- In order to take care of the uncertainties associated with machining operation, a new concept of mini-repository is introduced. Mini-repository keeps all doubtful data. For illustration of this concept, multiple linear regression is adopted for performance prediction (cutting force in turning) in the present study. (Neural network or any other soft computing method can also be used for performance prediction.) The amount of data in the the mini-repository and the deviation from the predicted result jointly determine whether to transfer the data to CDR or not. The detailed description is provided in Section 3.2.
- To eliminate duplicate or nearly similar data in the CDR, a concept based on Cook's distance is being used. Cook's distance ensures to keep only the influential or necessary data points. Cook's distance is described in detail in Section 3.3.1.

3.3 Overall plan of the proposed framework

It has been observed that a lot of machining data is present in the literature, but the same is not being effectively utilized. If the data from various sources are collected and preserved in one place, it can be used for the prediction of machining performance. This work attempts to develop a database repository that would impart extracted knowledge at the shop floor or process planning section and provide suitable instructions.

TH-3282_186103018

A conceptual plan for sharing the data among factories is depicted in Figure 3.1. The proposed CDR placed in a cloud server provides support both for data storage as well as for computing facility. Infrastructure as a Service (IAAS) is a cloud computing model used for accessing various services that include data storage, network and servers. In this case, IAAS provides the computing facility for CDR. The main focus of this work is towards data acquisition, drawing inferences from the data along with a new concept of dynamic reliability attached to inference and updating the database avoiding data-explosion. The value of the data and the associated reliability are the two major aspects of data that are projected in this chapter. The CDR initially contains data obtained from various reliable sources like literature including machining handbooks; with time the volume of data and its (dynamic) reliability keep on changing.

A scheme for data collection and prediction is shown in Figure 3.2. The user enters the process parameters in a computer, which searches the CDR and uses suitable codes to estimate the machining force. Estimation of machining force can be based on regression, neural networks, mechanistic model or any such method or the combination of methods. Section 3.3 describes the application of regression models for estimation of most likely, upper and lower estimates of main cutting force. If the prediction model is not available for the desired tool-work combination, a rough estimate can still be made with the model for a similar tool-work combination. A suitable correction factor can be employed for reducing the model error, based on the shop floor feedback. Any new experimental data-entry is included in the CDR assuming 50% chances of it being accurate. Thus, a reliability of 0.5 is attached to a new data-entry. The assumption of attaching a reliability of 0.5 to a new data-entry is based on a simple probability theory. Whenever any new information arrives, there can be two possibilities: 1) data-entry truly represent the process or 2) data-entry is erroneous. Hence, there must be some basis for either accepting or rejecting a new data-entry.

TH-3282_186103018

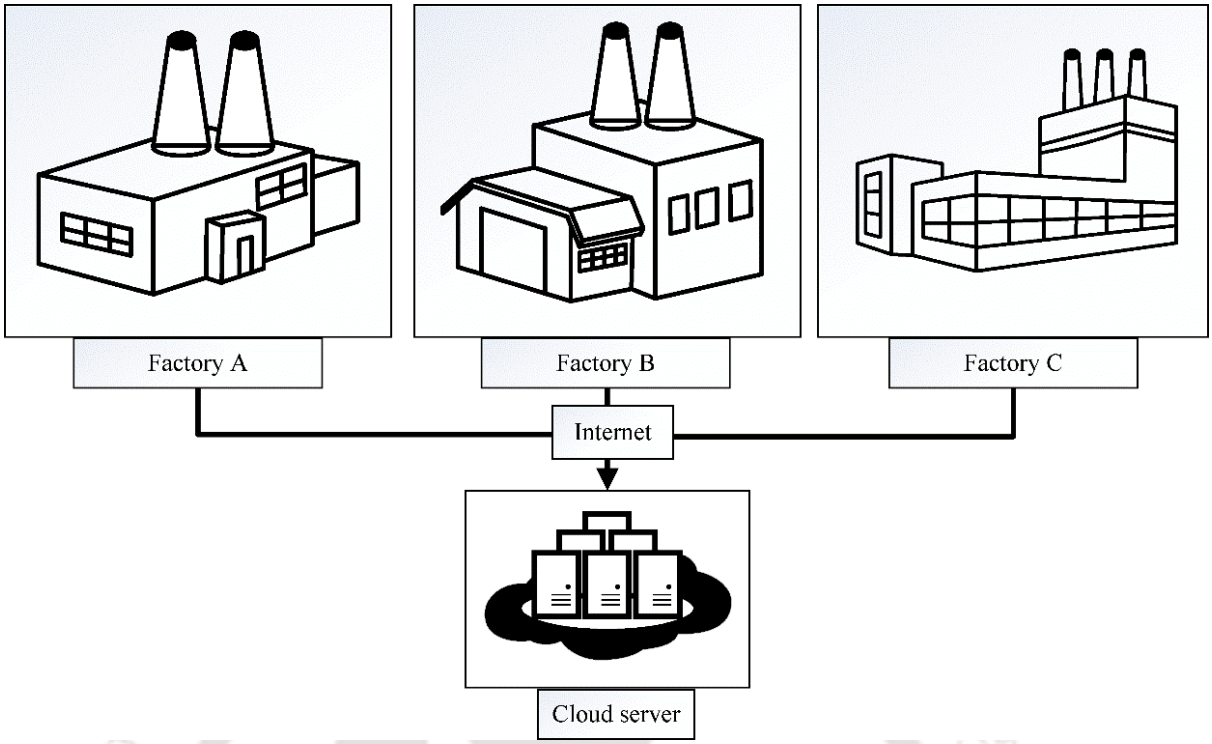

Figure 3.1 Conceptual plan for sharing of data among factories

Considering equal possibility of two events:

$$P(\text{Data is accurate}) = \frac{1}{2};\ P(\text{Data is erroneous}) = \frac{1}{2}. \tag{3.1}$$

Therefore, a new data-entry is stored by assigning a reliability of 0.5. In other words, there is a probability 0.5 of it being correct. Nevertheless, a value other than 0.5 may be assigned if there is any prior information based on the confidence of experts.

Apart from the information about cutting-tool and work-piece material, a variety of information can be collected. Often the information is incomplete. Several articles in the literature predict the cutting force based on only three parameters—cutting speed, feed and depth of cut. However, at times data about vibration and tool wear are also available. Besides, modern adaptive control computer numerical control (CNC) machines can have data from several sensors, e.g., acoustic emission, temperature and spindle motor current. In order to avoid complicacy in description, this chapter focuses on the cases when the domain of input variables comprises only cutting speed, feed and depth of cut. Of course, a brief description is provided for handling and utilizing other types of time-dependent signals. A detailed flowchart for enhancing the machining performance using Big Data Strategy is shown in Figure 3.3 and the corresponding related actions are listed in Table 3.1. The flowchart provides an outline about the proposed strategy in various uncertain

TH-3282_186103018

situations that are explained in detail. This framework can be extended to machining optimization; however, it is not the focus of the present chapter.

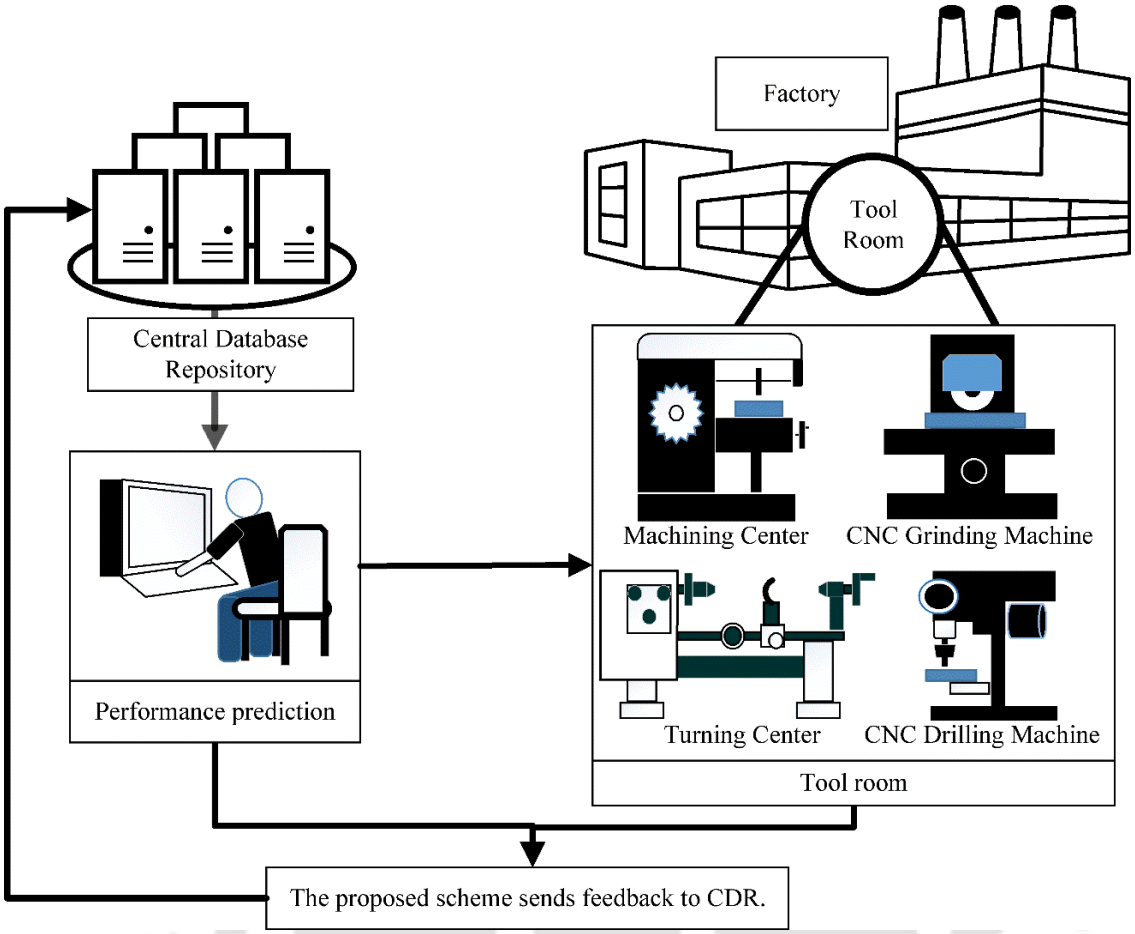

Figure 3.2 Proposed scheme for sending feedback to CDR based on the actual result from the shop floor

3.4 Methodology for data collection when feed, depth of cut and cutting speed are available along with main cutting force

Assume that following information is available about machining process: tool material, workpiece material, presence or absence of lubrication, cutting speed, feed, depth of cut and cutting force. There can be different scenarios, which have to be tackled in different ways. Sometimes the information can be entirely new and at other times, similar information may be available. In the sequel, different cases are discussed.

TH-3282_186103018

CASE 1: Existing cutting tool and workpiece combination

Whenever machining is performed for the existing cutting tool and workpiece combination, i.e., the tool-work combination is already present in the CDR. The process parameters in which machining is taking place are entered and prediction is made. After the actual machining, the feedback from the shop floor can be collected for updating the prediction model. The following are the two possible scenarios:

CASE 1A: The process parameters data lying outside the range of the data in CDR

Whenever the incoming process parameters for the existing cutting tool and workpiece combination are outside the range of data in CDR, extrapolated prediction is carried out. There is a high probability of the predicted value being inaccurate. The percentage error in the estimation depends on the closeness of the incoming process parameter with that of the upper and lower limits of the already preserved process parameters in the database. Prediction of extrapolated data should always be carried out with a caution. Nevertheless, after the completion of the actual machining operation, shop floor feedback can be obtained. The new information is then stored in CDR with a reliability of 0.5.

CASE 1B: The process parameters data lying within the range of the data in CDR

Whenever the incoming process parameters for the existing tool-work combination are within the range of the existing process parameters in CDR, estimation of the cutting force is carried out within 95% confidence interval or any such interval.

In case the feedback of the cutting force from the shop floor is within the estimated range, the decision whether to include the incoming data in the CDR or not is taken based on the Cook's and the Euclidean distances. It is explained in the following sub-section.

3.4.1 Concept of Cook's distance

A significant way to measure the influence of an observation is by using the Cook's distance. Cook's distance considers the residual of the output and the leverage of the point while estimating the level of influence. In other words, Cook's distance combines the value of outlier and leverage for estimating the level of influence. In the present study, the concept of Cook's distance is used with multiple linear regression for illustration only. It can be interpreted as a means to indicate the possible locations where it would be good to have a greater number of data points that can affect the future outcomes.

TH-3282_186103018

Cook's distance can also be used along with other methods such as neural network, mechanistic models or any such methods suitable for performance prediction. The leverage is a part of Cook's distance. The leverage indicates the extremity of the independent variables from the mean value without considering the dependent (output) variable. Cook's distance is given by the following equation (Larose, 2015)

$$D_i = \frac{(y_i - y_{i,p})^2}{(m+1)s^2}\left\{\frac{h_i}{(1-h_i)^2}\right\}, \tag{3.2}$$

where y_i is the actual obtained output for ith observation, $y_{i,p}$ is the corresponding predicted output, m is the number of predictors (three viz., cutting speed, feed and depth of cut, in this case), s is the standard error of the estimate and h_i is the leverage of the ith observation. The leverage is calculated as

$$h_i = \frac{1}{n} + \frac{(\ln V_p - \ln \overline{V})^2}{\sum_{i=1}^{n}\left(\ln V_i - \ln \overline{V}\right)^2} + \frac{(\ln f_p - \ln \overline{f})^2}{\sum_{i=1}^{n}\left(\ln f_i - \ln \overline{f}\right)^2} + \frac{(\ln d_p - \ln \overline{d})^2}{\sum_{i=1}^{n}\left(\ln d_i - \ln \overline{d}\right)^2}. \tag{3.3}$$

A data-entry is considered to be influential only when the value of Cook's distance exceeds one (Larose, 2015). The influential points i.e., the data points having Cook's distance more than one, will be included in CDR with 50% reliability. When the Cook's distance does not exceed one, the nearest data point is searched in the CDR and its reliability is improved. This strategy will help in avoiding data-explosion as it does not store non-influential data.

3.4.2 Concept of dynamic reliability

A methodology for finding the nearest data point is by evaluating Euclidean distance. All the process parameters are assumed to be coordinates in space. For estimating the distance between two data entries, Euclidean distance is evaluated using the following equation:

$$d_{\text{Euclidean}}(x, y) = \sqrt{\sum_{i=1}^{m}\left(x_i - y_i\right)^2}, \tag{3.4}$$

where x and y represent two points each having m attributes. In this case, m is three, corresponding to cutting speed, feed and depth of cut.

TH-3282_186103018

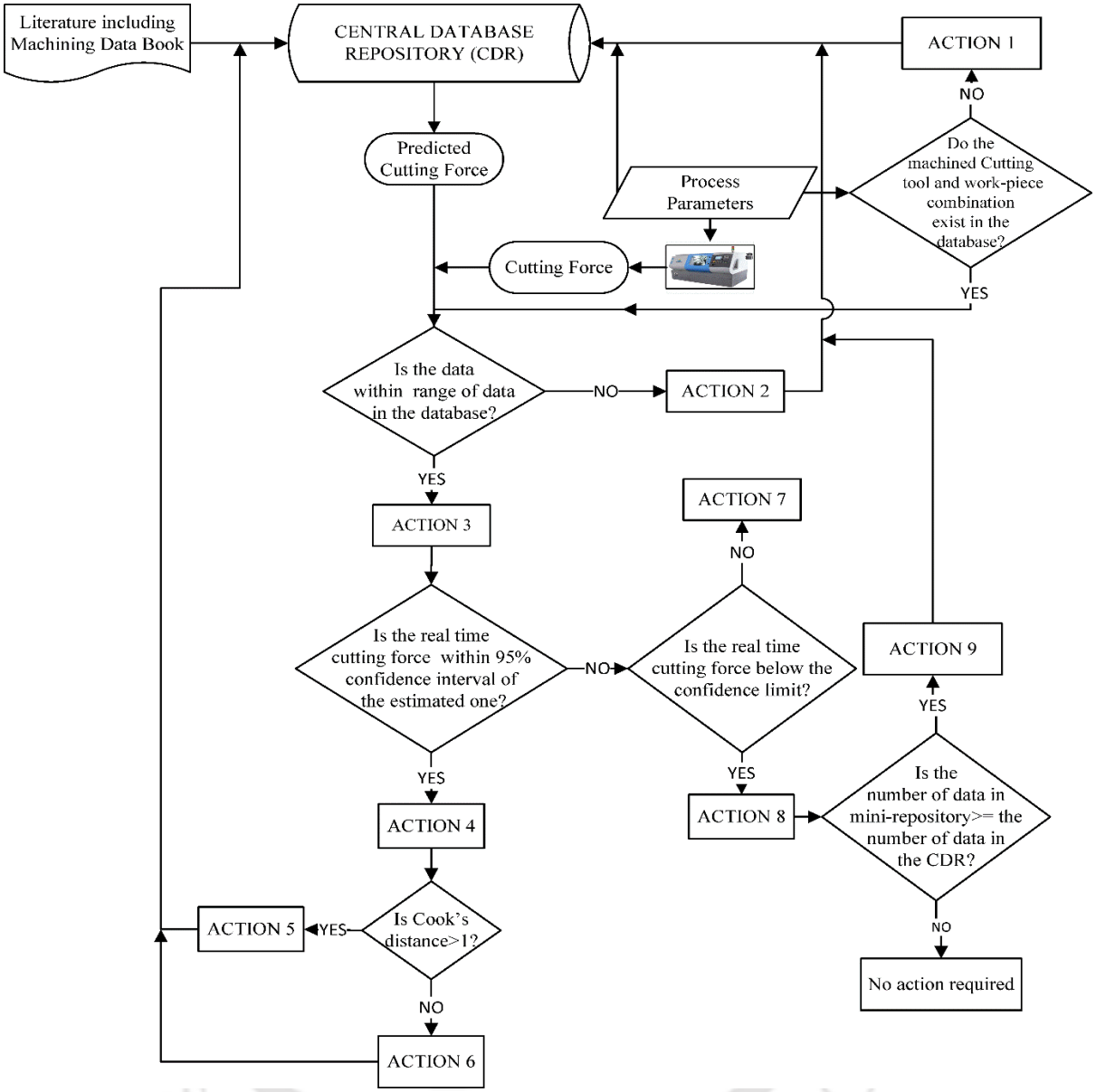

Figure 3.3 Flowchart for enhancing the machining performance using a Big Data strategy

TH-3282_186103018

Table 3.1 List of Actions

Action Number	Task
1	Estimate the cutting force with all the existing models in the database repository and choose the one which is having the least error. Reduce the model error further by updating the estimation with a suitable correction factor and include the information in the prediction module for the new tool-work combination.
2	Extrapolated prediction is carried out with a caveat and the incoming process parameter along with the output details are included in the corresponding module of database repository. Assign a reliability of 0.5 to these data.
3	Extract the output from prediction model from Central Database Repository (CDR).
4	Calculate the Euclidean and Cook's distance.
5	Include the incoming process parameter and output details in the corresponding module of database repository. Assign a reliability of 0.5 to these data.
6	Improve the reliability of the nearest data (based on Euclidean distance) in the database repository.
7	Store the data in separate module for the analysis of tool wear or chatter.
8	Save the data in a mini repository.
9	Merge the data with the data in the CDR pertaining to the same tool-work combination, leaving aside outliers (error above $\mu+2\sigma$ limit). Fit new regression models.

The Euclidean distance from the data-entry is calculated for all the existing data points in CDR. The data point having the minimum Euclidean distance will get its reliability updated. The enhancement of the reliability is done using the following equation based on probability theory:

$$\text{Updated Reliability} = 1-\{(1-\text{reliability of new data})\times(1-\text{current reliability})\}. \quad (3.5)$$

In absence of any other information, a new data can be assigned a reliability of 0.5. In that case, the updated reliability is given by

$$\text{Updated reliability} = 0.5\ (1+\text{current reliability}). \quad (3.6)$$

TH-3282_186103018

As an example, if there is a data-entry already in CDR with a reliability of 0.5 and a similar new data-entry is found, the reliability of the data is updated to 0.75. If the next time another similar data-entry is found, the reliability of the data is updated to 0.875. The reliability value keeps getting updated with more similar data as shown in Figure 3.4. For 7 data, reliability becomes more than 0.99. Thus, the present methodology focuses on building a compact, highly reliable and quality database.

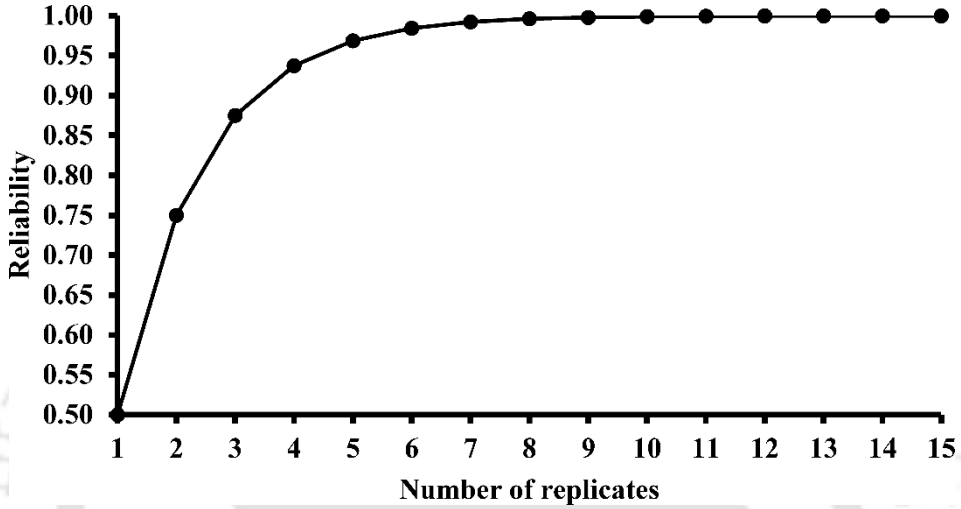

Figure 3.4 Improvement of reliability with number of replicates

3.4.3 Concept of mini-repository

In case the feedback of the cutting force from the shop floor is outside the predicted range, the scheme will look whether the feedback of the cutting force is below the lower limit or above the upper limit. If the cutting force is below the lower limit, the incoming data-entry will be stored in a separate mini-repository. Data in the mini repository will be merged with the data in the CDR, when the number of the data in the mini-repository becomes equal to the number of data kept in the CDR for a particular tool-work combination. It is accomplished in the following way:

If the number of data in mini-repository becomes equal to the number of data in CDR, then the mean value and standard deviation of unsigned error of all the data which are below the lower limit for a particular tool-work combination is evaluated. They are denoted by μ and σ, respectively. All the data that lie above the (μ+2σ) are considered as outliers and are excluded. The data that lie below the value of (μ+2σ) are included and are merged with the main data in the CDR by associating a reliability of 0.5 with the merged data.

TH-3282_186103018

If the feedback of the cutting force from the shop floor lies above the estimated upper limit, the condition of the cutting tool as well as vibration data is verified. One module can be prepared that analyses chatter based on the vibration and other supporting data. If the chatter is detected, the data can be stored in a mini-repository pertaining to machining data with chatter. If there is no chatter, but the tool is old, the data pertaining to tool wear is recorded and information is put in another mini repository. If it is ensured that there is no tool wear or chatter, the data is included in the CDR with 50% chances of the information being accurate.

Mini-repository contains all the data that does not match with the predicted result, thereby taking care of the uncertainties associated with a machining operation (turning for the present case). In fact, separate analysis can be carried out in mini-repository alone to identify the causes of such deviation from the predicted output. This chapter being conceptual in nature, details on analysing wear and chatter signals are omitted.

CASE 2: New cutting tool and workpiece combination

Whenever machining is performed for a new cutting tool and workpiece combination, the estimation of cutting force can be done by utilizing all the existing models inside the CDR. The model which is having the least error based on the feedback obtained from the shop floor can be chosen for further estimation. After the actual machining is carried out, the model can be updated based on the measurement of cutting force. In order to minimize the model error, a suitable correction factor may be estimated as follows:

$$\text{Correction factor} = \frac{\text{Feedback of the cutting force}}{\text{Predicted value}} \tag{3.7}$$

This correction factor is multiplied to any estimated value from the existing similar model. The new information with the incoming data-entry will be included in the CDR for a new cutting tool and workpiece combination with a reliability of 0.5.

3.5 Cutting force estimation with a 95% prediction interval

Cutting force is affected by the presence of tool wear and chatter. Researchers have used acoustic emission sensors, accelerometer, dynamometer, etc., for capturing the time varying signals (Sharma et al., 2008). The time varying signals can be stored and used for modelling of the cutting force equation. In the present chapter, it is assumed that the dependence of cutting force on all the process parameters as linear in a logarithmic scale.

TH-3282_186103018

For example, in order to estimate the cutting force in turning, the following mathematical model can be fitted:

$$F = KV^{\alpha} f^{\beta} d^{\gamma} w^{\delta} t^{\varepsilon} a^{\zeta} C^{\eta}, \tag{3.8}$$

where F is the main cutting force, V is the cutting velocity, f is the feed, d is the depth of cut, w is the height of wear land, t is the time elapsed, a is the acceleration and C is the average ring-down count obtained from an acoustic sensor. The exponents and constant K can be obtained through a multiple regression procedure. Rest of the procedure is similar to that described in Section 3.3. In order not to lose the focus of this chapter, further discussion will pertain to the case when only the information about feed, speed and depth of cut is available along with main cutting force.

3.6 Estimation of cutting force with 95% prediction interval

Cutting force mainly depends on cutting speed, feed and depth of cut. Assuming that sufficient quantity of data is available, in a sufficiently small ranges of process variables, the following mathematical model can be fitted:

$$F = KV^{\alpha} f^{\beta} d^{\gamma}, \tag{3.9}$$

where F is the main cutting force in N, V is the cutting velocity in m/min, f is the feed in mm/rev and d is the depth of cut in mm. The exponents α, β and γ as well as constant K need to be obtained through a multiple regression procedure. It is very difficult to estimate the form of cutting force equation for a wide range of process parameters. However, for a small range of parameters, the dependence of force on the process parameters can be assumed as linear in logarithmic scale. To assess the validity of this assumption, coefficient of determination should be estimated; a high value of coefficient of determination supports the assumption. Similar form of the cutting force equation has been observed in the literature (Ravindra et al., 1993; Axinte et al., 2001). Taking natural logarithm on both sides of Eq. 3.9:

$$\ln F = \ln K + \alpha \ln V + \beta \ln f + \gamma \ln d, \tag{3.10}$$

The linear equation obtained in Eq. 3.10 is used for the multiple-linear regression analysis, which amounts to solving the following unconstrained optimization problem to obtain the best-fit estimate:

TH-3282_186103018

$$\text{Minimize} \sum_{i=1}^{n} \{\ln F_i - (\ln K + \alpha \ln V_i + \beta \ln f_i + \gamma \ln d_i)\}^2, \tag{3.11}$$

where i is a typical data-entry among the total n data entries available for model fitting. Solution of Eq. 11 provides the optimum values of K, α, β and γ. This can be carried out for different cutting tool and work-piece combinations. Knowing the optimum values of K, α, β and γ, Eq. 9 can be used to estimate the main cutting force. However, it is always better to predict an estimate of an interval, in which the cutting force may lie with 95% confidence. The reliability of the all the data are initially assumed to be same. The value of the reliability gets updated in due course. The reliability value can be utilized as a weight factor in least square error and model can be fitted by minimizing the weighted least square error. The following equation is used for obtaining cutting force with 95% prediction interval (Larose, 2015)

$$\text{Cutting force with 95\% prediction interval} = \exp\left\{\ln \hat{F} \pm t(n-4, 5\%)\, s \sqrt{1 + \frac{1}{n} + \frac{(\ln V_p - \ln \bar{V})^2}{\sum_{i=1}^{n}\left(\ln V_i - \ln \bar{V}\right)^2} + \frac{(\ln f_p - \ln \bar{f})^2}{\sum_{i=1}^{n}\left(\ln f_i - \ln \bar{f}\right)^2} + \frac{(\ln d_p - \ln \bar{d})^2}{\sum_{i=1}^{n}\left(\ln d_i - \ln \bar{d}\right)^2}}\right\}, \tag{3.12}$$

where $\hat{F}$ represents the best-fit value of the cutting force for the entered data point, n is the total number of observations used in fitting the model, t (n–4, 5%) is a test statistic obtained from a t-table of two tailed t-test for the degree of freedom of (n–4) and 5% significance level, s is the standard error of the estimate, a bar denotes mean value of a variable, suffix 'i' represents the ith observation and suffix 'p' represents the data-entry for which prediction is being made.

3.7 Case studies

For better illustration of the proposed framework for data collection and prediction based on the stored data, four typical case studies in Section 3.5.1, 3.5.2, 3.5.3 and 3.5.4 are presented. It is assumed that main cutting force information is required for turning by a factory, which has the provision of providing feedback. It implies that the lathe machine is fitted with a force measuring sensor.

3.7.1 Data collection for existing cutting tool and work-piece combination

It is assumed that Factory A is accessing the CDR and it wants to machine S55C high carbon steel with a sintered carbide tool (Lin et al., 2001). It is found that the desired

TH-3282_186103018

cutting tool and workpiece combination is present in the CDR that is initially having 27 observations. All the data are having 50% chances of being accurate. Hence, all the data are having a reliability of 0.5. Prediction of cutting force is carried out using 'R', an open source statistical programming language. On executing the multiple-regression analysis, it loads the data file from the CDR in the 'R' environment to form a data-frame using the 'readr' library package. The two-dimensional table containing the information about the machining process is referred to as data frame in 'R'. Thereafter, the value of the process parameters i.e., cutting speed, feed and depth of cut are entered. On entering the details, there are two possibilities: i) The process parameters are within the range of data in CDR and ii) The process parameters are outside the range of data in CDR. In this case, the entered process parameters are within range. Let the cutting velocity, feed, depth of cut for the machined surface be 200 m/min, 0.30 mm/rev and 0.80 mm, respectively. Table 3.2 shows the range of values of cutting speed, feed and depth of cut that is stored in the database for sintered carbide and S55C high carbon steel.

Table 3.2 Initial range of values for sintered carbide and S55C high carbon steel

	V (m/min)	f (mm/rev)	d (mm)
MAXIMUM VALUE	202.6	0.32	1.25
MINIMUM VALUE	86.1	0.08	0.35

The value of coefficient of determination (R^2) in regression analysis depicts the fit of the model while considering all the factors. R^2 lies in between 0 and 1. The value of R^2 obtained for this case is 0.994, depicting a good fit. The result obtained with reference to terminology used in Eq. 3.10 is

$$\ln K = 7.82367,\ \alpha = -0.07280,\ \beta = 0.58656,\ \gamma = 0.74095, \tag{3.13}$$

$$\ln F = 7.82367 - 0.07280 \ln V + 0.58656 \ln f + 0.74095 \ln d. \tag{3.14}$$

The desired multiple-regression model obtained using Eq. 3.9 is

$$F = 2499.06(V)^{-0.07280}(f)^{0.58656}(d)^{0.74095}. \tag{3.15}$$

TH-3282_186103018

The best fit value predicted using Eq. 3.15 is 711 N. The lower limit and upper limit values of the cutting force predicted using Eq. 3.12 are 646 N and 782 N, respectively.

Feedback of cutting force is obtained during machining. Suppose that a value of 700 N is obtained, which is within the predicted interval limits. The next step is to find the level of influence that the entering observation has over the regression model. It is evaluated using the Cook's distance. Before evaluating Cook's distance in 'R', the columns containing information about the cutting speed, feed, depth of cut and cutting force are extracted from the data frame using the 'subset' function. The resulting two-dimensional table is then combined with the data-entry including the actual feedback about the cutting force. This leads to the formation of total 28 data points from the existing value of 27. On using 'cooks.distance' function in 'R', the Cook's distance of the data-entry is calculated. Out of the 28 numeric values obtained for this case, the last value is the Cook's distance for the entering data point. The Cook's distance comes out to be 0.00019, which is much less than one. Hence the entering observation is not influential. It is excluded from entering CDR, instead the reliability of the nearest data point is improved based on the Euclidean distance.

From the data frame in 'R' containing the machining information obtained from CDR, the columns containing the information about cutting speed, feed and depth of cut are extracted using the 'subset' function. The extracted information from the data frame is combined with the data-entry to from a data frame of 28 rows and 3 columns. Euclidean distance is then calculated by using the 'distance' function in 'R', resulting in a 28×28 matrix. The minimum value is found to be for the 6th observation. Therefore, the reliability of the sixth observation is improved to 0.75 using Eq. 6 and saved in the CDR. The updated number of the data for machining of S55C high carbon steel with sintered carbide tool is still 27. However, the reliability of the sixth observation gets updated.

3.7.2 Data collection for existing cutting tool and work-piece combination with any of the process parameters laying outside the range of data in CDR

In this case it is assumed that Factory B is accessing CDR and it also wants to machine S55C high carbon steel with sintered carbide tool. The user enters the cutting velocity, feed, depth of cut for the machined work-piece as 300 m/min, 0.30 mm/rev and 0.80 mm, respectively. It can be seen from Table 3.2 that the value of the cutting speed entered by the user lies outside the range of data in CDR. This indicates the data-entry is

TH-3282_186103018

outside the range. Hence, the extrapolated results are shown with a warning that the entered process parameters are outside the limits. Suppose the feedback of the cutting force is 680 N. This new information is included in the CDR with a reliability of 0.5 for later use. The updated number of data for machining of S55C high carbon steel with sintered carbide tool increases by one.

3.7.3 Data collection for existing cutting tool and workpiece combination, the process parameters lying within the range of data in CDR with the feedback of the cutting force below the acceptable interval limit

Suppose Factory C is accessing CDR and it also wants to machine S55C high carbon steel with sintered carbide tool, similar to Factory A and Factory B. On executing the multiple-regression model from the CDR, the user enters cutting speed, feed and depth of cut as 200 m/min, 0.30 mm/rev and 0.80 mm, respectively (as in Section 3.5.1). Therefore, the process parameters are well within range of data in CDR as is seen from Table 3.2. This time the feedback of the cutting force obtained is 600 N. However, the estimated lower and upper bound of the cutting force is 646 N and 782 N, respectively. As the actual cutting force is less than the lower limit, the new data-entry is stored in a separate mini-repository. In this case, the new data entry is not merged with the preserved data in CDR, rather it is stored in the mini-repository.

3.7.4 Data collection for new cutting tool and work-piece combination

Suppose Factory D wants to machine S45C steel bar with tungsten carbide tool (Lee and Tarng, 2000). It could not find this tool-work in CDR. The existing models present in the library are used for the prediction of the cutting force based on the input process parameters provided during machining. In this example, let the user enters cutting speed, feed and depth of cut as 135 m/min, 0.08 mm/rev and 0.6 mm, respectively. Let the feedback of the cutting force obtained from the shop floor be 263 N. All the models are utilized for finding the cutting force. The results are saved in a data frame. The one having the least error is selected for further estimation. Assuming the minimum absolute error comes out in case when the cutting tool is sintered carbide and work piece is S55C high carbon steel. The value predicted on substituting the entered process parameter in Eq. 3.15 is 272 N. The feedback of the cutting force obtained while machining is 263 N. Hence, an absolute error of 9 N is obtained. In order to reduce the error further, a suitable correction is found:

TH-3282_186103018

$$\text{Correction factor} = \frac{\text{Feedback of the cutting force}}{\text{Predicted value}} = \frac{263}{272} = 0.967. \qquad (3.16)$$

The inclusion of correction factor reduces the mean absolute error in predicting the cutting force. Thus, updated Eq. 3.15 along with the correction factor is used for further prediction of cutting force in case of tungsten carbide and S45C steel bar. All the new data are collected in the CDR for this cutting-tool and workpiece combination. This new data will, of course, get updated with sufficient number of trials on the shop floor.

The aforesaid procedure for estimating the cutting force using regression methodology is illustrative only. There can be several other methods for the estimation of cutting force. The main objective of this research work is to conceptually demonstrate a procedure of collecting data and building a highly reliable data bank which is termed as Central Database Repository (CDR) in this case. The challenge is not only to prepare a reliable database for a manufacturing environment that can be easily accessed via the internet, but also to protect it from hackers and malicious users who can manipulate the data stored in the cloud. Therefore, data confidentiality, integrity and availability become an integral part of the proposed CDR. Service provider for CDR need to ensure that there is at least a tested encryption scheme to protect the data. Preventing unauthorised access and periodic data backup are the other necessities. Researchers are thoroughly carrying out research to improve the level of encryption and to provide enhanced security and privacy to the data stored on a cloud-based platform (Namasudra, 2019; Sun, 2019). However, this is not the focus of present work; implementation of data security and privacy in the context of the proposed framework is left as a future task.

Most importantly the present work focuses on the usage of Cook's distance to evaluate the level of influence and for keeping only the important and influential data rather than keeping all the non-influential data. A novel feature of the proposed framework is the usage of the dynamic reliability, which keeps on updating with the available information.

3.8 Conclusion

With the advent of Industry 4.0 and increasing emphasis on using data analytics for distributed manufacturing, it is high time to explore the use of past data in enhancing machining performance. The proposed framework provides a systematic guidance for data collection and building a highly reliable and compact data bank for manufacturing industries. CDR supplies on demand data to any factory located within the reach of internet.

TH-3282_186103018

There is a provision to properly update the information present in CDR. The information stored in the data bank can be used for performance prediction that would help in reducing the unnecessary downtime. This is illustrated for an example of cutting force estimation for turning operation. For ease of illustration, a multiple-linear regression is used for the estimation of main cutting force within 95% prediction interval. In practice, a neural network, fuzzy set based or any other prediction model can also be used.

The purpose of this chapter is to project the novel idea of CDR, mini-repository and dynamic reliability. The dynamic reliability can also be used as a weight factor for minimizing the weighted least square error in multiple linear regression. Cook's distance has also been used as a parameter for measuring the level of influence that can be used for filtering out the non-influential data. In other words, the proposed framework illustrates the application of using data analytics in manufacturing conceptually. Hence, deliberately a small size of data has been used and necessary calculations are done using R, an open source statistical software. It is envisaged that future machine tools will be part of cyber-physical system and collection of data by cloud will not be a difficult task.

This chapter proposes the concept required for building a highly reliable databank keeping data explosion in mind for the manufacturing industries. The scope can be expanded towards including other machining processes such as milling, drilling and grinding. For better accuracy in the estimation of machining performance, one can also explore the use of support vector regression, classification & regression tree algorithm and neural network within the proposed framework.

TH-3282_186103018

TH-3282_186103018

Chapter 4
Efficient Storage and Utilization of the Captured Data: An example of Surface Roughness Estimation in Turning

4.1 Introduction

In modern day manufacturing, the ability to effectively preserve and utilize the captured data has become increasingly important. With the advancement in the sensing technologies and database management systems, manufacturing processes generate a huge amount of data that has the potential to provide valuable insights for process optimization and quality improvement. However, the challenge lies in effectively managing and extracting meaningful information from this captured data. This chapter focuses on the efficient storage and utilization of captured data, taking surface roughness estimation in turning processes as an example.

Surface roughness is a critical parameter in machining operations, as it directly influences the functional and aesthetic properties of machined components. There is also a significant pressure to control the surface roughness during machining operation (Silberschmidt et al., 2014; de Paiva et al., 2017). Traditionally, surface roughness measurements were carried out using tactile methods that involve physical contact with the workpiece. However, these methods were time-consuming, subjective, and may cause damage to delicate surfaces. In recent years, non-contact measurement techniques, such as optical profilometry and laser scanning, have emerged as viable alternatives. These techniques enable the capture of detailed surface information without physically contacting the workpiece, providing an opportunity to collect large amounts of data for surface roughness estimation.

There is a significant advantage of using the non-contact measurement in terms of data collection, the management and utilization of the captured data pose a serious challenge. The high volume of data makes it difficult to preserve, process and extract meaningful information effectively. Therefore, there is a need to develop efficient methods for storing and utilizing captured data to estimate surface roughness in turning processes.

TH-3282_186103018

Recent literature on machining indicated the use of Gaussian process regression (GPR), random forest, regression trees, support vector regression (SVR) and deep learning in machining. Evaluating surface roughness using GPR in an end milling operation was carried out by Zhang et al. (2014). The authors felt the need for improving the prediction accuracy by taking more sensor data, particularly vibration signals. Research is now focussed on integrating analytical and data-driven models to enhance the accuracy of prediction. On a similar note, Misaka et al. (2020) integrated data-driven prediction models such as regression and neural network, and combined it with an analytical approach for surface roughness prediction in a CNC turning operation. Yu and Liu (2020) modified the existing deep neural network (DNN) for surface roughness prediction in a CNC vertical machining centre. The authors integrated symbol rules and classification rules with the DNN to enhance the actual performance.

Techniques such as GPR and SVR tries to fit a function on the training dataset. This makes both the techniques difficult to be represented by fixed set of parameters. Every time a new data arrives, the set of parameters used to define the model also varies (Dutta et al., 2016; Lu et al., 2020). Thus, whenever any new prediction is made, such techniques requires all the past machining data. Including all the past data every time for prediction makes the process computationally expensive and time-consuming. In neural network models, the researchers need to ensure proper optimization of the weight function to avoid overfitting. In the least square regression models, it becomes difficult to fit a particular curve for a big data set.

This chapter attempts to build a robust methodology that can be applied in all circumstances. The fundamental concept is that if the whole region is divided into several cells, it will be easier to fit a function of simpler form for each cell and the procedure can be standardized. Also, after proper fitting, only the essential parameters of the model need to be stored instead of preserving the whole raw data; this will avoid data explosion. Removal of outliers and updating the model are also part of the proposed methodology. The proposed method also predicts the lower and upper estimates of surface roughness. It is to be mentioned that barring Kohli and Dixit (2005) and Sonar et al. (2006), researchers have not paid attention to predicting the lower and upper estimates of surface roughness and only concentrated on the most likely estimate. Considering the statistical nature of the problem, it is necessary to carry out interval estimation, which is the essential feature of the proposed method in this work. The proposed methodology builds upon the framework

TH-3282_186103018

suggested for predicting cutting force in turning as presented in Chapter 3; the prime focus of the framework work was on the acquisition of veracious data. The present chapter concentrates on efficient storage and prediction. The rest of the chapter is organized as follows. Section 4.2 describes the overall plan of the proposed methodology. Section 4.3 presents the data collection module. The surface roughness prediction and data updation procedure to be adopted is described in Section 4.4. Typical case studies are shown in Section 4.5. Section 4.6 concludes the chapter.

4.2 Basic features of the proposed methodology

The proposed methodology is divided into two major modules. One module is for data collection and the other module is for surface roughness prediction with model updating. Data collection module involves collecting data from various sources that include data measured from multiple sensors attached to a machine, data obtained from various analytical, numerical or mechanistic models and data gathered from the simulation of a machining process. All such hybrid data can be kept in a cloud-based repository. Industries can access such data using internet for prediction purposes. The existing range of data is divided into three major levels categorised as high, medium and low to represent as cells. Multiple-linear regression is used for model fitting in each cell. As the ranges of parameters in a small cell are narrow, multiple linear regression can provide a sufficiently accurate prediction. Coefficient of determination and in-process variations are considered for assessing the quality of the fit and to decide whether to further divide the existing cell. Only the parameters of the multiple linear regression model that are used for estimating the most likely, upper and lower estimate with 95% confidence are kept in the cloud data base pertaining to a specific cell and the raw data is erased from the memory. Parameters are stored with a dynamic reliability of 50% chance of it being accurate. Raw data is preserved only when the number of data pertaining to a cell is insufficient to fit the multiple-linear regression model.

The surface roughness prediction module carries out the prediction of surface roughness as well as model updating. Feedback is sent from the shop floor every time machining is carried out. Based on the process parameters, the specific cell for surface roughness estimation is identified. If the cell has insufficient data to fit the multiple regression model, the nearest neighbour estimate is used for the estimation of the most likely estimate till sufficient data is available in that cell for model fitting. The model parameters for the estimation of most likely, upper and lower estimate are then stored

TH-3282_186103018

specific to that cell. If the cell has sufficient data, surface roughness prediction is carried out with 95% confidence. When the actual surface roughness observed from the factory floor lies exterior to the interval estimates, the data is preserved in an isolated repository suspecting any process abnormality such as chatter and tool wear. When it is ensured that the process is stable and the repository contains sufficient amount of such data, the data is merged in the main repository keeping aside outliers. When the actual surface roughness obtained from the shop floor falls within the interval estimate, only the influential raw data are stored in the cloud assuming 50% chance of it being accurate. The level of influence is evaluated with the help of Cook's distance, as discussed in (Larose, 2015). A Cook's distance of greater than one indicates an influential observation. A non-influential data entry is not preserved instead when the number of such non-influential data reaches an optimum level, the dynamic reliability of the model parameters is improved. An influential observation is requested to preserve. Additionally, Euclidean distance is used for eliminating almost duplicate data. In lieu of storing almost duplicate data, the corresponding dynamic reliability of the data is enhanced; any new and distinct raw data is kept having a dynamic reliability of 0.5. When the number of raw data again reaches an optimum number, weighted multiple linear regression is carried out by considering the dynamic reliability as a weight factor. A new set of parameters are obtained from the weighted multiple linear regression analysis. The model parameters are updated by taking the weighted average of the new and the already existing model parameters with dynamic reliability acting as a weight. The updated parameters are again preserved in the cloud pertaining to a specific cell and the raw data are erased. This process continues and the model keeps updating itself with the availability of new and reliable data.

The basic outline of the proposed methodology is depicted in Figure 4.1. It is composed of two modules— 1. data collection and 2. prediction and model updating. Hybrid data are collected from various sources on a cloud-based platform. The stored data is further accessed by a factory via the internet for surface roughness prediction and a feedback is sent from the shop floor. The existing model is updated based on this feedback. The detailed procedure of data collection and surface roughness prediction with interval estimates are explained in detail in the subsequent sections.

TH-3282_186103018

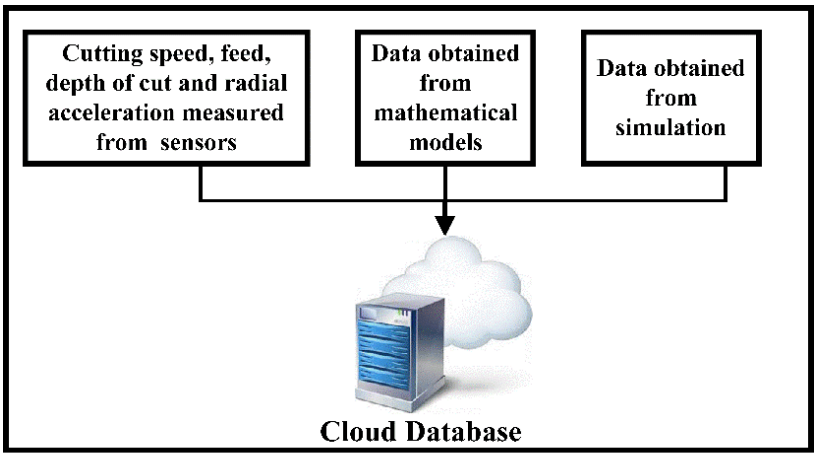

a. Data collection module

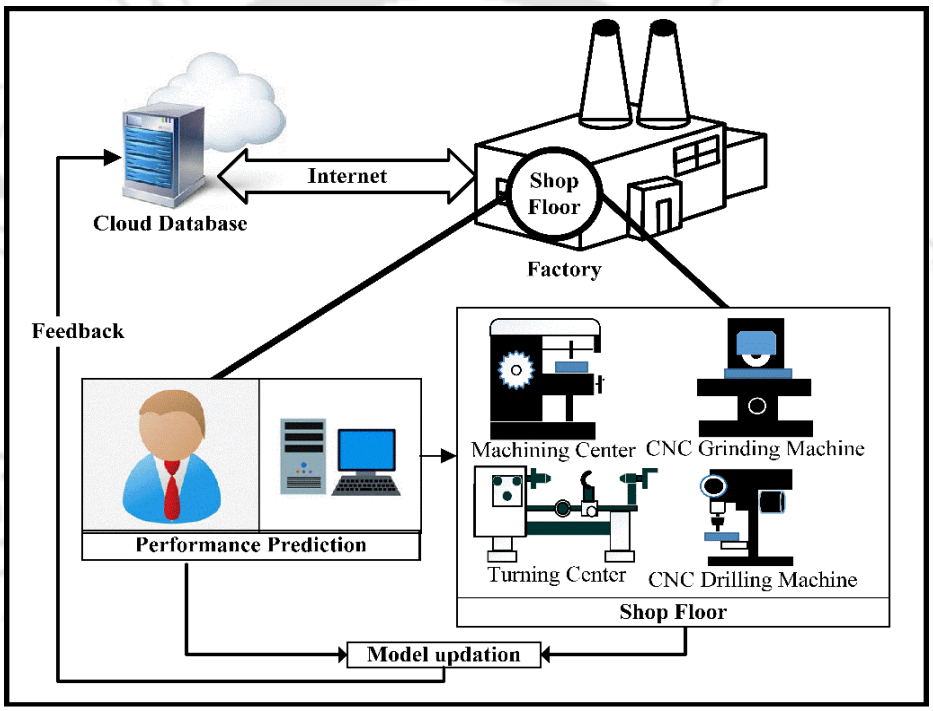

b. Surface roughness prediction and data updation module

Figure 4.1 The proposed structure: a. data collection module, b. surface roughness prediction and data updating module

4.3 Data collection procedure

The data collection module involves collecting data from various reliable sources that include data measured from various sensors attached to a machine, data obtained from various analytical, numerical or mechanistic models and data obtained from simulation of a machining process. The hybrid data that are collected are initially stored on a cloud-based repository named as central database repository (CDR) as discussed in Chapter 3. It is assumed that tool material, workpiece material, cutting speed, feed, depth of cut and radial

TH-3282_186103018

acceleration are known for surface roughness estimation in turning. For the present case, cutting speed, feed and depth of cut are the controllable parameters, and radial acceleration is the uncontrollable parameter. There are possibilities of having different scenarios, that are to be addressed in suitable ways.

A detailed flowchart for the data collection module is shown in Figure 4.2. The flowchart offers a glimpse of the proposed methodology. The data collection module can be extended to any machining processes such as turning, milling, drilling or grinding. However, the present chapter restricts turning operations only. In the proposed method, the feasible range of process parameters for surface roughness estimation in turning, namely cutting speed, feed, depth of cut and radial acceleration for a specific tool-work combination, is divided into three equal intervals. There are four input parameters that are divided into three equal intervals of high, medium and low level, thereby creating four-dimensional hypercube. However, it becomes difficult to visualize a four-dimensional cube. For the sake of better visualization, three cubes are considered with each cube representing a particular level of the fourth parameter. For the present case, radial acceleration is assumed as the fourth parameter. Each cube is further divided into cells as shown in Figure 4.3.

TH-3282_186103018

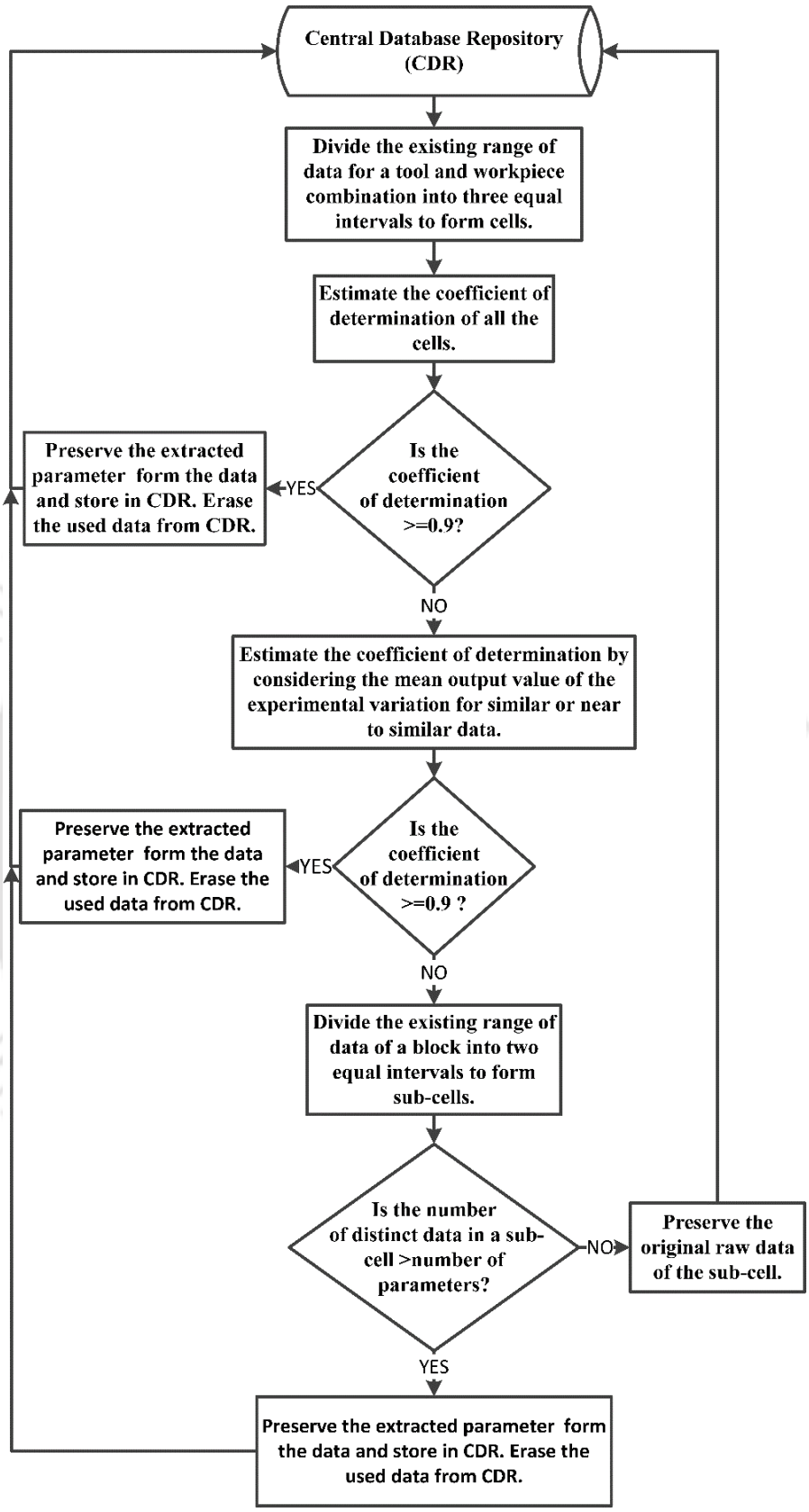

Figure 4.2 Flowchart for data collection module

TH-3282_186103018

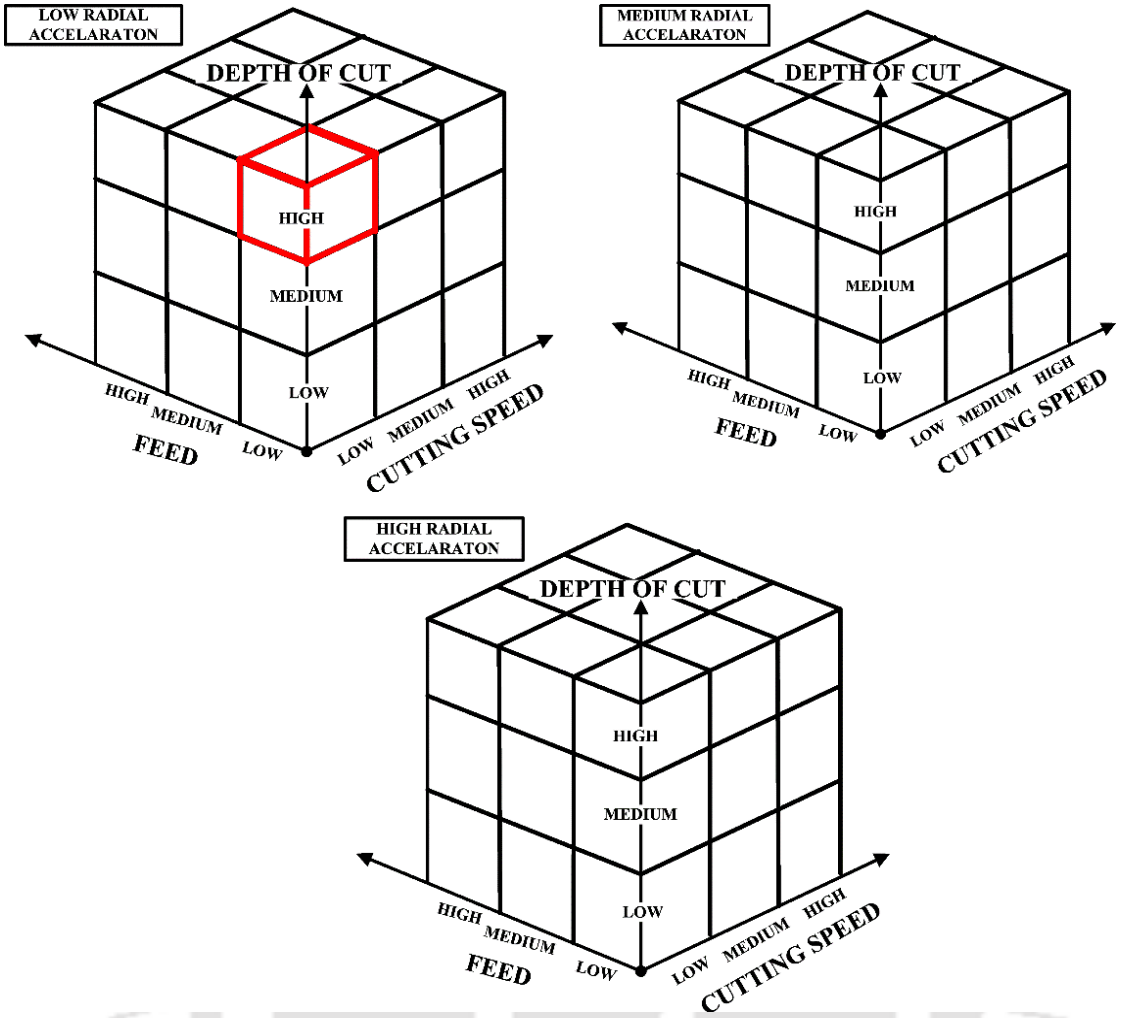

Figure 4.3 Three cubes showing four input process parameters divided into three equal intervals

The highlighted cell in Figure 4.3, represents a low cutting speed, low feed, high depth of cut and low radial acceleration. Each cell is modelled using multiple linear regression. As the ranges of process variables are significantly small, a piecewise linear or continuous model can be assumed. Model fitting is carried out using the following equation:

$$R_a = KV^{\alpha} f^{\beta} d^{\gamma} a^{\delta}, \tag{4.1}$$

where R_a is the surface roughness in μm, V is the cutting velocity in m/min, f is the feed in mm/rev, d is the depth of cut in mm and a is the radial acceleration in m/s^2. The exponents α, β, γ and δ as well as constant K are acquired by multiple regression analysis. Taking natural logarithm on both sides of Eq. 4.1:

$$\ln R_a = \ln K + \alpha \ln V + \beta \ln f + \gamma \ln d + \delta \ln a, \tag{4.2}$$

TH-3282_186103018

The following unconstrained optimization problem that is obtained from Eq. 4.2 is further evaluated to get the optimal-fit:

$$\text{Minimize} \sum_{i=1}^{n} \{\ln R_{ai} - (\ln K + \alpha \ln V_i + \beta \ln f_i + \gamma \ln d_i + \delta \ln a_i)\}^2, \tag{4.3}$$

where *i* is a usual data entry among *n* data entries accessible for model fitting in a particular cell.

In the present work, the optimal values of *K*, α, β, γ and δ are substituted in Eq. 4.1 to get the most likely estimate of surface roughness. The raw data that are already used for modelling for a specific cell are then erased. Besides *K*, α, β, γ and δ, there are other values that are required for estimating the lower and upper interval estimates for any new data. Surface roughness with 95% prediction interval is obtained using the following equation (Larose, 2015):

$$R_{a\text{pred}} = \exp\left(\ln \hat{R}_a \pm t(n-5, 5\%)\, s \sqrt{1 + \frac{1}{n} + \frac{(\ln V_p - \ln \bar{V})^2}{\sum_{i=1}^{n} \left(\ln V_i - \ln \bar{V}\right)^2} + \frac{(\ln f_p - \ln \bar{f})^2}{\sum_{i=1}^{n} \left(\ln f_i - \ln \bar{f}\right)^2} + \frac{(\ln d_p - \ln \bar{d})^2}{\sum_{i=1}^{n} \left(\ln d_i - \ln \bar{d}\right)^2} + \frac{(\ln a_p - \ln \bar{a})^2}{\sum_{i=1}^{n} \left(\ln a_i - \ln \bar{a}\right)^2}} \right), \tag{4.4}$$

where $R_{a\text{pred}}$ represents surface roughness with 95% prediction interval, $\hat{R}_a$ represents the most likely value of the surface roughness, *n* is the number of observations used for model fitting, *t*(*n*–5, 5%) is a test statistic obtained from a t-table of two tailed *t*-test for the degree of freedom of (*n*–5) respectively with 5% significance level, *s* is the standard error of the estimate, a bar indicates mean value of a variable, suffix '*i*' shows the i^{th} observation and suffix '*p*' shows the data-entry for which prediction is carried out. In order to evaluate the surface roughness with 95% prediction interval for a new data entry, a set of parameters are preserved. In case of four input process parameters, say for surface roughness estimation in this case, the 15 parameters shown in Table 4.1 are stored in each of the cells. *K*, α, β, γ and δ are preserved with a reliability of 0.5. These 15 values are collected for each cell instead of the large amount of past machining data for surface roughness. Thereby avoiding data explosion. If the number of raw data in any of the cell is insufficient to fit the multiple-regression model, the original raw data is preserved in the cell, as it is not possible to fit the model shown in Eq. 4.1. In due course when new and reliable data is allocated to such cell, Eq.4.1 is then used to model such cells having less data that is explained in Section 4.4.

TH-3282_186103018

The coefficient of determination is often used for judging the quality-of-fit of any model. For the present work, the coefficient of determination is evaluated for Eq. 4.2. A value closer to 1 indicates good fit. In case of regression models, coefficient of determination is largely affected by the choice of the input parameter values and the variations in the output parameters that are observed at each input parameter setting in case of replicated experiments (Cornell and Berger, 1987). In most of the cases, an output parameter follows Gaussian distribution. The present work does consider statistical variation in surface roughness while deciding if the coefficient of determination of the fit is satisfactory or not. Following decisions are taken depending on the situation.

CASE 1. Coefficient of determination greater than or equal to 0.9 for all the cells considering experimental variation: Preserve all the parameters shown in Table 4.1 in the CDR. Erase the used raw data from the memory. Assign a reliability of 0.5 to the regression coefficients and regression constant.

CASE 2. Coefficient of determination less than 0.9 for all the cells considering experimental variation: The variation within the dataset is further analysed. Researchers have observed that too much variation in the output for an input parameter setting, significantly lowers the value of the coefficient of determination (Cornell and Berger, 1987). A better way to judge the level of influence the statistical variation has on the existing dataset is to evaluate the mean value of the observed change in the output in case of replicated experiments.

In this chapter, the four input process parameters, viz., cutting speed, feed, depth of cut and radial acceleration, are assumed as coordinates in space. They can be written in the form of a vector. The method of normalization is adopted for finding similar or near to similar input process parameters for replicated experiments. For the purpose of identifying similar data entries, a data entry is identified to be fixed that is called as a fixed vector and all other data that are compared with respect to the fixed vector are called as variable vectors. To make it clearer, let there be '*n*' number of data collected from the shop floor. In that case the first data is considered as a fixed vector and the second data is considered as a variable vector. The fixed vector is compared with the variable vector. If similarity in the data is observed, the variable vector is not considered for model building and the output of the fixed vector is taken as the average output of the two vectors. After that the fixed vector is compared with the third data. If similarity is again observed, the variable vector is again ignored from model building. Now the output of the fixed vector becomes the

TH-3282_186103018

average output of three data. Thus, finally the mean value of the output of all the similar data is considered. Keeping aside the fixed vector, the rest of the similar data are disabled and not considered for model building. When similarity in the data is not observed, all such data are used for model building. The fixed vector and variable vector are represented by the following equations:

$$\text{Fixed Vector} = [V, f, d, a]^{T} \tag{4.5}$$

$$\text{Variable Vector} = [V_i, f_i, d_i, a_i]^{T} \tag{4.6}$$

where suffix 'i' represents the i^{th} variable vector. The process of normalization is adopted for evaluating the similarity between the fixed and the variable vector. The normalized value of the difference of the fixed vector and the variable vector is evaluated. If the evaluated value is less than or equal to ten percent of the normalized value of the fixed vector, the compared vector is then assumed to be similar or near to similar to the fixed vector. There can be two possible scenarios:

CASE 2A. Coefficient of determination of the cell is greater than or equal to 0.9 considering the mean output value of the replicated experiments: Fit the model using all the similar data that are temporarily ignored. Preserve all the obtained parameters shown in Table 4.1 for the allocated cell in CDR. Erase the used raw data from the memory. Assign a reliability of 0.5 to the regression coefficient and regression constant.

CASE 2B. Coefficient of determination of the cell is less than 0.9 considering the mean output value of the replicated experiments: Whenever the coefficient of determination is found to be less than 0.9, such cell is further divided into smaller cells for better model fitting using Eq. 4.1. The existing range is now divided into two equal ranges creating 16 sub-cells for four input process parameters. Model fitting is carried out and the value of coefficient of determination is evaluated. However, model fitting is possible only when there are sufficient data. There can be further two possible scenarios:

CASE 2B-I. Number of data are sufficient in the sub-cell to fit the multiple-linear regression model: Preserve all the parameters shown in Table 4.1 for the allocated sub-cell in CDR. Erase the used raw data from the memory. Assign a reliability of 0.5 to the regression coefficient and regression constant.

TH-3282_186103018

CASE 2B-II. Number of data are insufficient in the sub-cell to fit the multiple-linear regression model: Preserve the raw data allocated to such sub-cell. The nearest neighbour approach is adopted for evaluating the most likely estimate in case of cell having insufficient data that is explained further in Section 4.4. All the parameters pertaining to a specific cell are updated in the CDR.

Table 4.1 Necessary parameters to be preserved for surface roughness estimation

Sl. No.	Parameters	Significance
1	$\sum_{i=1}^{n}\left(\ln V_i - \ln \overline{V}\right)^2$	spread of the data
2	$\sum_{i=1}^{n}\left(\ln f_i - \ln \overline{f}\right)^2$	spread of the data
3	$\sum_{i=1}^{n}\left(\ln d_i - \ln \overline{d}\right)^2$	spread of the data
4	$\sum_{i=1}^{n}\left(\ln a_i - \ln \overline{a}\right)^2$	spread of the data
5	n	number of observations
6	$\ln \overline{V}$	mean value of the data
7	$\ln \overline{f}$	mean value of the data
8	$\ln \overline{d}$	mean value of the data
9	$\ln \overline{a}$	mean value of the data
10	$\sum_{i=1}^{n}\left(\ln R_{ai} - \ln \hat{R}_{ai}\right)^2$	sum of square of error
11	K	regression constant
12	α	regression exponent
13	β	regression exponent
14	γ	regression exponent
15	δ	regression exponent

4.4 Surface roughness prediction and data updating module

The surface roughness prediction module carries out prediction of the most likely, upper and lower estimate of the surface roughness. This module also updates the data in the cloud database. A detailed flowchart of the prediction and data updating module is depicted in Figure 4.4. The flowchart offers a glimpse of the proposed methodology. On the basis of input process parameters, a specific cell or sub-cell is identified. When the actual machining on the shop floor is completed, feedback is acquired for further estimation. The following are the major possibilities:

TH-3282_186103018

4.4.1 Insufficient number of data for model fitting

Due to insufficient data, multiple-linear regression model is difficult to fit. The raw data that are preserved in the cell are used for estimating the most likely estimate using the *k*-nearest neighbour approach. It is achieved using the following equation (Larose, 2015):

$$\hat{y}_{new} = \frac{\sum_{i=1}^{n} w_i y_i}{\sum_{i=1}^{n} w_i}. \tag{4.7}$$

where y_i represents the actual output of the existing observations, n is number of observations in the cell for model fitting, suffix 'i' indicates the ith observation out of n observations in the cell, w_i is the squared reciprocal of the Euclidean distance between the new data entry with the existing observation. The following equation is used for calculating the Euclidean distance:

$$d_{\text{Euclidean}}(x, y) = \sqrt{\sum_{i=1}^{m} (x_i - y_i)^2}, \tag{4.8}$$

where x and y represent two points with m attributes. In this case, m is four, corresponding to cutting speed, feed, depth of cut and radial acceleration. The upper and the lower estimate of the surface roughness is estimated by the following equation:

$$R_{a\text{interval}} = \hat{y}_{new} \pm (\sigma + \mu) \tag{4.9}$$

where $\hat{y}_{new}$ is the predicted surface roughness, σ is the standard deviation of the unsigned error of all the data and μ is the mean of the unsigned error of all the data. When there is only one observation in the cell, it is difficult to model using Eq. 4.7. In such a case, Euclidean distance is used to estimate the nearest data point from the surrounding cells. The existing and the nearest data points are then used to evaluate the most likely estimate. When sufficient quantities of data are assigned to such cell, model fitting is carried out using Eq. 4.1 and the parameters shown in Table 4.1 are preserved. The used raw data are then erased from the cell.

TH-3282_186103018

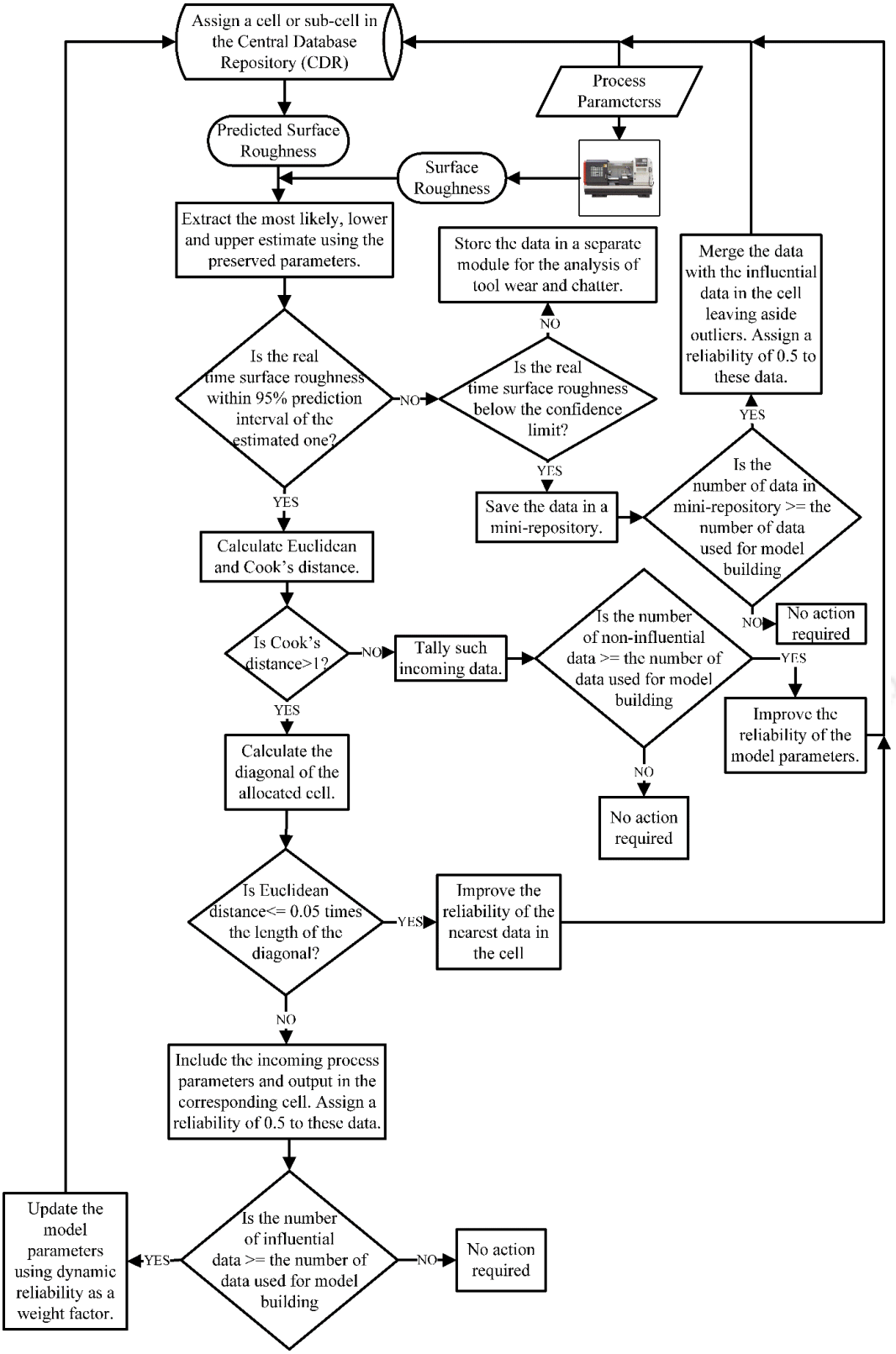

Figure 4.4 Flowchart for surface roughness prediction and data updating

TH-3282_186103018

4.4.2 Sufficient number of data for model fitting

Estimation of surface roughness with 95% prediction interval is carried out based on the preserved parameters. The most likely, lower and upper estimate is evaluated and decisions are taken based on the following possible cases:

CASE A. Actual surface roughness from the factory floor lies within the interval limits: Whenever the actual surface roughness lies within the interval estimate, the influence of the entering data entry is evaluated by Cook's distance (Larose, 2015). It is a standard approach to evaluate the effect of any new data entry using the following equation:

$$D_i = \frac{(y_i - y_{i,p})^2}{(m+1)s^2}\left\{\frac{h_i}{(1-h_i)^2}\right\}, \tag{4.10}$$

where y_i is the actual obtained output for i^{th} data entry, $y_{i,p}$ is the corresponding predicted output, m is the number of predictors (four viz., cutting speed, feed, depth of cut and radial acceleration, for surface roughness estimation in this case), s is the standard error of the estimate and h_i is the leverage of the i^{th} observation. The leverage for surface roughness is calculated as:

$$h_i = \frac{1}{n} + \frac{(\ln V_p - \ln \overline{V})^2}{\sum_{i=1}^{n}\left(\ln V_i - \ln \overline{V}\right)^2} + \frac{(\ln f_p - \ln \overline{f})^2}{\sum_{i=1}^{n}\left(\ln f_i - \ln \overline{f}\right)^2} + \frac{(\ln d_p - \ln \overline{d})^2}{\sum_{i=1}^{n}\left(\ln d_i - \ln \overline{d}\right)^2} + \frac{(\ln a_p - \ln \overline{a})^2}{\sum_{i=1}^{n}\left(\ln a_i - \ln \overline{a}\right)^2}. \tag{4.11}$$

Thus, for evaluating both Cook's distance and leverage, the already stored values are used for the estimation. When Cook's distance is more than or equal to one, the new data is considered as influential (Larose, 2015). Hence, there are two possibilities in this case.

CASE A-I. Cook's distance greater than or equal to one for the new data entry: The influential data entry is checked for similarity or closeness with any existing data that are preserved in the cell. If the Euclidean distance with any of the existing data entries are found to be less than five percent of the length of diagonal of the cell, then the new data is assumed to be close. The length of diagonal of the cell is given by:

$$L_{\text{diagonal}} = \sqrt{(V_2 - V_1)^2 + (f_2 - f_1)^2 + (d_2 - d_1)^2 + (a_2 - a_1)^2}. \tag{4.12}$$

TH-3282_186103018

where the suffix "2" represents upper limit and the suffix "1" represents lower limit of the parameter pertaining to a specific cell. The improvement in reliability of the closest data point is achieved using the following probability theory (Chatterjee et al., 2020):

$$R_{\text{eupdated}} = 1-\left\{\left(1-R_{\text{enew}}\right)\left(1-R_{\text{ecurrent}}\right)\right\}. \tag{4.13}$$

where R_{eupdated} is the updated reliability of the observation, R_{enew} is the reliability of the new observation and R_{ecurrent} is the reliability of the current observation. A new data is allocated with a reliability of 0.5 or there is 0.5 probability of it being correct. In that case, the reliability is updated by

$$R_{\text{eupdated}} = 0.5\left(1+R_{\text{ecurrent}}\right). \tag{4.14}$$

Thus, the enhancement of the reliability of the existing data is done using Eq. 4.14. Otherwise, if closeness of the new influential data is not observed with any of the existing data in the cell, the new data entry is preserved having a reliability of 0.5. Once the number of influential data becomes sufficient, the reliability associated with such data are considered as weights factor for the following equation:

$$\text{Minimize}\sum_{i=1}^{n}\{\ln R_{ai}-(\ln K+\alpha\ln V_i+\beta\ln f_i+\gamma\ln d_i+\delta\ln a_i)\}^2\times\text{Reliability of } i^{th}\text{ data}. \tag{4.15}$$

where i is a typical data entry among the n data entries available for model fitting.

The optimal new values of K, α, β, γ and δ are obtained from Eq. 4.15. The optimal new values of the regression parameters are also assigned with a reliability of 0.5. The values of all the five parameters are updated using the following equation:

$$x_{\text{updated}} = \frac{\left(x_{\text{current}}\times R_{\text{excurrent}}\right)+\left(x_{\text{new}}\times R_{\text{exnew}}\right)}{R_{\text{excurrent}}+R_{\text{exnew}}}. \tag{4.16}$$

where x_{updated} is the updated value of the regression parameter, x_{current} is the current value of the regression parameter, x_{new} is the new value of the regression parameter, $R_{\text{excurrent}}$ is the current reliability of the regression parameter value, R_{exnew} is the reliability of the new regression parameter value. The updated values are then preserved in the cell. Assign a reliability of 0.5 to all the parameters. The used influential raw data are then erased from the memory. The value of number of observations used for model fitting is also updated. The process continues with the storage of new influential data until it becomes sufficient again for model fitting and updating the regression parameters.

TH-3282_186103018

CASE A-II: Cook's distance less than one for the new data entry

The non-influential data entry is not preserved. Instead the number of new non-influential data is tallied. Whenever the number of such data becomes sufficient, the reliability of the regression parameters is improved according to the probability theory:

$$R_{\text{exupdated}} = 1-\left\{\left(1-R_{\text{exnew}}\right)\left(1-R_{\text{excurrent}}\right)\right\}. \tag{4.17}$$

where $R_{\text{exupdated}}$ is the updated reliability of the regression parameter value. The reliability of the new regression parameter value when the number of non-influential data becomes sufficient is assigned as 0.5. Hence, the reliability is updated by

$$R_{\text{exupdated}} = 0.5\left(1+R_{\text{excurrent}}\right). \tag{4.18}$$

The updated reliability of the model parameters is preserved. It is further used for updating the model parameters when the number of raw influential data becomes sufficient.

CASE B: Actual surface roughness from the factory floor lies exterior to the interval limits: The tool wear and chatter data are verified and preserved for later analysis pertaining to the assigned cell. Such data are also merged with the influential data, when the number of such data reaches a sufficient quantity for a specific cell. The procedure of merging the data is explained in details in Chapter 3. A similar strategy is also adopted in the present chapter when the actual surface roughness lies outside the interval estimate.

4.5 Case Studies

For demonstration purpose, the experimental data are taken from Kohli and Dixit (2005). They conducted turning experiments on an HMT NH–26 lathe machine to investigate the effect of four input parameters, i.e., cutting speed, feed, depth of cut and radial acceleration of vibration on the surface roughness. The work material was mild steel having hardness of 130 BHN, yield strength of 290 MPa and ultimate tensile strength of 477 MPa. The cutting tools used were of made of high-speed steel (HSS) and tungsten carbide. The diameter of the job varied from 30 mm to 46 mm, length was 240 mm, but the machining length of 110 mm was used for the experiments. Pocket Surf (Make: Mahr, GmbH) was used for measuring the centre line average (CLA) surface roughness. For measuring the radial acceleration of vibration, a piezoelectric type vibration meter (Make: Syscon, Model: SI-327A01) was used. Experiments were conducted for both wet and dry turning using HSS and carbide tool. However, in this work, wet turning using HSS tool is only considered for illustrating the effectiveness of the proposed methodology. Cutting

TH-3282_186103018

speed, feed and depth of cut are the controllable parameters. Radial acceleration is the uncontrollable parameter. The input process parameters ranged in the following manner: cutting speed: 25–110 m/min, feed: 0.04–0.16 mm/rev, depth of cut: 0.3–0.6 mm, radial acceleration of vibration: 0.37–3.66 m/s^2. For enhanced clarity of the case study, data collection and surface roughness prediction are shown as follows:

4.6 Data collection module

The methodology suggested in the present chapter is implemented by writing a code in R language, an open source statistical software; the hardware was Intel Core I5 with 8 GB RAM. The efficacy of the proposed scheme is tested by constructing a virtual lathe machine. In the virtual lathe machine, surface roughness prediction is carried out using the best neural network topology suggested by Kohli and Dixit (2005) with three hidden neurons. For a given process parameter, the virtual lathe provides centre line average (CLA) value of surface roughness. A total of 59 experiments were conducted for wet turning of mild steel with an HSS tool to analyse the effect of cutting speed, feed, depth of cut and radial acceleration on the surface roughness.

In this work, 35000 simulated data are generated for illustrating the case study as depicted in Figure 4.5. Such large amount of industrial big data are initially stored on a cloud server. Thus, in the data collection module, only simulated data produced by a virtual lathe is considered; in actual practice, it will be obtained directly from machine shops.

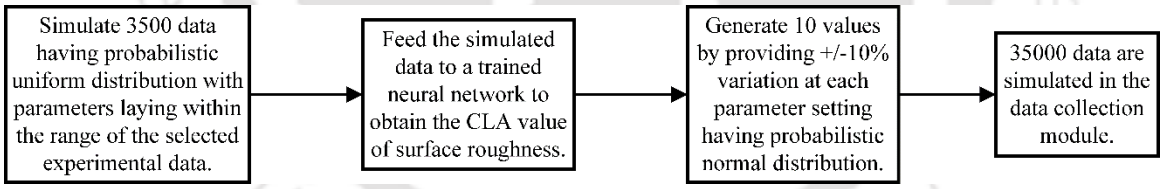

Figure 4.5 Data collection procedure

The existing range of the four input process parameters shown in Table 4.2 are categorised into high, medium and low to represent as cells. This results in the formation of 81 cells. The accumulated 35000 data are allocated to all the 81 cells based on the range of the input parameters as shown in Table 2. Model fitting is carried out in each cell as per Eq. 4.1. The coefficient of determination (R^2) is evaluated for all cells and if it is more than or equal to 0.9 considering variation in the output for a particular parameter setting, then the fifteen essential parameters are preserved as shown in Table 4.1. When the value of R^2 is less than 0.9, the mean value of the variable output is considered for model fitting and R^2 is again evaluated. If the value is greater than or equal to 0.9, the fifteen essential

TH-3282_186103018

parameters are preserved, otherwise the cell is further divided into high and low levels as already explained in details in Section 4.3. In the following two sections, cases of two typical cells are illustrated: 1) a cell with insufficient data for surface roughness estimation and 2) a cell with sufficient data for surface roughness estimation.

Table 4.2 Range of input parameters for the proposed methodology

	Cutting Speed (m/min)	Feed (mm/rev)	Depth of Cut (mm)	Radial Acceleration of vibration (m/s^2)
Low Range	25.00	0.040	0.30	0.37
	53.33	0.080	0.40	1.46
Medium Range	53.34	0.081	0.41	1.47
	81.66	0.120	0.50	2.56
High Range	81.67	0.121	0.51	2.57
	110.00	0.160	0.60	3.66

4.7 Surface roughness prediction for a cell with insufficient data

The cell where the range of input parameters ranged in the following manner: cutting speed: 25.00–53.33 m/min (low range), feed: 0.04–0.08 mm/rev (low range), depth of cut: 0.51–0.60 mm (high range), radial acceleration of vibration: 0.37–1.46 m/s^2 (low range) is having R^2 of 0.81 even after considering the mean value of the variation in the output. The aforesaid cell containing 340 observations is further divided into two major levels based on the range of the parameters resulting in the formation of 16 sub-cells. It is observed that there are insufficient data in almost all the sub-cells for model fitting. Hence, all the raw data are preserved for such sub-cells. Whenever sufficient data is allocated, then model fitting is carried out and the fifteen essential parameters are preserved. Any new information is preserved with a reliability of 0.5. For enhanced illustration of the scheme, data influx is further narrowed down to only the sub-cell as shown in Table 4.3 having the range of input process parameters ranged in the following manner: 25.00–39.165 m/min (low range), feed: 0.04–0.06 mm/rev (low range), depth of cut: 0.51–0.55 mm (low range), radial acceleration of vibration: 0.37–0.92 m/s^2 (low range). The aforesaid sub-cell has 10 observations and model fitting cannot be carried out. Hence all the raw data are preserved for surface roughness estimation.

TH-3282_186103018

Table 4.3 Range of parameters for the selected cell for further analysis

	Cutting Speed (m/min)	Feed (mm/rev)	Depth of Cut (mm)	Radial Acceleration of vibration (m/s^2)
Low Range	25.000	0.040	0.51	0.37
	39.165	0.060	0.55	0.92
High Range	39.166	0.061	0.56	0.93
	53.330	0.080	0.60	1.47

4.7.1 First set of data— prediction of the upper, lower and most likely estimate for the sub-cell with 50 new data

It is assumed that further machining is carried out on the shop floor. Feedback for fifty new data are obtained using the virtual lathe. Similar or near to similar input process parameters are identified using the method of normalization as explained in Section 4.3. The mean output value of the similar observations is considered. In this case all the 10 existing observations are similar. Hence, the mean output value is used.

Nearest neighbour regression requires at least two data points having dissimilar input parameters for prediction of surface roughness. The selected sub-cell has one identical input parameter, requiring at least one more data for estimating the most likely estimate. Euclidean distance is used to estimate the nearest data from the surrounding cells. The one having the least value is selected. It is achieved by using the 'distance' function in R. Using Eq. 4.7, the most likely estimate is evaluated with a caveat due to less amount of data. The upper and lower estimate is evaluated using Eq. 4.9. The initial prediction of the upper, lower and most likely estimate for the selected sub-cell using nearest neighbour approach is depicted in Figure 4.6. It is observed that 82% of the data lies within the interval estimate. After estimation of upper, lower and most likely estimate, all the allocated 50 data along with the already existing 10 data in the sub-cell are used for model fitting. The essential fifteen parameters are preserved in the sub-cell as depicted in Table 4.4.

TH-3282_186103018

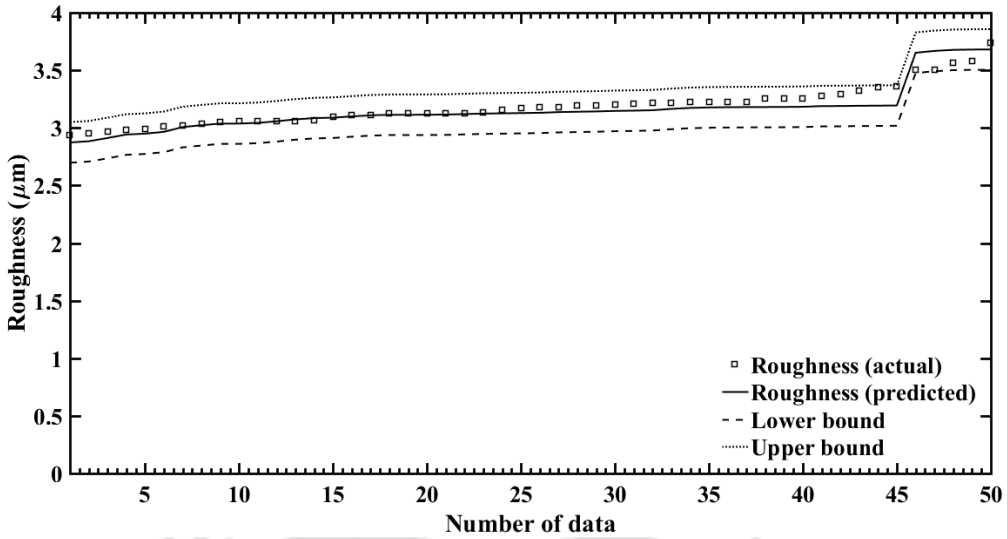

Figure 4.6 Prediction using nearest neighbour regression for selected sub-cell

Table 4.4 The parameter values for the selected sub-cell

Sl. No.	Parameters	Value
1	$\sum_{i=1}^{n}\left(\ln V_i - \ln \overline{V}\right)^2$	1.157338
2	$\sum_{i=1}^{n}\left(\ln f_i - \ln \overline{f}\right)^2$	0.781966
3	$\sum_{i=1}^{n}\left(\ln d_i - \ln \overline{d}\right)^2$	0.032594
4	$\sum_{i=1}^{n}\left(\ln a_i - \ln \overline{a}\right)^2$	3.798347
5	n	60
6	$\ln \overline{V}$	3.330855
7	$\ln \overline{f}$	– 2.99132
8	$\ln \overline{d}$	– 0.64335
9	$\ln \overline{a}$	– 0.54335
10	$\sum_{i=1}^{n}\left(\ln R_{ai} - \ln \hat{R}_{a\,i}\right)^2$	1.106679
11	K	11.83061, $R_{eK\text{current}} = 0.5$
12	α	0.02081, $R_{e\alpha\text{current}} = 0.5$
13	β	0.39127, $R_{e\beta\text{current}} = 0.5$
14	γ	0.255168, $R_{e\gamma\text{current}} = 0.5$
15	δ	0.058313, $R_{e\delta\text{current}} = 0.5$

4.7.2 Second set of data— Prediction of the upper, lower and most likely estimate for the sub-cell with 100 new data

Similarly, further machining is carried out. The values shown in Table 4.4 are used for estimating the upper, lower and most likely estimate for the new set of 100 data that are

TH-3282_186103018

simulated using the virtual lathe. The upper and lower estimate are predicted with 95% prediction interval as depicted in Figure 4.7. A flowchart showing the data distribution is shown in Figure 8. Approximately 64% of the data lies within the interval estimate. It is found that all the data that lies within the interval estimate are having a Cook's distance of less than one. Instead of preserving such data, only the value of the quantity is preserved. When the quantity exceeds 60, the reliability of the model parameter is improved. In this case, the quantity observed is 64 as depicted in Figure 4.8, i.e., more than the number of observations used for model building. Therefore, only the value of the reliability is updated in the Table 4.4. Using Eq. 4.18, the reliability of the regression parameter is improved to 0.75.

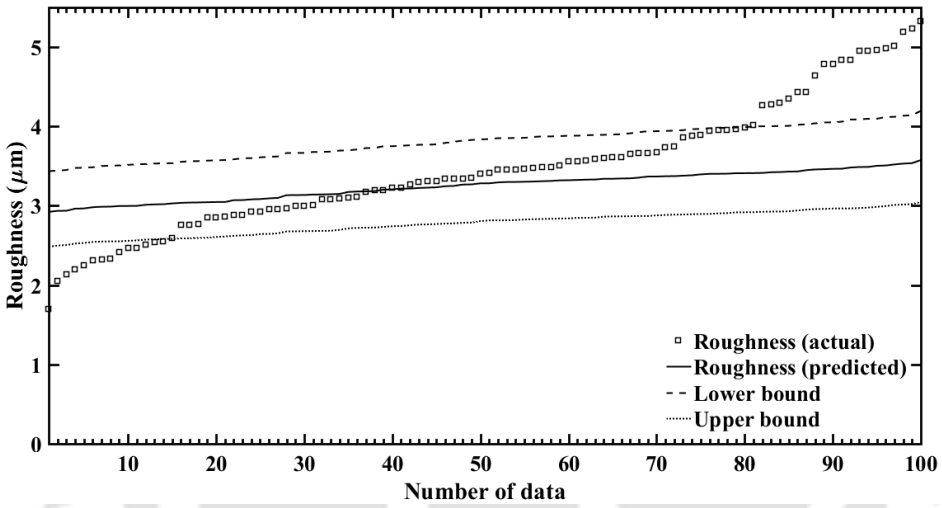

Figure 4.7 Prediction with 95% prediction interval in the sub-cell for the first set of 100 data

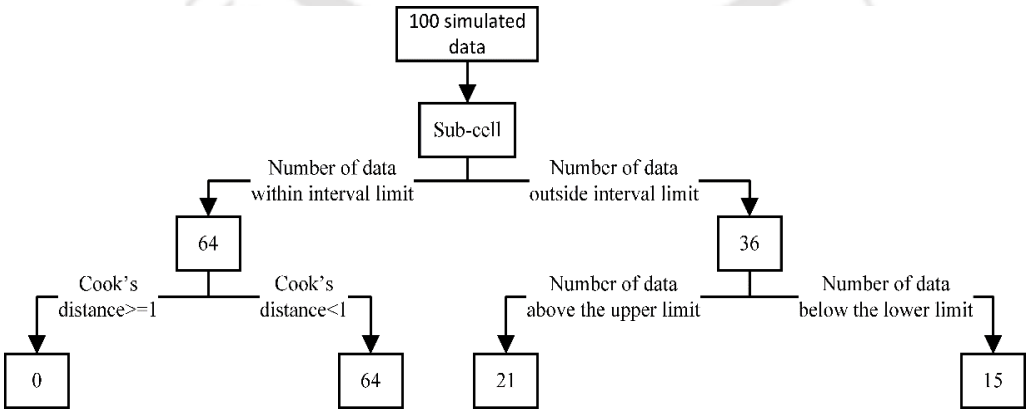

Figure 4.8 Data distribution for the first set of 100 data in the selected sub-cell

TH-3282_186103018

4.7.3 Third set of data— Prediction of the upper, lower and most likely estimate for the sub-cell with 150 new data

Feedback is again taken from the shop floor using the virtual lathe, that is used for simulating 150 data. The upper and lower estimate are predicted with 95% prediction interval as depicted in Figure 4.9. The data distribution is depicted in Figure 4.10. This time, 74.66% data are within the prediction limit. Out of the 38 data that are outside the prediction limit, 24 data are above the upper limit. Such data are checked for any process abnormality. It is observed that this time also all the data that lie within the prediction limit are having a Cook's distance of less than one. Therefore, the data are not preserved, instead the value of the quantity is preserved. This time again the cumulative value has exceeded 60. The reliabilities of the regression parameters are further improved to 0.875 using Eq. 4.18 that are updated in the Table 4.4.

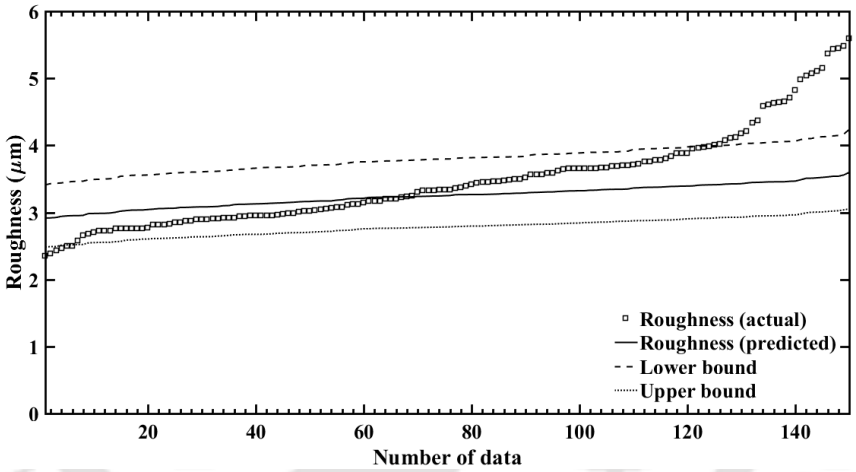

Figure 4.9 Prediction with 95% prediction interval in the selected sub-cell for the second set of 150 data

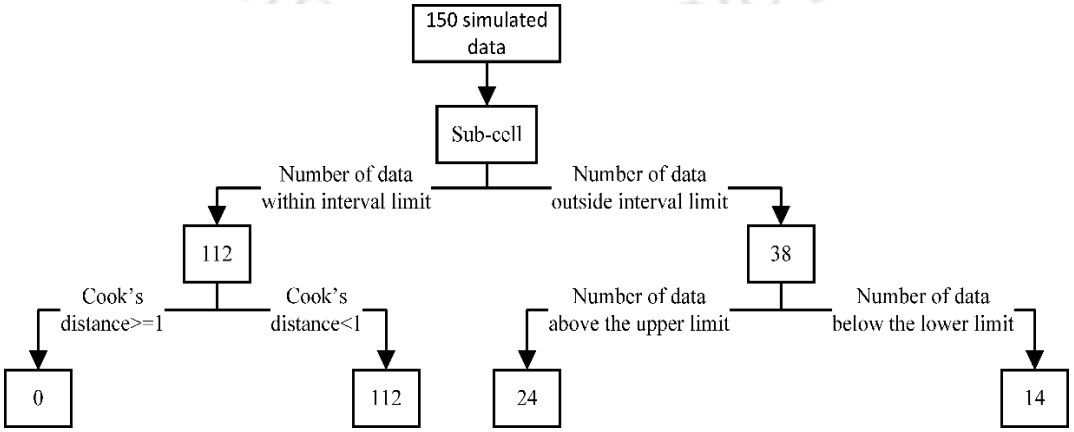

Figure 4.10 Data distribution for the second set of 150 data in the selected sub-cell

TH-3282_186103018

4.8 Surface roughness prediction and model updating for a cell having sufficient data

The cell where the range of input parameters ranged in the following manner: cutting speed: 25.00–53.33 m/min (low range), feed: 0.04–0.08 mm/rev (low range), depth of cut: 0.30–0.40 mm (low range), radial acceleration of vibration: 0.37–1.46 m/s^2 (low range) is having sufficient data. Additionally, the value of R^2 is observed to be 0.98 after considering the mean value of variation in the output. It indicates that the existing 370 observations are sufficient for model fitting. The essential fifteen parameters are preserved as depicted in Table 4.5.

Table 4.5 The parameter values for the selected cell

Sl. No.	Parameters	Value
1	$\sum_{i=1}^{n}\left(\ln V_i - \ln \overline{V}\right)^2$	18.33789
2	$\sum_{i=1}^{n}\left(\ln f_i - \ln \overline{f}\right)^2$	11.15223
3	$\sum_{i=1}^{n}\left(\ln d_i - \ln \overline{d}\right)^2$	2.345877
4	$\sum_{i=1}^{n}\left(\ln a_i - \ln \overline{a}\right)^2$	53.48355
5	n	370
6	$\ln \overline{V}$	3.625839
7	$\ln \overline{f}$	– 2.827693
8	$\ln \overline{d}$	– 1.047954
9	$\ln \overline{a}$	– 0.196141
10	$\sum_{i=1}^{n}\left(\ln R_{ai} - \ln \hat{R}_{ai}\right)^2$	0.01381064
11	K	5.270804, $R_{eK\text{current}} = 0.5$
12	α	0.3046234, $R_{e\alpha\text{current}} = 0.5$
13	β	0.06878103, $R_{e\beta\text{current}} = 0.5$
14	γ	1.390504, $R_{e\gamma\text{current}} = 0.5$
15	δ	-0.0088375, $R_{e\delta\text{current}} = 0.5$

4.8.1 First set of data— prediction of the upper, lower and most likely estimate for the cell with 300 new data

It is assumed that machining is carried out on the shop floor and feedback is taken from the shop floor using the virtual lathe. New set of 300 data are simulated having input parameters laying within the range of values pertaining to the selected cell. The values

TH-3282_186103018

shown in Table 4.5 are used for predicting the upper, lower and most likely estimate. The upper and lower estimate are predicted with 95% prediction interval as depicted in Figure 4.11. A flowchart showing the data distribution is depicted in Figure 4.12. It is observed that 87.67% of the data lies within the interval estimate. It is also observed that all the data that lies within the interval estimate are having a Cook's distance of less than one. Therefore, the data are not preserved, instead the value of the quantity is preserved. When the quantity exceeds 370, the reliability of the model parameter is improved. In this case, the quantity observed is 263 as depicted in Figure 4.12, i.e., less than the number of observations used for model building. Hence, the Table 4.5 is kept unchanged.

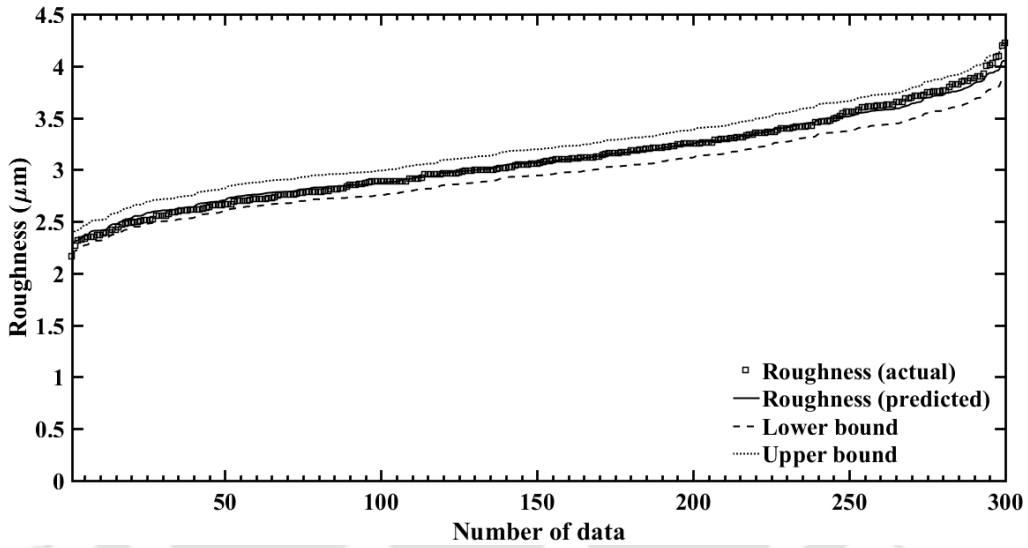

Figure 4.11 Prediction with 95% prediction interval in the selected cell for the first set of 300 data

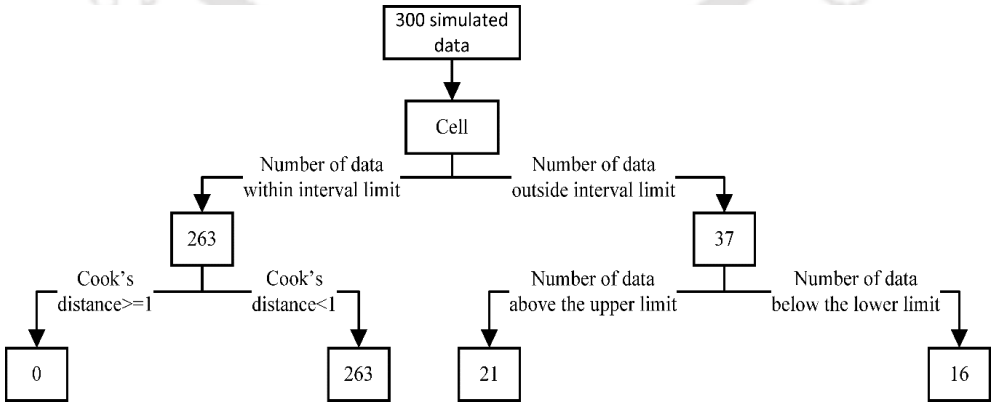

Figure 4.12 Data distribution for the first set of 300 data in the selected cell

TH-3282_186103018

4.8.2 Second set of data— Prediction of the upper, lower and most likely estimate for the cell with 300 new data

Feedback for 300 more data having input parameters laying within the range of values of the selected sub-cell are again taken using the virtual lathe. The upper and lower estimate are predicted using Table 4.5 with 95% prediction interval as depicted in Figure 4.13. A flowchart showing the data distribution is depicted in Figure 4.14. It is detected that 90.33% of the data lies within the interval estimate. It is also observed that all the data that lies within the interval estimate are having a Cook's distance of less than one. Therefore, the data are not preserved, and only the value of the quantity is preserved. This time the cumulative quantity is 534 i.e., more than 370. Hence, the reliability of the model parameter is only improved keeping all other parameters unchanged. The counter for tallying the number of non-influential data is then reset to zero. The reliabilities of the regression parameters are improved to 0.75 and the same is updated in Table 4.5.

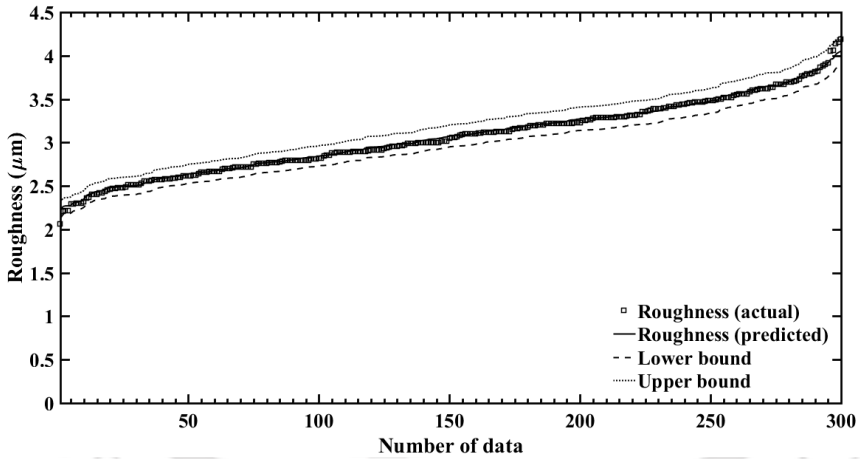

Figure 4.13 Prediction with 95% prediction interval in the selected cell for the second set of 300 data

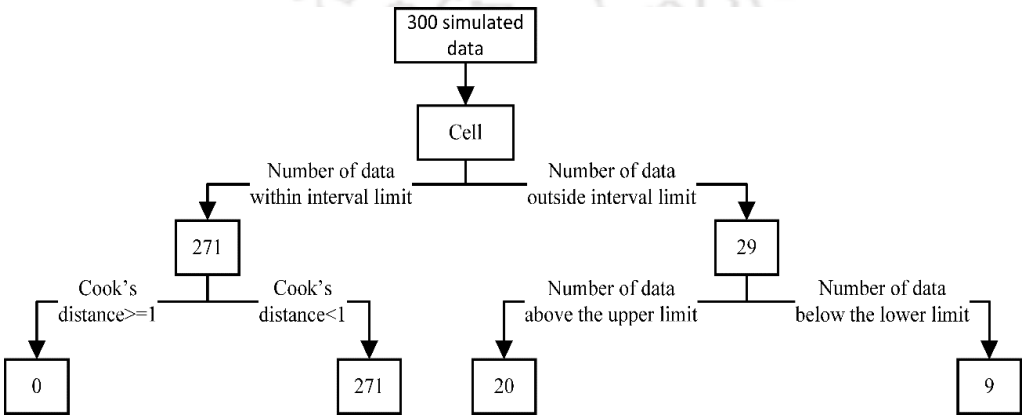

Figure 4.14 Data distribution for the second set of 300 data in the selected cell

TH-3282_186103018

4.8.3 Third set of data— Prediction of the upper, lower and most likely estimate for the cell with 300 new data

Similarly, for the third data set, 300 more data are simulated using the virtual lathe. The upper and lower estimate are predicted with 95% prediction interval as depicted in Figure 4.15. The data distribution is depicted in Figure 16. This time, 91% data are within the prediction limit. It is observed that this time also all the data that lie within the prediction limit are having a Cook's distance of less than one. Therefore, the data are not preserved, instead the number of such non-influential data are tallied and only the value of the quantity is preserved. This time the cumulative value has not exceeded 370. Hence, all the model parameters that are depicted in Table 4.5 are kept unchanged.

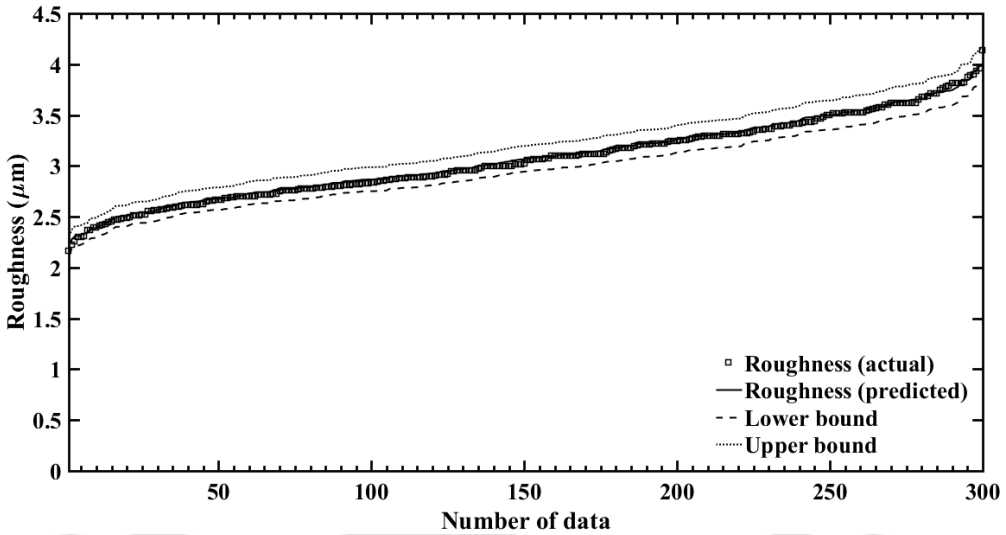

Figure 4.15 Prediction with 95% prediction interval in the selected cell for the third set of 300 data

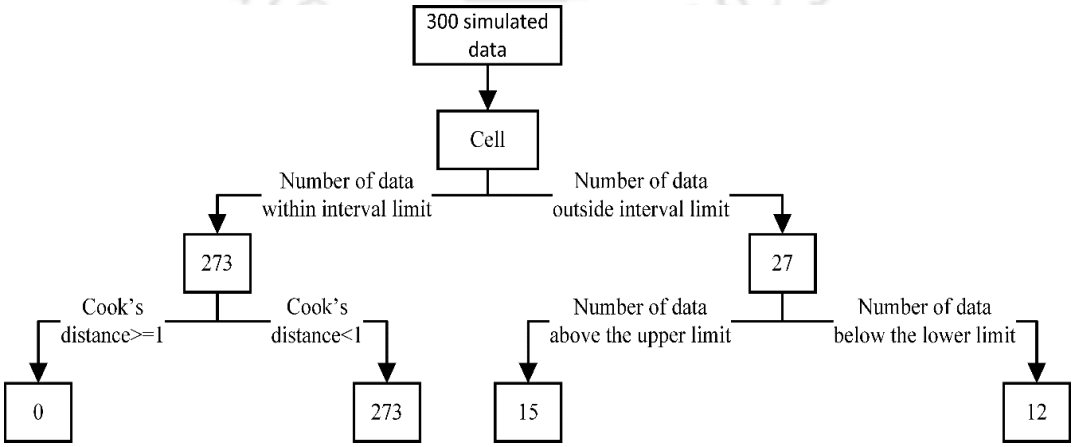

Figure 4.16 Data distribution for the third set of 300 data in the selected cell

TH-3282_186103018

It is evident that the proposed methodology predicts well when sufficient data are available that can be modelled properly according to Eq. 4.1. In brief, the whole region is divided into 81 cells for the 35000 data. Each cell requires only fifteen parameter values to represent the model. Only in case of large experimental variation, the existing cell is further divided into 16 sub-cells. In spite of that, the number of data required for estimating the upper, lower and most likely estimate is much lesser than many popular techniques such as GPR and SVR. This work attempts to highlight the following key aspects of the proposed methodology:

- The proposed scheme is simple to understand and easy to implement.
- The number of essential parameters required for prediction is limited to only fifteen per cell. There is no need to preserve the large amount of used raw data in the database. Thereby, reducing the burden on data storage devices.
- Surface roughness prediction is carried with 95% prediction interval using the preserved parameters.
- Model updating is carried out using the dynamic reliability factor that is associated, when there are sufficient number of influential data.
- Cook's distance is used for identifying the influential observation.
- Outliers have been considered while merging the data laying outside the interval limits.

4.9 Conclusion

The emergence of fourth industrial revolution created an increasing trend to use the past machining data for enhancement of the machining process. The current work deals with the prediction of surface roughness by utilising only the essential parameters that are required for estimating the upper, lower and most likely estimate. This would reduce the unnecessary burden on the cloud database without compromising the accuracy. There is a facility for updating the model with sufficient amount of influential data that are identified with the help of Cook's distance. 35000 data are used for demonstrating the proposed methodology.

The proposed methodology is validated by means of the data that are simulated by the virtual lathe for wet turning of steel using HSS tool. The strategy is observed to be considerably successful and uses minimum parameters for interval estimation as compared

TH-3282_186103018

to popular machine learning techniques. Examples are shown when insufficient data are available for model fitting in a cell. It is assumed that machining is carried out on the shop floor and feedback is taken. In the present chapter, it is achieved using the virtual lathe. Three separate sets of data are used to show the effectiveness of the proposed methodology. For first set of data, prediction is carried out using nearest neighbour approach and 82% of the simulated values falls within the interval estimate. The first set of data and the already existing raw data are then used for model fitting that are used further. It is observed that around 64% of the simulated values lies within the upper and lower estimate for the second set of data. The third dataset contains around 75% of the simulated values within the interval estimate. In the example when sufficient data are available for model fitting in a cell, three separate sets of data are also simulated using the virtual lathe to show the effectiveness of the proposed strategy. The first set data predicts around 87.67% of the simulated values within the upper and lower estimate. Similarly, the second set of data contains 90.33% and the third set of data contains 91% of the simulated data within the upper and lower estimate. Therefore, the results match well with the predicted and the simulated values of surface roughness with at least 87.67% of data laying within the interval limits. The main purpose of this chapter is to highlight the concept of using the minimum number parameters for evaluating the upper, lower and most likely estimate of surface roughness in an industrial big data environment. Thus, the methodology is applied when sufficiently large amount of machining data is accumulated in a real-life industrial situation and quick dissemination of information are required so that the burden of data storage can be reduced.

In future, industrial employment of the proposed methodology is planned to be undertaken. Additionally, the real-life implementation will not only include surface roughness prediction, but also all the estimation of cutting force and tool wear. This can include all the conventional machining processes such as turning, milling, drilling and grinding. Thus, the proposed methodology is an initial effort towards competent data storage and data utilization in manufacturing.

TH-3282_186103018

TH-3282_186103018

Chapter 5
Estimation of forging load in open and closed-die forging with the help of stored data

5.1 Introduction

The forging process involves the deformation of metals under high pressure conditions to shape it into the desired form. The accurate estimation of forging load is essential for ensuring the structural integrity of forged components, predicting tooling requirements, and optimizing process parameters. It is observed that empirical models tend to rely on material properties and friction condition. While these models can provide reasonable estimates, they are limited by their assumptions and may not accurately capture the complexities of the forging process in the absence of large database. This chapter aims to explore this aspect of using the stored data for the estimation of the forging load.

The utilization of stored data presents an opportunity to estimate forging load accurately and efficiently. By capturing and analysing data from various sensors and process monitoring systems, valuable information can be extracted to establish correlations between process variables and forging load. The challenge lies in effectively utilizing this stored data to develop reliable and robust estimation models that can be applied to different forging scenarios. Furthermore, the selection of appropriate data storage techniques and the pre-processing of stored data are critical for ensuring the accuracy and reliability of the estimation process.

There are a few attempts in the past that proposes the usage of expert system for timely and effective utilisation of the accumulated data in forging. One of the initial works in expert system was carried out by Osakada and Yang (1990). They used backpropagation neural network aided expert system for determining the forming method, number of forming steps and prediction of die fracture with die defect. Katayama et al. (2004) developed an expert system for the process design of a cold forging process. Expert system was also applied for determining the sequence of steps in manufacturing a part through axisymmetric cold forging (Kim and Park, 2006). Considering the uncertainty in forging process, fuzzy logic was applied. Fuzzy logic was used for the estimation of the dimensional errors occurring during actual forging operation (Park et al., 2007). Gangopadhyay et al. (2011) incorporated fuzzy logic in their expert system for the

TH-3282_186103018

prediction of forging load and axial stress. Gronostajski et al. (2016) used an expert system for determining the various wear mechanisms that degrade the forging tools during hot forging. Recently, deep learning techniques are also used in cold forging for condition monitoring of the machines (Glaeser et al., 2021). Thus, researchers are trying hard to effectively utilise data-driven technologies in forging.

In estimating the forging load, there are two uncertain parameters: flow stress and friction condition. Flow stress significantly influences the material flow in forging operation. Flow stress is generally modelled in the form of mathematical equation, whose parameters are determined from compression tests. However, modelling of friction is itself a challenging task (Dixit et al., 2020). A thorough knowledge and a lot of skill is required for the estimation of forging load using the existing analytical and numerical models. Data driven techniques can be effective in taking care of the various uncertainties associated with forging such as friction condition and flow stress. With time and usage, data driven models get updated and provide more accurate results based on the feedback received from the shop floor.

The central idea of this chapter is to use the knowledge of the most similar closed die forging products for forging load prediction of a new product. The most similar product is chosen by finding out the similarity in material, geometry and friction, which is then used for estimate the forging load. There are various uncertainties associated with the closed die forging process. Although some attempts have already been made in the application of fuzzy set theory for load estimation, it is the first application of fuzzy set theory for making accurate estimation based on the information of similar products. The forging load estimations are carried out in the form of lower, most-likely and upper estimate, from which one can construct a triangular membership function. The proposed algorithm is validated by taking several examples of varying product sizes, friction condition and material of four closed die forging products. All the validation data are obtained from FEM simulations using ABAQUS, which serves as a virtual factory. The data that are obtained from the FEM simulations are preserved in a ‘MySQL’ relational database. The database is accessed and the methodology is implemented by a code written in ‘R’, an open source statistical programming language with a graphical user interface (GUI). The scheme adopted for estimating the forging load in open and closed die forging is shown in Figure 5.1 and is discussed in details. The computational scheme could be repeated several times while the accuracy of the computation would be enhanced.

TH-3282_186103018

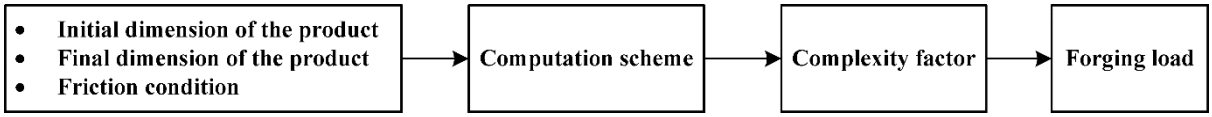

Figure 5.1 Scheme for estimating forging load

5.2 FEM simulation procedure adopted for axisymmetric forged products (open and closed die)

This section elaborates on the concept of virtual factory and its use to demonstrate the proposed methodology. The virtual factory sends feedback of the forging load to the proposed scheme. This is assumed to be analogous to the feedback obtained from the shop floor. Feedback of the forging load is obtained by carrying out FEM simulations using a commercially finite element package ABAQUS® version 6.13-1. The analysis using the virtual factory provides a more realistic assessment of the proposed scheme.

For better visualization, axisymmetric models of the closed die cold forging processes are considered for this study. Part module was used to create axisymmetric shape of the blank and die. During modelling of cold forging process, axisymmetric deformable shell part was created for the blank, while the axisymmetric discrete rigid wire part was created for the die. A reference point was created on the die. The motion or restraints of the entire die is applied through the aforesaid reference point only. The lower surface of the die was considered as master and the upper surface of the blank was considered as slave. Property module was created by assigning the blank as lead. Properties viz., density, Young's modulus and Poisson's ratio were taken as 11.29 × 103 kg/m3, 17 GPa and 0.42, respectively. The yield stress and the corresponding plastic strain was roughly estimated using the following flow stress equation

$$\sigma_o = 65.8\varepsilon^{0.27}. \tag{5.1}$$

where σ_o is the flow stress and ε is the equivalent plastic strain. The material properties of lead were taken from Fereshteh-Saniee and Jaafari (2002). An isotropic inertia mass is assigned to the die for all cases using the property module. For axisymmetric forging, parts were then placed in the global coordinate system with the help of assembly module. It was assumed that the velocity of both the upper and lower dies had same magnitude but opposite in direction. A typical generating plane needs to be considered, as the FEM simulation is axisymmetric in nature; the solid model was created by giving a full revolution to the plane about y-axis shown in Figure 5.2 and FEM model is shown in Figure 5.3. The die was kept

TH-3282_186103018

just above the blank without any gap as depicted in Figure 5.2 and Figure 5.3. The automatic time step increments were chosen for the dynamic explicit analysis in the step module. Surface to surface (explicit) interaction was considered between the blank and the die.

For executing the closed die forging simulation, a penalty-based friction formulation was considered. It is also assumed for the ABAQUS simulation that a Coulomb's coefficient of friction μ as 0.1 may be considered as lubricated condition and a value of μ as 0.25 may be considered as non-lubricated condition. Generally, the value of the Coulomb's coefficient of friction for cold forging varies between 0.05 and 0.15. Nevertheless, the value of μ as 0.25 can be considered as an extreme condition. Arbitrary Lagrangian-Eulerian (ALE) adaptive mesh control was used to mesh the blank for closed die forging in the step module. The ALE utilizes both the Lagrangian as well as Eulerian analysis to avoid distortion of the mesh elements under the closed die simulated condition. A quad element shape was chosen with medial axis algorithm for meshing the blank. The medial axis algorithm makes sure that the complete meshed region is divided into simpler regions for using the structured meshing technique to fill the regions with mesh elements. The blank was discretized with a 4-node bilinear axisymmetric quadrilateral, reduced integration, hourglass control (CAX4R) elements. The element size of 0.5 mm × 0.5 mm is adopted for the blank as shown in Figure 5.3. The die was discretized with a 2-node linear axisymmetric rigid link (RAX2) elements. The element size of 0.5 mm was adopted for the die. The load module was created to assign the load and boundary conditions to the model. The boundary conditions adopted for the axisymmetric case is shown in Figure 5.2. Here, *U*x and *U*y refer to displacements along x and y -axes, respectively and *UR*z is the rotational displacement about the z-axis. A downward velocity *V*y is given to die using the reference point along the y-axis.

In the last step, the job module was created and the model was submitted for the analysis. After the analysis, reaction force (forging load), was recorded. Forging load was also verified by dividing the total energy (internal + friction) with incremental displacement shown as

$$P = \frac{(IE_{\mathrm{i}} + FE_{\mathrm{i}}) - (IE_{\mathrm{i-1}} + FE_{\mathrm{i-1}})}{(V_{\mathrm{y}}\ t_{\mathrm{i}} - V_{\mathrm{y}}\ t_{\mathrm{i-1}})}. \tag{5.2}$$

TH-3282_186103018

where *P* is the forging load, *IE* is the internal energy, *FE* is the frictional energy, *Vy* is the die velocity, and *t* indicates the time at the ith instance and (*i*–1)th instance. The numerator denotes the total energy and the denominator denotes the incremental displacement. The information about the internal and frictional dissipation energy were obtained from output database (ODB) history of the simulation and ODB field output. FEM simulations were then carried out accordingly based on the closed die products and the information of the forging load were used as feedback from a virtual factory.

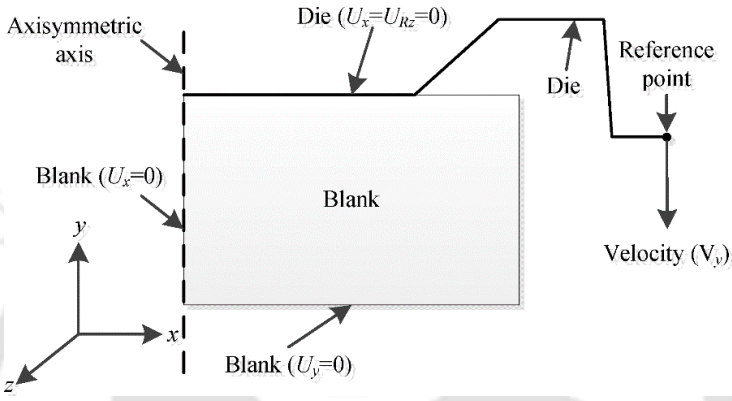

Figure 5.2 Axisymmetric closed die cold forging

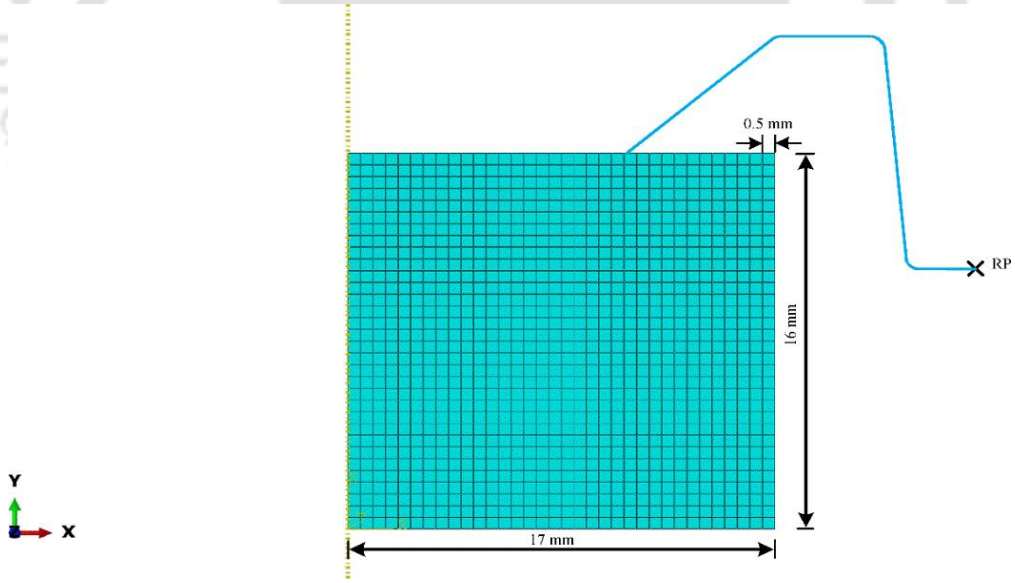

Figure 5.3 FEM model of the closed die forging

5.3 Proposed methodology for estimation of forging load in open die forging

The slab method analysis in upsetting an axisymmetric disk using Coulomb's model gives the following die pressure *p* at any radial coordinate *r* as (Ghosh and Mallik, 2010):

$$p = \sigma_o \exp\left\{\frac{2\mu}{H}(R-r)\right\}, \tag{5.3}$$

TH-3282_186103018

where σ_o is the flow stress, μ is the coefficient of friction, H is the height, R is the final radius of the disk and r is the radial coordinate. Total forging load P is obtained by integrating the die pressure p over the whole contact area of the disk with the platen shown as

$$P = \int_0^a 2\pi r p \mathrm{d}r, \tag{5.4}$$

On substituting Eq. 5.3 in Eq. 5.4 and on integration, the total forging load P is expressed as

$$P = \frac{\sigma_o \pi H}{\mu}\left[\frac{H}{2\mu}\left\{\exp\left(\frac{2\mu R}{H}\right)-1\right\}-R\right]. \tag{5.5}$$

An empirical relation for the estimation of forging load was given long back (Altan and Fiorentino, 1971) as

$$P = C_p \sigma_o A_p, \tag{5.6}$$

where C_p is the complexity factor and A_p is the plan area of the forging including flash. The aim of this chapter is to suggest a suitable value of C_p such that it can be used for any forging case. Equating Eq. 5.5 and Eq. 5.6, the shape complexity can be computed as

$$C_p = \frac{H}{\mu R^2}\left[\frac{H}{2\mu}\left\{\exp\left(\frac{2\mu R}{H}\right)-1\right\}-R\right]. \tag{5.7}$$

On substituting Eq. 5.7 in Eq. 5.6, the forging load is estimated. The suggested value of the complexity factor is applicable for any sizes and for any friction condition.

The efficacy of the proposed methodology for the estimation of forging load is further presented for the case of open die forging. FEM simulations are carried out and the information of the forging load obtained are assumed to be analogous to the feedback obtained from the shop floor. Prediction of forging load for geometrically similar shapes are carried out using the already existing information pertaining to size and friction condition. Results are discussed for open as well as closed die forging of axisymmetric shapes.

The value of the complexity factor is computed using Eq. 5.7 and the forging load is ultimately estimated using Eq. 5.6 for four different materials. They are JIS S25C steel (Shima and Mori, 1979), AISI 1015 steel (Dadras and Thomas Jr, 1983), AI 1100 aluminium (Park and Kobayashi, 1984) and commercially-pure aluminium (Hartley et al., 1980). The corresponding material properties and the hardening parameters are used for the

TH-3282_186103018

FEM simulation and for the estimation of σ_o. Results are presented for low aspect ratio and high aspect ratio.

5.3.1 Estimation of forging load for low aspect ratio (*R*/*H*)

In this case, the forging load is estimated for four materials viz., JIS S25C steel, AISI 1015 steel, AI 1100 aluminium and commercially-pure aluminium. The workpiece is of size 10 mm radius and 20 mm height, i.e., an aspect ratio of 0.5 is considered. Analysis is carried out for 10% as well as 40% reduction of the height. Forging takes place under lubricated as well as under non-lubricated condition. A value of μ as 0.1 may represent lubricated condition and a value of μ as 0.25 may represent non-lubricated condition. In cold forging, the Coulomb's coefficient of friction generally varies between 0.05 to 0.15; hence, μ as 0.25 can be considered as an extreme case. Simulations are carried out accordingly. The complexity factor for open die forging is estimated using Eq. 5.7 and is substituted in Eq. 5.6 for the estimation of forging load under both lubricated and non-lubricated condition as shown in Figure 5.4 and Figure 5.5. The obtained results show that there is good accuracy in the estimation of forging load for low aspect ratio. It is to be mentioned that for forging under lubricated as well as under non-lubricated condition, an error of less than 3% is achieved in all the cases.

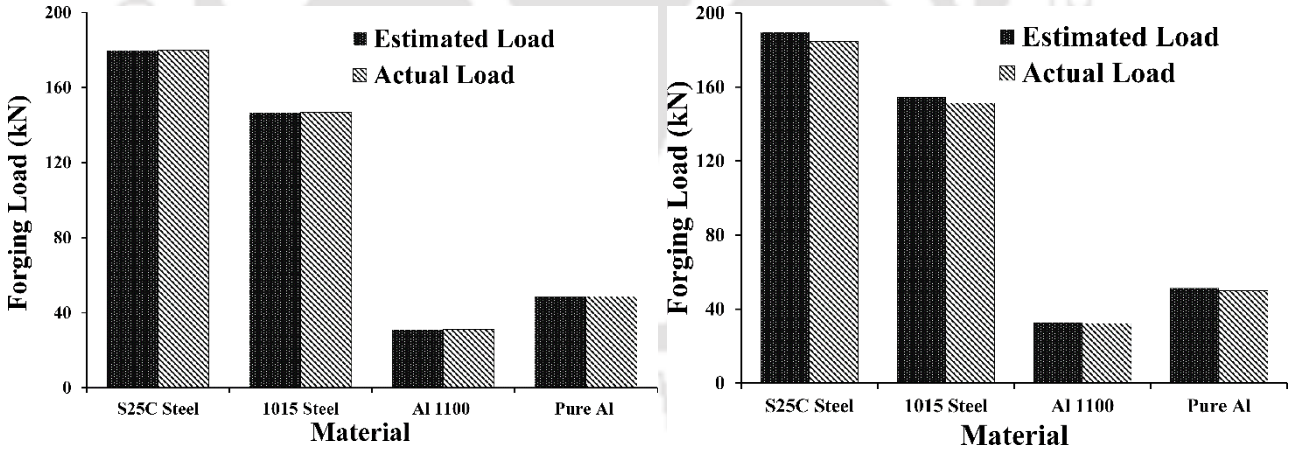

Figure 5.4 Estimation of forging load for 10% reduction (*R* = 10 mm and *H* = 20 mm) (a) lubricated condition, (b) non-lubricated condition

TH-3282_186103018

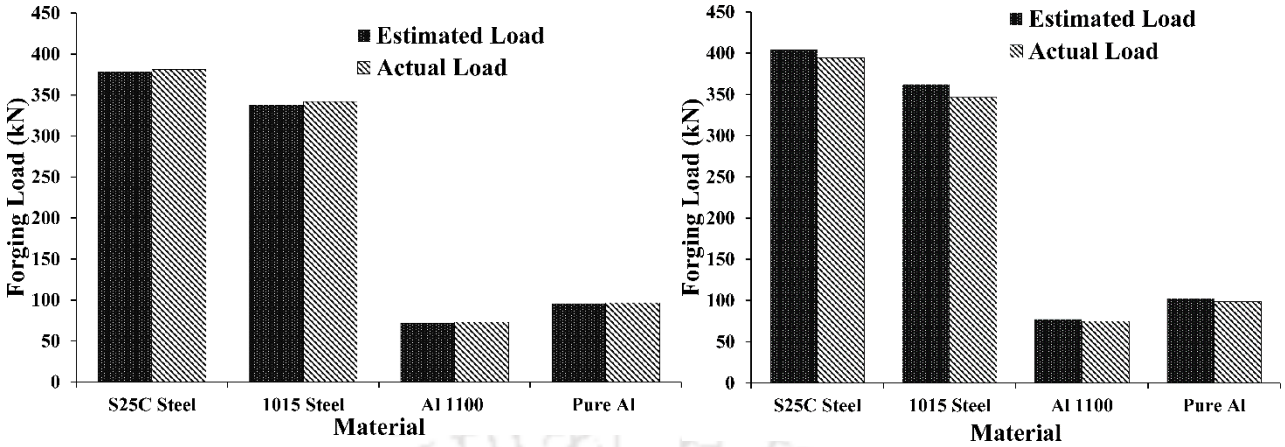

Figure 5.5 Estimation of forging load for 40% reduction (R = 10 mm and H = 20 mm) (a) lubricated condition, (b) non-lubricated condition

5.3.2 Estimation of forging load for high aspect ratio (R/H)

In this case also, forging load estimation is carried out for the four materials viz., JIS S25C steel, AISI 1015 steel, AI 1100 aluminium and commercially-pure aluminium. However, the workpiece is of size 40 mm radius and 10 mm height, i.e., an aspect ratio of 4 is considered. Analysis is carried out for 10% reduction in height. Forging takes place under lubricated as well as under non-lubricated condition. Forging load is estimated using Eq. 5.6 and the value of C_p is computed using Eq. 5.7. The estimated load is validated with the actual results obtained from simulation as shown in Figure 5.6. It can be seen from Fig. 5.6 that the estimated forging load matches well with the actual forging even at high aspect ratio. The maximum percentage error is observed to be around 3%.

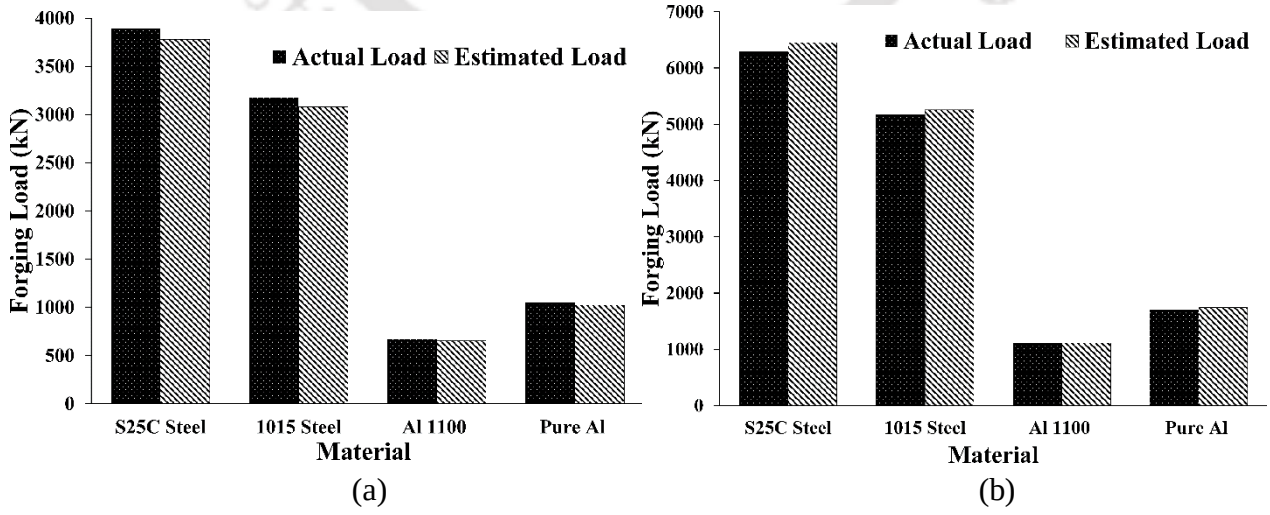

Figure 5.6 Estimation of forging load for 10% reduction (R = 40 mm and H =10 mm) (a) lubricated condition, (b) non-lubricated condition

TH-3282_186103018

5.4 Proposed methodology for estimation of forging load in closed-die forging

The proposed methodology is divided into two major segments. One segment involves identifying the closest shape from the database and the other segment involves using the closest shape for the estimation of forging load. Identification of the closest shape involves comparing the geometric attributes of the product to be forged with all the products available in the database. The database is kept in a cloud-based platform that can be accessed by industries using internet for estimation purpose. The procedure for estimating the closest shape is based on the nearest neighbour approach that is explained in details.

5.4.1 Identification of the geometrically closest shape from the database

The first step in the estimation of the forging load is to identify the geometrically closest product. Generally, humans use cognition for identifying the most similar product from a given set of products. The present chapter estimates a similarity index by comparing the information of the material, geometric features and friction condition for ascertaining if a new data entry is similar to an already existing product in the database. In this work, the initial shape of the axisymmetric products is assumed to be cylindrical and for the non-axisymmetric products, it is assumed to be prismatic. Similarity estimation is carried out by both non-numeric and numeric attributes of the product. Similarity measure for a non-numeric attribute is estimated as

$$\text{sim}(f_i, f_r) = \begin{cases} 1, & \text{if } f_i = f_r \\ 0, & \text{if } f_i \neq f_r \end{cases}, \tag{5.8}$$

where f_i is the non-numeric attribute of the new product and f_r is the non-numeric attribute of the compared product already preserved in the database. A value of 1 indicates perfect matching. On the other hand, a value of 0 indicates a prefect non-matching case. Following are the non-numeric attributes: (1) material and (2) friction condition— lubricated or non-lubricated.

The similarity measure for a numeric attribute is estimated as

$$\text{sim}(f_i, f_r) = 1 - \frac{|f_i - f_r|}{R_d}. \tag{5.9}$$

where f_i is the numeric attribute of the new product, f_r is the numeric attribute of the compared product already preserved in the database and R_d is the difference between the

TH-3282_186103018

maximum and minimum value of the attribute being compared. For the numeric data, a similarity measure of close to 1 indicates almost perfect closeness of two products; similarity measure of zero indicates no closeness. The final forged product is hypothetically enclosed in an enveloping cylinder for an axisymmetric product and in an enveloping prism for a non-axisymmetric cylinder. The essential numeric attribute preserved for evaluating the similarity of an axisymmetric product are as follows: (1) blank radius, (2) blank height, (3) envelope radius, and (4) envelope height. The essential numeric attribute preserved for evaluating the similarity of a non-axisymmetric product are as follows: (1) blank length, (2) blank width, (3) blank height, (4) envelope length, (5) envelope width and (6) envelope height. In addition to the aforesaid attributes, following three attributes are calculated from the already preserved information: (1) Blank volume, (2) Envelope volume and (3) Difference between the envelope volume and blank volume.

For evaluating the overall similarity, a nearest neighbor algorithm proposed by Kolodner (2014) for case-based reasoning has been used (Watson 1995). As per this, the overall similarity is given by the weighted average of the similarities of all the attributes. Although it is possible to explore various methods for the estimation of similarity, this method is easy to implement and quickly estimates the overall similarity to accurately suggest the most similar product. However, in the present work, all the attributes are assigned equal weightage. Therefore, the overall similarity is evaluated as

$$\text{sim}(\text{product}_\text{i}, \text{product}_\text{r}) = \frac{\sum_{i=1}^{n} \text{sim}(f_\text{i}, f_\text{r})}{n_a}. \tag{5.10}$$

where product_i is the unseen new product to be forged, product_r is the compared product from the database and n_a is the total number of attributes (numeric as well as non-numeric). With a new product, all the products of database are compared. The one having the highest overall similarity is chosen as the most similar model. In order to reduce the computational time, the comparison can be stopped as soon as a product with 0.95 similarity is found. The next step involves using the information of the most similar model for the estimation of the forging load using a semi-analytical model as discussed in the subsequent section.

5.4.2 Estimation of forging load using the geometrically closest shape

The second segment involves using the most similar forged product for the estimation of forging load for a new product. It is considered to be a challenging task, as it requires

TH-3282_186103018

effectively using the existing information of shape, size, geometry, material and friction condition. Forging load estimation using the already forged product data was recently suggested by Chatterjee et al. (2022). The present work is an extension of the earlier work that elaborates on finding the most similar product and on tackling the uncertainty associated with the material properties and friction condition for the estimation of forging load. It is the first application of using fuzzy set theory for making accurate forging load estimation based on the information of similar axisymmetric forged products. FEM simulations of axisymmetric products are carried out to supply forging data for the proposed scheme. Forging load feedback from the ABAQUS-simulations are assumed to signify feedback from an industrial environment. The rest of the research work deals with the uncertainty associated with the estimation of complexity factor and using it for accurately predicting the forging load.

Flow stress and friction condition are the two main uncertain parameters associated with the estimation of forging load. The uncertainty associated with both the parameters is dealt with by representing them as fuzzy parameters. The values of yield strength, strain hardening coefficient and coefficient of friction are considered to be fuzzy parameters in this study. There can be various methodologies that can be adopted to obtain the membership grade. The membership grades are generally obtained from experts. The values of the membership grade lie between 0 and 1, where 0 represents non-membership and 1 represents complete membership. For the sake of simplicity, a triangular membership function is considered in the study. In the triangular membership function, a membership grade of 0.5 represents either lower (l) or higher (h) bound estimates of the parameter under consideration. On the other hand, a membership grade of 1 always represents most likely (m) estimate of the parameter under consideration. Fuzzy arithmetic operation involves basic mathematics to deal with the fuzzy parameters at a particular membership grade.

For the fuzzy set-based load estimation in closed die forging, the following steps are considered:

I. Obtain the low (l), high (h) and most likely (m) estimates of the yield strength, strain hardening coefficient and coefficient of friction. Develop the fuzzy membership function corresponding to the membership grade.

II. The forging load for closed die forging is estimated by substituting all the deterministic parameters as fuzzy parameters and arithmetic operation as fuzzy

TH-3282_186103018

arithmetic operation. Generally, the four arithmetic operations, viz., addition, subtraction, multiplication and division are replaced with fuzzy arithmetic operations.

III. Fuzzy arithmetic operations are carried out for a particular membership grade α. If a particular fuzzy parameter is represented by A with an interval (a_1^{α}, a_2^{α}) and another fuzzy parameter is represented by B with an interval (b_1^{α}, b_2^{α}), then the fuzzy arithmetic operations for that specific membership grade is estimated as (Dixit and Dixit 2008)

$$\text{Fuzzy addition: } (a_1^{\alpha}, a_2^{\alpha}) + (b_1^{\alpha}, b_2^{\alpha}) = (a_1^{\alpha} + b_1^{\alpha}, a_2^{\alpha} + b_2^{\alpha}) \quad (5.11)$$

$$\text{Fuzzy subtraction: } (a_1^{\alpha}, a_2^{\alpha}) - (b_1^{\alpha}, b_2^{\alpha}) = (a_1^{\alpha} - b_2^{\alpha}, a_2^{\alpha} - b_1^{\alpha}) \quad (5.12)$$

$$\text{Fuzzy multiplication: } (a_1^{\alpha}, a_2^{\alpha}) \times (b_1^{\alpha}, b_2^{\alpha}) = (a_1^{\alpha} \times b_1^{\alpha}, a_2^{\alpha} \times b_2^{\alpha}) \quad (5.13)$$

$$\text{Fuzzy division: } (a_1^{\alpha}, a_2^{\alpha}) \div (b_1^{\alpha}, b_2^{\alpha}) = (a_1^{\alpha} \div b_2^{\alpha}, a_2^{\alpha} \div b_1^{\alpha}) \quad (5.14)$$

As the process parameters are fuzzy, the output obtained is also fuzzy, i.e., each output parameter possesses a range of values rather than a fixed value.

5.5 Forging load estimation in closed die forging

The methodology is illustrated for four closed die products. Forging is carried out under lubricated and as well as under non-lubricated condition. The computer aided design (CAD) model of the four products considered in this study is shown in Figure 5.7. The effect of radius, height, material and friction condition are considered for the estimation of forging load.

TH-3282_186103018

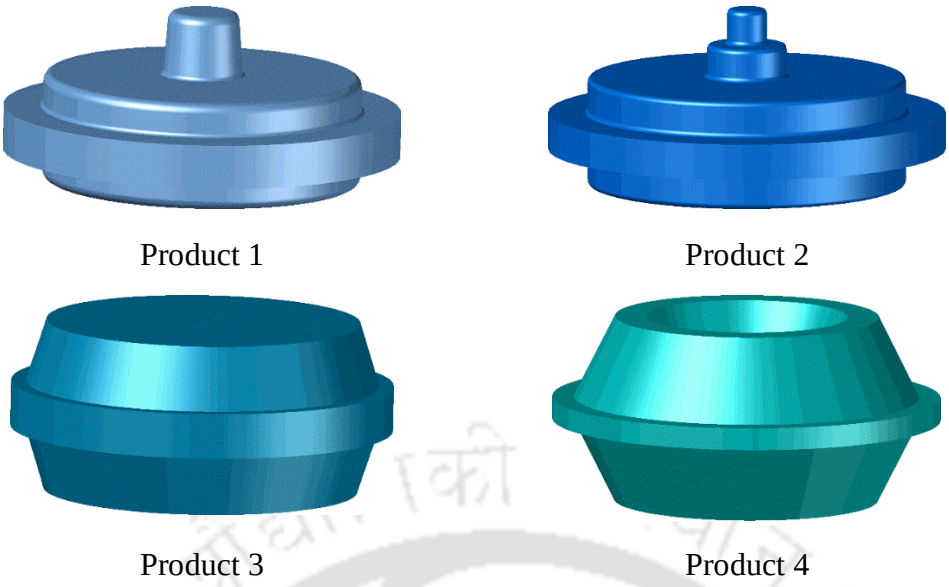

Figure 5.7 Four closed die products used in the study

5.5.1 Forging load estimation for varying sizes of the workpieces

Forging load is estimated for three possible scenarios, viz., varying the radius with height remaining constant, varying the height with radius remaining constant, and varying both radius and height. All the scenarios are explained by considering two models for the same product. In the sequel, three situations are explained.

Models vary in projected radius with no change in height. Two models with different radius and same height are considered. It is assumed that the information of the forging load for the workpiece with larger projected radius is available. The load estimation for the smaller workpiece is required under similar friction condition with the height remaining same. From Eq. 5.6, the estimated load P for the smaller model is evaluated as

$$P_{\text{small}} = \left(\frac{R_{\text{small}}}{R_{\text{large}}} \right)^2 \times P_{\text{large}}. \tag{5.15}$$

where R is the projected radius of the closed die model. Similar procedure is employed when information of the model with larger projected radius is available and information of the smaller model is required to be estimated for a similar friction condition. In fact, complexity factor can also be changed proportionately using Eq. 5.7. Later on, depending on the feedback of the actual simulated load, the complexity factor is preserved.

Models vary in height with no change in projected radius. Two models with different height and same projected radius are considered. It is assumed that the information

TH-3282_186103018

for the taller workpiece is available and it is required to estimate the forging load of the smaller workpiece with unchanged friction condition. The C_p of the smaller workpiece is estimated as

$$\left(C_p\right)_{\text{closed-short}} = \frac{C_p \text{ from Eq. 5.7 for short model}}{C_p \text{ from Eq. 5.7 for tall model}} \times \left(C_p\right)_{\text{closed-tall}}. \tag{5.16}$$

On substituting the roughly estimated C_p in Eq. 5.6, the forging load is estimated. Similar methodology is again adopted in case when the information is available for shorter model and load estimation is required for the taller model under similar friction condition. On obtaining the feedback from the shop floor, the value of the complexity factor is preserved in the database.

Models vary in height and projected radius. In the last scenario, two models with different height and projected radius are considered. The information of the small model is available and load is required to be estimated for the large model under similar friction condition. The value of C_p for the large model is roughly estimated as

$$\left(C_p\right)_{\text{closed-large}} = \frac{C_p \text{ from Eq. 5.7 for small model}}{C_p \text{ from Eq. 5.7 for large model}} \times \left(C_p\right)_{\text{closed-small}}. \tag{5.17}$$

The value of C_p is substituted in Eq. 5.6 to obtain the estimated value of the forging load. The methodology remains the same when information is available for the larger model under similar friction condition. Nevertheless, the C_p is preserved in the database based on the feedback of the simulated forging load.

5.5.2 Forging load estimation for varying friction condition

Two models with similar height and projected radius are considered. However, the friction condition in this case is different and information of the non-lubricated condition exits. There is a need to estimate the forging load for lubricated condition. The complexity factor is roughly evaluated as

$$\left(C_p\right)_{\text{closed-lubriacted}} = \frac{C_p \text{ from Eq. 5.7 for } \mu \text{ of lubricated case}}{C_p \text{ from Eq. 5.7 for } \mu \text{ of non-lubricated case}} \times \left(C_p\right)_{\text{closed-nonlubriacted}}. \tag{5.18}$$

The methodology remains the same when information is available for the lubricated case and estimation is required for the non-lubricated model. On obtaining the simulated feedback of the forging load, the value of the complexity factor is preserved for further usage.

TH-3282_186103018

5.5.3 Forging load estimation for varying materials

For varying materials, the methodology remains the same in case when sizes and friction conditions vary, as explained in Section 5.5.1 and 5.5.2. Nevertheless, the simulated value of the complexity factor is always preserved for further usage pertaining to a specific material. The results based on varying geometry, friction condition and material are presented in Section 5.6 and 5.7.

5.6 System Structure

In the proposed fuzzy set-based estimation of forging load, the cloud supports the forging data and computing facilities. Industries can obtain data as well as computational services as required. The simulated forging data are preserved in forging database that is maintained by a web server. The fuzzy set-based optimization of forging load is implemented by writing a code in 'R', an open source statistical programming language with graphical user interface (GUI). The user interacts with the system by providing all the geometric information and the material properties of the new product to be forged. The system in turn suggests the upper, most-likely and lower estimates of forging load, thereby providing a guideline for the process planner to allocate a suitable forging machine.

The methodology suggests in preserving the available shop floor information of the axisymmetric forged products. In this study, all the initial blanks are considered to be cylindrical in shape. For illustration purpose, 'MySQL' relational database system is used to store the forging data in web server. The forging data viz. material, blank radius, blank height, projected radius, projected height, friction condition and complexity factor are preserved. The 'MySQL' database is accessed by using the 'dbConnect' function in 'R. The 'dbConnect' requires username, password, name of the database and the host internet protocol (IP) address for accessing remotely. Every webserver has a specific IP address referred to as the domain name. After establishing the connection with the database, 'dbSendQuery' is used to fetch the complete dataset in the 'R' programming environment for estimating the most similar product available in the database. After estimating the upper, most likely and lower estimates of the forging load, again a connection is established with the database using the 'dbConnect' function. The new data is updated in the database using the function 'dbWriteTable'. Finally, the database is disconnected from the 'R' environment using the function 'dbDisconnect', so as to ensure only authorized personnel can only access and edit the database.

TH-3282_186103018

The industries using the proposed scheme, contribute to the aforesaid forging data that is maintained by the web server. Whenever a product is required to be forged, the most similar data is retrieved and the information is used for estimating the lower, most-likely and higher estimate of the forging load. The web-based system permits the industries to remotely access the information stored in the database. The user needs to submit the information such as material, blank height, blank radius, projected radius, projected height, friction condition, material hardening parameters. The scheme in turn suggest an interval estimation the forging load. The feedback of the FEM simulated forging load is taken that is further used for approximately estimating the complexity factor to be preserved in the forging database as suggested in Figure 5.8. The scheme is analogous to the operators suggesting forging load based on his experience and intuition.

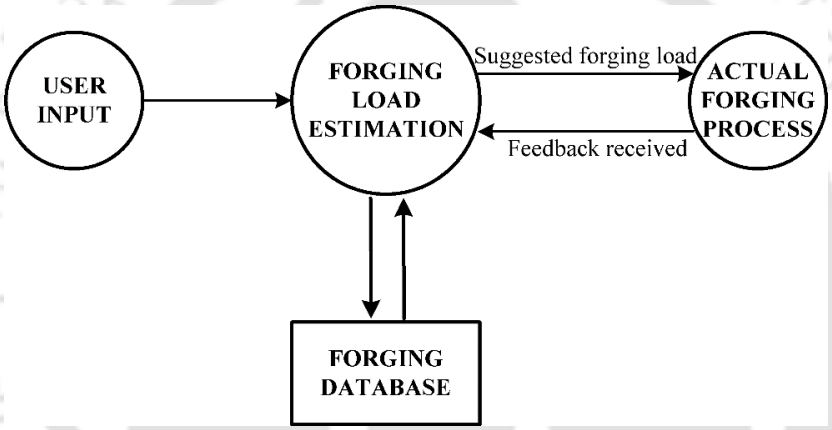

Figure 5.8 Scheme for the estimation of forging load

5.7 Case Studies

The adoption of fuzzy logic helps to deal with the uncertainty associated with the estimation of forging load. As already discussed in detail, the hardening parameters and friction condition are considered as fuzzy. In this study, it is assumed that there may be a variation of ±10% in the estimation of yield stress and a variation of ±20% in the estimation of hardening coefficients respectively (Dixit and Dixit 1996). Depending on the geometric dimensions of the model and their corresponding flow stress equation, the lower, most likely and upper values are estimated accordingly. For the coefficient of friction, there are two possibilities: lubricated condition and non-lubricated condition. For lubricated condition, the coefficient of friction for low, most likely and high estimates are considered as 0.02, 0.10 and 0.15 respectively. For non-lubricated condition, the coefficient of friction for low, most likely and high estimates are considered as 0.15, 0.22 and 0.32 respectively.

TH-3282_186103018

Forging load is estimated for three possible scenarios, viz., varying the height with radius remaining constant, varying the radius with height remaining constant and by varying both radius and height. All the four products are considered to be made out of lead. The developed GUI for estimating the forging load based on the information of similar model is shown in Figure 5.9. Figure 5.9 (a) and Figure 5.9 (b) show the input parameters entered by the user. Based on the input parameters and the information of the similar model, the scheme predicts the lower, most-likely and upper estimates of the forging load in kN as shown in Figure 5.9 (c). It is interfaced with MySQL, a relational database platform for preserving the forging data that is handled by the administrator. Whenever any request is made to access the database, the web server handles such request. It is proposed that the manufacturing industries at different locations can access the GUI through their web browsers and operate at their locations.

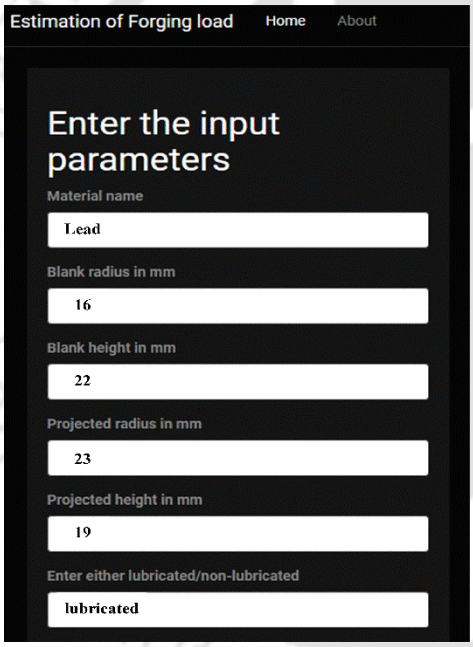

(a) Input screen 1

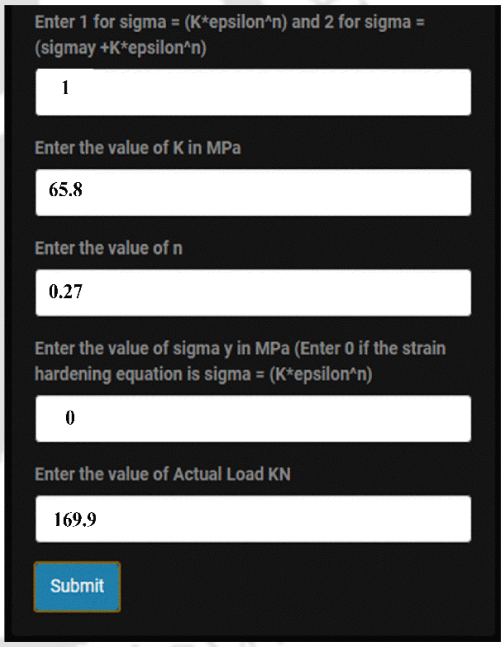

(b) Input screen 2

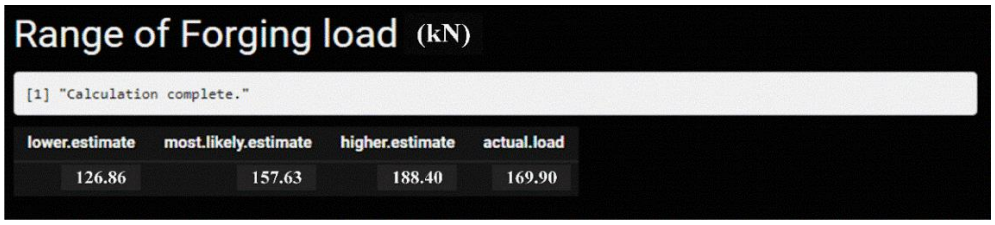

(c) Final display of the forging load estimation

Figure 5.9 Snapshots of the user interface

TH-3282_186103018

5.7.1 Forging load estimation for models with varying height and constant radius

For demonstrating the effect of height on the estimation of forging load, product 1 as shown in Figure 5.7 is first considered. The different models of product 1 with varying heights and radius remaining same are shown in Figure 5.10. The initial dimensions of all the models shown in Figure 5.10 are presented in Table 5.1. FEM simulations are carried out for the eight models of Product 1 under lubricated condition. The scheme uses the information of the geometrically closest shape to predict the forging load. The virtually simulated load that is assumed to be generated from the shop floor is found to be 219.7 kN for Model 1 with the corresponding value of C_p as 2.19. The information obtained is further used for the estimation of forging load for the rest of the models. Only in the first instance, Model 1 is used to predict the forging load of Model 2, as there is only one model available in the database. As both the models are having similar projected radius, forging load is estimated using Eq. 5.6 under similar lubricated condition. The lower, most likely and higher estimates of load for Model 2 are 179.9 kN, 219.8 kN and 266.1 kN respectively. The simulated forging load is obtained as 181.2 kN. The actual simulated load is observed to lie close to the lower estimate of the forging load. The C_p is preserved in the database based on the actual simulated load for Model 2. The complete results are presented in Table 5.1 and Figure 5.11.

From Model 3, evaluation of the similarity index is carried out based on the methodology discussed in Section 5.4.1. It is observed that Model 2 is having higher similarity compared to Model 1 due to the geometric closeness. A similarity index value of 0.722 is observed. The complexity factor of model 2 is used for the estimation of model 3. It is observed that the lower, most likely and higher estimates of load for model 3 are 148.7 kN, 180.4 kN and 216.9 kN respectively. The simulated forging load is obtained as 153.5 kN. It is observed that the simulated load lies within the lower and the most likely estimate.

Similarly, for estimating the forging load of Model 4, estimation of similarity index is carried out by comparing the Model 4 with the rest of the models. It is observed that the overall similarity is the highest is case of Model 3. A similarity index value of 0.770 is observed. Thus, the complexity factor of Model 3 is fetched to be used for estimating the forging load of Model 4. It is observed that the lower, most likely and higher estimates of load for Model 4 are obtained as 126.8 kN, 153.2 kN and 183.4 kN respectively. The simulated forging load is obtained as 139.8 kN. In this case also, the actual simulated load is observed to lie between the lower and the most likely estimate.

TH-3282_186103018

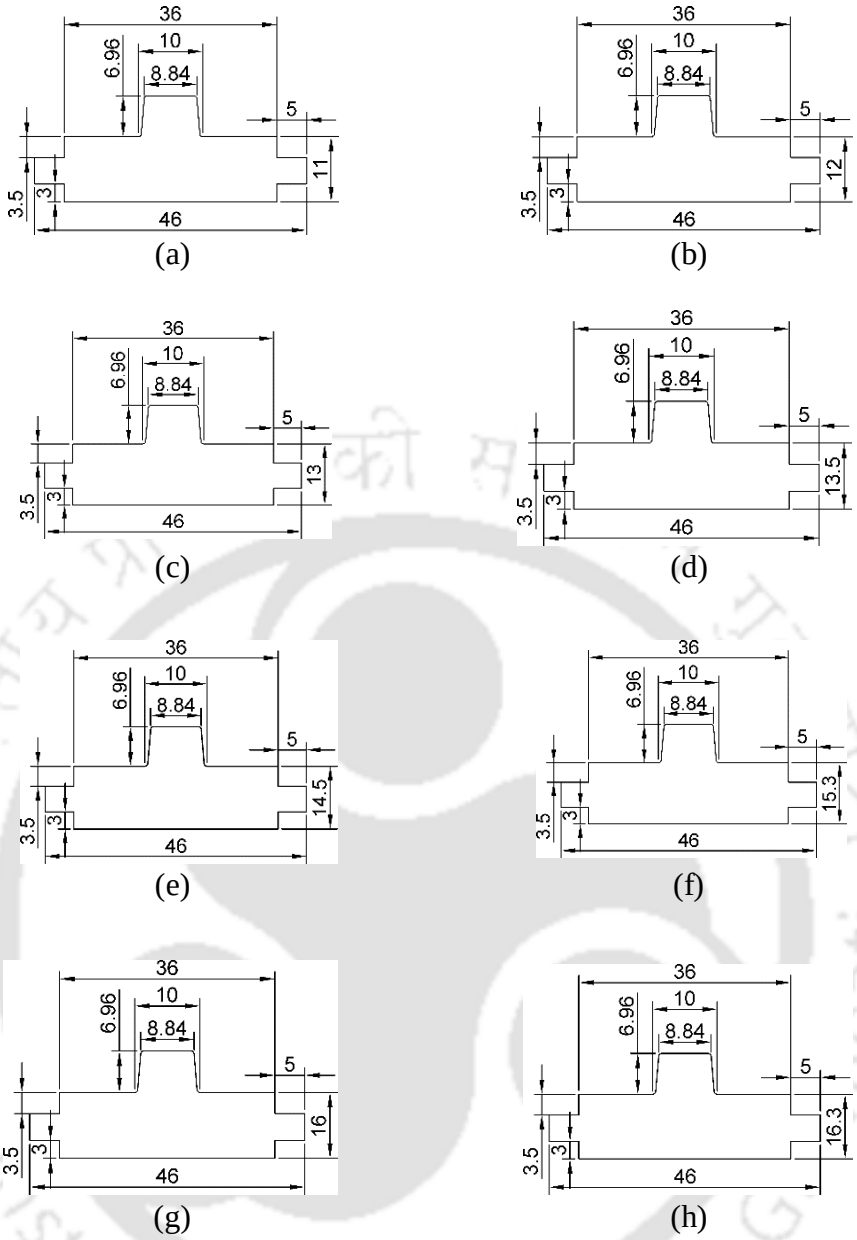

Figure 5.10 Closed die forged Product 1: (a) Model 1, (b) Model 2, (c) Model 3, (d) Model 4, (e) Model 5, (f) Model 6, (g) Model 7 and (h) Model 8

As the process is repeated for the rest of the models, the data is increasing and so is the value of the overall Similarity index. It is observed that a value of overall similarity greater than 0.85 suggests a more accurate value of the complexity factor. The actual load in case of Model 5, Model 6, Model 7 and Model 8 matches well with the most likely estimate. All the new forging information are preserved in the 'MySQL' database. The results of all the models of product 1 are shown in Table 5.1. Figure 5.11 provides a visual description of the results.

TH-3282_186103018

Table 5.1 Forging load estimation for varying height of Product 1

Product	Model	Blank radius (mm)	Blank height (mm)	Friction condition	Simulated (actual) load (kN)	Similarity index	Similar product	Similar model
1	1	16	20	lubricated	219.7	–	–	–
1	2	16	22	lubricated	181.2	–	1	1
1	3	16	24	lubricated	153.5	0.722	1	2
1	4	16	26	lubricated	139.8	0.770	1	3
1	5	16	28	lubricated	132.4	0.873	1	4
1	6	16	30	lubricated	133.4	0.899	1	5
1	7	16	32	lubricated	135.8	0.881	1	6
1	8	16	34	lubricated	134.0	0.909	1	7

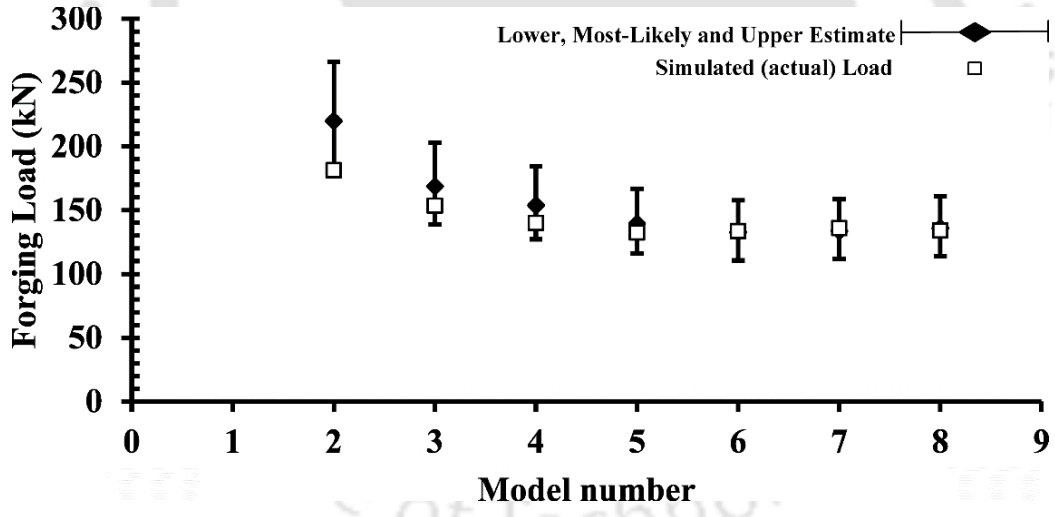

Figure 5.11 Predicted values versus simulated values for Product 1

Product 2 is also considered to understand the effect of height for the prediction of forging load. The models of Product 2, shown in Figure 5.12 are used for further analysis. The initial dimensions of all the models of Product 2 are shown in Table 5.2. Similar to Product 1, FEM simulations are carried out under lubricated condition for the four models shown. This time, the aim is to initially use the information of Product 1 in Product 2 and then subsequently use the information of Product 2.

TH-3282_186103018

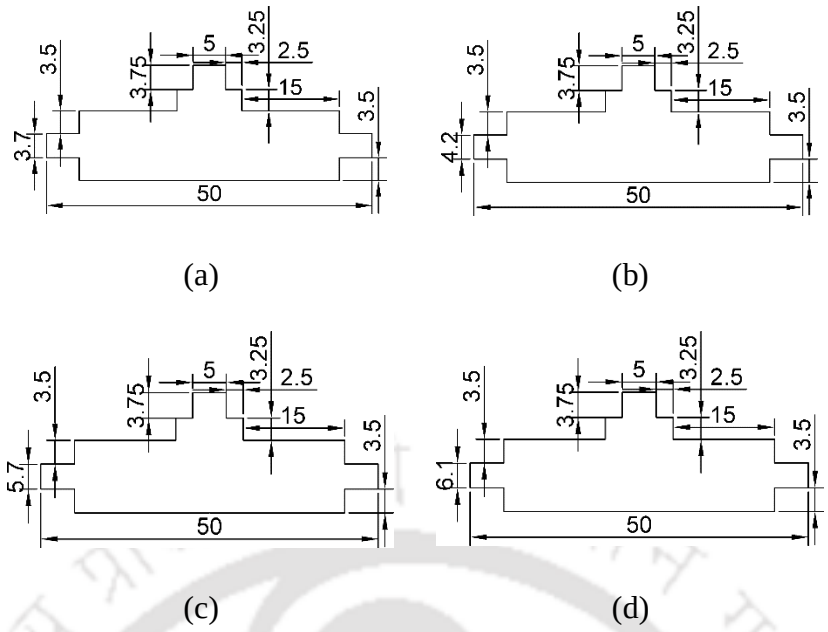

Figure 5.12 Closed die forged Product 2: (a) Model 1, (b) Model 2, (c) Model 3 and (d) Model 4

The overall similarity for Model 1 of Product 2 is estimated with all the models of Product 1 using the procedure explained in Section 5.4.1. Based on the value of the similarity obtained, the specific model is used for estimation. For Product 2 also all the models are simulated under lubricated condition. Among all the models of Product 1, Model 2 of product 1 is having the highest similarity index with Model 1 of Product 2. The similarity index is estimated to be 0.621. The complexity factor of the chosen model is fetched from the forging database. The retrieved value of C_p is further used to estimate the low, most likely and high estimates of closed die forging load for Model 1 of Product 2. The low, most likely and high estimates of forging load for Model 1 of Product 2 are 172.36 kN, 211.35 kN and 255.2 kN respectively. The feedback of the simulated load is 261.7 kN. The simulated load is observed to be lie just outside the interval estimate. The complexity factor based on the information of the simulated load is preserved in the database. It can be seen from Table 5.2that overall similarity for the model used for estimating the forging load is much less than 1. Hence, the actual simulated load lies outside the interval estimates.

The methodology adopted for Product 1 to estimate the forging load is also adopted for Product 2. For Model 2 of Product 2, the overall similarity is estimated. In this case, the overall similarity is highest when compared with Model 1 of Product 2. The value is estimated as 0.92. The value of the complexity factor for Model 1 is fetched and is used for estimation of Model 2. The three estimates of forging load are estimated as 211.4 kN, 260.7

TH-3282_186103018

kN and 318.8 kN. The simulated load is 253.6 kN. The simulated load again lies within the estimated range and matches well with the most-likely estimate. Similarly, overall similarity is estimated for the rest of the two models of Product 2, i.e., Model 3 and Model 4. For Model 3, the closest model is estimated to be Model 2 of Product 2 and for Model 4, the closest model is estimated to be Model 3 of Product 2. In both the cases, the overall similarity is estimated to be approximately 0.9. Hence, the simulated load for both Model 3 and Model 4 matches well with the most-likely estimate as shown in Table 5.2 and Figure 5.13.

Table 5.2 Forging load estimation for varying height of Product 2

Product	Model	Blank radius (mm)	Blank height (mm)	Friction condition	Simulated (actual) load (kN)	Similarity index	Similar product	Similar model
2	1	18	18	lubricated	261.7	0.621	1	2
2	2	18	20	lubricated	253.6	0.920	2	1
2	3	18	22	lubricated	243.8	0.880	2	2
2	4	18	24	lubricated	231.4	0.920	2	3

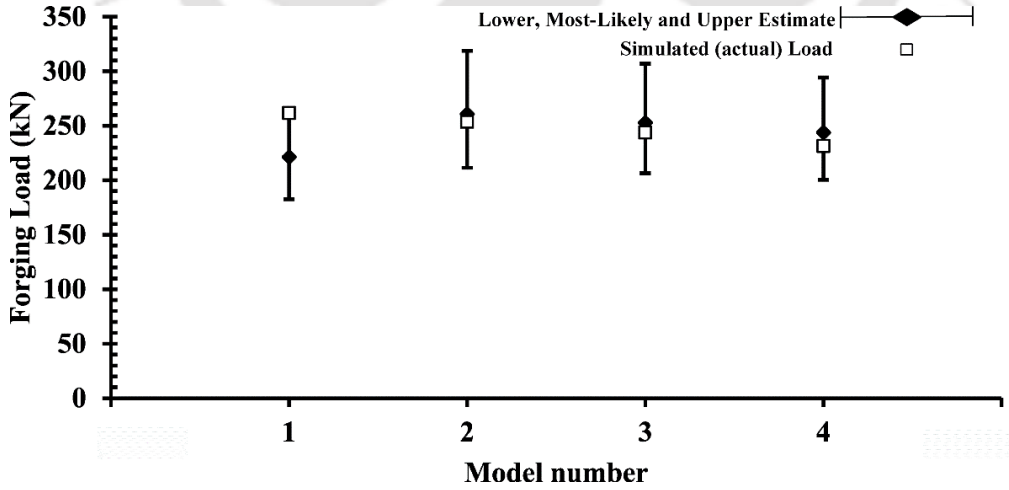

Figure 5.13 Predicted values versus simulated values for Product 2

TH-3282_186103018

5.7.2 Forging load estimation for models with varying height and radius

For demonstrating the effect of both height and radius for the estimation of forging load, Product 3 as shown in Figure 5.7 is now considered. The initial dimensions of all the models shown in Figure 5.14 are presented in Table 5.3. Closed die forging is simulated for the eight models of Product 3 with different height and projected radius as shown in Figure 5.14. The scheme uses the existing information of Product 1 and Product 2 for the prediction of Product 3.

On comparing the overall similarity for Model 1 of Product 3 with all the existing models of Product 1 and Product 2, Model 7 of Product 1 is having the highest overall similarity. A value of 0.779 is observed. The corresponding value of the complexity factor is fetched from the database that is used to predict the forging load for Model 1 of Product 3. The estimated values of low, most likely and high estimates are 149.5 kN, 284.4 kN and 439.4 kN respectively. The simulated load observed is 347.5 kN. As the value of the overall similarity is less than 0.85 and the shape is completely new in the database, the simulated load lies outside the interval estimate. The complexity factor is preserved based on the simulated load observed. The preserved complexity factor is further used for the estimation of forging load.

Model 2 of Product 3 is then compared with rest of the available Models in the database. Model 1 of Product 3 is estimated to have the highest overall similarity. A value of 0.85 is evaluated. The corresponding complexity factor is fetched from the database that is used for interval estimation. It is found that the simulated load lies well within the lower and the most-likely estimate. Based on the simulated load, the complexity factor is preserved. The process continues with the estimation of the similarity of the rest of the models of Product 3. Estimation of the forging load is carried out accordingly. With the value of overall similarity exceeding 0.85, the scheme is found to suggest reasonably accurate complexity factor. As the simulated load matches well with the most likely estimate as shown Table 5.3 and Figure 5.15. It is also observed from Eq. 4 and Figure 5.15 that projected radius is have a greater effect on the estimation of forging load.

TH-3282_186103018

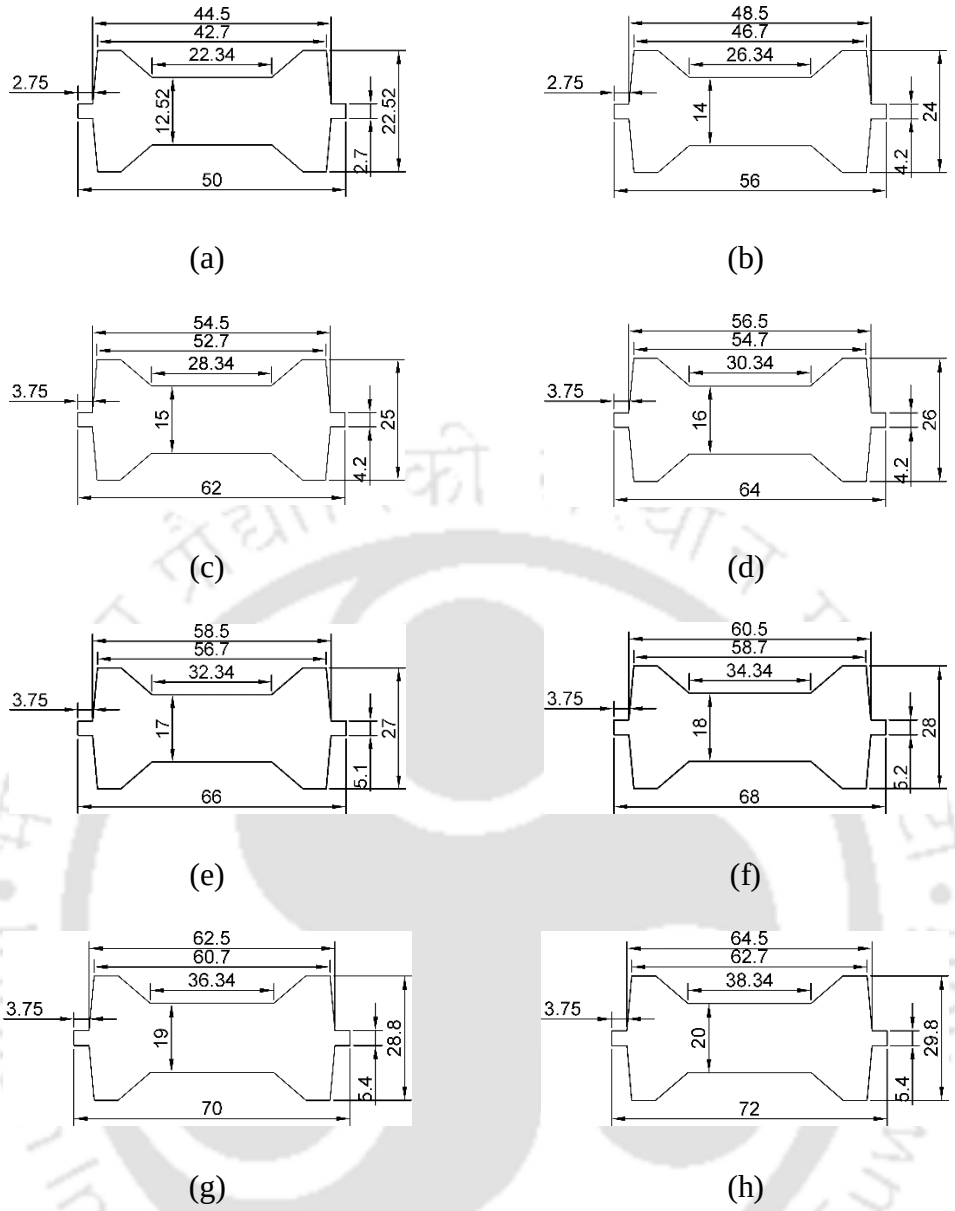

Figure 5.14 Closed die forged Product 3: (a) Model 1, (b) Model 2, (c) Model 3, (d) Model 4, (e) Model 5, (f) Model 6, (g) Model 7 and (h) Model 8

TH-3282_186103018

Table 5.3 Forging load estimation for varying height and radius of Product 3

Product	Model	Blank radius (mm)	Blank height (mm)	Friction condition	Simulated (actual) load (kN)	Similarity index	Similar product	Similar model
3	1	17	32	lubricated	347.5	0.779	1	7
3	2	19	35	lubricated	395.3	0.845	3	1
3	3	20	38	lubricated	434.7	0.872	3	2
3	4	21	41	lubricated	526.5	0.889	3	3
3	5	22	44	lubricated	587.6	0.898	3	4
3	6	23	47	lubricated	655.4	0.904	3	5
3	7	24	50	lubricated	729.3	0.905	3	6
3	8	25	53	lubricated	782.2	0.909	3	7

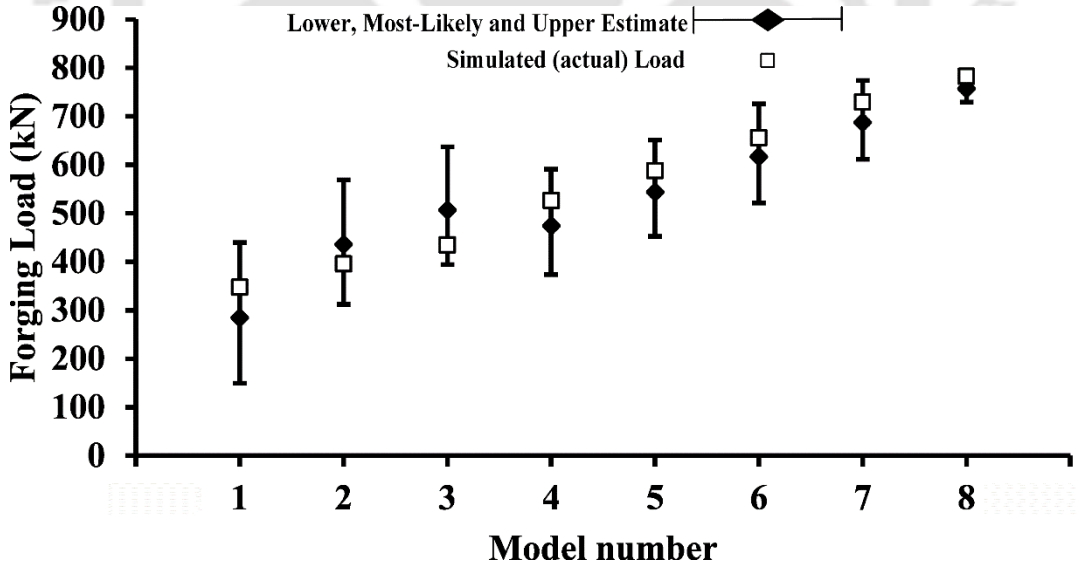

Figure 5.15 Predicted values versus simulated values for Product 3

5.7.3 Forging load estimation for models with varying radius and constant height

For demonstrating the effect of radius for the estimation of forging load, Product 4 shown in Figure 5.7 is now considered. The initial dimensions of all the models shown in Figure 5.16 are presented in Table 5.4. FEM simulations are carried out for the eight

TH-3282_186103018

models of Product 4 with different projected radius and similar height under lubricated condition. The scheme computes the overall similarity for Model 1 of Product 4 with all the existing models till now. It is observed that Model 1 of Product 3 is having the highest overall similarity. The Similarity index is evaluated to be 0.859. Thus, Model 1 of Product 3 is used for the prediction of forging load for Model 1 of Product 4. On fetching the value of C_p for Model 1 of Product 3, the low, most likely and high estimate for closed-die forging load under lubricated condition are estimated to be 123.3 kN, 293.9 kN and 495.4 kN respectively. The simulated load observed is 307.6 kN. The most-likely estimate is close to the simulated load. The complexity factor for Model 1 of Product 4 is preserved based on the obtained simulated load to be used for further estimation of forging load.

The scheme continues with the estimation of the Similarity index for Model 2 of Product 4 with the rest of the existing models. Model 1 of Product 4 is estimated to have the highest Similarity index with Model 2 of Product 4. The Similarity index is 0.945. The chosen complexity factor is fetched and is used for estimation. In this case, the low, most likely and higher load are computed as 207.9 kN, 359.4 kN and 536.6 kN respectively. The simulated load is 419.3 kN. It is observed that the simulated load lays well within the interval estimate. The actual complexity factor is preserved based on the obtained simulated load.

Similarly, the Similarity index is again computed for Model 3 of Product 4 with all the existing models. Model 2 of Product 3 is estimated to have the highest Similarity index. The complexity factor for the model 2 is fetched from the database for estimation purpose. For Model 3, the value of the low, most likely and high estimate of forging load are computed to be 356.0 kN, 490.6 kN and 646.6 kN respectively. The simulated load is observed to be 466.5 kN. The simulated load is again observed to lie well within the interval estimate. The process continues with the rest of the models of Product 4 and the results are shown in Table 5.4 and Figure 5.17.

TH-3282_186103018

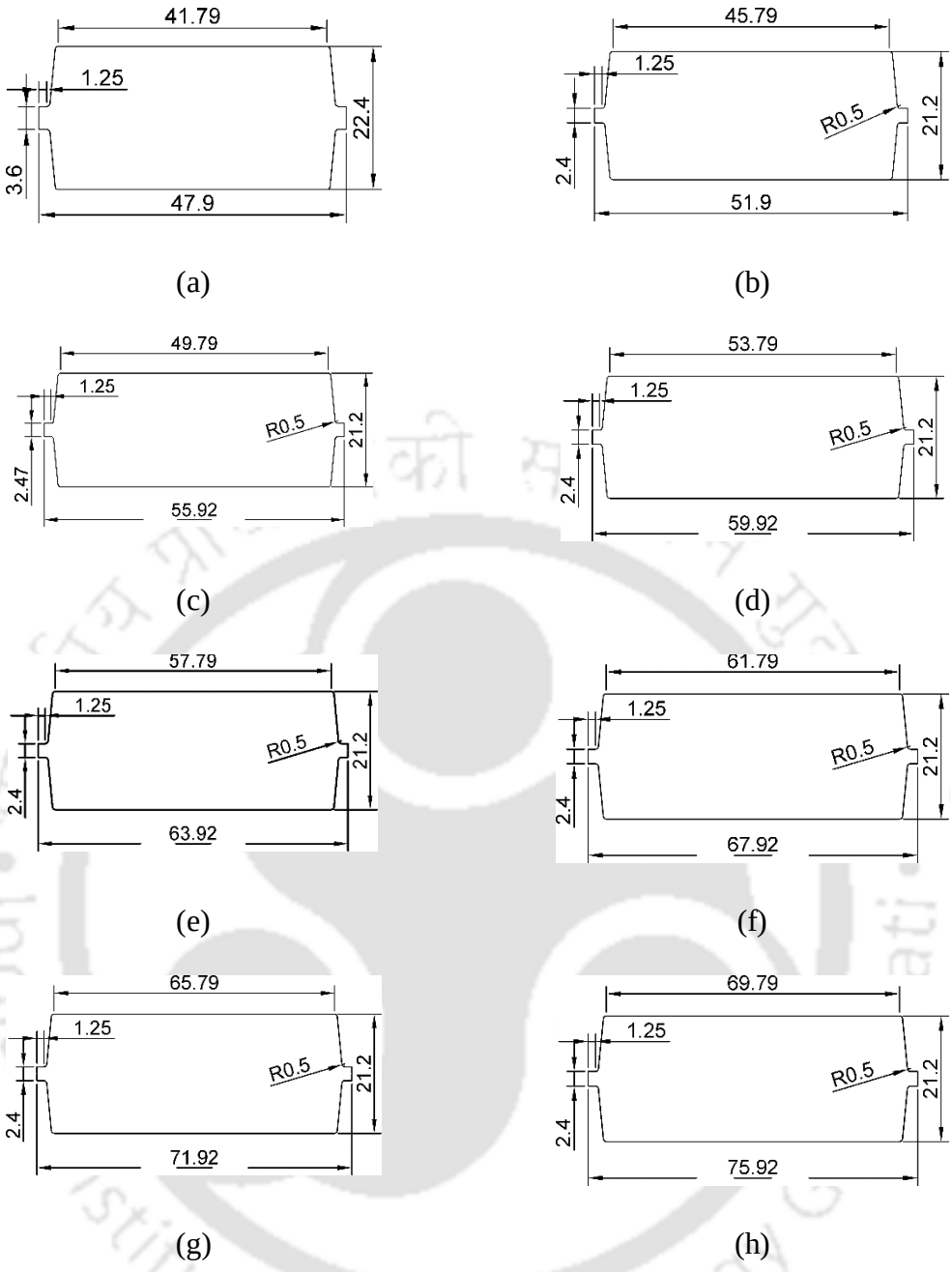

Figure 5.16 Closed die forged Product 4: (a) Model 1, (b) Model 2, (c) Model 3, (d) Model 4, (e) Model 5, (f) Model 6, (g) Model 7 and (h) Model 8

TH-3282_186103018

Table 5.4 Forging load estimation for varying radius of Product 4

Product	Model	Blank radius (mm)	Blank height (mm)	Friction condition	Simulated load (kN)	Similarity index	Similar product	Similar model
4	1	17	32	lubricated	307.6	0.859	3	1
4	2	18.25	32	lubricated	419.3	0.945	4	1
4	3	19.5	32	lubricated	466.5	0.936	4	2
4	4	23	32	lubricated	559.3	0.913	4	3
4	5	24.75	32	lubricated	621.4	0.912	4	4
4	6	26.25	32	lubricated	689.6	0.941	4	5
4	7	28	32	lubricated	756.8	0.942	4	6
4	8	29.75	32	lubricated	829.6	0.945	4	7

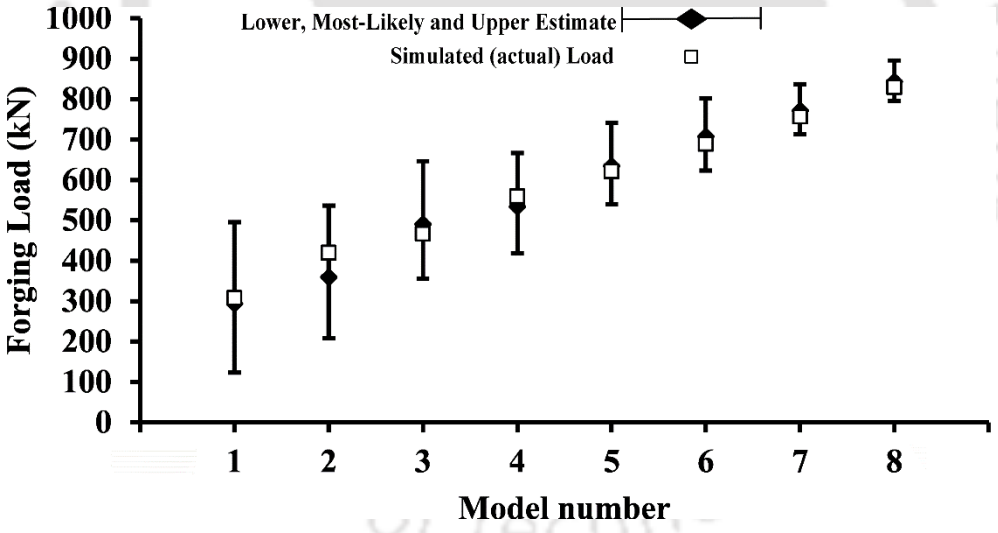

Figure 5.17 Predicted values versus simulated values for Product 4

5.7.4 Forging load estimation for various friction condition

To demonstrate the effect of only friction in the estimation of forging load in closed die forging, Product 2 is considered for the analysis. The forging load information of Model 4 already exists under lubricated condition. However, there is a need to estimate the forging load of Model 4 under non-lubricated condition. In this case, the Similarity index is again estimated for Model 4 under non-lubricated condition with the rest of the existing models

TH-3282_186103018

under lubricated condition. It is estimated that Model 4 under lubricated condition is estimated to have the highest Similarity index. A Similarity index of 0.889 is obtained. The complexity factor for the Model 4 under lubricated condition is chosen and is used for the estimation of forging load. In this case, the low, most likely and high estimate of closed-die forging load are computed as 213.7 kN, 258.2 kN and 326.0 kN respectively. The simulated load observed is 286.5 kN. The simulated load is observed to lie close to the most likely estimate. The actual complexity factor is preserved based on the values of the actual simulated load.

In the next case, there is a need to estimate the forging load for Model 3 of Product 2 under non-lubricated condition. In this is case, the complexity factor for Model 4 of Product 2 under non-lubricated condition is estimated to have the highest value of similarity with a magnitude of 0.979. Hence, on the using the complexity factor of Model 4, the low, most likely and high estimate of forging load for Model 3 are estimated as 233.5 kN, 297.3 kN and 375.2 kN respectively. The simulated load obtained is 294.6 kN. Due to the Similarity index being very close to one, the simulated load matches well with the most-likely estimate of forging load. The process continues with the estimation of the Similarity index of Model 2 and Model 1 under non-lubricated condition and the forging load is estimated accordingly. It is observed that in both model 2 and model 1, the most-likely estimate matches well with the simulated load due to the high Similarity index obtained in both the cases as shown in Table 5.5 and Figure 5.18.

Table 5.5 Estimation of forging load for two friction conditions of Product 2

Product	**Model**	**Friction condition**	**Blank radius (mm)**	**Blank height (mm)**	**Simulated load (kN)**	**Similarity index**	**Similar product**	**Similar model**	**Friction condition**
2	4	non-lubricated	18	24	286.5	0.889	2	4	lubricated
2	3	non-lubricated	18	22	294.6	0.979	2	4	non-lubricated
2	2	non-lubricated	18	20	309.5	0.969	2	3	non-lubricated
2	1	non-lubricated	18	18	318.3	0.971	2	2	non-lubricated

TH-3282_186103018

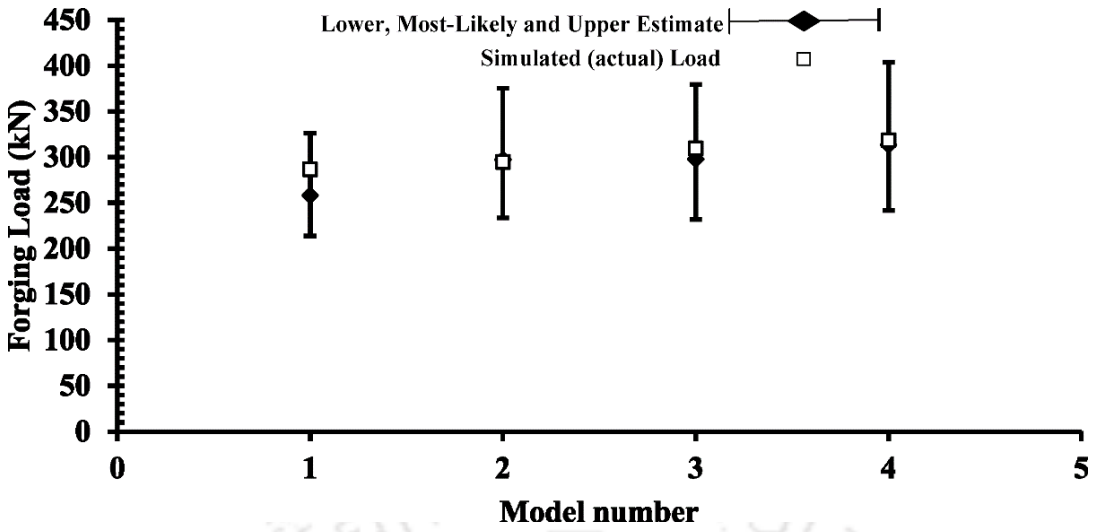

Figure 5.18 Predicted values versus simulated values for Product 2 under non-lubricated condition

5.7.5 Forging load estimation for different material

The products analyzed in the study till now are made out of lead. In order to demonstrate the effect of material in the estimation of forging load in closed die forging, Model 1 of Product 2 is only considered. Predictions are carried out under lubricated condition. It is already known that the material is lead for Model 1 of Product 2. However, there is a need to estimate the forging of geometrically similar model made of Al 1100 aluminum and AISI 1015 steel. Material properties of Al 1100 viz., density, Young's modulus and Poisson's ratio were considered as 2.7×10^3 kg/m^3, 69 GPa and 0.3, respectively. The yield stress and the corresponding plastic strain for the FEM simulation was roughly estimated using the following flow stress equation

$$\sigma_o = 62.74 + 110.1\varepsilon^{0.68}. \tag{5.19}$$

Material properties of AISI 1015 steel viz., density, Young's modulus and Poisson's ration were considered as 7.85×10^3 kg/m^3, 208 GPa and 0.3, respectively. The yield stress and the corresponding plastic strain for the FEM simulation of AISI 1015 steel was roughly estimated using the following flow stress equation

$$\sigma_o = 275 + 515.23\varepsilon^{0.6}. \tag{5.20}$$

The material properties and the hardening parameters of Al 1100 were taken from Park and Kobayashi (1984), and AISI 1015 steel were taken from Dadras and Thomas Jr (1983). The complexity factor for Model 1 of Product 2 under lubricated condition made

TH-3282_186103018

out of lead is fetched from the database. It is used to evaluate the forging load for a geometrically same model made out of Al 1100. The Similarity index is estimated to be 0.889. The low, most likely and high estimate of forging load for the Al 1100 specimen under lubricated condition are 529.7 kN, 649.6 kN and 789.3 kN, respectively. The simulated load is observed to be 662.9 kN. Due to high geometric similarity, the simulated load matches well with the most-likely estimate. The complexity factor based on the simulated load is preserved.

In the next case, the same specimen is made out of AISI 1015 steel. In the first instance, the complexity factor of lead is used for the estimation and in the second instance, the complexity factor of Al 1100 is used for the estimation. When the complexity factor of lead is used, the low, most-likely and high estimate of forging load are 2452.3 kN, 3015.4 kN and 3673.1 kN, respectively. When the complexity actor of Al 1100 is used the low, most-likely and high estimate of forging load are 2506.3 kN, 3081.8 kN and 3953.9 kN, respectively. The simulated load is 2928.4 kN. In both the instances, the simulated load matches well with the most-likely estimate as shown in Table 5.6 and Figure 5.19. It is also observed that the magnitude of the hardening parameters of AISI 1015 steel is greater than the hardening parameters of Al 1100 aluminum. This can be understood by the increased level of uncertainty in the estimation of forging load for AISI 1015 steel as compared to Al 1100 aluminum.

Table 5.6 Estimation of forging load for two different materials of Product 2

Product	Model	Material	Blank radius (mm)	Blank height (mm)	Friction condition	Simulated load (kN)	Similar product	Similar model	Base Material
2	1	Al 1100	18	18	lubricated	662.9	2	1	Lead
2	1	AISI 1015	18	18	lubricated	2928.4	2	1	Lead
2	1	AISI 1015	18	18	lubricated	2928.4	2	1	Al 1100

TH-3282_186103018

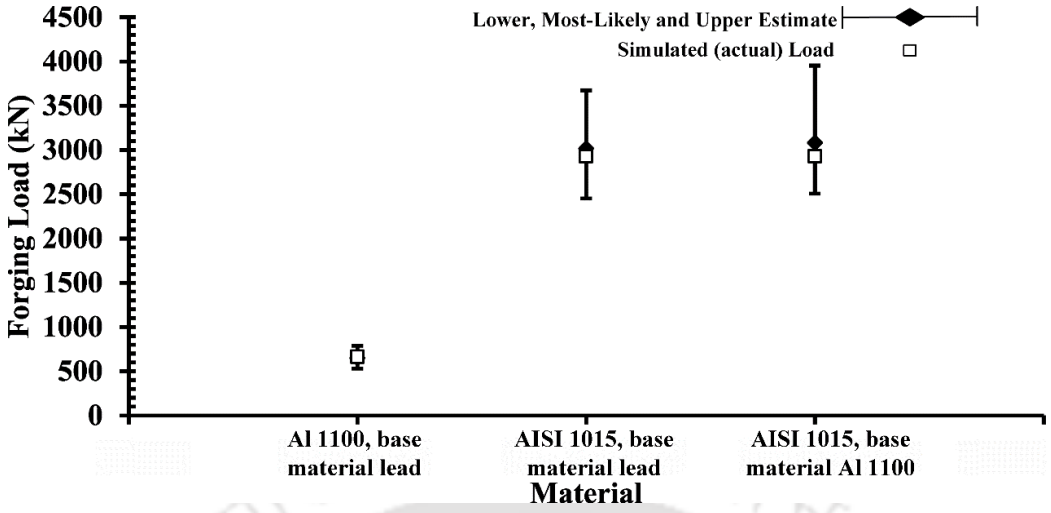

Figure 5.19 Predicted values versus simulated values for Product 2 for different materials

5.8 Conclusion

There has been an increase in the application of data-driven techniques in metal forming. Especially with the advancement of data storage technologies, data handling and its subsequent usage have increased. This work also aims to utilize the existing closed die forged data for the estimation of forging load based on size, material and friction condition. The following are the noteworthy outcomes from this chapter:

- A methodology is suggested for the computation of complexity factor in closed die forging of axisymmetric products. The database in this work is preserved in a 'MySQL' relational database.
- Estimation of forging load in closed die forging is carried out for four different products that vary in size, friction condition and material using fuzzy set-based methodology. All the predictions are carried out as low, most likely and high estimate.
- All the forging load estimations are carried out based on the Similarity index approach. The Similarity index depends on the material, friction condition and geometric dimension. The nearest neighbor is evaluated and one with the highest magnitude of similarity is chosen as the model for estimation purpose.
- The Similarity index determines the closeness of the most-likely estimate with the simulated load. A value close to 1 will suggest more accurate most-likely estimate.

Geometric closeness is essential for the estimation of forging load in closed die forging. Accuracy is superior when the model used for estimation purpose is geometrically closest to the desired model.

TH-3282_186103018

Chapter 6
Improving the prediction with the help of Kalman filter: A case study of closed-die forging

6.1 Introduction

Estimation of forging load is crucial for the process planners and designers. FEM is a well-known powerful computational tool for this purpose. However, FEM comes at a high computation cost and requires skill as well as proper input data. Therefore, in order to quickly estimate the forging load, empirical model is a viable option only with the help of an experienced operator or engineer. In order to reduce the dependency, Industry 4.0 proposes to use AI without sacrificing the accuracy of the prediction. This chapter falls into the broad category of AI based estimation of forging load. On this aspect, a preliminary work was presented in Chapter 5, where a strategy was proposed to preserve the shop floor data and use it for the estimation of forging load. The strategy was mainly focused towards fuzzy-set based estimation of closed-die forging load of axisymmetric products as already discussed.

A few researchers in the past have highlighted the fact that the shop floor data may contain noise and might not be prudent to use it in the raw form. They attempted to use filters for estimation in manufacturing. One such popular filter is Butterworth filter. It is mainly used for eliminating the noise from the captured signals due to the presence of various external disturbances. Besides Butterworth filter, researchers have used moving average filter for reducing the unwanted noise. Kalman filter is another technique that has been used for the quick estimation in the presence of uncertainties. It has been also been applied in the arena of metal forming.

Closed-die forging is a complex manufacturing process. However, due to uncertainties and measurement noise, achieving precise predictions in closed-die forging can be challenging. It is also evident from literature that Kalman filter has not been used for accurate estimation of forging load using a machine learning approach, although it has been found very effective in optimal control systems. It is a very effective tool for eliminating the noisy data. Hence, this chapter intends to demonstrate feasibility and effectiveness of Kalman filter for the estimation of forging load. The overview of the proposed methodology of forging load estimation is described in Section 6.2. Subsequent

TH-3282_186103018

sections carry out the task of detailing. The methodology is based on predicting the forging load based on the similar forgings. Hence, Section 6.3 proposes a method for identification of geometrically closest shapes. Estimation of forging load for a closed-die forged product based on the empirical information from similar product is described in Section 6.4. Fine tuning of the estimate using Kalman filtering is described in Section 6.5. FEM simulation procedure for the closed die forging process is presented in Section 6.6. Results and conclusions are discussed in Section 6.7 and 6.8 respectively.

6.2 Overview of the Proposed Methodology

The proposed methodology consists of three major segments. The first segment involves creating and using the database for accurate estimation of the forging load. The second segment involves using a semi-analytical model for estimating the closed-die forging load in the form of low, most-likely and high estimate. The third segment is about Kalman filtering of the estimate.

The adopted scheme for estimating the closed-die forging load is depicted in Figure 6.1. Database creation includes accumulating data from various sources that consists of data measured from sensors attached to a forging machine and data accumulated from numerical simulations of a closed-die forging process. Such hybrid data can be preserved in an open source relational database management system such as in MySQL. Forging Industries requiring can it for estimation of the forging load. Following information is stored in the database: (1) material, (2) for axisymmetric products: blank radius and height; for non-axisymmetric products: height, width and length, (3) maximum enveloping cylinder and cube for the finished axisymmetric and non-axisymmetric products, respectively, (4) friction condition: lubricated or non-lubricated, (5) a complexity factor associated with product.

Whenever a new product is forged on the shop floor, the geometric features of the new product is compared with the already preserved information in the database. The one having the most similar geometric feature is chosen for further estimation of the forging load for the new product. In this chapter, the feedback of the actual forging load is obtained from finite element method (FEM) simulations using ABAQUS. The results of the FEM simulations are assumed to represent a virtual factory shop floor.

A semi-analytical model is then used to estimate the closed-die forging load using the information of the most similar product. All the estimations are carried out in the form of the low, most-likely and high estimate. The obtained estimation of the forging load is

TH-3282_186103018

then fine-tuned by Kalman filtering. Kalman filter processes the information obtained from the semi-analytical model as well as the information obtained from the shop floor. Shop floor information contains noise. It is not judicious to use such data in a raw form. Kalman filter uses a weight factor termed as Kalman Gain that depends on the uncertainty in the estimation suggested by the semi-analytical model and the uncertainty in the data measured from the shop floor. The estimated weight factor also suggests the weightage to be given for the result obtained from the semi-analytical model and the weightage to be given for the information obtained from the shop floor. Interval estimations are then carried out accordingly. When the actual forging load from the factory shop floor lies exterior to the interval estimates, the new information is checked for any abnormality in the process. When it is assured that the forging process is stable, the new information is then preserved in the database. The detailed procedure for the accurate estimation of the closed-die forging load are explained in details in the subsequent sections.

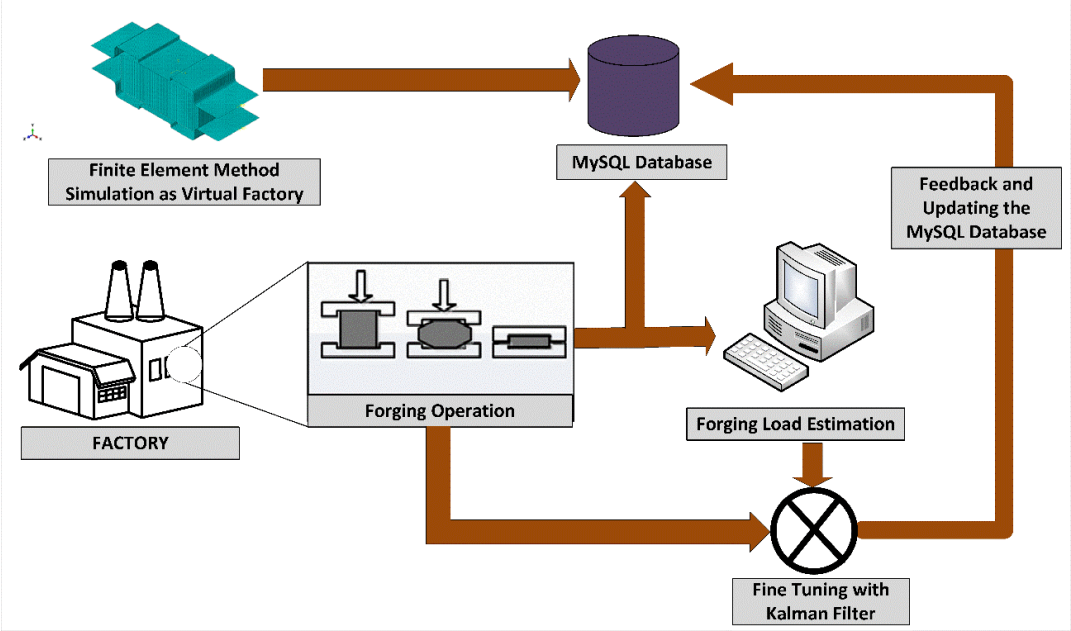

Figure 6.1 Basic overview of the proposed methodology

6.3 Estimation of the Closed-Die Forging Load using a Semi-Analytical Model

The first step in the estimation of forging load using a semi-analytical approach requires identifying the geometrically closest product from the database. A detailed procedure is already explained in Section 5.4 of Chapter 5. Similar approach is adopted for the present case study.

TH-3282_186103018

A typical plane strain compression of a solid billet is shown in Figure 6.2. The thickness of the workpiece at the given instant is h and the complete width of the workpiece is $2L$. It is assumed that the coefficient of friction μ at the interface between the dies and the workpiece is constant.

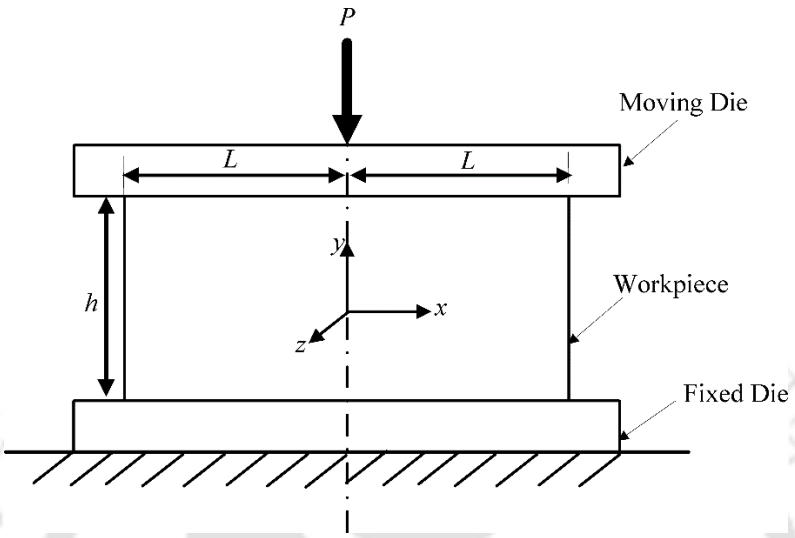

Figure 6.2 Open die forging of a solid billet

The slab method procedure in an open die forging for plane strain compression of solid billet using Coulomb's model gives the following expression for die pressure at any location (Ghosh and Mallik 2010)

$$p = \frac{2\sigma_o}{\sqrt{3}} \exp\left\{\frac{2\mu}{h}(L-x)\right\}, \tag{6.1}$$

where σ_o is the flow stress, μ is the coefficient of friction, h is the height of the billet, L is the semi-width of the billet and x is coordinate of the location. The total forging load P is obtained by integrating the die pressure p over the complete width $2L$ of the billet. It is given by

$$P = \frac{2}{\sqrt{3}} \frac{\sigma_o bh}{\mu} \left[\exp\left(\frac{2\mu L}{h} - 1\right)\right]. \tag{6.2}$$

However, in a simplistic manner, the forging load in case of open and closed-die forging can be calculated empirically as shown in Eq. 5.6.

For a solid billet under plane strain compression, equating Eq. 6.2 and 5.6, the initial value of complexity factor C_p is evaluated as

TH-3282_186103018

$$C_{\mathrm{p}} = \frac{2}{\sqrt{3}} \frac{h}{\mu L} \left[\exp\left(\frac{2\mu L}{h} - 1 \right) \right]. \tag{6.3}$$

On substituting the above value of C_{p} in Eq. 5.6, the forging load is estimated. In the similar manner, the initial value of complexity factor for forging of an axisymmetric billet can be expressed as shown in Eq. 5.7.

The main challenge is to suggest an accurate complexity factor for closed die forged products such that it can accurately estimate the closed-die forging load. The procedure proposed in this chapter keep on updating the complexity factor depending on the availability of the data.

6.3.1 Forging load estimation for varying sizes of the workpieces

Forging load is required to be estimated for unseen new products using the most similar product. For estimating the closed-die forging load using Eq. 5.6, a rough estimate of the complexity factor is required. Such estimated C_{p} is then used for the unseen product. A rough value of C_{p} is calculated using the following procedure. Consider two models with different geometries— Model 1 and Model 2. It is assumed that the information of the forging load for Model 1 is available. The load estimation for Model 2 is required. The initial guess value of C_{p} is estimated for both Model 1 and Model 2 using Eq. 6.3 (for non-axisymmetric model) or Eq. 5.7 (for axisymmetric model). The updated value of the C_{p} for Model 1 is calculated using the information of the actual load obtained from the shop floor. One simplistic assumption is to consider that the ratio of the initial guess values of C_{p} for Model 1 and Model 2 is equivalent to the updated value of the C_{p} for Model 1 and Model 2. It is represented as

$$\frac{\left(C_{\mathrm{p}}\right)_{\mathrm{guess1}}}{\left(C_{\mathrm{p}}\right)_{\mathrm{guess2}}} = \frac{\left(C_{\mathrm{p}}\right)_{\mathrm{updated1}}}{\left(C_{\mathrm{p}}\right)_{\mathrm{updated2}}}. \tag{6.4}$$

The complexity factor for Model 2 is calculated using Eq. 6.4. It is substituted in Eq. 5.6 to obtain the closed-die forging load. Based on the actual feedback of the simulated load, the complexity factor for Model 2 is further updated.

6.3.2 Fuzzy Estimations of the Closed-Die Forging Load

Flow stress and friction condition are the two main uncertain parameters associated with the estimation of forging load. The uncertainty associated with both the parameters is

TH-3282_186103018

dealt with by representing them as fuzzy parameters. The values of yield strength, strain hardening coefficient and coefficient of friction are considered as fuzzy parameters. There can be various methodologies that can be adopted to obtain the membership grade. The membership grades are generally obtained from experts. The values of the membership grade lie between 0 and 1, where 0 represents non-membership and 1 represents complete membership. For the sake of simplicity, a triangular membership function is considered in the study. In the triangular membership function, a membership grade of 0.5 represents either lower (*l*) or higher (*h*) bound estimates of the parameter under consideration. On the other hand, a membership grade of 1 always represents most likely (*m*) estimate of the parameter under consideration.

For demonstration purpose, it is assumed that there may be a variation of ±10% in the estimation of yield stress and a variation of ±20% in the estimation of hardening coefficients respectively (Dixit and Dixit 1996). Depending on the geometric dimensions of the model and their corresponding flow stress equation, the lower, most likely and upper value is estimated accordingly. For the coefficient of friction, there are two possibilities: lubricated condition and non-lubricated condition. For lubricated condition, the coefficient of friction for low, most likely and high estimate are considered as 0.02, 0.10 and 0.15 respectively. For non-lubricated condition, the coefficient of friction for low, most likely and high estimate are considered as 0.15, 0.22 and 0.32 respectively. Substituting all the fuzzy parameters in Eq. 6.6, the of low, most-likely and high estimate of the complexity factors can be obtained. With the help of these estimates, a linear triangular fuzzy number can be constructed. Further fine tuning of the estimations is carried out using Kalman Filter as discussed in Section 6.4.

6.4 Kalman Filter for fine tuning of the estimated closed-die forging load

Kalman filter is a recursive estimator that incorporates the feedback from the previously estimated value to improve the estimate of the current state from a set of noisy data (Barker et al., 1995). In this work, Kalman filter is applied to fine tune the already estimated forging load in the form of low, most-likely and high estimates. A detailed flowchart for fine tuning of the estimated forging load with a Kalman Filter is depicted in Figure 6.3. Kalman filter starts with an already available information of the forging load. The forging load gets updated depending on the actual feedback obtained from the shop floor. The present work focusses on estimation of the closed-die forging load (*F*). Hence, it is a one-dimensional problem and matrices of standard Kalman filter equations reduce to

TH-3282_186103018

scalars. For the present work, the initial estimation of the forging load is obtained from the semi-analytical model as described in the last section. The fuzzy estimation from the semi-analytical model is represented as

$$\tilde{F}=(F_{\mathrm{l}}, F_{\mathrm{m}}, F_{\mathrm{u}}), \tag{6.5}$$

where F_{l} is the lower estimate of the forging load, F_{m} is the most-likely estimate and F_{u} is the upper estimate. The next step is to estimate the error in the model. The error in overestimation is expressed as the difference between the upper and the most likely estimates of the forging load, i.e.,

$$E_{\mathrm{oest}} = F_{\mathrm{u}} - F_{\mathrm{m}}. \tag{6.6}$$

Similarly, the error in the overestimation is expressed as the difference between the most likely and lower estimates of the forging load, i.e.,

$$E_{\mathrm{uest}} = F_{\mathrm{m}} - F_{\mathrm{l}}. \tag{6.7}$$

The error of the most-likely estimation is taken as the maximum of E_{oest} and E_{uest}.

In Kalman filter, data obtained from the sensor is used for updating the current model estimation. Here, an FEM simulation model acts as a virtual factory and supplies the data of forging load in lieu of sensor-data. The error in the FEM simulation data is assumed to be ±10% of the value obtained. Thus, the error in the measurement, i.e. the observation error is represented as E_{mea}, which is equal to 0.1 times the forging load (F_{mea}). The error in the measurement is represented as E_{mea} and the FEM forging load as F_{mea}. Updating the current state estimation is dependent on the evaluation of a correction factor that is commonly termed as Kalman Gain K_{G} and is expressed as

$$K_{\mathrm{G}} = \frac{E_{\mathrm{est}}}{E_{\mathrm{est}} + E_{\mathrm{mea}}}, \tag{6.8}$$

where E_{est} is E_{oest} and E_{uest} for overestimation and underestimation, respectively.

The value of K_{G} can vary between 0 and 1. A value close to 1 indicates that sensor data (FEM data here) is more reliable than the forging load suggested by the semi-analytical model. On the other hand, a K_{G} value close to 0 indicates unreliable sensor data and relatively reliable estimation from the semi-analytical model. The updated forging load is given by

TH-3282_186103018

$$F_{\mathrm{m}}^{\mathrm{u}} = F_{\mathrm{m}} + K\left(F_{\mathrm{mea}} - F_{\mathrm{m}}\right). \tag{6.9}$$

Based on the updated forging load, the complexity factor of Eq. 5.6 is also updated and recorded. The errors in the estimation are updated as

$$E_{\mathrm{est}}^{\mathrm{u}} = \left(1-K\right)E_{\mathrm{est}}. \tag{6.10}$$

The updated errors in the estimation used to evaluate or update the upper and lower estimates of the forging load. The updated error in the estimation is also recorded in the database. Mathematically,

$$F_{\mathrm{u}}^{\mathrm{u}} = F_{\mathrm{m}}^{\mathrm{u}} + E_{\mathrm{oest}};\ F_{\mathrm{l}}^{\mathrm{u}} = F_{\mathrm{m}}^{\mathrm{u}} - E_{\mathrm{uest}}. \tag{6.11}$$

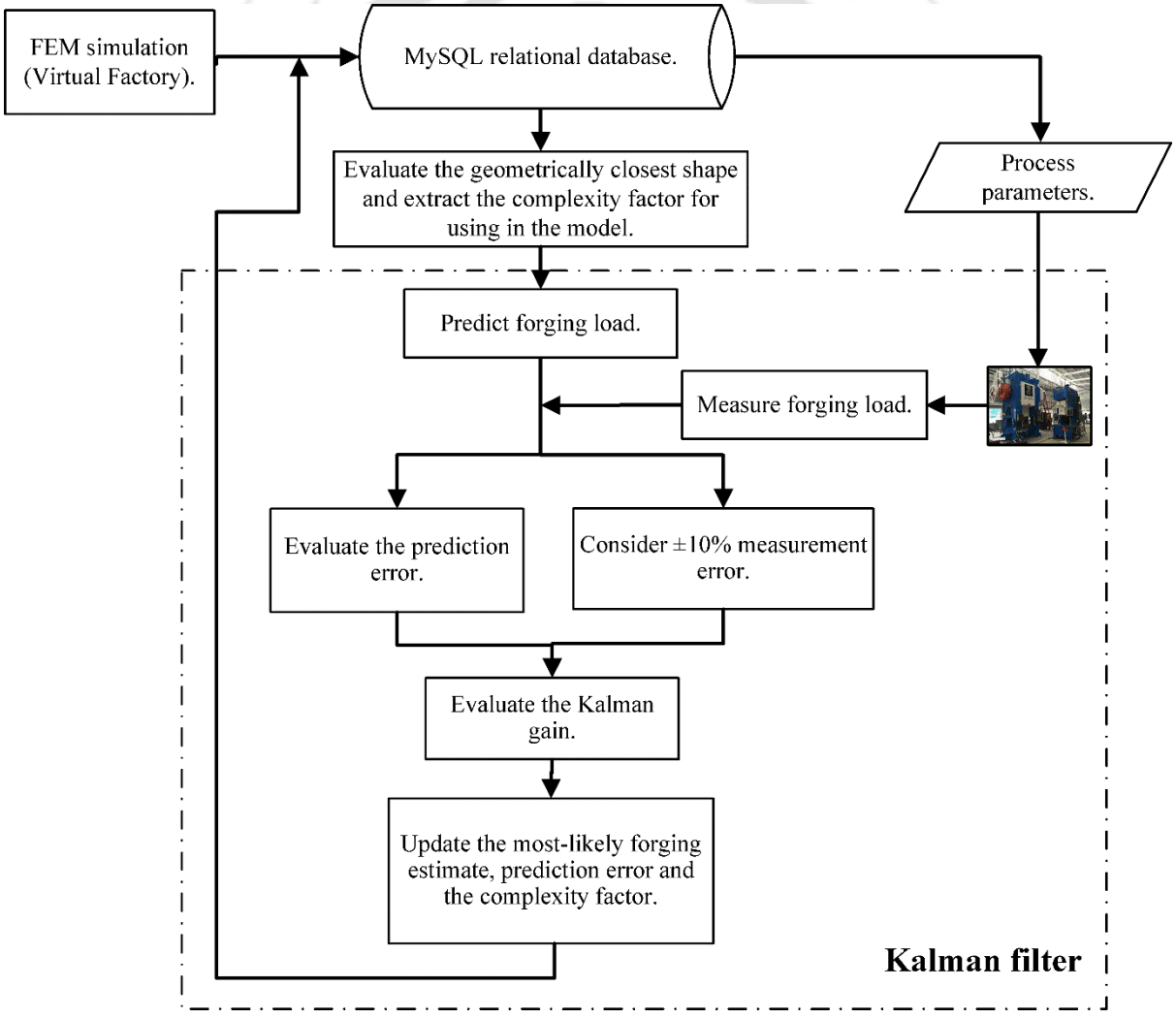

Figure 6.3 Flowchart for Kalman filtering for the model estimated forging load

The information is preserved in the database. Whenever similar product is forged, the preserved information is used for suggesting a suitable value of the forging load.

TH-3282_186103018

The proposed method is demonstrated through several examples presented in Section 6.7. Before that Section 6.6 briefly describes FEM simulation procedure. As already mentioned, FEM simulation module acts as a virtual factory here. In actual scenario, instead of FEM simulated data, the shop floor data will be obtained.

6.5 FEM Simulation of non-axisymmetric closed die forged products

Due to unavailability of shop floor sensor data, FEM simulation module was used to generate data of forging load. Simulation module acts as a virtual factory. The virtual factory sends feedback of the forging load obtained by carrying out FEM simulations using a commercially finite element package ABAQUS® version 6.13-1.

For better visualization, three-dimensional (3D) models of the closed-die cold forging processes were created. Part module was used to create the blank and the dies. During modelling of cold forging process, 3D deformable solid extruded part was created for the blank, while the upper and lower dies were represented by 3D discrete rigid parts. One reference point was created on each of the upper and lower dies. The motion or restraints of the entire die was applied through the created reference points. The interacting surface of the dies was considered as master and the interacting surface of the blank was considered as slave. Property module was created by assigning the blank as AISI 1015 steel. Density, Young's modulus and Poisson's ratio were taken as 7.85×10^3 kg/m^3, 208 GPa and 0.3, respectively. The yield stress and the corresponding plastic strain was estimated using the following flow stress equation (Dadras and Thomas Jr 1983):

$$\sigma_o = 275 + 515.23\,\varepsilon^{0.6}. \tag{6.12}$$

Parts were positioned in the global coordinate system with the help of assembly module. The velocity of both the upper and lower dies had same magnitude but opposite directions. The automatic time step increments were chosen for the dynamic explicit analysis in the step module. Surface to surface (explicit) interaction was considered between the blank and the die.

For executing the closed die forging simulation, a penalty-based friction formulation was considered. For the ABAQUS simulation, Coulomb's coefficient of friction μ of 0.1 was considered as lubricated condition and a value of μ of 0.25 was considered as non-lubricated condition. Generally, the value of the Coulomb's coefficient of friction for cold forging varies between 0.05 and 0.15. The value of μ as 0.25 can be

TH-3282_186103018

considered as an extreme case. Simulations are carried out for lubricated conditions. Arbitrary Lagrangian-Eulerian (ALE) adaptive mesh control was used to mesh the blank for closed die forging in the step module. The ALE utilizes both the Lagrangian as well as Eulerian analysis to avoid distortion of the mesh elements under the closed-die simulated condition. The quadrilateral elements, were chosen with medial axis algorithm for meshing the blank. The medial axis algorithm makes sure that the complete meshed region is divided into simpler regions for using the structured meshing technique to fill the regions with mesh elements. The blank was discretized with an 8-node linear brick, reduced integration, hourglass control (C3D8R) elements. The element size of 0.5 mm × 0.5 mm × 0.5 mm was adopted for the blank. The upper and lower dies were discretized with a 4-node 3D bilinear rigid quadrilateral (R3D4) elements. The element size of 0.5 mm × 0.5 mm was adopted for both the dies. Mess sensitivity analysis of perfectly plastic workpiece suggested a mesh size of 0.5 mm as appropriate (Dixit et al., 2022). Boundary conditions were assigned to the upper and lower dies in the load module. The boundary conditions are applied on the created reference points of each of the upper and lower dies. The translational and rotational motion of the lower die is restricted in *x*, *y* and *z* direction. The translational and rotational motion for the upper die is restricted in the *x* and *z* direction. A downward velocity is given to the upper die using the reference point along the *y*-axis as shown in Figure 6.4.

In the last step, the job module was created and the model was submitted for analysis. After the analysis, reaction force (forging load), was recorded to represent the data obtained from a virtual factory. The recorded data is then for the analysis of the proposed scheme with several examples as discussed in Section 6.7.

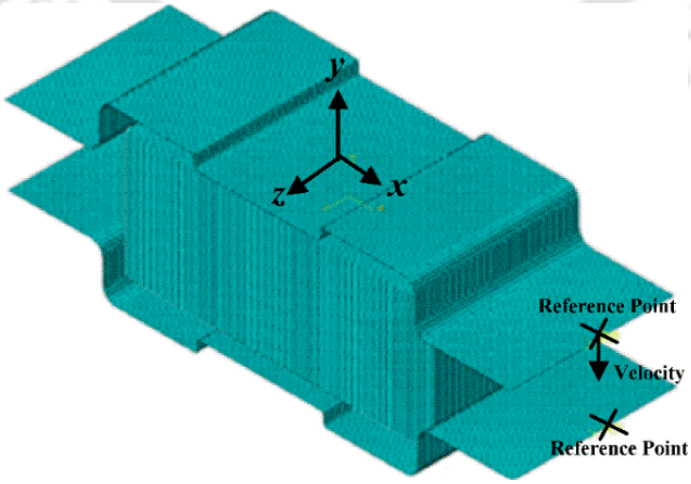

Figure 6.4 FEM model of the closed-die forging process

TH-3282_186103018

6.6 Results and discussion

The proposed methodology is illustrated for six closed-die forged products shown in Figure 6.5, comprising three axisymmetric and three non-axisymmetric products. All the forging simulations are carried out under both lubricated as well as non-lubricated condition. The complete methodology is implemented by writing a code in 'R', an open source statistical programming language.

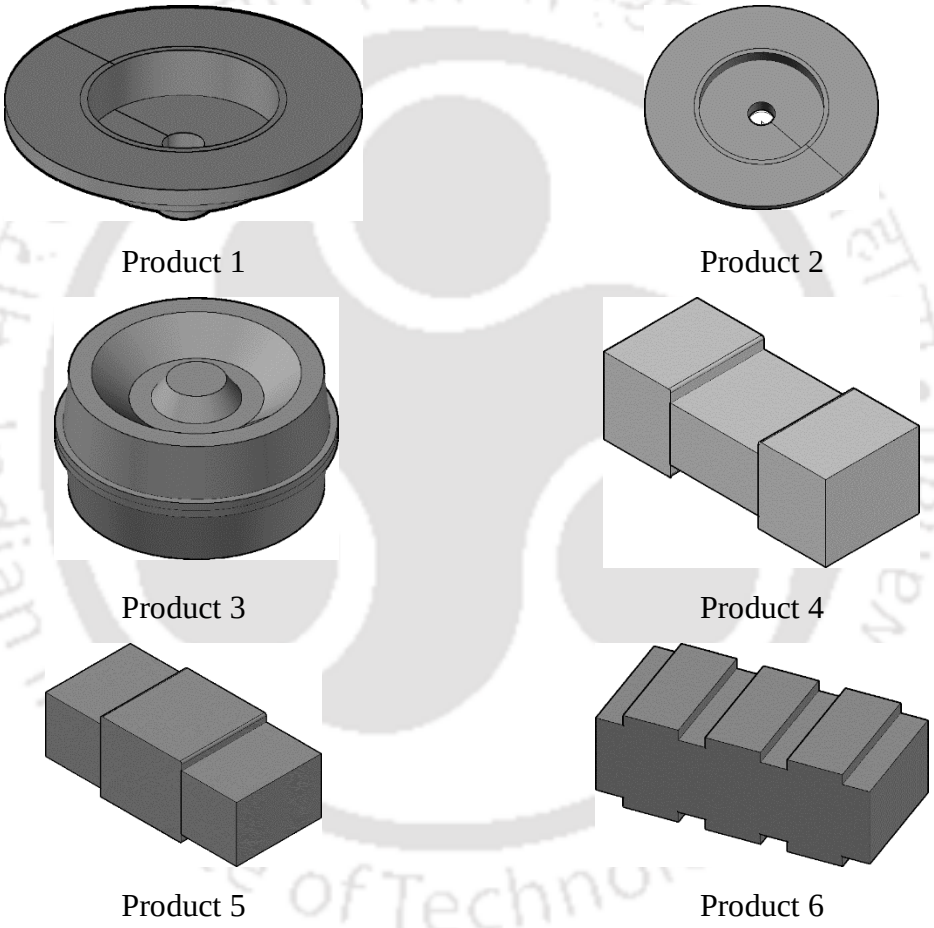

Figure 6.5 Six closed die forged products considered in the study

This work utilizes 'MySQL' relational database system to preserve all the forging data. As the complete methodology is implemented in 'R', the 'MySQL' database is accessed by using the 'dbConnect' command in 'R'. The 'dbConnect' requires username, password, name of the database and the host internet protocol (IP) address for accessing remotely. Every webserver has a specific IP address referred to as the domain name. After establishing the connection with the database, 'dbSendQuery' command is written to fetch

TH-3282_186103018

the desired dataset in the 'R' programming environment. After estimating the upper, most likely and lower estimate of the forging load, the new information is updated in the 'MySQL' relational database. Updation is carried out using the function 'dbWriteTable'. Finally, the database is disconnected from the 'R' environment using the function 'dbDisconnect', so as to ensure only authorized personnel can only access and edit the database.

6.6.1 Forging Load Estimation when there is no fluctuation in the sensor reading

It is assumed that Product 1 as shown in Figure 6.5 is desired to be forged. Consider two models of Product 1, Model 1 and Model 2 as shown in Figure 6.6. The blank radius and blank height for Model 1 was 15 mm and 5 mm respectively. The blank radius and blank height for model 2 was 17 mm and 5 mm respectively. FEM simulation was carried out for Model 1 under lubricated condition. The simulated load for Model 1 was 315.3 kN with the corresponding value of C_p was estimated as 2.57. The information obtained is further used for the estimation of forging load for Model 2. The semi-analytical model estimation of the lower, most likely and higher estimates of load for Model 2 were 224.2 kN, 348.8 kN and 534.8 kN respectively. The simulated forging load was 362.2 kN. However, on applying Kalman filter, the lower, most-likely and upper estimates were suggested as 331.3 kN, 359.8 kN and 390.1 kN, thereby reducing the deviation of the most-likely estimate from 3.65% to 0.59%. The complexity factor based on the most likely estimate suggested by applying the Kalman filter and the deviation of the upper and lower estimates with the most-likely estimates were also preserved in the database. In the next iteration, Model 2 is again desired to be forged. The preserved complexity factor and the model error for the already forged Model 2 are retrieved. In the second iteration, the suggested pessimistic, most-likely and optimistic estimates are 331.3 kN, 359.8 kN and 390.1 kN respectively. The simulated forging was again observed as 362.2 kN. On further fine tuning with Kalman filter, the lower, most-likely and upper estimate of the forging load for Model 2 was estimated as 344.8 kN, 360.8 kN and 377.2 kN respectively. It is observed that the deviation of the most-likely estimate with the upper and the lower estimates was reducing. A total of 20 iteration was carried out for estimating the forging load for Model 2. As there is no fluctuation in the simulated load, the deviation of the most-likely estimate with the upper estimate as well as the deviation of the most-likely estimate with the lower estimate were reducing with each iteration as shown in Figure 6.7. In other words, the reliability of the estimation was improving with each iteration.

TH-3282_186103018

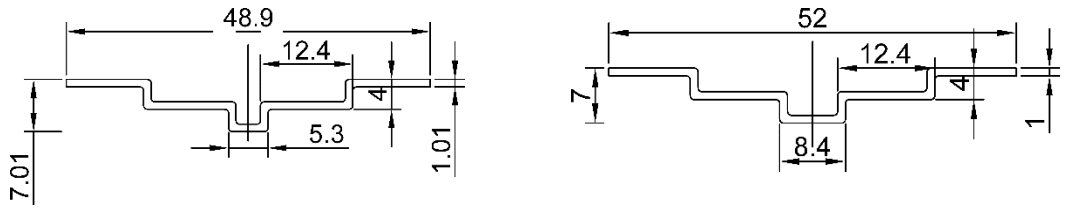

Model 1 Model 2

Figure 6.6 Closed Forged Product 1

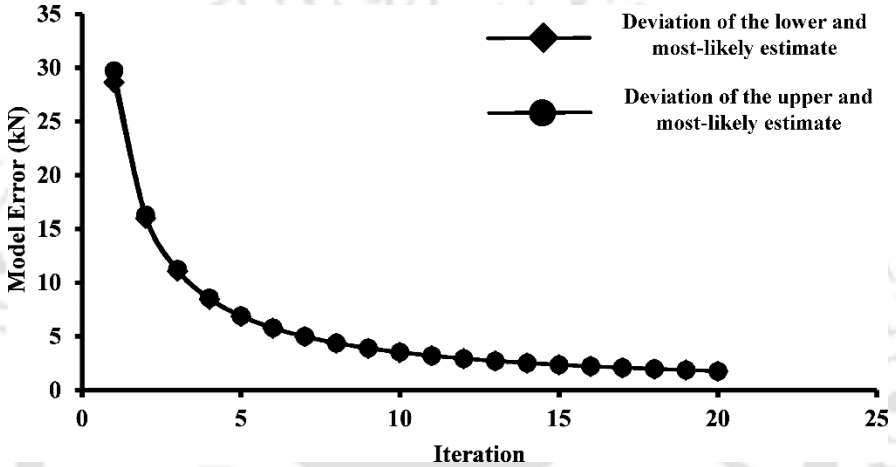

Figure 6.7 Model error when there is no fluctuation in the simulated load

6.6.2 Forging Load Estimation when there is a fluctuation in the sensor reading

In the second instance, the information of the complexity factor preserved for Model 1 of Product 1 is again used for estimating the forging load for Model 2. The simulated load for Model 1 was 315.3 kN with the corresponding value of C_p was estimated as 2.57. In the first iteration, the semi-empirical model suggested the lower, most-likely and upper estimate of the forging as 224.18 kN, 348.80 kN and 534.76 kN. Model 2 is simulated under lubricated condition. The simulated load observed was 362.2 kN. On fine tuning with Kalman filter, the lower, most-likely and upper estimates of the load are 331.3 kN, 359.8 kN and 390.1 kN. Nevertheless, the deviation of the most-likely estimates from the upper and lower estimates reduces from 3.65% to 0.59%. From the second iteration, the FEM simulated load that indicates the sensor reading fluctuates for Model 2. In order to highlight the fluctuation in the simulated load for Model 2, the coefficient of friction is slightly perturbed. It is already highlighted in Section 6 that the coefficient of friction for cold forging varies between 0.05 to 0.15. For the first iteration, the coefficient of friction

TH-3282_186103018

considered was 0.1. For the second iteration, the coefficient of friction considered was 0.05 and the corresponding simulated load observed was 311.3 kN. The lower, most-likely and upper estimate of the load suggested by the model was 331.3 kN, 359.8 kN and 390.1 kN respectively. On Fine tuning with Kalman filter, the lower, most-likely and upper estimates were estimated as 321.1 kN, 336.0 kN and 351.2 kN. It can be seen that the deviation of the most-like estimate with the lower and the upper estimate reduces from the first iteration. It is interesting to note that as the simulated load shifts from 362.2 kN to 311.3 kN, the Kalman filter suggested most likely estimate also changes from 359.8 kN to 336.0 kN. The process is repeated for 20 iterations with random perturbation in friction value. The deviation of the most-likely estimate with the simulated load is shown in Figure 6.8. It can be noticed that the most-likely estimates try to shift towards the simulated load observed.

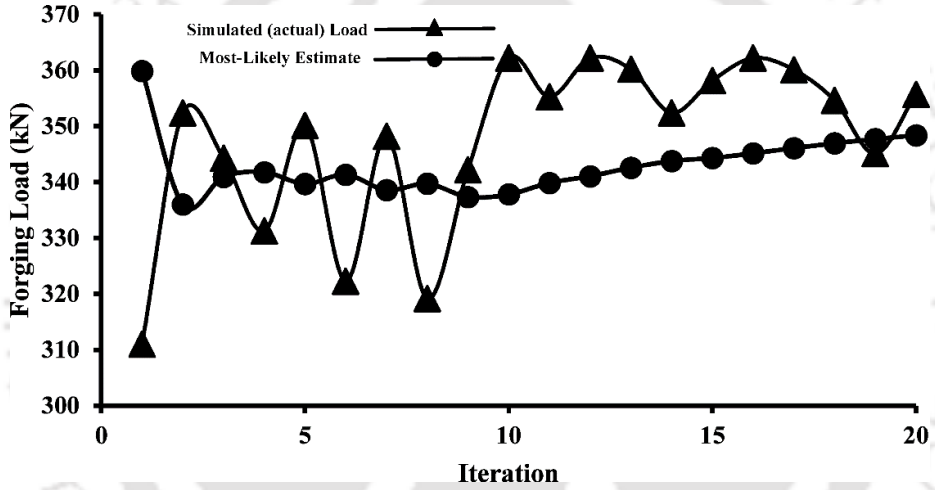

Figure 6.8 Model error when there is fluctuation in the simulated load

6.6.3 Forging Load Estimation when the friction condition and size changes for axisymmetric products

In the third instance, different models of Product 1 as shown in Figure 6.9 is considered. All the initial dimensions of the eight models are presented in Table 6.1. The process starts with the FEM simulation of Model 1 under non-lubricated condition. The simulated load for Model 1 was 802.3 kN with the corresponding value of C_p as 3.17. The complexity factor of Model 1 is preserved for further estimation of the forging load.

In the next iteration, Model 2 is desired to be forged under lubricated condition. Considering Model 1 as the base model, forging load estimation was carried out for Model 2 using the semi-analytical model. The estimated lower, most-likely and upper estimate of the forging load for Model 2 were 252.9 kN, 558.2 kN and 1083.4 kN respectively. The FEM simulated forging load was observed as 548.2 kN. On fine tuning with Kalman filter,

TH-3282_186103018

the lower, most-likely and higher estimate of the forging load were estimated as 492.1 kN, 549.3 kN and 611.2 kN respectively. The complexity factor is preserved based on the Kalman filter suggested most-likely estimate and the deviation of the upper and lower with the most-likely estimate. The iteration continues with Model 3 desired to be forged under lubricated condition. The overall similarity is evaluated by comparing Model 1 and Model 2 using the methodology discussed in Section 3. Model 2 was observed to have a higher similarity with Model 3 as compared to Model 1. The preserved complexity factor was retrieved for Model 2 for estimating the forging load. The semi-analytical suggested lower, most-likely and upper estimate of the forging load were 358.8 kN, 625.5 kN and 1057.3 kN respectively. The FEM simulated load observed was 615.2 kN. The Kalman filter suggested lower, most-likely and upper estimate of the forging load were 569.2 kN, 619.2 kN and 673.4 kN respectively.

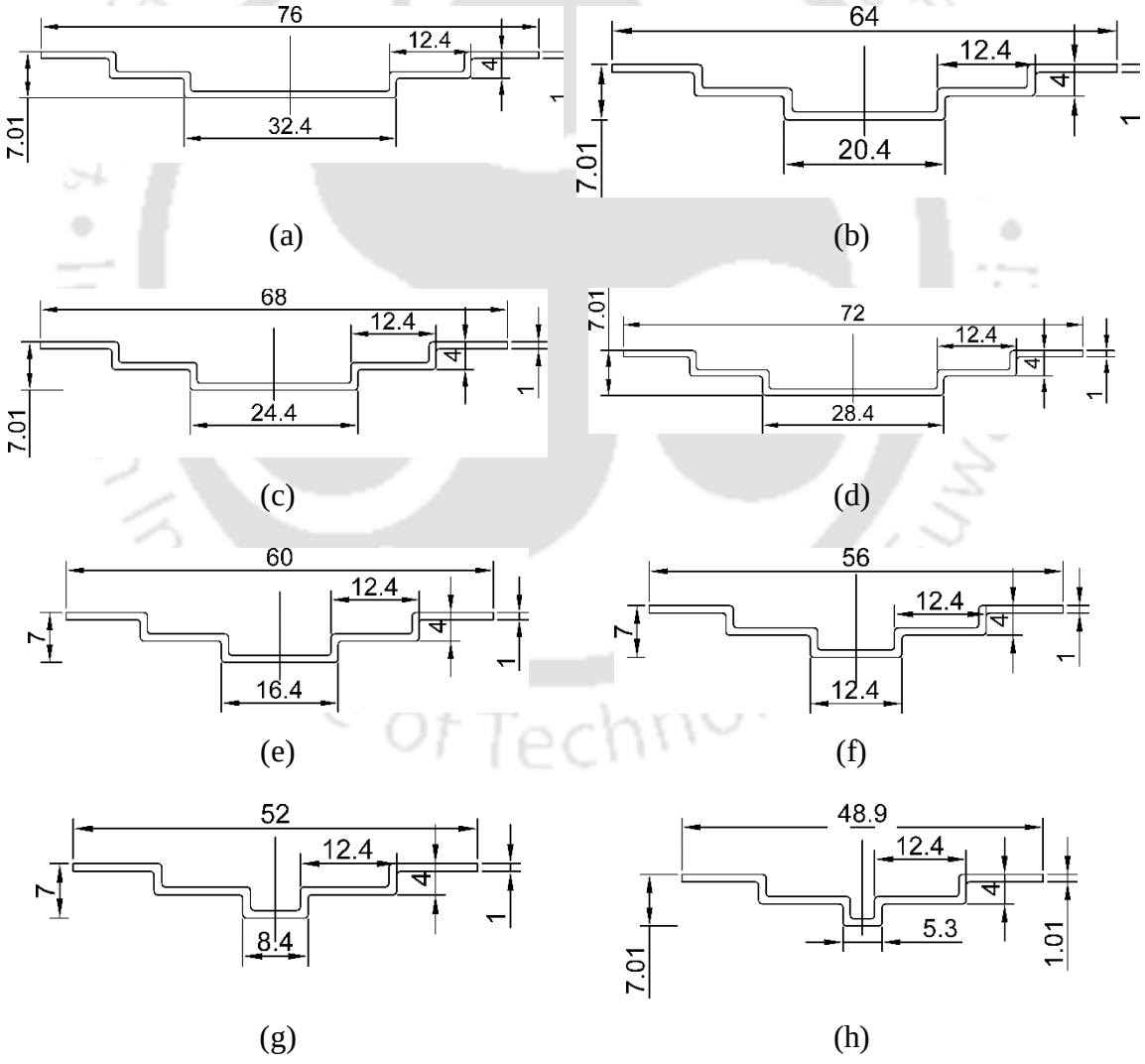

Figure 6.9 Closed die forged Product 1: (a) Model 1, (b) Model 2, (c) Model 3, (d) Model 4, (e) Model 5, (f) Model 6, (g) Model 7 and (h) Model 8

TH-3282_186103018

The complexity factor based on the Kalman filter suggested most-likely estimate and the deviation of the upper and lower with the most-likely estimate were then preserved. Similar methodology is adopted for rest of the six models for Product 1. It was observed that the model error reduces as the information increases for a product. The results are presented in Table 6.1. Figure 6.10 and 6.11 provides a visual description of the results from the semi-analytical and on fine tuning with Kalman filter.

Table 6.1 Forging load estimation for Product 1

Product	Model	Blank radius (mm)	Blank height (mm)	Semi-analytical most-likely estimate (kN)	Simulated (actual) load (kN)	Kalman filter most-likely estimate (kN)	Base model	Base product	Friction condition
1	1	29	5	–	802.3	–	–	–	non-lubricated
1	2	23	5	558.2	548.2	549.3	1	1	lubricated
1	3	25	5	625.5	615.2	619.2	2	1	lubricated
1	4	27	5	697.1	702.0	701.4	3	1	non-lubricated
1	5	15	5	322.5	315.3	315.2	2	1	lubricated
1	6	19	5	411.6	421.6	419.8	5	1	non-lubricated
1	7	17	5	348.8	362.3	359.9	6	1	lubricated
1	8	21	5	481.8	490.1	488.8	6	1	lubricated

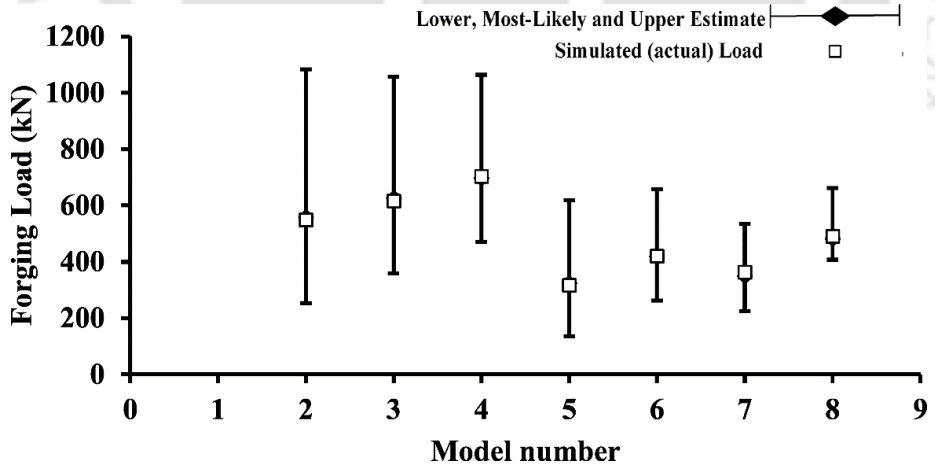

Figure 6.10 Predicted values versus simulated values for Product 1 using semi-analytical model

TH-3282_186103018

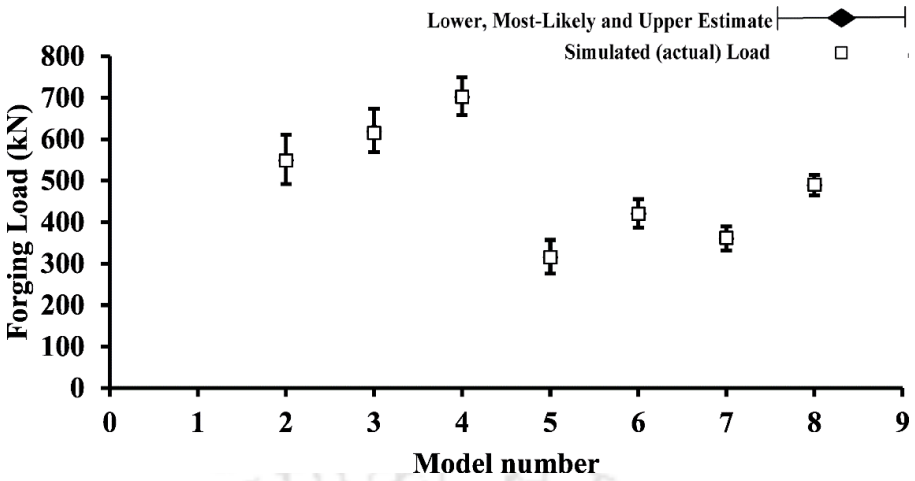

Figure 6.11 Predicted values versus simulated values for Product 1 using Kalman filter

The information of the complexity factor preserved for all the models of Product 1 were used for the estimation of the forging load for Product 2. All the models of Product 2 are shown in Figure 6.12. Initially, Model 1 of Product 2 was required to be forged. Similar to the methodology described for Product 1, the scheme evaluates the overall similarity of all the available models for Product 1. It was observed that Model 3 of Product 1 was having the highest overall similarity index. The preserved complexity factor for Model 3 was then used to estimate the forging load for Model 1 of Product 2. Model 1 is desired to be forged under lubricated condition. The semi-analytical model estimated lower, most-likely and upper estimate of the forging load were 404.6 kN, 669.8 kN and 1074.0 kN respectively. The FEM simulated load under non-lubricated condition for Model 1 was 560.3 kN. Kalman filter suggested lower, most-likely and upper estimate of the forging load were 531.3 kN, 573.4 kN and 622.5 kN respectively. The complexity factor based on the Kalman filter suggested most-likely estimate and the deviation of the upper and lower with the most-likely estimate are preserved. Similar methodology is adopted for rest of the seven models for Product 2. The results are presented in Table 6.2. Figure 6.13 and 6.14 provides a visual description of the results from the semi-analytical model and on fine tuning with Kalman filter.

TH-3282_186103018

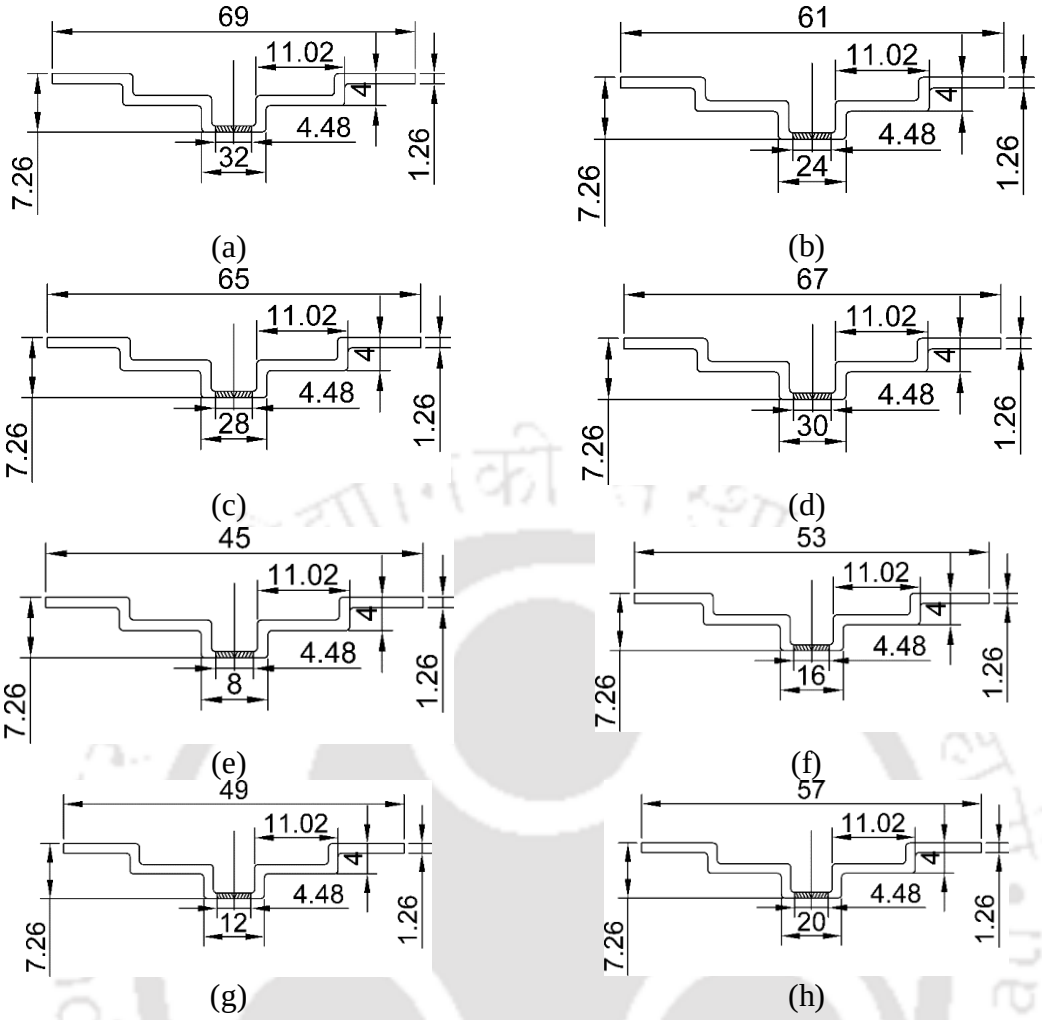

Figure 6.12 Closed die forged Product 2: (a) Model 1, (b) Model 2, (c) Model 3, (d) Model 4, (e) Model 5, (f) Model 6, (g) Model 7 and (h) Model 8

Table 6.2 Forging load estimation for Product 2

Product	Model	Blank radius (mm)	Blank height (mm)	Semi-analytical most-likely estimate (kN)	Simulated (actual) load (kN)	Kalman filter most-likely estimate (kN)	Base model	Base product	Friction condition
2	1	46	3	669.8	560.3	573.4	3	1	lubricated
2	2	40	3	431.6	427.6	427.7	1	2	non-lubricated
2	3	42	3	487.8	490.3	489.7	2	2	lubricated
2	4	44	3	556.1	526.5	529.8	3	2	non-lubricated
2	5	32	3	246.1	224.8	227.6	2	2	non-lubricated
2	6	36	3	312.6	320.3	318.7	5	2	lubricated
2	7	34	3	256.8	266.5	266.6	6	2	lubricated
2	8	38	3	371.5	375.3	374.5	6	2	lubricated

TH-3282_186103018

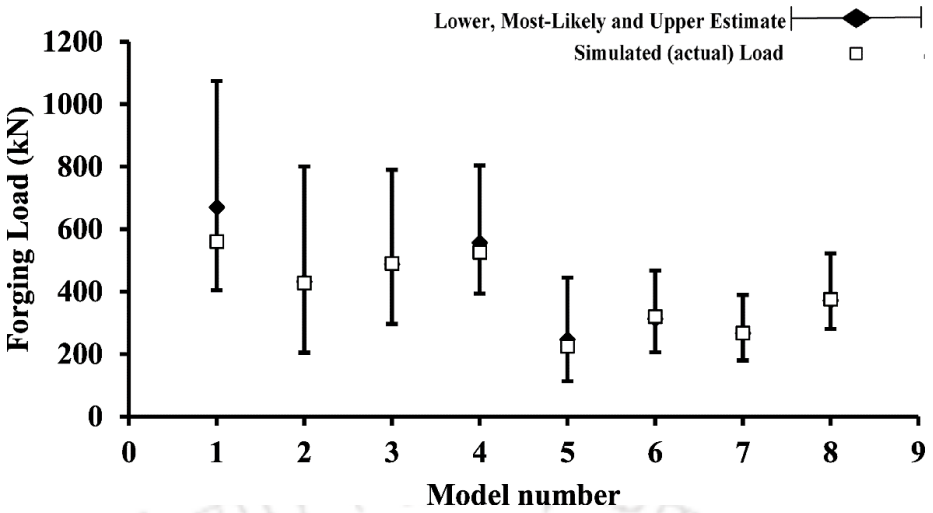

Figure 6.13 Predicted values versus simulated values for Product 2 using semi-analytical model

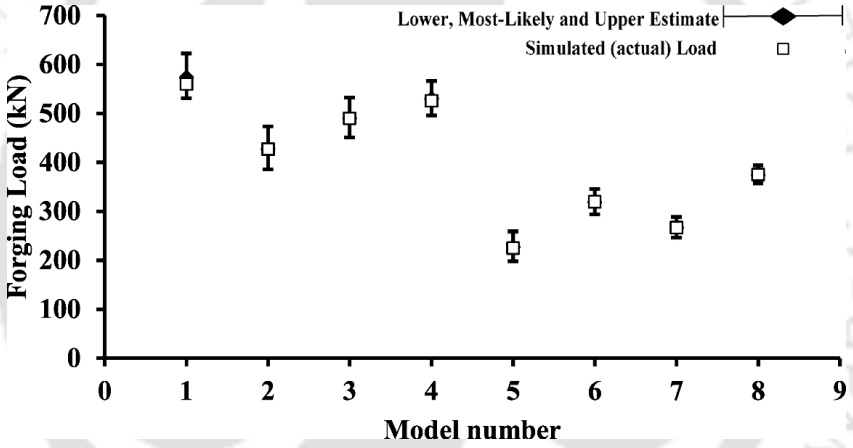

Figure 6.14 Predicted values versus simulated values for Product 2 using Kalman filter

The process continues with the different models of Product 3 are shown in Fig. 6.15. The initial dimensions of all the models are presented in Table 6.3. In case of Product 3, the information of all the available models of Product 1 and Product 2 were used to suggest the most similar product. It was observed that Model 3 of Product 1 was having the highest similarity index. The preserved complexity factor was retrieved. Model 1 of Product 3 was desired to be forged under non-lubricated condition. The semi-analytical model suggested lower, most-likely and upper estimate of the forging load were 368.2 kN, 571.3 kN and 859.5 kN respectively. The simulated forging load was observed as 540.2 kN. Kalman filter suggested lower, most-likely and upper estimate of the forging load were 494.3 kN, 536.4 kN and 585.7 kN respectively. The complexity factor based on the Kalman filter suggested most-likely estimate and the deviation of the upper and lower with the most-likely estimate

TH-3282_186103018

are preserved. The process continues for the rest of the seven models of Product 3. The results are presented in Table 6.3. Figure 6.16 and 6.17 provides a visual description of the results from the semi-analytical and on fine tuning with Kalman filter.

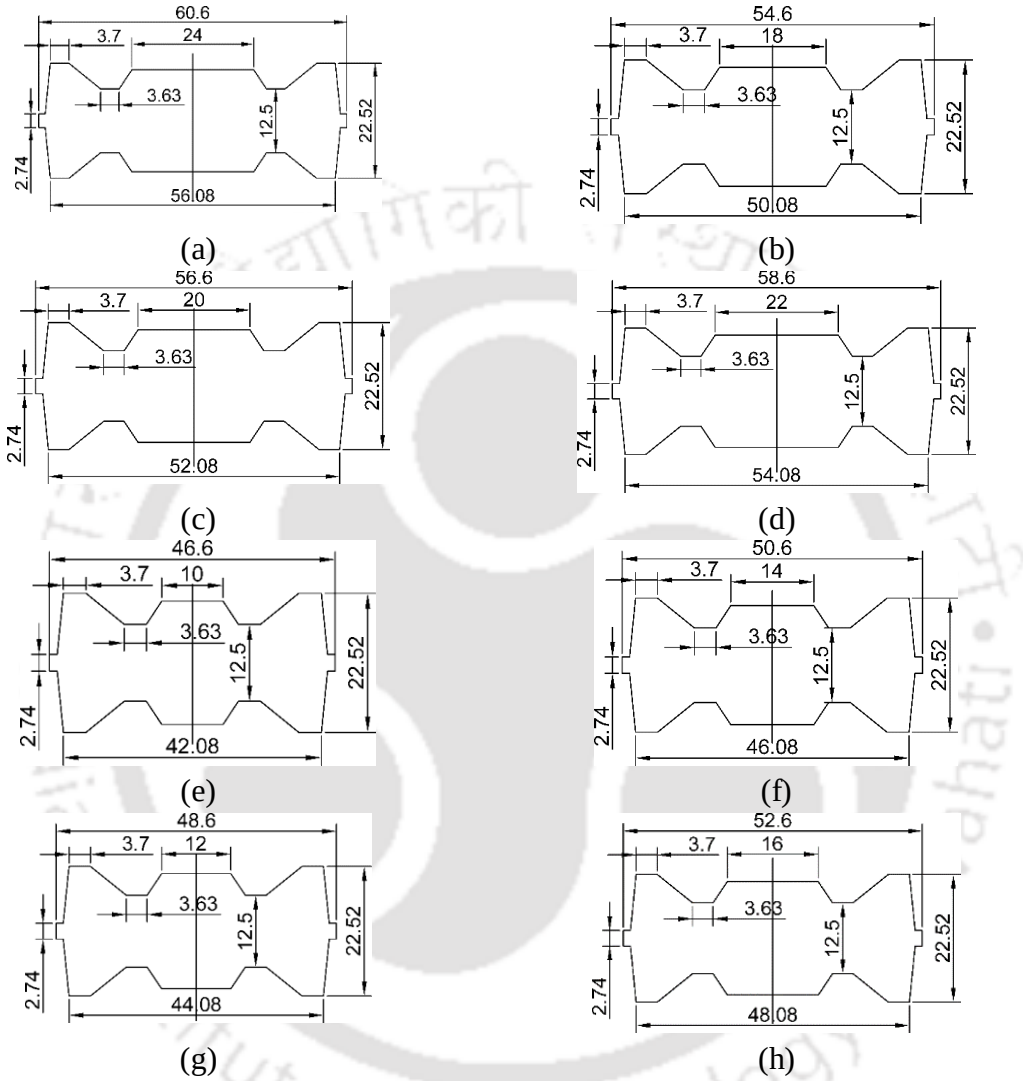

Figure 6.15 Closed die forged Product 3: (a) Model 1, (b) Model 2, (c) Model 3, (d) Model 4, (e) Model 5, (f) Model 6, (g) Model 7 and (h) Model 8

TH-3282_186103018

Table 6.3 Forging load estimation for Product 3

Product	Model	Blank radius (mm)	Blank height (mm)	Semi-analytical most-likely estimate (kN)	Simulated (actual) load (kN)	Kalman filter most-likely estimate (kN)	Base model	Base product	Friction condition
3	1	24	32	571.3	540.2	536.4	3	1	non-lubricated
3	2	21	32	418.3	431.1	430.1	1	3	lubricated
3	3	22	32	487.8	470.3	468.1	2	3	lubricated
3	4	23	32	534.2	505.6	501.6	3	3	non-lubricated
3	5	17	32	237.7	289.2	277.9	2	3	lubricated
3	6	19	32	340.2	361.3	358.7	5	3	lubricated
3	7	18	32	271.8	328.8	325.7	6	3	lubricated
3	8	20	32	368.6	395.6	394.3	6	3	lubricated

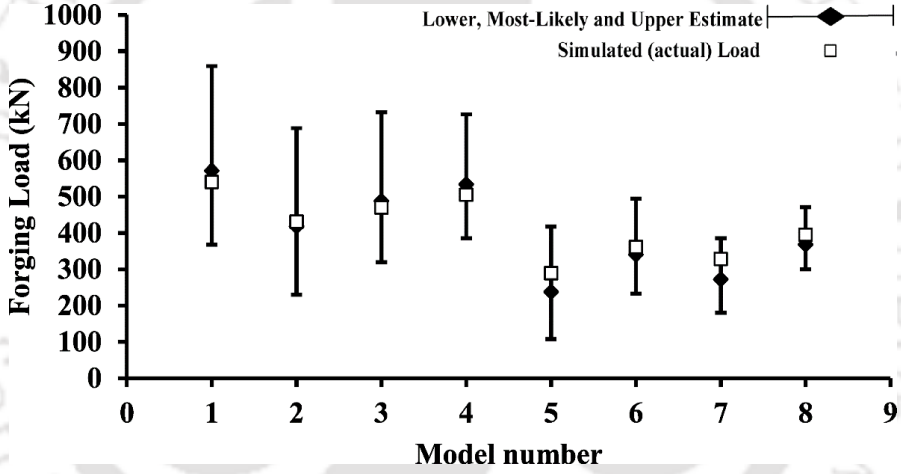

Figure 6.16 Predicted values versus simulated values for Product 3 using semi-analytical model

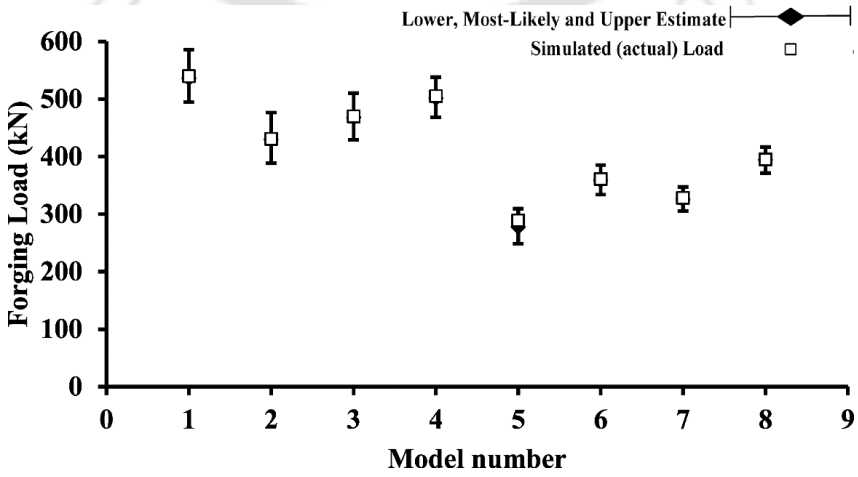

Figure 6.17 Predicted values versus simulated values for Product 3 using Kalman filter

TH-3282_186103018

6.6.4 Forging Load Estimation when the friction condition and size changes for non-axisymmetric products

Forging load estimation is carried out for non-axisymmetric products. The process starts with Product 4 as shown in Figure 6.18. All the initial dimensions of the eight models are presented in Table 6.4. All the axisymmetric models are made of AISI 1015 steel. The process starts with the FEM simulation of Model 1 under non-lubricated condition. The simulated load for Model 1 was 783.4 kN with the corresponding value of C_p as 1.59. The complexity factor of Model 1 is preserved for further estimation of the forging load. In the next iteration, Model 2 is desired to be forged under lubricated condition. Considering Model 1 as the base model, forging load estimation was carried out for Model 2 using the semi-analytical model. The estimated lower, most-likely and upper estimate of the forging load for Model 2 were 484.4 kN, 759.4 kN and 1131.8 kN respectively. The FEM simulated forging load was observed as 710.1 kN. On fine tuning with Kalman filter, the lower, most-likely and higher estimate of the forging load were estimated as 666.8 kN, 719.7 kN and 781.5 kN respectively. The complexity factor is preserved based on the Kalman filter suggested most-likely estimate and the deviation of the upper and lower with the most-likely estimate. The iteration continues with Model 3 desired to be forged under lubricated condition. The overall similarity is evaluated by comparing Model 1 and Model 2 using the methodology discussed in Section 3. Model 2 was observed to have a higher similarity with Model 3 as compared to Model 1. The preserved complexity factor was retrieved for Model 2 for estimating the forging load. The semi-analytical suggested lower, most-likely and upper estimate of the forging load were 548.4 kN, 789.9 kN and 1116.0 kN respectively. The FEM simulated load observed was 720.0 kN. The Kalman filter suggested lower, most-likely and upper estimate of the forging load were 680.9 kN, 732.7 kN and 791.6 kN respectively. The complexity factor based on the Kalman filter suggested most-likely estimate and the deviation of the upper and lower with the most-likely estimate were then preserved. Similar methodology is adopted for rest of the six models for Product 4. It was observed that the model error reduces as the information increases for a product. The results are presented in Table 6.4. Figure 6.19 and 6.20 provides a visual description of the results from the semi-analytical and on fine tuning with Kalman filter.

TH-3282_186103018

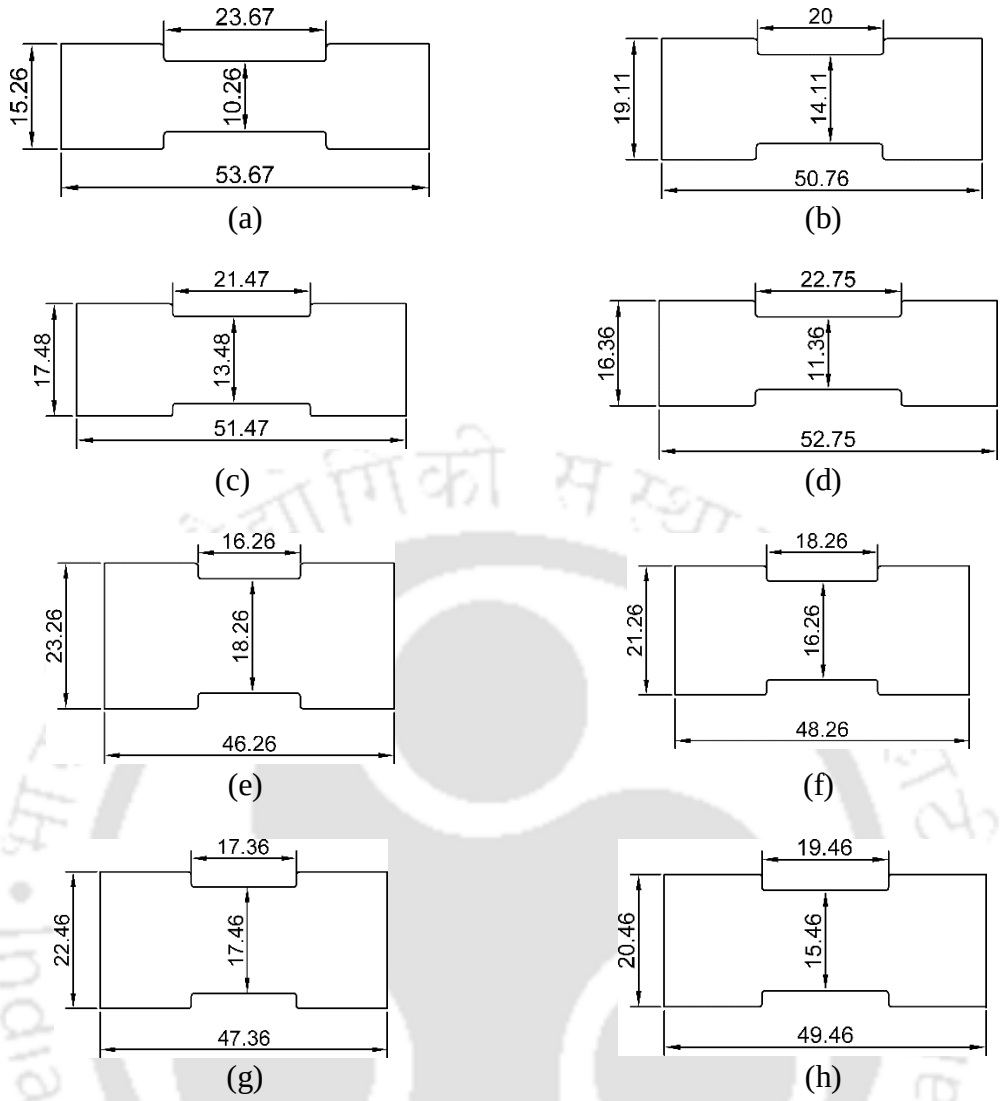

Figure 6.18 Closed die forged Product 4: (a) Model 1, (b) Model 2, (c) Model 3, (d) Model 4, (e) Model 5, (f) Model 6, (g) Model 7 and (h) Model 8

Table 6.4 Forging load estimation for Product 4

Product / Model	Blank width (mm)	Blank depth (mm)	Blank height (mm)	Product depth (mm)	Semi-analytical most-likely estimate (kN)	Simulated (actual) load (kN)	Kalman filter most-likely estimate (kN)	Base model	Base product	Friction condition
4/1	52	20	16	21.8	–	783.4	–	–	–	non-lubricated
4/2	49	20	20	21.5	759.4	710.1	717.7	1	4	lubricated
4/3	50	20	18	21.6	789.9	720.0	732.6	2	4	lubricated
4/4	51	20	17	21.7	850.8	745.9	760.0	3	4	non-lubricated
4/5	45	20	24	21.1	653.5	636.2	638.9	2	4	lubricated
4/6	47	20	22	21.3	683.0	665.8	669.5	5	4	non-lubricated
4/7	46	20	23	21.2	661.8	651.4	653.7	6	4	lubricated

TH-3282_186103018

4/8	48	20	21	24.4	718.8	682.4	689.8	6	4	lubricated

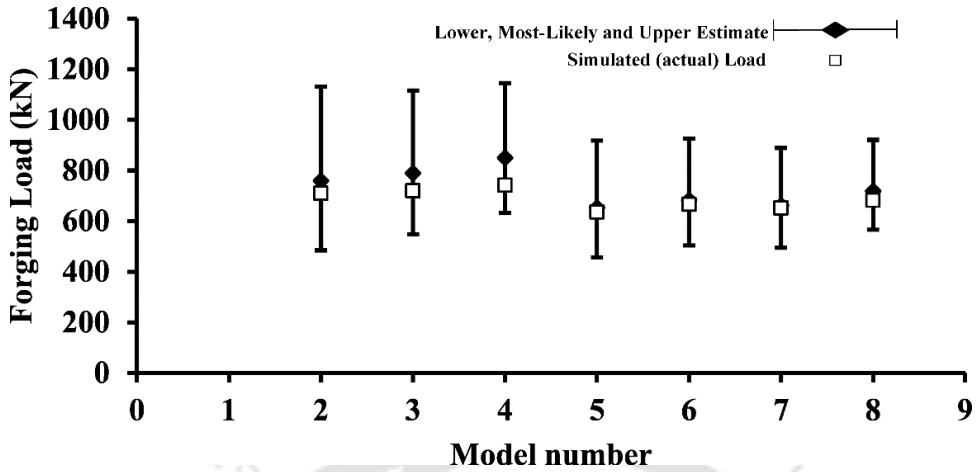

Figure 6.19 Predicted values versus simulated values for Product 4 using the semi-analytical model

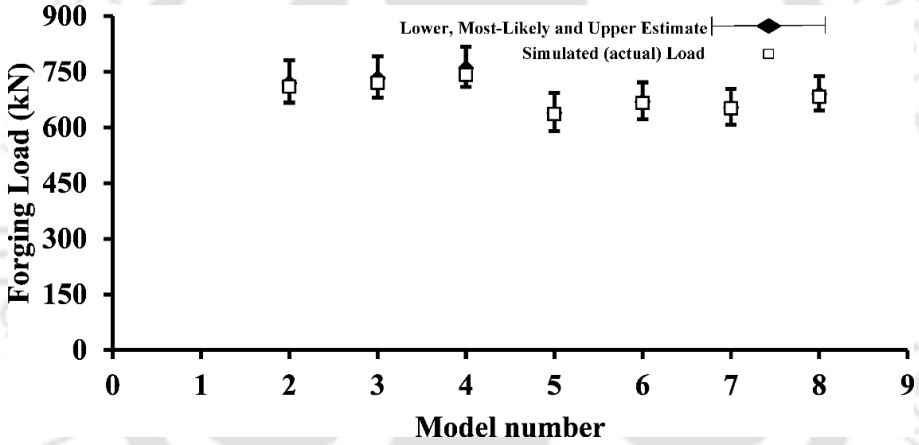

Figure 6.20 Predicted values versus simulated values for Product 4 using Kalman filter

The information of the complexity factor preserved for all the models of Product 4 were used for the estimation of the forging load for Product 5. All the models of Product 5 are shown in Figure 6.21. Initially, Model 1 of Product 5 was required to be forged. Similar to the methodology described for Product 4, the scheme evaluates the overall similarity of all the available models for Product 4.

TH-3282_186103018

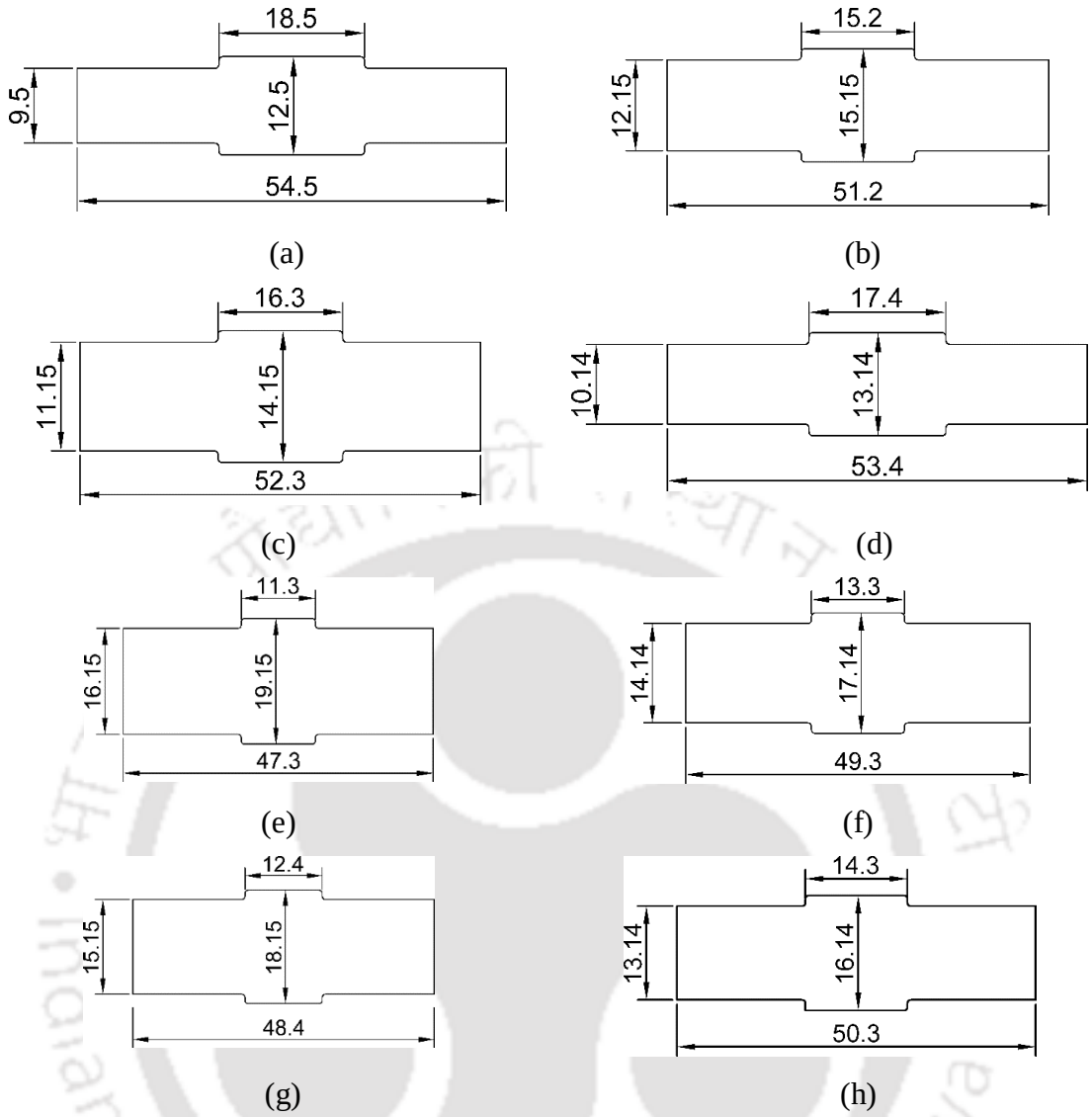

Figure 6.21 Closed die forged Product 5: (a) Model 1, (b) Model 2, (c) Model 3, (d) Model 4, (e) Model 5, (f) Model 6, (g) Model 7 and (h) Model 8

It was observed that Model 3 of Product 4 was having the highest overall similarity index. The preserved complexity factor for Model 3 was then used to estimate the forging load for Model 1 of Product 5. Model 1 is desired to be forged under lubricated condition. The semi-analytical model estimated lower, most-likely and upper estimate of the forging load were 503.2 kN, 771.5 kN and 1133.8 kN respectively. The FEM simulated load under non-lubricated condition for Model 1 was 653.2 kN. Kalman filter suggested lower, most-likely and upper estimate of the forging load were 624.2 kN, 671.3 kN and 726.6 kN respectively. The complexity factor based on the Kalman filter suggested most-likely estimate and the deviation of the upper and lower with the most-likely estimate are preserved. Similar methodology is adopted for rest of the seven models for Product 5. The

TH-3282_186103018

results are presented in Table 6.5. Figure 6.22 and 6.23 provides a visual description of the results from the semi-analytical and on fine tuning with Kalman filter.

Table 6.5 Forging load estimation for Product 5

Product / Model	Blank width (mm)	Blank depth (mm)	Blank height (mm)	Product depth (mm)	Semi-analytical most-likely estimate (kN)	Simulated (actual) load (kN)	Kalman filter most-likely estimate (kN)	Base model	Base product	Friction condition
5/1	53	20	16	23.8	771.5	653.2	671.3	3	4	lubricated
5/2	50	20	19	23.6	657.3	603.2	613.2	1	5	non-lubricated
5/3	51	20	18	23.7	692.1	620.1	632.5	2	5	lubricated
5/4	52	20	17	23.8	731.7	639.0	654.1	3	5	non-lubricated
5/5	46	20	23	23.2	568.2	551.4	553.3	2	5	non-lubricated
5/6	48	20	21	23.4	604.4	577.8	583.2	5	5	lubricated
5/7	47	20	22	23.3	583.4	566.3	569.9	6	5	lubricated
5/8	49	20	20	23.5	631.2	591.6	599.3	6	5	lubricated

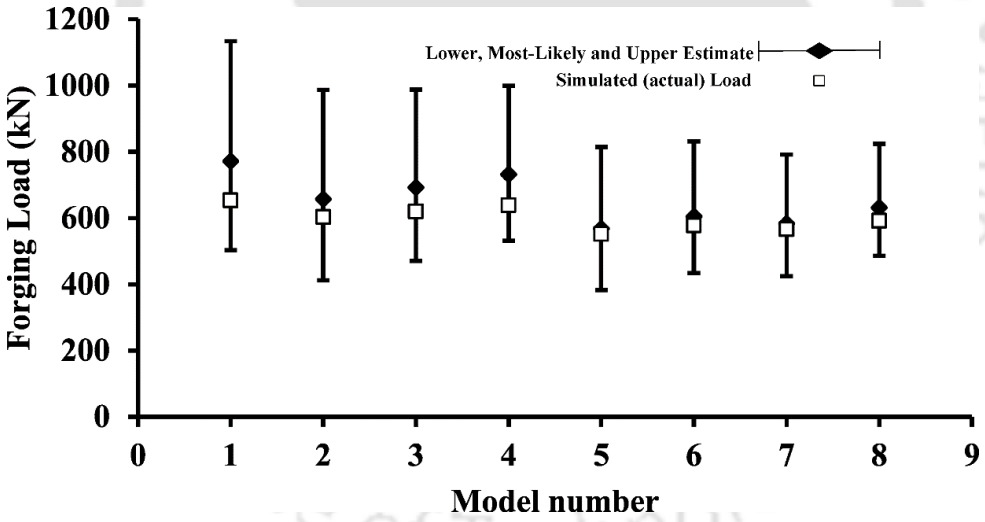

Figure 6.22 Predicted values versus simulated values for Product 5 using the semi-analytical model

TH-3282_186103018

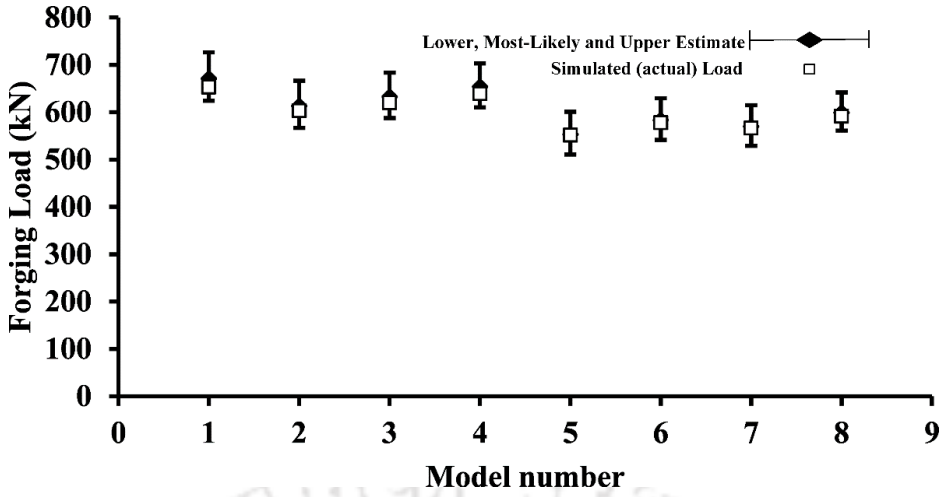

Figure 6.23 Predicted values versus simulated values for Product 5 using Kalman filter

The process continues with the different models of Product 6 are shown in Figure 6.24. The initial dimensions of all the models are presented in Table 6.6. In case of Product 6, the information of all the available models of Product 4 and Product 5 were used to suggest the most similar product. It was observed that Model 3 of Product 4 was having the highest similarity index. The preserved complexity factor was retrieved. Model 1 of Product 6 was desired to be forged under non-lubricated condition. The semi-analytical model suggested lower, most-likely and upper estimate of the forging load were 368.2 kN, 556.1 kN and 809.4 kN respectively. The simulated forging load was observed as 477.9 kN. Kalman filter suggested lower, most-likely and upper estimate of the forging load were 455.9 kN, 490.3 kN and 530.5 kN respectively. The complexity factor based on the Kalman filter suggested most-likely estimate and the deviation of the upper and lower with the most-likely estimate are preserved. The process continues for the rest of the seven models of Product 6. The results are presented in Table 6.6. Figure 6.25 and 6.26 provides a visual description of the results from the semi-analytical and on fine tuning with Kalman filter.

TH-3282_186103018

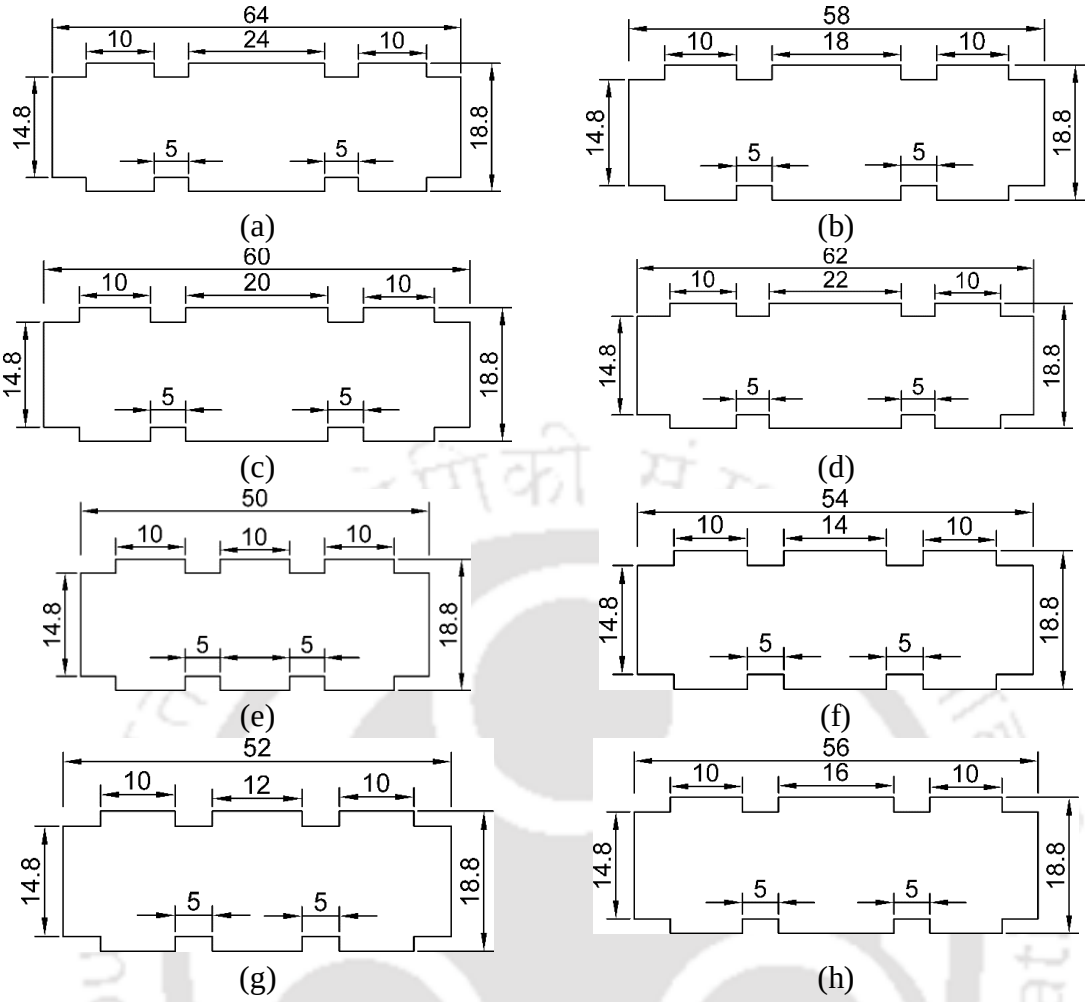

Figure 6.24 Closed die forged Product 6: (a) Model 1, (b) Model 2, (c) Model 3, (d) Model 4, (e) Model 5, (f) Model 6, (g) Model 7 and (h) Model 8

Table 6.6 Forging load estimation for Product 6

Product / Model	Blank width (mm)	Blank depth (mm)	Blank height (mm)	Product depth (mm)	Semi-analytical most-likely estimate (kN)	Simulated (actual) load (kN)	Kalman filter most-likely estimate (kN)	Base model	Base product	Friction condition
6/1	63	20	20	22.8	556.1	477.9	490.3	3	4	non-lubricated
6/2	57	20	20	22.6	483.1	431.2	440.2	1	6	lubricated
6/3	59	20	20	22.7	508.0	447.1	457.3	2	6	lubricated
6/4	61	20	20	22.8	532.4	462.0	473.4	3	6	non-lubricated
6/5	49	20	20	22.2	395.2	363.5	365.2	2	6	lubricated
6/6	53	20	20	22.4	435.2	397.7	404.5	5	6	lubricated
6/7	51	20	20	22.3	410.8	381.0	386.6	6	6	lubricated
6/8	55	20	20	22.5	458.7	414.4	422.3	6	6	lubricated

TH-3282_186103018

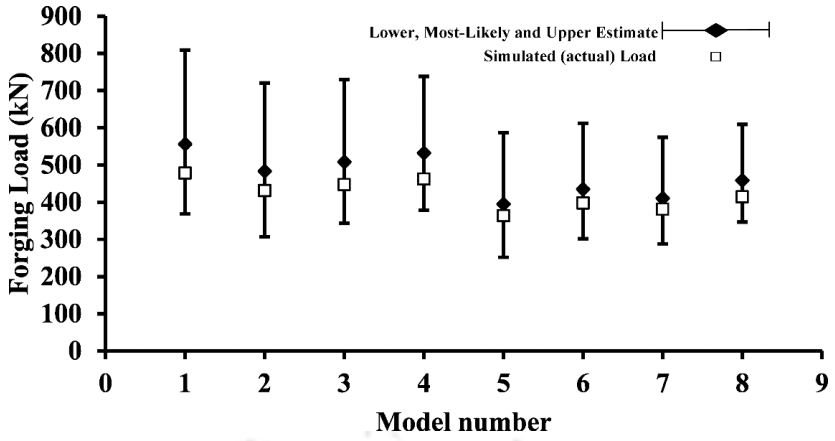

Figure 6.25 Predicted values versus simulated values for Product 6 using the semi-analytical model

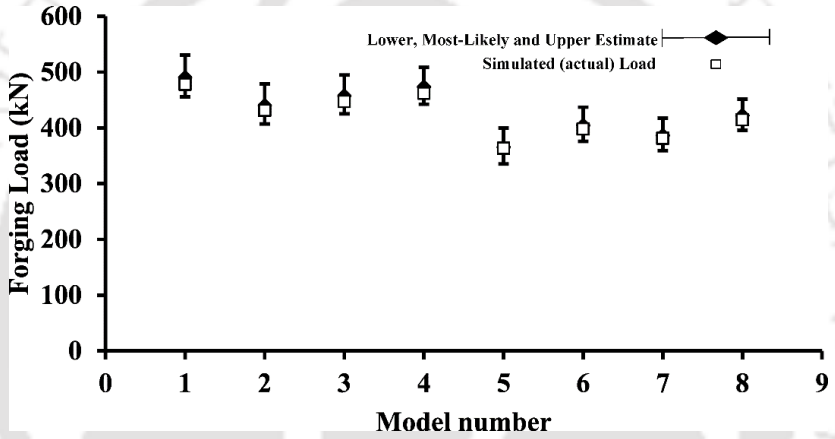

Figure 6.26 Predicted values versus simulated values for Product 6 using Kalman filter

6.7 Conclusion

Application of data-driven techniques is increasing in the metal forming industries. One application can be in the estimation of forging load in a closed die forging process. In this work, the Kalman filter has been used for making an optimal estimate of the forging load based on semi-analytical model and shop floor data. Due to scarcity of the shop floor data, FEM simulations were used to mimic a virtual shop floor. Several case studies ascertained that use of Kalman filter helps in better prediction of the forging load. It provides a way to update the prediction model based on the latest data on the shop floor. In case, the shop floor forging process is stable, the Kalman factor helps in reducing the estimation error drastically, for example from 51% to 8% in one case study. If the process is not stable, the Kalman filter will try to follow the process but after smoothening out the fluctuations due to noise. It is a computationally efficient method. There is a lot of scope to use Kalman filter for predicting other crucial parameters of metal forming.

TH-3282_186103018

TH-3282_186103018

Chapter 7
Epilogue

7.1 Introduction

With the advent of Industry 4.0, manufacturing industries are trying to effectively utilize the generated manufacturing data for enhancing the performance of manufacturing processes. The recent technological advancement especially in the field of information technology has made it possible to preserve and gain insights from the large amount of captured data. The main aim towards data-driven intelligence is quick and accurate performance estimation that can ultimately reduce the unnecessary downtime. However, the accuracy of such data driven intelligence depends on the veracity of the captured data. Additionally, there is also a pressure to reduce the unnecessary burden on data storage platform.

Significant researches have been carried out on physics-based, numerical-based and empirical modelling techniques for performance estimation of manufacturing processes, viz., machining and metal forming. A review of the works that are available in the literature reveal that physics-based models take a lot of assumptions that may be far away from reality. Most importantly, physics-based models require an exact knowledge of the material behavior during deformation that is difficult to ascertain. With the advancement of the processing power of computers, numerical models became popular. FEM is a powerful numerical tool that provide quick performance estimation by creating a digital copy in lieu of actual experimentation. However, such tools are not only computationally expensive, but also can take several hours to simulate products with complicated geometry. Lastly, the empirical models can provide a quick estimation accurately. However, the main challenge lies in creating a large database for the successful implementation of such models. For overcoming such hindrance, researchers are trying to create an intelligent database model that can preserve veracious data for accurate performance estimation of manufacturing processes and also avoid unnecessary burden on data storage. These two vital aspects of data-driven intelligence have not been investigated properly in the past. The focus of the thesis is towards suggesting a well-structured methodology that can be implemented in the shop floor for filtering the captured veracious data and also towards effective utilization of the preserved data to avoid data explosion. The scope of the thesis is limited to two typical manufacturing processes, viz., turning and forging.

TH-3282_186103018

7.2 Overall Conclusions

The noticeable conclusions that can be drawn from the present thesis can be listed as follows:

- A well-structured methodology is presented for preserving the veracious data in a Central Data Repository (CDR). Doubtful data are preserved in a mini-repository. Such data are further checked for any process abnormality. If it is ascertained that there is no process abnormality, such data is then used for modelling keeping aside outliers. A novel concept of dynamic reliability is attached with data, eliminating the chances of data duplication.
- Identification of the outliers in the database is carried out by evaluating the Cook's distance. Cook's distance has been used as a parameter for measuring the level of influence that can be used for filtering out the non-influential data. Most importantly, Cook's distance helps in assessing the stability and reliability of a model by analysing the influence of individual observation. Hence, only influential data are preserved in the database. The efficacy of the framework is presented through an example of cutting force estimation in turning.
- Efficient storage and utilization of shop floor data is carried out by an example of surface roughness estimation in turning operation. The strategy to preserve only the essential model parameters instead of preserving the complete data. Preserving only the model parameters eliminates the risk of data explosion. Additionally, the complete dataset is divided into three major levels categorised as high, medium and low to represent as cells. Multiple-linear regression is used for model fitting in each cell. As the range of process variables are significantly small, a piecewise linear or continuous model is assumed.
- Surface roughness estimations are carried out in the form of low, most-likely and high estimates. Estimations are carried out when there is sufficient as well as when there is insufficient data. Based on the process parameters, the specific cell for surface roughness estimation is identified. In case of insufficient data, the nearest neighbour estimate is used for the estimation of the most-likely estimate. Till sufficient data is available for model fitting. The model parameters are then preserved to that specific cell. Results demonstrates that at least 64% of the simulated values lies within the interval estimates when there is insufficient data and 88% of the simulated values lies within the interval estimates when there is sufficient data.

TH-3282_186103018

- A robust procedure is presented for estimating a suitable value of the complexity factor. The complexity factor is mainly influenced by size and friction condition. In open-die forging, the semi-analytical model can accurately estimate the complexity factor for estimating the forging load. FEM simulations are carried out to represent a virtual factory. The maximum observed error is about 3% in all the cases.
- In closed-die forging, the forging load is estimated based on the information of the most similar product available in the database. The most similar product is chosen by evaluating the similarity index. The similarity index depends on the material, friction condition and geometric dimension. The similarity index is estimated and the one with the highest magnitude is chosen as the most similar model. The information of the complexity factor is retrieved from the most similar product available in the database.
- Fuzzy set theory is then used to estimate the closed-die forging load in the form of low, most-likely and high estimates. Flow stress and friction condition are considered as fuzzy parameters. FEM simulations are carried out for both lubricated and non-lubricated conditions. The complexity factor of the most similar product is then used for the estimation of forging load in the form of low, most-likely and high estimates. Four axisymmetric closed-die forged products are considered. Simulation are carried out for varying sizes of the four products, friction conditions and materials. A maximum deviation of 22% is observed of the most-likely estimate with the simulated load in a typical case. Fuzzy set theory captures reality in an efficacious way.
- Kalman filter is an effective tool to improve the estimate of the current state from a set of noisy data based on the feedback from the previously estimated value. Kalman filter is applied to fine tune the already estimated forging load in the form of low, most-likely and high estimates. Six closed-die forged axisymmetric and non-axisymmetric products are considered. A number of models for each product are considered for demonstrating the methodology. Simulation are carried out for both lubricated as well as for non-lubricated conditions. Kalman filter drastically reduces the error from 51% to 8% in a typical case.

7.3 Scope of Future Work

On the basis of the review and the work carried out in this thesis, some of the key challenges and areas where future researchers can be directed as follows:

TH-3282_186103018

- This thesis considers effective utilization of data in turning and forging processes. However, the significance of the methodology proposed in this thesis extends beyond these specific processes. The methodology developed in this work can be applied to other processes as well.
- The present study uses virtual data for testing the algorithms. However, to validate the real-world applicability and robustness of the proposed algorithms, it becomes important to carry out test using a real-life data.
- Future work can be expanded towards improving the level of data encryption for providing enhanced security and privacy of the preserved data. This will add an extra layer of protection to keep the preserved data safe and private. It will ensure lesser occurrence of security breaches in future.

TH-3282_186103018

References

Abburi, N.R. and Dixit, U.S. 2006. A knowledge-based system for the prediction of surface roughness in turning process. Robotics and Computer-Integrated Manufacturing, 22(4), pp.363–372.

Abidin, N.W.Z., Ab Rashid, M.F.F. and Mohamed, N.M.Z.N., 2019. A review of multi-holes drilling path optimization using soft computing approaches. Archives of Computational Methods in Engineering, 26(1), pp.107–118.

Adnan, M.M., Sarkheyli, A., Zain, A.M. and Haron, H., 2015. Fuzzy logic for modeling machining process: a review. Artificial Intelligence Review, 43(3), pp.345–379.

Al-Athel, K.S. and Gadala, M.S. 2011. The use of volume of solid (VOS) approach in simulating metal cutting with chamfered and blunt tools. International Journal of Mechanical Sciences, 53(1), pp.23–30.

Albrecht, P., 1965. Dynamics of the metal-cutting process. ASME Journal of Engineering for Industry, 87, pp. 429–441.

Alexandrov, S., Lyamina, E. and Jeng, Y.R., 2017. A general kinematically admissible velocity field for axisymmetric forging and its application to hollow disk forging. The International Journal of Advanced Manufacturing Technology, 88, pp.3113–3122.

Alon, N. and Kalai, G., 1985. A simple proof of the upper bound theorem. European Journal of Combinatorics, 6(3), pp.211–214.

Altan T and Fiorentino RJ. 1971. Prediction of loads and stresses in closed-die forging. Journal of Manufacturing Science and Engineering, 93(2), pp. 477–484.

Altan, T. and Boulger, F.W., 1973. Flow stress of metals and its application in metal forming analyses, 95(4), pp. 1009–1019.

Altan, T. and Fiorentino, R.J., 1971. Prediction of loads and stresses in closed-die forging.

Altan, T. and Knoerr, M. 1992. Application of the 2D finite element method to simulation of cold-forging processes. Journal of Materials Processing Technology, 35(3-4), pp.275–302.

Altintas, Y and Spertce, A. 1991. End Milling Force Algorithm for CAD Systems, CIRP Annals, 40(1), pp. 31–34.

Armarego, E.J.A. and Deshpande, N.P. 1991. Computerized end-milling force predictions with cutting models allowing for eccentricity and cutter deflections. CIRP Annals, 40(1), pp.25–29.

Arrazola, P.J., 2010. Investigations on the effects of friction modeling in finite element simulation of machining. International journal of mechanical sciences, 52(1), pp.31–42.

Astakhov, V.P., 1998. Metal cutting mechanics. CRC press, Boca Raton, USA.

Astakhov, V.P., 2011. Authentication of FEM in metal cutting. Finite element method in manufacturing processes, pp.1–43.

TH-3282_186103018

Avitzur, B. and Kohser, R.A., 1978. Disk and strip forging with side-surface foldover—Part 1: velocity field and upper-bound analysis. Journal of Manufacturing Science and Engineering, 100(4), pp. 421–427.

Avitzur, B. and Sauerwine, F., 1978. Limit analysis of hollow disk forging—part 1: upper bound, ASME Journal of Manufacturing Science and Engineering, 100(3), pp. 340–344.

Axinte, D.A., Belluco, W. and De Chiffre, L. 2001. Evaluation of cutting force uncertainty components in turning. International Journal of Machine Tools and Manufacture, 41(5), pp.719-730.

Azouzi, R. and Guillot, M. 1997. On-line prediction of surface finish and dimensional deviation in turning using neural network-based sensor fusion. International Journal of Machine Tools and Manufacture, 37(9), pp.1201–1217.

Barker AL, Brown DE and Martin WN. 1995. Bayesian estimation and the Kalman filter. Computers & Mathematics with Applications, 30(10), pp.55–77.

Belhadi, A., Zkik, K., Cherrafi, A. and Yusof, M. 2019. Understanding the capabilities of Big Data Analytics for manufacturing process: insights from literature review and multiple case study. Computers & Industrial Engineering, p.106099.

Bhattacharyya P and Sengupta D. 2009. Estimation of tool wear based on adaptive sensor fusion of force and power in face milling. International Journal of Production Research, 47(3), pp. 817–833.

Binsaeid S, Asfour S, Cho S and Onar A. 2009. Machine ensemble approach for simultaneous detection of transient and gradual abnormalities in end milling using multisensor fusion. Journal of Materials Processing Technology, 209(10), pp. 4728–4738.

Calamaz, M., Limido, J., Nouari, M., Espinosa, C., Coupard, D., Salaün, M., Girot, F. and Chieragatti, R. 2009. Toward a better understanding of tool wear effect through a comparison between experiments and SPH numerical modelling of machining hard materials. International Journal of Refractory Metals and Hard Materials, 27(3), pp.595–604.

Chandrasekaran, M., Muralidhar, M. and Dixit, U.S. 2013. Online optimization of multipass machining based on cloud computing. The International Journal of Advanced Manufacturing Technology, 65(1-4), pp.239–250.

Chandrasekaran, M., Muralidhar, M., Krishna, C.M. and Dixit, U.S. 2010. Application of soft computing techniques in machining performance prediction and optimization: a literature review. The International Journal of Advanced Manufacturing Technology, 46(5-8), pp.445–464.

Chandrasekaran, M., Muralidhar, M., Krishna, C.M. and Dixit, U.S. 2012. Online machining optimization with continuous learning. Computational Methods for

TH-3282_186103018

Optimizing Manufacturing Technology: Models and Techniques, IGI Global, pp. 85–110.

Chandrasekharan, V., S. G. Kapoor, and R. E. DeVor. 1995. A mechanistic approach to predicting the cutting forces in drilling: with application to fiber-reinforced composite materials. 559-570. ASME Journal of Engineering for Industry, 117, pp. 559–57.

Chatterjee K, Dixit US, Zhang J and Petrov PA. A Methodology for data-driven estimation of forging load. In: Recent Advances in Manufacturing Processes and Systems. Springer, Singapore, 2022, pp. 11–22.

Chatterjee K., Zhang, J. and Dixit, U.S. 2020. Data-driven framework for the prediction of cutting force in turning. IET Collaborative Intelligent Manufacturing, 2(2), pp. 87–95.

Chatterjee, K., Zhang, J. and Dixit, U.S. 2021. Estimation of surface roughness in a turning operation using industrial big data. International Journal of Machining and Machinability of Materials, 23(3), pp.209–240.

Chattopadhyay, A.B., 2011. Machining and Machine Tools (With CD). John Wiley & Sons.

Chen, C.C. and Kobayashi, S., 1978. Rigid-plastic finite-element analysis of ring compression. Applications of Numerical Methods of Forming Processes, 28, pp.163–174.

Chen, C.C. and Kobayashi, S., 1980. Rigid-plastic finite element analysis of plane-strain closed-die forging. Materials and Processing Congresses, 1978-1979, pp.167–183.

Cherukuri, H., Perez-Bernabeu, E., Selles, M.A. and Schmitz, T.L., 2019. A neural network approach for chatter prediction in turning. Procedia Manufacturing, 34, pp.885–892.

Dadras P, Thomas Jr JF. 1983. Analysis of axisymmetric upsetting based on flow pattern observations. International Journal of Mechanical Sciences, 25(6), pp. 421–427.

Das, M.K. and Tobias, S.A., 1967. The relation between the static and the dynamic cutting of metals. International Journal of Machine Tool Design and Research, 7(2), pp.63–89.

Davim, J.P., Astakhov, V.P. and Outeiro, J.C., 2008. Metal cutting mechanics, finite element modelling. Machining: fundamentals and recent advances, pp.1–27.

de Paiva, R.L., da Silva, R.B., Jackson, M.J. and Abrão, A.M., 2017. The influence of cutting fluid concentration on surface integrity of VP80 steel and the influence of cutting fluid flow rate on surface roughness of VPATLAS steel after grinding. Journal of Manufacturing Science and Engineering, 139(12), p.121003.

Dixit, P.M. and Dixit, U.S., 2008. Modelling of Metal Forming and Machining Processes: By Finite Element and Soft Computing Methods, Springer, London.

Dixit, U.S. and Dixit, P.M. 1996. A finite element analysis of flat rolling and application of fuzzy set theory. International Journal of Machine Tools and Manufacture, vol. 36(8), pp.947–969.

TH-3282_186103018

Dixit, U.S. and Dixit, P.M., 1996. A finite element analysis of flat rolling and application of fuzzy set theory. International Journal of Machine Tools and Manufacture, 36(8), pp.947–969.

Dixit, U.S. and Narayanan, R.G., 2013. Metal forming: technology and process modelling. McGraw-Hill Education, New Delhi.

Dixit, U.S., Raj, A., Petrov, P.A. and Matveev, A.G., 2022. Numerical simulations for studying the influence of friction in forging. Advances in Materials and Processing Technologies, 8(3), pp. 2752–2774.

Dixit, U.S., Yadav, V., Pandey, P.M., Roy, A. and Silberschmidt, V.V., 2020. Modeling of friction in manufacturing processes. Mechanics of Materials in Modern Manufacturing Methods and Processing Techniques, Elsevier, Amsterdam, pp. 415–444.

Doi, S. and Kato, S., 1956. Chatter vibration of lathe tools. Transactions of the American Society of Mechanical Engineers, 78(5), pp.1127–1133.

Dölen M, Kaftanoglu B and Lorenz RD. 2004. A cutting force estimator for CNC machining centers. CIRP Annals, 53(1), pp. 313–316.

Domblesky, J.P., Shivpuri, R. and Painter, B. 1995. Application of the finite-element method to the radial forging of large diameter tubes. Journal of materials processing technology, 49(1-2), pp.57–74.

Duro JA, Padget JA, Bowen CR, Kim HA and Nassehi A. 2016. Multi-sensor data fusion framework for CNC machining monitoring. Mechanical Systems and Signal Processing, 66, pp.505–520.

Dutta, S., Pal, S.K. and Sen, R. 2016. On-machine tool prediction of flank wear from machined surface images using texture analyses and support vector regression. Precision Engineering, 43, pp.34–42.

Ebrahimi, R. and Najafizadeh, A., 2004. A new method for evaluation of friction in bulk metal forming. Journal of Materials Processing Technology, 152(2), pp.136–143.

Endres, W. J., Sutherland, J. W DeVor, R. E., and Kapoor, S. G., 1990. A Dynamic Model of the Cutting Force System in the Turning Process, Proc. ASME Symposium on Monitoring and Control for Manufacturing Processes, PED, 44, pp. 193–212

Fang, N. and Jawahir, I.S., 2002. An analytical predictive model and experimental validation for machining with grooved tools incorporating the effects of strains, strain-rates, and temperatures. CIRP Annals, 51(1), pp.83–86.

Fang, N., Jawahir, I.S. and Oxley, P.L.B., 2001. A universal slip-line model with non-unique solutions for machining with curled chip formation and a restricted contact tool. International Journal of Mechanical Sciences, 43(2), pp.557–580.

Fang, N., Pai, P.S. and Edwards, N., 2016. Neural network modeling and prediction of surface roughness in machining aluminum alloys. Journal of Computer and Communications, 4(5), pp.1–9.

TH-3282_186103018

Fereshteh-Saniee, F and Jaafari, M., 2002. Analytical, numerical and experimental analyses of the closed-die forging. Journal of Materials Processing Technology, 125, pp.334–340.

Frank, A.G., Dalenogare, L.S. and Ayala, N.F., 2019. Industry 4.0 technologies: Implementation patterns in manufacturing companies. International Journal of Production Economics, 210, pp.15–26.

Fu, Hao-Jen, R. E. DeVor, and Shiv Gopal Kapoor., 1984. A mechanistic model for the prediction of the force system in face milling operations. ASME Journal of Engineering for Industry, 106, pp. 81–88.

Gagliardi, F., Ambrogio, G., Ciancio, C. and Filice, L. 2017. Metamodeling technique for designing reengineered processes by historical data. Journal of Manufacturing Systems, 45, pp.195–200.

Gangopadhyay T, Pratihar DK, Basak I. 2011. Expert system to predict forging load and axial stress. Applied Soft Computing, 11(1), pp.744–753.

Ghosh A and Mallik AK. 2010. Manufacturing Science, 2nd Edition. Affiliated East West Press, New Delhi.

Ghosh N, Ravi YB, Patra A, Mukhopadhyay S, Paul S, Mohanty AR and Chattopadhyay AB. 2007. Estimation of tool wear during CNC milling using neural network-based sensor fusion. Mechanical Systems and Signal Processing, 21(1), pp.466–479.

Gisbert, C., Bernal, C. and Camacho, A.M., 2015. Improved analytical model for the calculation of forging forces during compression of bimetallic axial assemblies. Procedia engineering, 132, pp.298–305.

Glaeser, A., Selvaraj, V., Lee, S., Hwang, Y., Lee, K., Lee, N., Lee, S. and Min, S. 2021. Applications of deep learning for fault detection in industrial cold forging. International Journal of Production Research, vol. 59(16), pp. 4826–4835.

Glynn, D., Lyons, G. and Monaghan, J., 1995. Forging sequence design using an expert system. Journal of materials processing technology, 55(2), pp.95–102.

Gronostajski, Z., Hawryluk, M., Kaszuba, M., Marciniak, M., Niechajowicz, A., Polak, S., Zwierzchwoski, M., Adrian, A., Mrzygłód, B. and Durak, J. 2016. The expert system supporting the assessment of the durability of forging tools. The International Journal of Advanced Manufacturing Technology, 82(9-12), pp.1973–1991.

Gugax, P.E. and Mathias, E., 1980. Experimental full cut milling dynamics. CIRP Annals, 29(1), pp.61–66.

Guo, Y., Ye, F., Zhou, Y. and Zhang, Z. 2020. Fault diagnosis of multi-channel data in a forging process using the linear support higher-order tensor machine. International Journal of Computer Integrated Manufacturing, 33(8), pp.810–822.

TH-3282_186103018

Gurney, J.P. and Tobias, S.A., 1961. A graphical method for the determination of the dynamic stability of machine tools. International Journal of Machine Tool Design and Research, 1(1-2), pp.148–156.

Gygax, P.E., 1979. Dynamics of single-tooth milling. Annals of the CIRP, 28(1), pp.65–70.

Hahn, R.S., 1951. On the temperature developed at the shear plane in the metal cutting process. Journal of Applied Mechanics-Transactions of the ASME, 18(3), pp. 323–323.

Hanafi, I., Khamlichi, A., Cabrera, F.M., López, P.J.N. and Jabbouri, A. 2012. Fuzzy rule based predictive model for cutting force in turning of reinforced PEEK composite. Measurement, 45(6), pp.1424–1435.

Hartley, P., Pillinger, I., 2006. Numerical simulation of the forging process. Computer Methods in Applied Mechanics and Engineering, 195(48-49), pp. 6676–6690.

Hartley, P., Sturgess, C.E.N., Rowe, G.W. 1980. Influence of friction on the prediction of forces, pressure distributions and properties in upset forging. International Journal of Mechanical Sciences 22(12), pp.743–753.

Hong, M.S. and Ehmann, K.F., 1995. Generation of engineered surfaces by the surface-shaping system. International Journal of Machine Tools and Manufacture, 35(9), pp.1269–1290.

Hu, S., Liu, F., He, Y. and Hu, T. 2012. An on-line approach for energy efficiency monitoring of machine tools. Journal of Cleaner Production, 27, pp.133–140.

Illoul, L. and Lorong, P., 2011. On some aspects of the CNEM implementation in 3D in order to simulate high speed machining or shearing. Computers & Structures, 89(11–12), pp.940–958.

Jang, D.Y. and Liou, J.H., 1998. Study of stress development in axi-symmetric products processed by radial forging using a 3-D non-linear finite-element method. Journal of materials processing technology, 74(1-3), pp.74–82.

Ji, W., Yin, S. and Wang, L., 2019. A big data analytics-based machining optimisation approach. Journal of Intelligent Manufacturing, 30(3), pp. 1483–1495.

Jin, X. and Altintas, Y., 2011. Slip-line field model of micro-cutting process with round tool edge effect. Journal of Materials Processing Technology, 211(3), pp.339–355.

Jun, M.B., Goo, C., Malekian, M. and Park, S., 2012. A new mechanistic approach for micro end milling force modeling. Journal of Manufacturing Science and Engineering, 134(1).

Jung-Ho, C. and Noboru, K., 1985. An analysis of metal forming processes using large deformation elastic-plastic formulations. Computer methods in applied mechanics and engineering, 49(1), pp.71–108.

TH-3282_186103018

Kamble, D.N. and Nandedkar, V.M., 2011. Slab method modification and its experimental investigation for hot forming process. Materials and Manufacturing Processes, 26(5), pp.677–683.

Karpat, Y. and Özel, T., 2008. Mechanics of high speed cutting with curvilinear edge tools. International Journal of Machine Tools and Manufacture, 48(2), pp.195–208.

Katayama, T., Akamatsu, M., Tanaka, Y. 2004. Construction of PC-based expert system for cold forging process design. Journal of Materials Processing Technology, 155, pp.1583–1589.

Khaleed, H.M.T., Samad, Z., Othman, A.R., Abdul Mujeebu, M., Badarudin, A., Abdullah, A.B., Ab-Kadir, A.R., Anjum Badruddin, I. and Salman Ahmed, N.J. 2011. Computer-Aided FE Simulation for Flashless Cold Forging of Connecting Rod Without Underfilling. Arabian Journal for Science and Engineering, 36(5), pp.855–865.

Kim, C. and Park, C.W. 2006. Development of an expert system for cold forging of axisymmetric product. International Journal of Advanced Manufacturing Technology 29(5-6), pp.459–474.

Kim, H.S. and Im, Y.T., 1995. Expert system for multi-stage cold-forging process design with a re-designing algorithm. Journal of materials processing technology, 54(1–4), pp.271–285.

Kline, W.A. and DeVor, R.E., 1983. The effect of runout on cutting geometry and forces in end milling. International Journal of Machine Tool Design and Research, 23(2-3), pp.123–140.

Kline, W.A., DeVor, R.E. and Lindberg, J.R., 1982. The prediction of cutting forces in end milling with application to cornering cuts. International Journal of Machine Tool Design and Research, 22(1), pp.7–22.

Kline, W.A., DeVor, R.E. and Zdeblick, W.J., 1980, May. A mechanistic model for the force system in end milling with application to machining airframe structures. North American Manufacturing Research Conference Proceedings, 18, p. 297.

Ko, J.H. and Heisel, U. 2007. Mechanistic cutting force model for micro ball-end milling. Proceedings of the 2nd international conference on micromanufacturing, South Carolina, USA, Paper no. ICOMM07-0031.

Koenigsberger, F. and Sabberwal, A.J.P., 1961. An investigation into the cutting force pulsations during milling operations. International Journal of Machine Tool Design and Research, 1(1-2), pp.15–33.

Kohli, A., & Dixit, U. S. 2005. A neural-network-based methodology for the prediction of surface roughness in a turning process. The International Journal of Advanced Manufacturing Technology, 25(1-2), pp. 118–129.

Kolarits, F.M. and DeVries, W.R., 1991. A mechanistic dynamic model of end milling for process controller simulation, Journal of Manufacturing Science and Engineering, 113(2), pp. 176–183.

TH-3282_186103018

Kolodner J. 2014. Case-based reasoning. Morgan Kaufmann, San Mateo.

Kronenberg, M. 1966. Machining science and application. Pergamon Press, London, 217, p.219.

Kudo, H., 1960. Some analytical and experimental studies of axi-symmetric cold forging and extrusion—I. International Journal of Mechanical Sciences, 2(1-2), pp.102–127.

Kudo, H., 1961. Some analytical and experimental studies of axi-symmetric cold forging and extrusion—II. International Journal of Mechanical Sciences, 3(1-2), pp.91–117.

Kuntoğlu, M. and Sağlam, H., 2019. Investigation of progressive tool wear for determining of optimized machining parameters in turning. Measurement, 140, pp.427–436.

Laghari, R.A., Li, J., Laghari, A.A. and Wang, S.Q., 2019. A Review on Application of Soft Computing Techniques in Machining of Particle Reinforcement Metal Matrix Composites. Archives of Computational Methods in Engineering, pp.1–15.

Larose, D.T., 2015. Data mining and predictive analytics. John Wiley & Sons, New Delhi.

Lazar, N., 2019. The Big Picture: Crowdsourcing Your Way to Big Data. Chance, 32(2), pp.43–46.

Lazarova-Molnar, S., Mohamed, N. and Al-Jaroodi, J., 2019. Data analytics framework for Industry 4.0: enabling collaboration for added benefits. IET Collaborative Intelligent Manufacturing, 1(4), pp.117–125.

Lee, B.Y. and Tarng, Y.S., 2000. Cutting-parameter selection for maximizing production rate or minimizing production cost in multistage turning operations. Journal of Materials Processing Technology, 105(1-2), pp.61–66.

Lee, C.H. and Kobayashi, S., 1973. New solutions to rigid-plastic deformation problems using a matrix method, Journal of Manufacturing Science and Engineering, 95(3), pp. 865–873.

Lee, E.H., Mallett, R.L. and McMeeking, R.M., 1977. Stress and deformation analysis of metal-forming processes. Numerical Modelling of Manufacturing Processes, ASME, PVP-PB-025, p.19.

Lee, J., Kao, H.A. and Yang, S., 2014. Service innovation and smart analytics for industry 4.0 and big data environment. Procedia CIRP, 16, pp.3–8.

Lee, R.S. and Hsu, Q.C. 1992. Development of an integrated process planning-based CAE system for cold forging. Proceedings of the Institution of Mechanical Engineers, Part B: Journal of Engineering Manufacture, 206(3):215–25.

Lenz, J., Wuest, T. and Westkämper, E., 2018. Holistic approach to machine tool data analytics. Journal of Manufacturing Systems, 48, pp.180-191.

Li, G.J. and Kobayashi, S., 1984. Analysis of spread in rolling by the rigid-plastic, finite element method. In Numerical analysis of forming processes (pp. 777-786). Wiley New York.

TH-3282_186103018

Liang, M., Yeap, T., Rahmati, S. and Han Z. 2002. Fuzzy control of spindle power in end milling processes. International Journal of Machine Tools and Manufacture, 42(14), pp.1487–1496.

Liang, Y.C., Lu, X., Li, W.D. and Wang, S., 2018. Cyber Physical System and Big Data enabled energy efficient machining optimisation. Journal of Cleaner Production, 187, pp.46–62.

Lieber, D., Stolpe, M., Konrad, B., Deuse, J. and Morik, K., 2013. Quality prediction in interlinked manufacturing processes based on supervised & unsupervised machine learning. Procedia Cirp, 7, pp.193–198.

Lin, W.S., Lee, B.Y. and Wu, C.L., 2001. Modelling the surface roughness and cutting force for turning. Journal of Materials Processing Technology, 108(3), pp.286–293.

Liu, M.K., Tseng, Y.H. and Tran, M.Q., 2019. Tool wear monitoring and prediction based on sound signal. The International Journal of Advanced Manufacturing Technology, 103(9-12), pp.3361–3373.

Lou KN and Lin CJ. 1997. An intelligent sensor fusion system for tool monitoring on a machining centre. The International Journal of Advanced Manufacturing Technology, 13(8), pp.556–565.

Lu, J., Zhang, Z., Yuan, X., Ma, J., Hu, S., Xue, B. and Liao, X. 2020. Effect of machining parameters on surface roughness for compacted graphite cast iron by analyzing covariance function of Gaussian process regression. Measurement, 157, pp.107578.

Mamalis, A.G., Petrossian, G.L. and Manolakos, D.E. 1999. Open-die forging of sintered cylindrical billets: an analytical approach. Journal of Materials Processing Technology, 96(1-3), pp.112–116.

Mamalis, A.G., Petrossian, G.L., Manolakos, D.E. 1999. Open-die forging of sintered cylindrical billets: an analytical approach. Journal of Materials Processing Technology, 96(1–3), pp.112–116.

Maranhão, C. and Davim, J.P., 2010. Finite element modelling of machining of AISI 316 steel: numerical simulation and experimental validation. Simulation Modelling Practice and Theory, 18(2), pp.139–156.

Meinhold RJ and Singpurwalla ND. 1983. Understanding the Kalman filter. The American Statistician, 37(2), pp.123–127.

Merchant, H.E.M. and Ernst, H., 1941. Chip formation, friction and high-quality machined surfaces. Surface treatment of metals. Am Soc Met, 29, pp.299–378.

Merchant, M.E., 1944. Basic mechanics of the metal-cutting process. Journal of Applied Mechanics, 11(3), A168–A175.

Merchant, M.E., 1998. An interpretive look at 20th century research on modeling of machining. Machining Science and Technology, 2(2), pp.157–163.

TH-3282_186103018

Merritt, H.E., 1965. Theory of Self Excited Machine, Tool Chatter (Research-1). Journal of Manufacturing Science and Engineering, 87(17), pp. 447–454.

Mirkoohi E, Bocchini P and Liang SY. 2018. An analytical modeling for process parameter planning in the machining of Ti-6Al-4V for force specifications using an inverse analysis. The International Journal of Advanced Manufacturing Technology, 98(9), pp.2347–2355.

Misaka, T., Herwan, J., Ryabov, O., Kano, S., Sawada, H., Kasashima, N. and Furukawa, Y. 2020. Prediction of surface roughness in CNC turning by model-assisted response surface method. Precision Engineering, 62, pp.196–203.

Mittal, K.K. and Jain, P.K., 2014. An overview of performance measures in reconfigurable manufacturing system. Procedia engineering, 69, pp.1125–1129.

Monaghan, J.M., 1993. Stress analysis of a cold forging process applied to a countersunk headed fastener. Journal of materials processing technology, 39(1-2), pp.191–211.

Montgomery, D., and Altintas, Y., 1991, Mechanism of Cutting Force and Surface Generation in Dynamic Milling, ASME Journal of Engineering for Industry, 113, pp. 160–168.

Mori, K. and Osakada, K., 1984. Simulation of three-dimensional deformation in rolling by the finite-element method. International Journal of Mechanical Sciences, 26(9-10), pp.515–525.

Mori, K., Osakada, K., Nakadoi, K. and Fukuda, M., 1984. Simulation of three-dimensional deformation in metal forming by the rigid-plastic finite element method. Advanced Technology of Plasticity, 2, p.1009.

Moshksar, M.M. and Ebrahimi, R. 1998. An analytical approach for backward-extrusion forging of regular polygonal hollow components. International Journal of Mechanical Sciences, 40(12), pp.1247–1263.

Mou, W., Jiang, Z. and Zhu, S. 2019. A study of tool tipping monitoring for titanium milling based on cutting vibration. The International Journal of Advanced Manufacturing Technology, 104(9), pp.3457–3471.

Mourtzis, D., Vlachou, E. and Milas, N. 2016. Industrial Big Data as a result of IoT adoption in manufacturing. Procedia CIRP, 55, pp. 290–295.

Movahhedy, M.R., Gadala, M.S. and Altintas, Y. 2000. Simulation of chip formation in orthogonal metal cutting process: an ALE finite element approach. Machining Science and Technology, 4(1), pp.15–42.

Namasudra, S., 2019. An improved attribute-based encryption technique towards the data security in cloud computing. Concurrency and Computation: Practice and Experience, 31(3), pp.4364.

Niaki, F.A., Michel, M. and Mears, L. 2016. State of health monitoring in machining: Extended Kalman filter for tool wear assessment in turning of IN718 hard-to-machine alloy. Journal of Manufacturing Processes, 24, pp.361–369.

TH-3282_186103018

Nigm, M.M., Sadek, M.M. and Tobias, S.A., 1977. Determination of dynamic cutting coefficients from steady state cutting data. International Journal of Machine Tool Design and Research, 17(1), pp.19–37.

O'Donovan, P., Leahy, K., Bruton, K. and O'Sullivan, D.T., 2015. An industrial big data pipeline for data-driven analytics maintenance applications in large-scale smart manufacturing facilities. Journal of Big Data, 2(1), pp.1–26.

O'Connell, M., Painter, B., Maul, G. and Altan, T., 1996. Flashless closed-die upset forging-load estimation for optimal cold header selection. Journal of Materials Processing Technology, 59(1-2), pp.81–94.

Oh, S., 1982. Finite element analysis of metal forming processes with arbitrarily shaped dies. International Journal of Mechanical Sciences, 24(8), pp.479–493.

Oñate, E. and Zienkiewicz, O.C., 1983. A viscous shell formulation for the analysis of thin sheet metal forming. International Journal of Mechanical Sciences, 25(5), pp.305–335.

Osakada, K., Yang, G.B., Nakamura, T. and Mori, K., 1990. Expert system for cold-forging process based on FEM simulation. CIRP annals, 39(1), pp.249–252.

Ota, H. and Kono, K., 1974. On chatter vibrations of machine tool or work due to a regenerative effect and time lag. Transaction of the ASME. pp. 1337–1346.

Ozel, T., Llanos, I., Soriano, J. and Arrazola, P.J., 2011. 3D finite element modelling of chip formation process for machining Inconel 718: comparison of FE software predictions. Machining Science and Technology, 15(1), pp.21–46.

Park, J.J. and Kobayashi, S., 1984. Three-dimensional finite element analysis of block compression. International journal of mechanical sciences, 26(3), pp.165–176.

Park, K.S., Kim, B.J. and Moon, Y.H. 2007. Application of fuzzy expert system to estimate dimensional errors of forging products having complicated shape. Journal of Materials Processing Technology, 187, pp.720–724.

Pérez-Canales, D., Álvarez-Ramírez, J., Jáuregui-Correa, J.C., Vela-Martínez, L. and Herrera-Ruiz, G. 2011. Identification of dynamic instabilities in machining process using the approximate entropy method. International Journal of Machine Tools and Manufacture, 51(6), pp.556–564.

Rai, R., Tiwari, M.K., Ivanov, D. and Dolgui, A., 2021. Machine learning in manufacturing and industry 4.0 applications. International Journal of Production Research, 59(16), pp.4773–4778.

Rangwala, S.S. and Dornfeld, D.A., 1989. Learning and optimization of machining operations using computing abilities of neural networks. IEEE Transactions on Systems, Man, and Cybernetics, 19(2), pp.299–314.

Rao, A.V.S. and Pratihar, D.K., 2007. Fuzzy logic-based expert system to predict the results of finite element analysis. Knowledge-Based Systems, 20(1), pp.37–50.

Ravindra, H.V., Srinivasa, Y.G. and Krishnamurthy, R., 1993. Modelling of tool wear based on cutting forces in turning. Wear, 169(1), pp.25–32.

TH-3282_186103018

Ren, H. and Altintas, Y., 2000. Mechanics of machining with chamfered tools. J. Manuf. Sci. Eng., 122(4), pp.650–659.

Risbood, K.A., Dixit, U.S. and Sahasrabudhe, A.D., 2003. Prediction of surface roughness and dimensional deviation by measuring cutting forces and vibrations in turning process. Journal of Materials Processing Technology, 132(1-3), pp.203–214.

Sagar, R. and Juneja, B.L., 1980. An upper bound solution for closed die forging of hexagonal shapes. International Journal of Machine tool design and research, 20(1), pp.67–72.

Saljé, E., 1956. Self-excited vibrations of systems with two degrees of freedom. Transactions of the American Society of Mechanical Engineers, 78(4), pp.737–747.

Schermann, T., Marsolek, J., Schmidt, C. and Fleischer, J., 2006. Aspects of the Simulation of a Cutting Process with ABAQUS/Explicit Including the Interaction between the Cutting Process and the Dynamic Behaviour of the Machine Tool. Proceedings of the 9th CIRP International Workshop on Modelling of Machining Operations, Bled, Slovenia (2006), pp. 163–170.

Sela, A., Ortiz-de-Zarate, G., Arrieta, I., Soriano, D., Aristimuño, P., Medina-Clavijo, B. and Arrazola, P.J., 2019. A mechanistic model to predict cutting force on orthogonal machining of Aluminum 7475-T7351 considering the edge radius. Procedia CIRP, 82, pp.32–36.

Shah, S.N., Lee, C.H. and Kobayashi, S. 1974. Compression of tall, circular, solid cylinders between parallel flat dies. In Proceedings of the International Conference on Production Engineering, Tokyo, pp. 295–300.

Shang, C. and You, F., 2019. Data Analytics and Machine Learning for Smart Process Manufacturing: Recent Advances and Perspectives in the Big Data Era. Engineering, 5(6), pp. 1010–1016.

Sharma, V. and Pandey, P.M., 2019. Mechanistic based cutting force model during ultrasonic assisted turning with self-lubricating cutting inserts. Journal of Advanced Manufacturing Systems, 18(01), pp.133–155.

Sharma, V.S., Sharma, S.K. and Sharma, A.K., 2008. Cutting tool wear estimation for turning. Journal of Intelligent Manufacturing, 19(1), pp.99–108.

Shaw, M.C. and Cookson, J.O., 2005. Metal cutting principles (Vol. 2). New York: Oxford university press.

Shima, S. and Mori, K. 1979. Analysis of metal forming by the rigid-plastic finite element method based on plasticity theory for porous metals. In H. Lippmann (eds) Metal Forming Plasticity, Springer, Berlin, pp. 305–317.

Shin, S.J., Woo, J. and Rachuri, S. 2014. Predictive analytics model for power consumption in manufacturing. Procedia CIRP, 15, pp.153–158.

TH-3282_186103018

Shin, S.J., Woo, J., Rachuri, S. and Seo, W., 2019. An energy-efficient process planning system using machine-monitoring data: A data analytics approach. Computer-Aided Design, 110, pp.92–109.

Silberschmidt, V.V., Mahdy, S.M., Gouda, M.A., Naseer, A., Maurotto, A. and Roy, A., 2014. Surface-roughness improvement in ultrasonically assisted turning. Procedia Cirp, 13, pp.49–54.

Sonar, D. K., Dixit, U. S. and Ojha, D. K. 2006. The application of a radial basis function neural network for predicting the surface roughness in a turning process. The International Journal of Advanced Manufacturing Technology, 27(7-8), pp.661–666.

Stephenson, D.A. and Agapiou, J.S., 2016. Metal cutting theory and practice. CRC press.

Subramanian, T.L. and Altan, T., 1980. A practical method for estimating forging loads with the use of a programmable calculator. Journal of Applied Metalworking, 1(2), pp.60–68.

Sun H, Zhang X and Wang J. 2016. Online machining chatter forecast based on improved local mean decomposition. The International Journal of Advanced Manufacturing Technology, 84(5), pp.1045–1056.

Sun, J.X., Li, G.J. and Kobayashi, S., 1983, May. Analysis of spread in flat-tool forging by the finite element method. In Proc. North American Manufacturing Research Conference, pp. 224–231.

Sun, P.J., 2019. Privacy Protection and Data Security in Cloud Computing: A Survey, Challenges, and Solutions. IEEE Access, 7, pp.147420–147452.

Sutherland, J.W. and DeVor, R. E., 1988. A dynamic model of the cutting force system in the end milling process. Sensor and Controls for Manufacturing ASME PED, 33, pp. 53–62.

Tamang, S.K., Chandrasekaran, M., Palanikumar, K. and Arunachalam, R.M., 2019. Machining performance optimisation of MQL-assisted turning of Inconel-825 superalloy using GA for industrial applications. International Journal of Machining and Machinability of Materials, 21(1-2), pp.43–65.

Tao, F. and Qi, Q., 2017. New IT driven service-oriented smart manufacturing: framework and characteristics. IEEE Transactions on Systems, Man, and Cybernetics: Systems, 49(1), pp. 81–91.

Tao, F., Qi, Q., Liu, A. and Kusiak, A., 2018. Data-driven smart manufacturing. Journal of Manufacturing Systems, 48, pp.157–169.

Tiwari, K., Shaik, A. and Arunachalam, N. 2018. Tool wear prediction in end milling of Ti-6Al-4V through Kalman filter based fusion of texture features and cutting forces. Procedia Manufacturing, 26, pp.1459–1470.

Tjøtta, S. and Heimlund, O., 1992. Finite-element simulations in cold-forging process design. Journal of materials processing technology, 36(1), pp.79–96.

TH-3282_186103018

Tlusty, J. and Polacek, M., 1963. The Stability of the Machine Tool Against Self-Excited Vibration in Machining. Proceedings of the ASME Production Engineering Research Conference, pp. 465-474.

Tlusty, J., 1975. Dynamics of cutting forces in end milling. Ann CIRP, 24(1), pp.21–25.

Tobias, S.A. and Fishwick, W., 1958. The chatter of lathe tools under orthogonal cutting conditions. Transactions of the American Society of Mechanical Engineers, 80(5), pp.1079–1087.

Uhlmann, E., Gerstenberger, R., Graf von der Schulenburg, M., Kuhnert, J. and Mattes, A., 2009. The Finite-Pointset-Method for the Meshfree Numerical Simulation of Chip Formation. Proceedings of the 12th CIRP Conference on Modelling of Machining Operations, 1, pp. 145–151.

Usui, E. and Hirota, A., 1978. Analytical prediction of three-dimensional cutting process—part 2: chip formation and cutting force with conventional single-point tool. Journal of engineering for industry, 100(2), pp.229–235.

Usui, E., 1988. Progress of "predictive" theories in metal cutting. JSME International Journal. Ser. 3, Vibration, Control Engineering, Engineering for Industry, 31(2), pp.363–369.

Utsumi, K., Shichiri, S. and Sasahara, H., 2019. Determining the effect of tool posture on cutting force in a turn milling process using an analytical prediction model. International Journal of Machine Tools and Manufacture, p.103511.

Van Luttervelt, C.A., Childs, T.H.C., Jawahir, I.S., Klocke, F., Venuvinod, P.K., Altintas, Y., Armarego, E., Dornfeld, D., Grabec, I., Leopold, J. and Lindstrom, B., 1998. Present situation and future trends in modelling of machining operations progress report of the CIRP Working Group 'Modelling of Machining Operations'. CIRP Annals, 47(2), pp.587–626.

Vijayaraghavan, V., Garg, A., Gao, L., Vijayaraghavan, R. and Lu, G., 2016. A finite element-based data analytics approach for modeling turning process of Inconel 718 alloys. Journal of Cleaner Production, 137, pp.1619–1627.

Vogler, M.P., DeVor, R.E. and Kapoor, S.G., 2003. Microstructure-level force prediction model for micro-milling of multi-phase materials. J. Manuf. Sci. Eng., 125(2), pp.202–209.

Wang, H., Dong, H., Ke, Y. and Sun, J., 2019. Modeling and analysis of force prediction in milling process of unidirectional fiber reinforced polymer composites. The International Journal of Advanced Manufacturing Technology, 101(9-12), pp.3073–3080.

Wang, H.P. and Wysk, R.A., 1986. An expert system for machining data section. Computers & Industrial Engineering, 10(2), pp.99–107.

Wang, X. and Jawahir, I.S., 2002. Prediction of tool-chip interface friction and chip-groove effects in machining with restricted contact grooved tools using the universal slip-line model. Key Engineering Materials, 233, pp.469–476.

TH-3282_186103018

Wang, X. and Jawahir, I.S., 2004. Web-based optimization of milling operations for the selection of cutting conditions using genetic algorithms. Proceedings of the Institution of Mechanical Engineers, Part B: Journal of Engineering Manufacture, 218(6), pp.647–655.

Ward, M.J., Miller, B.C., Davey, K., 1998. Simulation of a multi-stage railway wheel and tyre forming process. Journal of Materials Processing Technology, 80, pp. 206–212.

Watson I. 1995. An introduction to case-based reasoning. Progress in Case-based Reasoning, Springer, Berlin, pp. 3–16

Woo, J., Shin, S.J., Seo, W. and Meilanitasari, P. 2018. Developing a big data analytics platform for manufacturing systems: architecture, method, and implementation. The International Journal of Advanced Manufacturing Technology, 99(9-12), pp.2193–2217.

Wu, J. and Liu, Z., 2010. Modeling of flow stress in orthogonal micro-cutting process based on strain gradient plasticity theory. International Journal of Advanced Manufacturing Technology, 46, pp. 143–149.

Wu, X., Zhu, X., Wu, G.Q. and Ding, W., 2014. Data mining with big data. IEEE Transactions on Knowledge and Data Engineering, 26(1), pp.97–107.

Wu, Y. and Dong, X., 2016. An upper bound model with continuous velocity field for strain inhomogeneity analysis in radial forging process. International Journal of Mechanical Sciences, 115, pp.385–391.

Wu, Y., Dong, X. and Yu, Q., 2015. Upper bound analysis of axial metal flow inhomogeneity in radial forging process. International Journal of Mechanical Sciences, 93, pp.102–110.

Yamada, Y., Wifi, A.S. and Hirakawa, T., 1979. Analysis of large deformation and stress in metal forming processes by the finite element method. Metal Forming Plasticity, Springer-Verlag, Berlin, p. 158

Yang DY, Choi Y, Kim JH. 1991. Analysis of upset forging of cylindrical billets considering the dissimilar frictional conditions at two flat die surfaces. International Journal of Machine Tools and Manufacture, 31(3), pp.397–404.

Yang Y, Geng Y and Wang W. 2022. Sensor Fault Detection and Isolation based on Zonotopic Kalman Filter for Accelerometer System in Drilling Tools. Measurement, p.112329.

Yazdi, M.S., Bagheri, G.S. and Tahmasebi, M. 2012. Finite volume analysis and neural network modeling of wear during hot forging of a steel splined hub. Arabian Journal for Science and Engineering, 37(3), pp.821–829.

Ye, F., Guo, Y., Xia, Z., Zhang, Z. and Zhou, Y. 2021. Feature extraction and process monitoring of multi-channel data in a forging process via sensor fusion. International Journal of Computer Integrated Manufacturing, 34(1), pp.95–109.

TH-3282_186103018

You, S. J., and Ehmann, K. F., 1991, Synthesis and Generation of Surfaces Milled by Ball Nose End Mills under Tertiary Cutter Motion, ASME Journal of Engineering for Industry, 113(1), pp. 17–24.

Yu, J. and Liu, G. 2020. Knowledge-based deep belief network for machining roughness prediction and knowledge discovery. Computers in Industry, 121, pp. 103262.

Zhang, G. M., and Kapoor, S. G., 1991a, Dynamic Generation of Machined Surfaces, Part 1: Description of a Random Excitation System, ASME Journal of Engineering for Industry, 113, pp. 137–144.

Zhang, G. M,, and Kapoor, S. G., 1991b, Dynamic Generation of Machined Surfaces, Part 2: Construction of Surface Topography, ASME Journal of Engineering for Industry, 113, pp. 145–153.

Zhang, G., Li, J., Chen, Y., Huang, Y., Shao, X. and Li, M. 2014. Prediction of surface roughness in end face milling based on Gaussian process regression and cause analysis considering tool vibration. The International Journal of Advanced Manufacturing Technology, 75(9-12), 1357–1370.

Zhang, J., Xie, G., Peng, Q. and Gu, P., 2023. Product evolution analysis for design adaptation using big sales data. Proceedings of the Institution of Mechanical Engineers, Part B: Journal of Engineering Manufacture, 237(8), pp.1241–1253.

Zhang, X., Yu, T. and Wang, W., 2019. Cutting forces modeling for micro flat end milling by considering tool run-out and bottom edge cutting effect. Proceedings of the Institution of Mechanical Engineers, Part B: Journal of Engineering Manufacture, 233(2), pp.470–485.

Zhang, Y., Wang, Y., Liu, Y., Lv, D., Fu, X., Zhang, Y. and Li, J. 2019. A concentricity measurement method for large forgings based on laser ranging principle. Measurement, 147, p.106838.

Zheng, L., Yang, X.M., Zhang, Z.H. and Liu, T.I., 2008. A web-based machining parameter selection system for life cycle cost reduction and product quality enhancement. Computers in Industry, 59(2-3), pp.254–261.

Zheng, T., Ardolino, M., Bacchetti, A. and Perona, M. 2021. The applications of Industry 4.0 technologies in manufacturing context: a systematic literature review. International Journal of Production Research, 59(6), pp.1922–1954.

Zhou, J., Ren, J. and Yao, C., 2017. Multi-objective optimization of multi-axis ball-end milling Inconel 718 via grey relational analysis coupled with RBF neural network and PSO algorithm. Measurement, 102, pp.271–285.

Zienkiewicz, O.C., Oñae, E. and Heinrich, J.C., 1981. A general formulation for coupled thermal flow of metals using finite elements. International Journal for Numerical Methods in Engineering, 17(10), pp.1497–1514.

TH-3282_186103018

Publications

Journal papers

1. Chatterjee K., Zhang, J. and Dixit, U.S., 2020, "Data-driven framework for the prediction of cutting force in turning," IET Collaborative Intelligent Manufacturing, 2(2), pp. 87–95.
2. Chatterjee, K., Zhang, J. and Dixit, U.S., 2021, "Estimation of surface roughness in a turning operation using industrial big data," International Journal of Machining and Machinability of Materials, 23(3), pp.209–240.
3. Chatterjee, K., Zhang, J. and Dixit, U.S. 2023, "Kalman Filtering for Estimation of Closed-Die Forging Load Based on Shop Floor Data". Proceedings of the Institution of Mechanical Engineers, Part C: Journal of Mechanical Engineering Science, p.09544062231202324.

Conference presentations

1. Chatterjee, K., Zhang, J. and Dixit, U.S. "A framework for enhancing machining performance using big research data analytics," 40th MATADOR International Conference on Advanced Manufacturing and Design, July 8–10, 2019, Hangzhou, China. (Abstract published).
2. Chatterjee, K., Dixit, U.S., Zhang, J. and Petrov, P.A. "A methodology for data-driven estimation of forging load," 2nd International Conference on Recent Advances in Manufacturing, June 10–12, 2021, NIT Surat, India (online mode). (Published as Book Chapter # 1).
3. Chatterjee, K., Dixit, U.S. and Zhang, J. "Fuzzy set-based estimation of Closed die Forging Load using the Shop Floor Data," North East Research Conclave (NERC-2022), May 20–22, 2022, IIT Guwahati, India. (Published as Book Chapter # 2)

Book chapters

1. Chatterjee, K., Dixit, U.S., Zhang, J. and Petrov, P.A., 2022, "A Methodology for Data-Driven Estimation of Forging Load," Recent Advances in Manufacturing Processes and Systems, Ed. Dave, H.K., Dixit, U.S. and Nedelcu, D., Springer Nature, Singapore, pp. 11–22.
2. Chatterjee, K., Dixit, U.S. and Zhang, J., 2022, "Fuzzy Set Based Estimation of Closed-Die Forging Load using the Shop Floor Data," Artificial Intelligence and Data Science based R&D interventions: Proceedings of NERC 2022, Ed. Bhattacharjee, R., Neog, D.R., Mopuri, K.R. and Vipparthi, S.K., Springer Nature, Singapore, pp. 157–185.

TH-3282_186103018